



저작자표시-동일조건변경허락 2.0 대한민국

이용자는 아래의 조건을 따르는 경우에 한하여 자유롭게

- 이 저작물을 복제, 배포, 전송, 전시, 공연 및 방송할 수 있습니다.
- 이차적 저작물을 작성할 수 있습니다.
- 이 저작물을 영리 목적으로 이용할 수 있습니다.

다음과 같은 조건을 따라야 합니다:



저작자표시. 귀하는 원저작자를 표시하여야 합니다.



동일조건변경허락. 귀하가 이 저작물을 개작, 변형 또는 가공했을 경우에는, 이 저작물과 동일한 이용허락조건하에서만 배포할 수 있습니다.

- 귀하는, 이 저작물의 재이용이나 배포의 경우, 이 저작물에 적용된 이용허락조건을 명확하게 나타내어야 합니다.
- 저작권자로부터 별도의 허가를 받으면 이러한 조건들은 적용되지 않습니다.

저작권법에 따른 이용자의 권리는 위의 내용에 의하여 영향을 받지 않습니다.

이것은 [이용허락규약\(Legal Code\)](#)을 이해하기 쉽게 요약한 것입니다.

[Disclaimer](#)



Master's Thesis

Developing a Strong Pre-Trained Base Model for Plant Leaf Disease Classification

Department of Artificial Intelligence Convergence
Graduate School, Chonnam National University

David Jona Richter

August 2025

Developing a Strong Pre-Trained Base Model for Plant Leaf Disease Classification

Department of Artificial Intelligence Convergence
Graduate School, Chonnam National University

David Jona Richter

Supervised by Professor Kyungbaek Kim

A dissertation submitted in partial fulfillment of the requirements for the
Master of Science in Artificial Intelligence Convergence

Committee in Charge:

Yeong-Jun Cho _____

Seok-Bong Yoo _____

Kyungbaek Kim _____

August 2025

Preface

This thesis was written as part of a Digital Agriculture project that our laboratory (DNS Lab at Chonnam National University) was tasked with. As part of the multi-year project, this thesis covers the first year of this project's work and will therefore be continued in future years. As such, in this first year, we set ourselves the goal of finding the most suitable datasets, models and methods for plant leaf disease classification as well as build a foundation model for the field.

Contents

List of Figures	x
List of Tables	xiv
List of Abbreviations	xviii
List of Terms	xx
1 Introduction and Motivation	1
1.1 Introduction	1
2 Literature Review	7
2.1 Previous Work	7
2.1.1 Literature Review Papers	7
2.1.2 Using Distributed Methods	9
2.1.3 Transfer-Learning CNN	11
2.1.4 Analysis	17
3 Background	22
3.1 Image Classification using Deep Learning	22
3.1.1 Domain Adaptation	25
3.1.1.1 Transfer-Learning	25
3.1.1.2 Fine-Tuning	26
3.1.1.3 One-Shot Learning	27
3.1.1.4 Few-Shot Learning	27
3.1.2 Base Models & Foundational Models	27

3.2	Plant Pathology using Deep Learning	29
3.2.1	Disease Types	29
3.2.1.1	Bacterial	29
3.2.1.2	Viral	30
3.2.1.3	Fungal	30
3.2.2	Datasets	30
3.2.2.1	Lab Datasets	31
3.2.2.2	Field Datasets	31
3.2.2.3	Hybrid Datasets	32
4	Datasets	33
4.1	Lab Datasets	36
4.1.1	Plant Village (plantVillage)	36
4.1.2	Tomato Village (tomatoVillage)	36
4.1.3	Potato Disease Leaf Dataset (pld)	36
4.1.4	Tea Sickness Dataset (tea)	37
4.2	Field Datasets	37
4.2.1	Cassava Leaf Disease Classification (cassava)	37
4.2.2	CD&S Dataset (cds)	37
4.2.3	Cucumber Disease Recognition Dataset (cucumber)	37
4.2.4	DiaMOS Plant (diaMos)	38
4.2.5	Paddy Doctor (paddy)	38
4.2.6	Plant Pathology 2020 - FGVC7 (fgvc7)	38
4.2.7	Plant Pathology 2021 - FGVC8 (fgvc8)	38
4.2.8	PDD271: Plant Disease Recognition Dataset (pdd271)	39
4.2.9	Strawberry Disease Detection Dataset (sms)	39
4.3	Hybrid Datasets	39
4.3.1	plantDoc	39
4.3.2	Taiwan Tomato (taiwanTomato)	40
4.3.3	Potato Leaf Disease Dataset in Uncontrolled Environment (novelPotato)	40
4.3.4	Rice Leaf Diseases Dataset (rldd)	40

4.3.5	Sugarcane Leaf Dataset (sugar)	40
5	Models	42
5.1	ResNet	42
5.2	VGG	42
5.3	Inception	43
5.4	EfficientNet	43
5.5	NASNet	43
5.6	MobileNet	44
5.7	ConvNeXt	44
5.8	DenseNet	44
6	Benchmarking	45
6.1	Benchmarking Methods	45
6.1.1	Datasets	46
6.1.2	Models	46
6.1.3	Benchmark Workflow	47
6.2	Benchmarking Results	48
6.2.1	ViT comparison	52
7	Data Augmentation Assessment	54
7.1	Augmentation Techniques	54
7.1.1	Color	55
7.1.2	Noise	55
7.1.3	Transformation	55
7.2	Augmentation Methodology	57
7.3	Augmentation Results	59
8	Dataset Construction	61
8.1	Dataset Construction Methods	61
8.1.1	Class Cleanup	62
8.1.2	Dataset Method Availability	63

9	Model Construction	65
9.1	Baseline Model search	66
9.2	Model Improvement Methodology	67
9.2.1	Model Architecture	67
9.2.2	Possible Improvements	69
9.2.3	Successful Improvements	70
9.2.3.1	Swish Activation (SiLU)	72
9.2.3.2	Channel Attention	73
9.2.3.3	Combined Model	73
9.3	Transfer-Learning	74
9.3.1	PLDC-6	74
9.3.2	Transfer-Learning Methodology	77
9.3.3	Results	77
9.3.3.1	Frozen	79
9.3.3.2	Unfrozen	84
9.3.3.3	Transfer-Learning Results Summary	91
9.4	One-Shot and Few-Shot Learning	92
9.4.1	Dataset	92
9.4.2	Methodology	92
9.4.3	Results	93
9.4.3.1	Cross-Domain One-Shot Classification	94
9.4.3.2	Cross Domain Few-Shot Classification	94
9.4.3.3	One and Few-Shot Result Summary	94
10	Discussion	96
11	Future Work	98
12	Conclusion	100
A	Appendix Datasets	121
A.1	Lab Datasets	121
A.1.1	Plant Village	121

A.1.2	Tomato Village	123
A.1.3	Potato Disease Leaf Dataset (PLD)	124
A.1.4	Tea Sickness Dataset	125
A.2	Field Datasets	126
A.2.1	Cassava Leaf Disease Classification	126
A.2.2	CD&S Dataset	127
A.2.3	Cucumber Disease Recognition Dataset	128
A.2.4	DiaMOS Plant	129
A.2.5	Paddy Doctor	130
A.2.6	Plant Pathology 2020 - FGVC7	131
A.2.7	Plant Pathology 2021 - FGVC8	133
A.2.8	PDD271: Plant Disease Recognition Dataset	134
A.2.9	Strawberry Disease Detection Dataset	135
A.3	Hybrid Datasets	136
A.3.1	plantDoc	136
A.3.2	Taiwan Tomato	139
A.3.3	Potato Leaf Disease Dataset in Uncontrolled Environment	140
A.3.4	Rice Leaf Diseases Dataset	141
A.3.5	Sugarcane Leaf Dataset	143
B	Appendix Datasets	144
B.1	ResNet	144
B.2	VGG	145
B.3	ConvNeXt	146
B.4	DenseNet	147
C	Appendix Benchmark	148
D	Appendix Augmentation	176
E	Dataset Construction	182

F	Appendix PLDC-6 Datasets	185
F.1	iBean	185
F.2	Soybean	186
F.3	Classes PLDC-6	187

List of Figures

1.1	Publications per year for "deep learning AND plant leaf disease" papers based on Web of Science data in recent years.	4
2.1	The frequency of datasets used in reviewed papers.	17
2.2	Frequency of used dataset types in papers review for this work.	18
2.3	Availability of datasets newly introduced in review papers.	18
2.4	The most used model families that were used in the review papers.	19
2.5	The most used models in review work.	20
3.1	This figure explains how kernels parse over the image and extract feature maps from them.	23
3.2	Kernel operation visualized.	23
3.3	Max Pooling process explained and visualized. 2 max pooling operations are shown in this figure.	24
3.4	Flatten and Pooling visually explained.	25
3.5	A fully connected neural network classifier top.	25
3.6	Transfer-Learning method visualized	26
3.7	Bacterial Diseases	29
3.8	Examples of Viral Diseases	30
3.9	Fungal Disease Examples	30
4.1	Sample of Tomato Leaf images taken under Lab conditions from the Plant Village dataset [19].	34
4.2	Sample of Potato Leaf images taken taken in the field conditions from the novel Potato dataset [65].	35

6.1	The workflow used during benchmarking	49
7.1	The different color based data augmentation techniques used in this paper visualized. Images are taken from the novelPotato [65] dataset.	56
7.2	The noise based data augmentation technique used in this paper visualized. Images are taken from the novelPotato [65] dataset.	57
7.3	The different transformation based data augmentation techniques used in this paper visualized. Images are taken from the novelPotato [65] dataset.	58
9.1	DenseNet201's architecture before modification	68
9.2	A visual comparison of the ReLU and the SiLU/Swish activation functions.	73
9.3	Flowchart of the Channel Attention Block.	74
9.4	The proposed PLDC-Net architecture based on the DenseNet201 baseline model with a Channel Attention Block and Swish-1 SiLU activations.	75
9.5	The result graph of the frozen Transfer-Learning (TL) results on the frozen 10-90 split.	80
9.6	The result graph of the frozen TL results on the frozen 30-70 split.	81
9.7	The result graph of the frozen TL results on the frozen 50-50 split.	82
9.8	The result graph of the frozen TL results on the frozen 70-30 split.	82
9.9	The result graph of the frozen TL results on the frozen 90-10 split.	83
9.10	The result graph of the unfrozen TL results on the unfrozen 10-90 split.	85
9.11	The zoomed in result graph of the unfrozen TL results on the unfrozen 10-90 split.	86
9.12	The result graph of the unfrozen TL results on the unfrozen 30-70 split.	87
9.13	The result graph of the unfrozen TL results on the unfrozen 50-50 split.	87
9.14	The result graph of the unfrozen TL results on the unfrozen 70-30 split.	88
9.15	The zoomed in result graph of the unfrozen TL results on the unfrozen 70-30 split.	89
9.16	The result graph of the unfrozen TL results on the unfrozen 90-10 split.	90
9.17	The zoomed in result graph of the unfrozen TL results on the unfrozen 90-10 split.	90

A.1	Class Distribution of the Plant Village Dataset.	122
A.2	A sample image of each class present in the Plant Village Dataset.	122
A.3	Class Distribution of the Tomato Village Dataset.	123
A.4	A sample image of each class present in the Tomato Village Dataset.	124
A.6	A sample image of each class present in the PLD Dataset.	124
A.5	Class Distribution of the PLD Dataset.	125
A.8	A sample image of each class present in the Tea Dataset.	125
A.7	Class Distribution of the Tea Dataset.	126
A.9	Class Distribution of the Cassava Dataset.	127
A.10	A sample image of each class present in the Cassava Dataset.	127
A.11	Class Distribution of the CD&S Dataset.	128
A.12	A sample image of each class present in the CD&S Dataset.	128
A.13	Class Distribution of the Cucumber Dataset.	129
A.14	A sample image of each class present in the Cucumber Dataset.	129
A.15	Class Distribution of the diaMOS Dataset.	130
A.16	A sample image of each class present in the diaMOS Dataset.	130
A.17	Class Distribution of the Paddy Doctor Dataset.	131
A.18	A sample image of each class present in the Paddy Doctor Dataset.	131
A.19	Class Distribution of the FGVC7 Dataset.	132
A.20	A sample image of each class present in the FGVC7 Dataset.	132
A.21	Class Distribution of the FGVC8 Dataset.	133
A.22	A sample image of each class present in the FGVC8 Dataset.	133
A.23	Class Distribution of the PDD271 Dataset.	134
A.24	A sample image of each class present in the PDD271 Dataset.	135
A.25	Class Distribution of the Strawberry Dataset.	135
A.26	A sample image of each class present in the Strawberry Dataset.	136
A.27	Class Distribution of the plantDoc Dataset.	137
A.28	A sample image of each class present in the plantDoc Dataset.	138
A.29	Class Distribution of the Taiwan Tomato Dataset.	139
A.30	A sample image of each class present in the Taiwan Tomato Dataset.	140
A.31	Class Distribution of the Novel Potato Dataset.	141

A.32	A sample image of each class present in the Novel Potato Dataset.	141
A.33	Class Distribution of the RLDD Dataset.	142
A.34	A sample image of each class present in the RLDD Dataset.	142
A.35	Class Distribution of the Sugarcane Dataset.	143
A.36	A sample image of each class present in the Sugarcane Dataset.	143
B.1	A ResNet block with the residual connection. The stride in is defaulted to 1 but set to 2 if this is the first block in the layer-block. Based on TensorFlow implementation [127].	144
B.2	VGG block of convolutional layers with pooling. Based on TensorFlow implementation [127].	145
B.3	ConvNeXt block with large kernel, pointwise convolutions, GELU and residual connections. Based on TensorFlow implementation [127].	146
B.4	DenseNet block with bottleneck and dense connection connections. Based on TensorFlow implementation [127].	147
F.1	Class Distribution of the iBean Dataset.	185
F.2	A sample image of each class present in the iBean Dataset.	186
F.3	Class Distribution of the Soybean Dataset.	186
F.4	A sample image of each class present in the Soybean Dataset.	187

List of Tables

6.1	List of all the datasets considered in this benchmark with all key-metrics. . . .	46
6.2	A list of all the models that will be considered for the benchmark in this work. The metrics were obtained from the official TensorFlow implementations via the model summary [127].	47
6.3	The average performance metrics for each models averaged per dataset. All values are the 5 run average and all of the metrics are based on the test dataset, except for epochs which are taken during testing. FT stands for fine-tuned. . . .	50
6.4	This list displays the average performance metrics of each model averaged across all datasets and iterations. Again, all of the metrics are based on the test dataset, except for epochs which are taken during testing. FT stands for fine-tuned.	51
6.5	The model average accuracy rankings represent the models average accuracy across all datasets and rank them accordingly, while the average model rank takes the model rank per dataset (based on accuracy per dataset) and averages that value.	52
6.6	Model ranking comparisons (same methods as in Table 6.5), including the comparison with ViT.	53
7.1	List of methods and values for color augmentation.	55
7.2	The noise augmentation method with the values used during augmentation. . .	55
7.3	Transformation augmentation methods.	57
7.4	List of all the datasets considered in the augmentation experiments runs.	59
7.5	Models used for the augmentation experiments.	59
7.6	Datasets sizes for the different augmented datasets.	59

7.7	The average test scores of each augmentation techniques across all models and datasets.	60
7.8	The test scores for each augmentation method across all models based on the dataset.	60
8.1	List of all the datasets that are considered to be part of the new benchmarking dataset. Given are all key metrics and performance metrics from the benchmarking [125].	62
8.2	Classes that were deleted from the dataset and the reason they were.	62
8.3	Classes that were combined in order to create unique classes for the final dataset.	63
8.4	Metrics of the new dataset.	63
9.1	Constant setup during model training and evaluation across all architectures. . .	66
9.2	List of the models that were compared in the benchmark.	66
9.3	Baseline model performance comparison.	66
9.4	Model modification comparison results. Here DN201 stands for DenseNet201. The Train, Val and Test columns list the accuracy for each set.	71
9.5	The 2 datasets used to combine into PLDC-6 for TL testing.	76
9.6	Metrics of the new PLDC-6 dataset.	76
9.7	Train-Test split results for TL experiments	78
9.8	Model parameter comparison for frozen and un-frozen models.	79
9.9	The results of the frozen TL results on the frozen 10-90 split. The percentage values given are the test F-1 scores.	79
9.10	The results of the frozen TL results on the frozen 30-70 split. The percentage values given are the test F-1 scores.	80
9.11	The results of the frozen TL results on the frozen 50-50 split. The percentage values given are the test F-1 scores.	81
9.12	The results of the frozen TL results on the frozen 70-30 split. The percentage values given are the test F-1 scores.	82
9.13	The results of the frozen TL results on the frozen 90-10 split. The percentage values given are the test F-1 scores.	83

9.14	The results of the unfrozen TL results on the unfrozen 10-90 split. The percentage values given are the test F-1 scores.	85
9.15	The results of the unfrozen TL results on the unfrozen 30-70 split. The percentage values given are the test F-1 scores.	86
9.16	The results of the unfrozen TL results on the unfrozen 50-50 split. The percentage values given are the test F-1 scores.	87
9.17	The results of the unfrozen TL results on the unfrozen 70-30 split. The percentage values given are the test F-1 scores.	88
9.18	The results of the unfrozen TL results on the unfrozen 90-10 split. The percentage values given are the test F-1 scores.	89
9.19	iBean dataset used for few-shot learning.	92
9.20	The results of both models One-Shot Learning on the iBean dataset.	94
9.21	The results of both models Five-Shot Learning on the iBean dataset.	94
A.1	Information about the Plant Village Dataset.	121
A.2	Information about the Tomato Village Dataset.	123
A.3	Information about the PLD Dataset.	124
A.4	Information about the Tea Leaf Dataset.	125
A.5	Information about the Cassava Dataset.	126
A.6	Information about the CD&S Dataset.	127
A.7	Information about the Cucumber Dataset.	128
A.8	Information about the diaMOS Dataset.	129
A.9	Information about the Paddy Doctor Dataset.	130
A.10	Information about the FGVC7 Dataset.	131
A.11	Information about the FGVC8 Dataset.	133
A.12	Information about the PDD271 Dataset.	134
A.13	Information about the Strawberry Dataset.	135
A.14	Information about the plantDoc Dataset.	136
A.15	Information about the Taiwan Tomato Dataset.	139
A.16	Information about the Novel Potato Dataset.	140
A.17	Information about the RLDD Dataset.	141

A.18	Information about the Sugarcane Dataset.	143
C.1	The models rank per dataset for each combination. Column name legend: 1 = cassava, 2 = cds, 3 = cucumber, 4 = diaMos, 5 = fgvc7, 6 = fgvc8, 7 = novelPotato, 8 = paddy, 9 = pdd271, 10 = plantDoc, 11 = plantVillage, 12 = pld, 13 = rldd, 14 = sms, 15 = sugar, 16 = taiwanTomato, 17 = tea, 18 = tomatoVillage, 19 = Avg. Rank, 20 = Worst Rank, 21 = Best Rank, 22 = Avg. Rank STD.	149
C.2	All of the results obtained during benchmarking. Each of the 23 model 18 dataset combinations are given. Each row represents the 5 run average results. Results originate from [125].	150
D.1	Full results obtained during augmentation experiments. Results originate from [133].	176
F.1	Information about the iBean Dataset.	185
F.2	Information about the Soybean Dataset.	186

List of Abbreviations

BM	Base Model
CA	Channel Attention
CBAM	Convolutional Block Attention Module
CNN	Convolutional Neural Network
DL	Deep Learning
DSC	Depthwise Separable Convolution
DwC	Depthwise Convolution
FAO	Food and Agriculture Organization of the United Nations
FtC	Factorized Convolutions
FL	Federated Learning
FM	Foundational Model
FSL	Few-Shot Learning
FT	Fine-Tuning
GAN	Generative Adversarial Network
HSI	Hyperspectral Imaging
MIB	Mobile Inverted Bottleneck
ML	Machine Learning

MSP Multi-Scale Processing
OSL One-Shot Learning
PwC Pointwise Convolution
RL Reinforcement Learning
SA Spatial Attention
SE Squeeze & Excitation
SVM Support Vector Machine
TL Transfer-Learning
UAV Unmanned Aerial Vehicle
ViT Vision Transformer

List of Terms

Base Model A pre-trained model that can be used as a baseline to be trained on a new dataset, allowing the model to benefit from the pre-trained weights and learn faster and more robust.

Channel Attention An attention mechanism for Convolutional Neural Network (CNN) models that operates on the channel axis. This method uses Global Average Pooling and Global Max Pooling, before feeding them into separate Autoencoders, adding the results and creating importance weights via sigmoid to weigh channel by their importance.

Convolutional Block Attention Module This block combines Channel Attention (CA) and Spatial Attention (SA) by stacking them on top of each other, CA first then SA. This allows the Convolutional Block Attention Module (CBAM) to identify the importance of feature maps across the channel axis as well as the width and height dimensions.

Convolutional Neural Network A Deep Learning Model type that is commonly used for image data, as it uses spatially aware and parameter efficient filters to iterate over the pixels.

Deep Learning A Machine Learning method that uses Deep Neural Networks to learn. Deep Learning models can handle large and high dimensional data and generalize upon it. These models can also handle numerous tasks, from simple classification and clustering, to fully generative models that can produce high quality imagery for example.

Depthwise Convolution Depthwise convolutions are a type of convolutional layer that applies a filter to only 1 channel at a time. While regular 2D convolution kernels are as deep as the input layer, Depthwise Convolution (DwC) are only 1 channel deep and only applied to one. These layers are often followed by Pointwise Convolution (PwC).

Depthwise Separable Convolution Depthwise Separable Convolution combine the ideas of Depthwise Convolution and Pointwise Convolution by stacking them on top of each other. Like this, they form a parameter efficient alternative to regular convolutions, that still consider information across height, width, and channels by combining DwC (height and width) and PwC (channel).

Factorized Convolutions A convolutional method that splits convolutional kernels into two 1D kernels instead of a 2D kernel when considering a single channel. A 3x3 kernel would for example be replaced by a 3x1 and a 1x3 kernel. This is done to reduce parameter count.

Federated Learning A Distributed Methodology to Deep Learning. It uses decentralized data which provides high security and privacy. Local models get trained on local data and are then aggregated on a central server to a global model and redistributed.

Few-Shot Learning A way of domain adaptation using limited data per class to generate class embeddings, which can then be used to compare to future test images and predict classes. No backpropagation is needed, embeddings are generated in forward runs after the global average pooling layer.

Fine-Tuning Fine-Tuning refers to the process of Transfer-Learning with un-frozen weights. This can be carried out on its own, but also often sees application after frozen TL has already concluded.

Food and Agriculture Organization of the United Nations The United Nations agency tasked with defeating world hunger and improving food security.

Foundational Model A large scale Deep Learning (DL) model with a large number of parameter that was trained on a large scale dataset. Foundational Models are often used for TL tasks.

Generative Adversarial Network A Generative Adversarial Network is a generative DL method that train a generator network that generates synthetic images and a discriminator network that is trained to classify these generated images against a real dataset, which leads

to both networks competing, through which the generator will be able to generate images that are almost indistinguishable from the dataset.

Hyperspectral Imaging Hyperspectral Imaging describes the imaging process in which hundreds of wavelengths (in the visible and near-infrared spectrum) are captured and stored for each pixel (unlike the usual three (RGB) in regular photography). These extra channels contain a lot of extra information, especially relevant in the field of plant diseases.

Machine Learning Statistical Methods or Algorithms that allow computers to learn without implicit instructions from data in a way that generalizes to before unseen data.

Mobile Inverted Bottleneck A DL method used in CNN that uses PwC to inflate the number of channels, before using a a depthwise separable block of DwC followed by PwC.

Multi-Scale Processing A DL method used in CNN where different sized kernels are present in an architecture, often in parallel, to observe the image and its features at different scales and receptive fields.

One-Shot Learning A method for domain adaptation using extremely limited data, with only 1 image per class to generate class embeddings, which are then used to compare to future test image embeddings to predict classes. No backpropagation is needed, embeddings are generated in forward runs after the global average pooling layer and remebered by the model.

Pointwise Convolution A convolutional layer method where the kernel is of size 1x1 but parses over each channel. Often used to either bottleneck CNN, re-arrange channel features, or after DwC to take into account information across channels.

Reinforcement Learning A branch of deep learning. Reinforcement Learning (RL) agents are not instructed how to operate, but are rather given an objective through a reward function that they need to optimize by choosing actions based on the state and rewards that influence the environment to reach said goal.

Spatial Attention Spatial Attention is a attention mechanisms that focuses on spatial features on the dimensions of width and height. To do that it uses Max Pooling reduction and

Average Pooling reduction across all channel to condense them to 1 channel each, before a sigmoid activated convolutional layer estimates importance weights for each pixel that will be multiplied to the features maps.

Squeeze & Excitation Squeeze & Excitation is a attention block that operates on the channel dimension. It uses Global Average Pooling to reduce the channels to one value per channel, before using an Autoencoder setup to reduce layers to their essential information and then a sigmoid layer to rank layers by importance.

Support Vector Machine A Support Vector Machine is a Machine Learning method that classifies data by optimizing a line or hyperplane in an N-dimensional space, by maximizing the distance between the classes.

Transfer-Learning Transfer-Learning is a Deep Learning technology, often used with image data and CNN, in which a pre-trained network architecture and its weights are downloaded and then applied to train a model using said weights to learn on a new and different dataset. Often this refers to training with frozen CNN weights.

Unmanned Aerial Vehicle A Unmanned Aerial Vehicle is a type of aircraft that is capable of flying without an pilot on board. Unmanned Aerial Vehicle are often either controlled through remote control or even capable of autonomous flight. Unmanned Aerial Vehicle can be drones (quadrotor, multi-rotor), helicopters or fixed-wing aircraft.

Vision Transformer A Vision Transformer is a DL model for vision tasks based on the idea of transformers, which utilize multi-head attention. ViT comply with that idea by embedding images into patches which can then be turned into vectors that work well with transformers.

Developing a Strong Pre-Trained Base Model for Plant Leaf Disease Classification

David Jona Richter

Department of Artificial Intelligence Convergence

Graduate School, Chonnam National University

Supervised by Professor Kyungbaek Kim

(Abstract)

Plants, crops and their yields are essential to our very existence. Our society heavily relies on agriculture and farmers for food, but diseases and pests cause large losses every year. As such it is vital to ensure that diseases can be spotted early and treated accordingly and stopping the spread while still possible. Manual and traditional methods require knowledgeable personal to walk through the field and check for symptoms "by hand" or using laboratory equipment such as microscopes to analyze the plants for diseases. This is, obviously, very laborious and very time consuming and also requires trained manpower. This resulted in the desire and need to automate this process. Machine Learning (ML) methods have been applied as a result and they have garnered promising results, but ML has its shortcomings. It needs researchers to extract features from the data, especially for image data (regular images, multispectral images, and hyperspectral images alike). Deep Learning (DL) methods can not only overcome said problem, but also tend to perform better than traditional ML. Convolutional Neural Network (CNN) models are especially efficient as they can automatically extract features from images without any manual feature construction before then feeding the features to a classifier (both ML or DL). Many different DL models have since been proposed and tested to identify plant diseases to varying degrees of success, most of them being CNN architectures using image data as input. CNN, and all other DL methods, require large amounts of data to train properly, making

datasets largely influential to the final performance of the model. Despite the importance that datasets pose to the field, there still seems to be somewhat of a discrepancy between what is publicly available for use and what would be required to sufficiently train fully capable models. To overcome these shortcomings, as part of this thesis open datasets for the field of plant leaf disease classification have been identified as well as models that can be trained on them and extensive benchmarks have been carried out to identify their suitability. Then a new dataset was constructed based on those findings as well as on the findings of a augmentation applicability study, which will be used to train a new Base Model based on the DenseNet201 architecture, which managed to outperform the baseline model on said new dataset as well as outperforming it on plant leaf disease classification domain specific Transfer-Learning experiments on another new dataset. This new model manages to train models through Transfer-Learning (TL) faster, more robust, more stable, and with less data than general Foundational Model (FM) would, overcoming a large number of issues that the field still suffers from.

Keywords: Deep Learning; Convolutional Neural Networks; Plant Pathology; Plant Leaf Disease Classification; Plant Disease

1. Introduction and Motivation

1.1 Introduction

One of the most important issues that still very much impacts humankind, even to this day, is hunger. Not only is the problem still relevant today, it also trending in the wrong direction, with recent reports projecting that world hunger will only worsen [1]. These reports by the Food and Agriculture Organization of the United Nations (FAO) have reported an increase of 7.5% to 9.1% of to the number of people suffering from undernourishment worldwide in only a 5 year span from 2019 to 2024 [1]. These numbers correlate to about 750 million people that were affected by undernourishment in 2023 with the trends only increasing. While world-wide the numbers currently measure in at the afore mentioned 9.1%, regional number are much mire dire in certain parts of the world, with Africa having a 20.4% share of the population that is affected [1]. On top of that, the recent COVID-19 pandemic also negatively impacted this trend and contributed to another 130 million potentially being subject to undernourishment [1]. So while many people in developed countries might not feel it first hand, hunger, to this day, remains a problem affecting hundreds of millions of people world-wide and therefore deserves and requires attention to solving it.

Crops play a pivotal role in that. Crops, according to the Food and Agriculture Organization of the United Nations (FAO), contribute heavily to the food supply of humans everywhere. Plant based products (cereals, fats and oils, sugar, fruit and vegetables, roots, tubers and pulses) are the biggest source of calorie consumption with over 80% while also being responsible for about 60% of the protein supply [2] with numbers being even more significant in Africa (nearly 80% of proteins and over 90% of calories). Crop production has increased by over 50% between 2000 and 2021 [2] and is expected to further increase by another 50% from its 2012 numbers to 2050. All this proves how pivotal and important agriculture, crop production and and its yields

are to food security world-wide and how important it is to make sure that crop production remains as efficient and reliable as possible.

FAO reports, however, showcase that about 40% of planted crops are lost to some kind of pests or diseases every year [3]. With prognoses of diseases continuously spreading to new locations, the impact of diseases and the resulting losses are likely to increase [3]. Plant disease pandemics are also said to be increasingly more likely to spread and be more severe than in the past [4]. To try and limit the impact felt by disease infections to the planted crops, detecting them early is of high importance [5]. Because of this accurate, fast and reliable detection of plant diseases is becoming more and more important. Field disease monitoring is traditionally carried out manually through field scouting [6], where trained staff would go out into the field where the crop seeds have been sown, to check the plants for signs of diseases. Staff needs to be well trained to make sure they can properly identify the symptoms accurately and in a timely manner to prevent negative results [7], and since plants need to be checked periodically, multiple times during the growing stages [8], the whole process is rather laborious.

One way of accelerating this process is through the application of Deep Learning (DL) models. Image classification models can be utilized to identify whether or not plants are infected and if they are they can classify what disease they are infected with [9, 10, 11, 12, 13]. Through advances in computer imaging and computer vision, new methods are becoming increasingly stronger and more capable of handling tasks such as this one. Recent years have brought forth better and more advanced models that exceed in the field of categorizing images into their respective classes. Complex models such as that do, however, rely on high quality datasets that are: big enough, diverse enough, high resolution, and representative of the task that they are supposed to be trained for.

Such datasets are, however, sparse and especially in the field of plant leaf disease detection ideal datasets are not a given [14, 11]. The most popular dataset, PlantVillage, is a lab dataset taken in ideal conditions, which tends to train models that are not as capable when used in field [15]. PlantVillage being this popular is understandable, considering that not everyone has the opportunity to create their own dataset, and even if they do, doing so is very time consuming. On top of that, PlantVillage comes with over 50,000 images and with 38 classes including multiple plants and multiple diseases per plant. All images are of high quality and so is the dataset as a whole. The only downside one can bring up is that it is taken in lab.

Most new datasets collected by researchers are kept private (not open to access by the public) [10], further amplifying this limitation currently faced in the field. With most researchers using PlantVillage as the dataset in their work (see Figure 2.1), a certain level of comparability is available across studies (although many studies only use subsets). However, with PlantVillage being a lab dataset and therefore rather easy for DL models and CNN to learn, most models achieve very high scores, making said comparability somewhat tricky, since all models score incredibly well. This means that even weaker models will perform well on this data and that most models only differentiate themselves from each other by very small margins.

To improve the current state of plant leaf disease classification using DL methods, in this thesis a number of open datasets and powerful CNN models have been identified and underwent an extensive set of benchmarking experiments in order to identify the validity of each model and dataset for this specific field. Based on the findings of this benchmark, along with findings of another set of experiments to identify the applicability of image augmentation methods for plant leaf classification task (to overcome the issue of limited data availability), a new dataset was constructed. This new dataset, which was built by choosing 9 pre-existing datasets, now has 80 classes across 25 different plants with over 300,000 images (of which 280,000 are used for training and validation and are augmented, and 24,507 are un-augmented test images). This dataset is perfectly balanced on the training side with each class having exactly 3,500 images per class before train-val splitting. This dataset was then used to train the best performing models (according to the benchmarks) to find the most powerful model available and improve upon it to create a new Base Model (BM) specifically for this field. The model chosen as a baseline was DenseNet201, which was improved upon by adding advanced activation functions as well as adding Channel Attention (CA) mechanisms to it. Lastly, this new pre-trained architecture was compared to a ImageNet pre-trained DenseNet201 to showcase the validity, need, and power of this new Base Model.

FM are large scale models trained on a large scale datasets that can then be used as BM to train (using Transfer-Learning (TL)) new models in related, or unrelated areas [16]. A new and domain-related Base Model, a model trained on data that is domain-specific or at least domain-related data, comes with many benefits, as it can generate potentially better Transfer-Learning models, do that faster, less computationally expensive and in a more robust manner [17]. The resulting model manages to outperform general FM in a TL task significantly, performing better

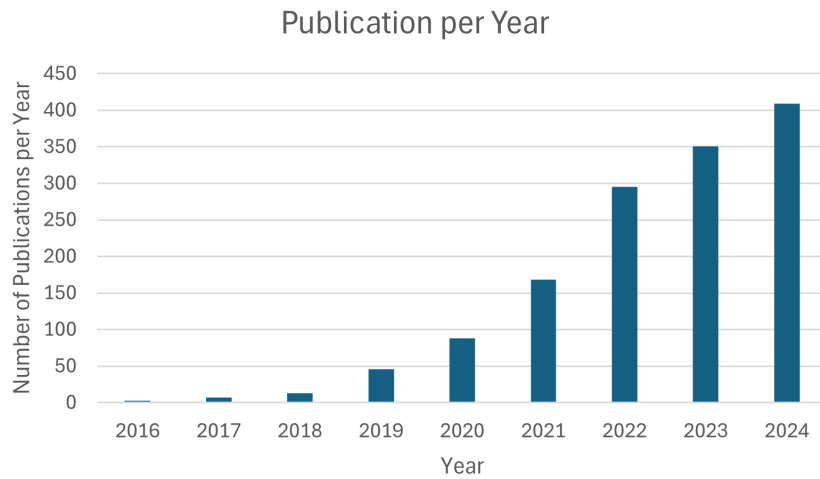


Figure 1.1: Publications per year for "deep learning AND plant leaf disease" papers based on Web of Science data in recent years.

while also being faster, more stable, more robust, and also capable of learning robust features on significantly less data. This proves that the idea of designing, creating, training and using a domain informed Federated Learning (FL) model for the field of plant leaf disease classification is a step that can be immensely helpful and that the methods proposed in this thesis manage to perform well and as a result manage to overcome many of the issues this field currently faces, when compared to current methods.

As part of this thesis, the following contributions were made to the field of plant leaf disease classification using DL techniques.

- Current literature of using CNN FM for plant leaf disease classification is reviewed
- Open and relevant datasets were collected, introduced, described and analyzed
- Current image classification CNN FM are introduced, explained, and analyzed
- These datasets and models are benchmarked in a extensive set of experiments and the results are analyzed
- Using the benchmarking results, the best performing models and datasets are identified
- Augmentation methods to improve plant leaf disease classification datasets to better perform are tested

- Based on the models identified in the benchmark and the augmentation techniques a new large scale dataset is created
- A new model is constructed based on DenseNet201 (which performed well in benchmarks) that outperforms baseline models
- That model is trained on the newly constructed dataset to create a new plant leaf disease classification field specific BM
- That new BM is compared to a baseline FM in a TL experiments on a different plant leaf disease dataset with unseen classes

The rest of this thesis is structured as follows: First the current literature in the field of plant leaf disease classification will be reviewed to identify current trends, best practices, and weaknesses in Chapter 2. Chapter 3 will explain basic methods and technologies relating to both Deep Learning (DL) techniques with a focus on Convolutional Neural Network (CNN) and also looks at plant leaf disease classification in relation with DL. Chapter 4 will introduce current open plant leaf disease datasets and quantify them for better understanding, comparison, and for later usage in building a large scale dataset for training a new model. Chapter 5 introduces and explains foundational CNN models found frequently in current literature. These models will be used in the benchmark to study their applicability in the field and to use them as a baseline for improvements. Chapter 6 explains the methodology used to run the benchmarking experiments and analyzes the results, showcasing how different models and datasets are more or less suited to be applied to the field of plant leaf disease classification. In Chapter 7 different augmentation techniques will be tested to see if they can be beneficial to not only overcome the low number of data availability, but if they can also improve performance. Next, in Chapter 8 the new dataset used to train the Foundational Model will be presented and explained, along with the requirements to recreate that dataset. Then, in Chapter 9, the architecture of the new DenseNet201 based model will be presented along with the experimental results validating it (as well as results with other architectures that were considered), before exposing the now pre-trained model to new data to test it for TL capabilities, comparing it to a DenseNet201 that is pretrained on ImageNet data. Chapter 10 discusses the results and findings obtained in the making of this thesis. In the next chapter, Chapter 11, possible future directions

will be presented and discussed, before Chapter 12 concludes this work. The appendices offer additional information and results corresponding to the related chapters.

2. Literature Review

This chapter will review relevant review papers for the field of plant leaf disease classification, as well as a few papers that use distributed methods and also numerous papers that are focusing on CNN TL approaches for plant leaf disease classification.

2.1 Previous Work

In this section previous work will be summarized and then analyzed. A more extensive review can be found in [18]. The review in this thesis is based upon said referenced review.

2.1.1 Literature Review Papers

The survey paper by Demilie [13] summarizes a large number of papers in the field of plant disease detection using both ML and DL methods. The paper showcased that this field experienced a huge uptick in publications starting in 2019. In this work the author found that DL methods generally outperformed ML methods, but it was noted that a hybrid using a CNN as a feature extractor and then a ML method as a classifier, Support Vector Machine (SVM) for example also performs well. Most papers managed to achieve scores of 95% and more, with various modern and advanced CNN models being among the best performing models (some of which used Transfer-Learning). As for plants, tomato plants and their diseases are by far the most researched plants (around 39% of the surveyed papers) with rice plants being the second most popular (16%). Additionally, it was found that most of the surveyed studies used the PlantVillage [19] dataset, due to its availability and size. The dataset is, however, created under lab conditions, and future work would benefit from a dataset recorded in field.

Nagaraju et al. [9] discuss papers published between 2015 and 2019 in their review, with a focus on Hyperspectral Imaging (HSI). A total of roughly 80 papers were introduced in

the review and among them were many papers that also introduced datasets. Here too it was brought up that networks using the CNN methodology are the most powerful networks (and applicable to many different plant types) for image based plant leaf disease detection and that CNN SVM hybrid models also perform well. Image pre-processing is also discussed in the form of mainly image resizing. It is noted that 60x60 pixels, 96x96 pixels, 128x128 pixels and 256x256 pixels are the most commonly used sizes.

Li et al. [10] review Deep Learning for plant disease detection and classification in their work. The authors state that most symptoms are visible on the leaf, which is why researchers often use leaf images as input for their models. They also argue that the switch from ML to DL can be attributed to ever larger datasets, more and more powerful computers and graphics cards, and ever better and more functional code libraries for DL. This paper puts a focus on TL and on working with small sample datasets, where methods like Few-Shot Learning are well suited and often applied, which allow the model to train with very small training data. When discussing data augmentation the authors note that color should not be changed when using traditional augmentation, but also mention the power and validity of Generative Adversarial Network (GAN). Visualization methods were also compiled and presented, as were full disease recognition systems and HSI (which are well suited for early disease detection).

Lu et al. [11] summarize DL for the use in plant disease classification task. The paper lists common fungal, bacterial and viral infections for a set of common plants. According to the authors, the major disadvantages that traditional ML methods pose are: low performance, lack of data, manual feature extraction, and that plants are separated from their roots to be classified. problems that DL does not suffer from. The paper discusses several classification networks in detail, listing their architecture, pros, cons, novel aspects and other interesting details. Other facts are also disclosed, such as the fact that making CNNs deeper only works until a certain depth, at which the network will not benefit from the additional layers, but rather suffers from them in the form of slower training. This paper also intensively covers augmentation methods. As for evaluation metrics, the author note the popularity of accuracy across the field. The main issues of DL in plant disease identification are the lack of data, especially data taken in the field as data taken in the lab does not tend to generalize well to real field conditions. With PlantVillage, a dataset with lab condition images, being the biggest publicly available dataset, and most in field datasets being closed source or too small, there is a lack for a sufficiently

sized in-field dataset. In cases where the background of an image is too busy, segmenting images first in an effort to detach the leaf from the background could be useful. The paper also explains various factors that impact the disease symptoms, those being: the stage the disease is in, whether or not the plant is affected by multiple diseases whose symptoms would then impact each other, as well as extrinsic factors such as humidity, temperature, soil conditions, sunlight and wind.

Sarkar et al. [12] summarize the field of DL for plant leaf disease identification from 2010 to 2022. The paper goes in depth on the root causes to many different plant diseases for many different plants. It also covers different types of noise and how they impact the performance. The paper also offers many different graphs and statistics analyzing previous publications and also provides an in-depth overview over many different ML and DL algorithms alongside their strengths and weaknesses. One method mentioned specifically is TL, as it outperforms many models that are trained from scratch. One interesting point brought up by the authors is the fact that climate change has an impact on plant leaf diseases as the change in temperature accelerates infection rates. Another topic that is covered in depth in this work is the explanation of more advanced image pre-processing techniques such as Sobel edge detection, CIELAB, top-hat transformations, and more. On top of that it also covers a number of different data augmentation methods as well as methods for image segmentation. Additionally feature selection and extraction is also included. Different classification methods are also explained, ranging from traditional ML to more modern DL methods. The paper also mentions the current interest in hybrid and ensemble methods.

2.1.2 Using Distributed Methods

In [20] Mamba et al. present their findings following a set of experiments for crop disease detection using Federated Learning (FL) methods on the PlantVillage dataset [19]. The authors set out to compare and contextualize how different approaches, that are common outside the FL scope, perform once they are applied with FL. They ran a multitude of experiments, in which they iterated over: the dataset (different plant types with different amounts of diseases/classes), the communication rounds, the local agent's epochs and the number of clients. When iterating over the number of agents (3, 5, 7), they found that less agents (3) performed better than when adding more, this was partially due to the fact that the overall amount of data remained the

same. So once there were more agents data had to be split into smaller subsets. ResNet [21] (or ResNet50 to be specific) did the best, with MobileNet [22] (MobileNet-v2) not being far off while being a much smaller model. When iterating over the number of communication rounds (10, 30, 50, 100) ResNet again performed best (with MobileNet again doing very well too), while some models did best with 30 while other models tended to do better with more rounds. The local epoch experiment (1, 5) showed that more local epochs improved performance with ResNet and MobileNet yet again standing out. The Dataset experiment showed that the models performed differently on different set, with grapes being the easiest and tomatoes being the toughest (tomatoes have more classes than the rest). Overall this has shown that ResNet and MobileNet translate the best to Federated Learning in this case and that it is important to consider communication rounds, local epochs, number of agents and dataset carefully as they all impact the performance of the models.

Mehta et al. apply Federated Learning to predict wheat disease severeness [23]. A CNN was used that took 256x256 pixel Greyscale images as input, that were normalized to be in the range of 0 to 1. After applying data augmentation on the collected image dataset (spinning and turning) the set contained 9,967 images of which 1,000 were used for validation with the remaining 8,967 making up the training set. The dataset contained 5 diseases and therefore 5 classes, with those being leaf rust, Fusarium head blight, wheat stripe mosaic virus, powdery mildew, and Septoria leaf blotch. The global model converged at around 90% accuracy, although the paper fails to explain how the severity is actually being calculated or applied to the model. Hyperparameters as well as the model architecture are also not included in the paper.

In [24], Dhiman et al. train a novel DL model (a VGGNet model with Transfer-Learning (TL)) to predict the disease severity of citrus fruits. Here the fruit itself, post harvesting, is analyzed, not the plant it grew on. The image data was gathered from publicly available datasets (PlantVillage, Kaggle) and was then annotated by an expert (horticulture scientist). The expert used only exterior features such as size, color and shape, not considering internal features. The resulting dataset contains bounding boxes for any imperfections that state the severity (healthy, low, medium, high) of said imperfection and it consists of about 4,000 annotated images.

[25] explores the application of Unmanned Aerial Vehicle (UAV) in combination with FL for pest detection. The experiment conducted here was carried out at 4 different sites (4 clients), where each site had a UAV setup that carried out real-time pest analysis. The model is capable

of detecting pest such as mosquito's, grasshoppers, sawflies, mites and beetles, among others. A total of 9 pest classes was present in the dataset. Data would be collected on site by the UAV in the proposed method, but for this work data was collected via Kaggle and Google image search queues and then pre-processed (resized) and augmented (mirroring and rotation) which resulted in a dataset in 5,400 images overall. This data was then used for training on an EfficientNetB3 architecture. The proposed methodology outperformed previous works and reached a accuracy score of 99.55% according to the authors.

Idoje et al. also utilize Federated Learning in [26]. In this paper the objective of the FL model is the classify the crop types in smart farm environments. One big difference here is that the data is tabular climatic data (rainfall, potential of Hydrogen (pH), humidity and temperature) as opposed to image data. The federated learning model was tested across different optimizes (Adam and SGD). The models using SGD did not perform well and the model using Adam with a rather large starting learning rate also failed to reach high accuracy. The model using Adam and a smaller stating learning rate of 0.001 however managed to reach 90%.

2.1.3 Transfer-Learning CNN

Hammou et al. [27] use DenseNet169 and InceptionV3 on the PlantVillage dataset, using only the classes that were dedicated to tomato plant leaves. This resulted in a subset of roughly 18,000 imaes across 10 tomato leaf classes. Both models were pretrained on the ImageNet dataset. The models were trained for 100 epochs and both models managed 100% accuracy.

Tej et al. [28] implemented ResNet50 as well as ResNet152 in their study. Said study introduces a new dataset which was collected by the authors in Tunisia. The dataset contains tomato and pepper images and totals 488 images, which were the augmented (using rotation, brightness, contrast, saturation, flip, gaussian blur) to increase the dataset to 8,400 images, belonging to 7 classes (1,200 each). The trained models (after 100 epochs) managed scores of: 92.7% / 83.3% (ResNet50) and 98.85% / 92% (ResNet152) with the first value being the augmented data and the second one being trained without the augmented data.

Nagi et al. [29] made use of MobileNet, AlexNet, VGG16, and VGG19 in their study, in which they trained all 4 models on the PlantVillage dataset. They did, however, not use all classes, but rather only classes that contained grape plant images. As such, the final dataset contained 4 classes and 3,423 images. After training for 30 epochs the AlexNet reached roughly

95.5%, VGG16 managed roughly 97%, VGG19 managed roughly 97.5%, and MobileNet reached roughly 98%.

Li et al. [30] use RegNet, ShuffleNet, MobileNetV3, and EfficientNet-B0 in their work, training them on an apple plant leaf dataset that they themselves collected in China. The dataset consists of 5 classes with 2,141 images before augmentation (rotation, translation, brightness, scaling). ShuffleNet (90.2%), MobileNetV3 (93.4%), and EfficientNet-B0 (94.3%) managed their highest accuracy with the Adam optimizer, while RegNet managed its best score (99.9%) with Ranger (Adam 99.8%).

Naik et al. [31] compared a large number of models, namely AlexNet, DarkNet53, DenseNet201, EfficientNet-B0, InceptionV3, MobileNetV2, NasNetLarge, ResNet101, ShuffleNet, SqueezeNet, VGG19, and XceptionNet. The dataset used in this study was collected by the authors in India. It contains chili leaf images which make up 5,100 images in 6 classes. Training was carried out for 30 epochs and the resulting models managed: AlexNet 97.65%, DarkNet53 98.82%, DenseNet201 97.84%, Efficient-B0 97.55%, Inceptionv3 96.86%, MobileNetV2 97.35%, NasNetLarge 96.18%, ResNet101 97.55%, ShuffleNet 97.45%, SqueezeNet 97.35%, VGG19 97.84%, and XceptionNet 98.63% on the augmented dataset (rotation, brightness, contrast, saturation, flip, gaussian blur).

Pradhan et al. [32] made use of DenseNet201, DenseNet169, InceptionV3, InceptionResNetV2, MobileNet, MobileNetV2, ResNet50, VGG16, VGG19, and Xception in their work and train the models on the PlantVillage dataset apple classes (2,537 images in 4 classes). Models were trained for 30 epochs and managed 98.75% (DenseNet201), 97.52% (DenseNet169), 94.87% (InceptionV3), 95.27% (InceptionResNetV2), 98.66% (MobileNet), 98.29% (MobileNetV2), 74.29% (ResNet50), 98.26% (VGG16), 97.00% (VGG19), and 95.11% (Xception).

Reda et al. [33] focus on smaller and more lightweight models in MobileNet, MobileNetV2, NasNetMobile, and EfficientNetB0. The dataset of choice in this paper was again PlantVillage. In this case PlantVillage was not cut to a subset, but rather used over 60,000 images belonging to 39 classes. Training was carried out for a total of 30 epochs, after which the EfficientNetB0 without any frozen layers achieved over 99%, which made it the best performing model.

Mafukidze et al. [34] use InceptionV3, DenseNet121, DenseNet201, MobileNetV2, VGG16, EfficientNetB0, ResNet50, and LeNet to classify the 4 maize classes of the augmented PlantVillage dataset. Through shearing, rotation, flipping, saturation changes, mean filtering, and crop-

ping the dataset was enlarged from 4,188 to 46,898 images. After 500 epochs, the models managed 99% accuracy, except for LeNet, which reached 94%.

Latif et al. [35] utilize GoogleNet, VGG16, VGG19, DenseNet201, and AlexNet to then train them on a rice leaf dataset that they obtained from Kaggle. 2,164 images were originally included in the dataset which was then enlarged via augmentation methods. GoogleNet managed 89.63%, VGG16 95.62%, VGG19 96.08%, DenseNet201 94.24%, and AlexNet reached 92.63%.

Bruno et al. [36] use different EfficientNet architectures (B0 to B7) to categorize 39 classes of PlantVillage data. Augmentation was not applied in this work and the training was concluded after the early stopping callback with patience determined that the model had converged.

Eunice et al. [37] opted for 4 separate pretrained CNN models (DenseNet121, ResNet50, VGG16, and InceptionV4) for their experiments. The dataset used was PlantVillage, again. 38 classes with 54,305 images were used in this work and the dataset was also exposed to augmentation. The models were trained for 30 epochs, which led to 99.78% (InceptionV4), 84.27 (VGG16), 99.82 (ResNet50), and 99.87% (DenseNet121).

Albahli et al. [38] implemented AlexNet, VGG19, InceptionV3, ResNet50, DenseNet201, MobileNetV2, EfficientNet, and EfficientNetV2 to train them on 3 datasets, those being PlantVillage, PlantDoc, and CD&S. The datasets were filtered to only include corn classes and augmented with rotation, flipping, translation, scaling, and color jittering. As a result of that the final dataset spanned 8,231 images across 5 classes. The models were trained for a baseline of 25 epochs, but with early stopping (patience 10) enabled. Results show test accuracies of 87.12% (AlexNet), 90.34% (VGG19), 92.82% (InceptionV3), 87.58% (ResNet50), 94.17% (DenseNet201), 84.38% (MobileNetV2), 93.52% (EfficientNet), and 94.37% (EfficientNetV2).

Novtahaning et al. [39] tested EfficientNet-B0, ResNet152, VGG16, InceptionV3, Xception, MobileNetV2, DenseNet 201, InceptionResNetV2, and NasNetMobile to then build and ensemble a model from among them. A open coffee plant leaf image dataset from Kaggle was used for training which included 6 classes of 260 images each (1,300 total images). Training was carried out for 30 epochs after which VGG16 reached 94.2%, InceptionV3 83.9%, ResNet152 93.8%, Xception 85.4%, MobileNetV2 74.6%, DenseNet201 83.8 InceptionResNetV2 86.9%, NASNetMobile 83.8, and EfficientNet-B0 95.0%, all using the Adam optimizer. Due to these results the authors decided to build an ensemble network using EfficientNet-B0,

ResNet152, and VGG16.

Alirezazadeh et al. [40] use the DiaMos pear leaf dataset in their work to train EfficientNetB0, MobileNetV2, ResNet50, InceptionV3, and VGG19 in combination with CBAM. The dataset, augmented with mirroring, rotation, and color variation, contained 4 classes and 3,006 images and the models were trained on it for 100 epochs. The results (ResNet50: 69.90%, ResNet50+CBAM: 71.36%, VGG19: 73.09%, VGG19+CBAM: 73.42%, InceptionV3: 76.62%, InceptionV3+CBAM: 77.87%, MobileNetV2: 82.06%, MobileNetV2+CBAM: 83.99%, EfficientNetB0: 85.82%, EfficientNetB0+CBAM: 86.89%) that the CBAM block managed to increase performance for all models.

Fulle et al. [41] train MobileNetV3-Small, NASNetMobile, MobileNetV2, and DenseNet121 on a dataset which the authors themselves collected in field in Ethiopia and then shared online. The dataset is a Enset plant leaf dataset consisting of 2 classes and 1,228 images before augmentation which were enhanced to a total of 7,580 after augmentation (shearing, flipping, and brightness changes). The models were in training for 30 epochs and the performed with test accuracies of 76.68% (NASNetMobile), 94.33% (MobileNetV2), 99.28% (DenseNet121), and 99.93% (MobileNetV3-Small).

Mavaddat et al. [42] make use of the VGG16, InceptionV3 and Resnet152v2 models and train them on an open rice leaf dataset. The dataset is made up of 5,932 images in 4 classes. The 3 models were trained for 30 epochs each and achieved 100% after the application of Fine-Tuning (FT).

Paiva et al. [43] present a large scale comparison of 12 different models on the iCassava dataset. VGG16, VGG19, ResNet50, ResNet50V2, ResNet101V2, ResNet152V2, InceptionV3, InceptionResNetV2, MobileNetV2, DenseNet121, DenseNet169, and DenseNet201 were chosen to be the model being compared in this study. The cassava leaf dataset was augmented before training by applying rotations, brightness adjustments, zooming, and flipping. The resulting set has 5 classes and 21,397 images. 20 epochs were set for training with early stopping with the patience set to 7. The results were: VGG16 with 60.63%, VGG19 with 62.90%, ResNet50 with 73.46%, ResNet50V2 with 72.34%, ResNet101V2 with 71.64%, ResNet152V2 with 70.14%, InceptionV3 with 69.91%, InceptionResNetV2 with 69.67%, MobileNetV2 with 71.17%, DenseNet121 with 73.27%, DenseNet169 with 74.77%, and DenseNet201 with 70.84%.

Mohapatra et al. [44] make use of AlexNet in combination with a rice plant leaf disease dataset from Kaggle. The dataset contains 3 classes with 1,732 images and AlexNet will be trained on it for 50 epochs after which it managed 98.80%.

Diker et al. [45] combine pretrained ResNet101 and MobileNet with ML classifiers like Random Forrest (RF) and SVM, as well as also using regular neural networks as classifiers. The dataset used here is a dataset that was collected by the authors and they decided to make it public for further use. The images were collected in turkey and are of olive tree plant leaves. Classes are set to be 2 (healthy and unhealthy) and the dataset accounts for a total of 954 images. The best performing combination was achieved using ResNet101 with k-fold set to 10, and while using SVM as the classifier, where the model managed to reach 98.63%.

Lanjewar et al. [46] use a Kaggle dataset for potato plant leaf diseases with NASNetMobile, VGG19, and DensNet169, ResNet50V2, InceptionV3, and Xception. The 1,500 image dataset was augmented through rotation and flipping and it contains 3 classes. The resulting models managed, on the test set, 95.33% (NASNet), 95.67% (VGG19), 99.67% (DenseNet169), 97.00% (ResNet50V2), 97.00% (InceptionV3), 96.00% (Xception) after 100 epochs of training.

Ramya et al. [47] use AlexNet on a dataset combined from different online sources. The dataset was augmented which resulted in 22,411 images across 10 classes. Training was only carried out for 15 epochs, after which the model managed an accuracy score of 99.7% on the validation dataset.

Shaheed et al. [48] apply the PlantVillage dataset to ResNet50, VGG16, Xception, and InceptionV3. PlantVillage was reduced to only include 3 classes, those being of potato images, and the dataset was augmented with rotating, shearing, and shifting images after augmentation. 100 epochs were set to be the training period and the best pretrained model (Xception) ended on accuracy score of 98.84%.

An et al. [49] also uses AlexNet as the model of choice selected for training in their paper. In this paper, however, the dataset was reduced to include only classes containing corn images. As such, the final dataset was made up of 4 classes totaling 2,013 images (augmentation was applied). Training was carried out over 20 epochs after which the model ended up with 95.7% using SGD and 95% using Adam.

Salam et al. [50] opted to use MobileNetV3Small, ResNet50, and VGG19 for the research.

The mulberry leaf dataset used was one that was collected by the authors in field in Bangladesh. The dataset was increased from 1,091 images to 6,000 images post augmentation (rotating, flipping, transformations, translation, zoom). Results show that MobileNet reached an average of 92.5% on 5 folds k-fold, VGG19 reached 90.89% and ResNet50 achieved 94.4%.

Bania et al. [51] use ResNet101 and a potato leaf dataset with 3 classes and 2,152 images after augmentation (flipping, rotation, and translation). The resulting model performed with 95.13%.

Hang et al. [52] utilized Xception, MobileNetV2, NASNetMobile, and MobileNet to train them on their own dataset, which was captured in China. It contains soybean images and was enhanced using CycleGan. CycleGan generated synthetic images that increased the dataset size from 2,820 to 8,456 (7 classes). After 1,000 epochs of training the model reached test accuracies 91.00% (Xception), 91.21% (MobileNetV2), 90.39% (NASNetMobile), 80.57% (MobileNet).

Haikal et al. [53] applied GoogleNet, ResNet34, and MobileNetV3 to the paddyDoc dataset (post augmentation). The dataset contains 10,799 images which are split into 4 classes. Additionally it was split in 2, one version containing 3,000 images in lab and the other version contained the remaining 7,799 images taken in field. The models were trained for 100 epochs each, with a focus on augmentation methods, before being evaluated. These results showed that models using augmentation were performing better than ones that did not.

Shah et al. [54] employ VGG16, VGG19, InceptionV3, InceptionRes-NetV2, Xception, and ResNet50V2 in their study, by training them on a field grape leaf dataset that the authors collected in India. Said dataset contains 300 original images which were extended to 1,600 images via augmentation (cropping, rescaling, transformation, resizing, rotation, adjusting brightness, contrast, sharpness). Training was only carried out for 10 epochs and the models ended up with accuracy scores of VGG16: 95%, VGG19: 96%, InceptionV3: 94%, InceptionRes-NetV2: 94%, Xception: 96%, ResNet50V2: 98%.

Mazumder et al. [55] inspect MobileNetV2, DenseNet121, ResNet152V2, DenseNet169, DenseNet201, InceptionV3, NASNetLarge, InceptionResNetV2, EfficientNetV2S, EfficientNetV2L, and a DenseNet201 with attention modules. The dataset contains images of banana and black gram leaf images with roughly 2,000 images reserved for training (3 classes for banana leaves and 5 for black gram). The models were trained for 50 epochs with early stop-

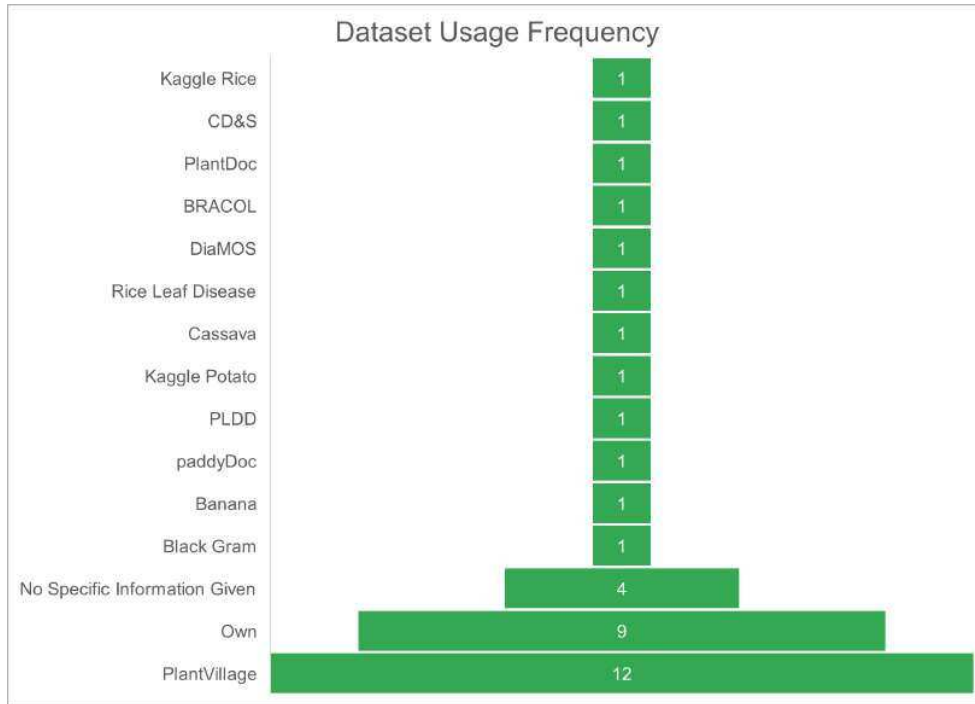


Figure 2.1: The frequency of datasets used in reviewed papers.

ping enabled and MobileNetV2 was best with 93% (besides the modified DenseNet201 with 99.50%) on the black gram data, while DenseNet201 was the best regular model with 82.3% (modified DenseNet201 90.12%).

Winiarti et al. [56] explore MobileNetV2, and VGG16 on a combined dataset of Kaggle chili leaves and leaves that the authors collected by themselves in field in Indonesia. The resulting full dataset spans 250 images across 5 classes. VGG16 reached 88% while MobileNetV2 reached 94%.

Batool et al. [57] experiment with InceptionV3, AlexNet, and VGG16 on the PlantVillage dataset. They limited themselves to only using the tomato classes, of which there are 10 with roughly 16,000 images. After 80 epochs of training, the models reached 95% (AlexNet and InceptionV3) and 96% (VGG16).

2.1.4 Analysis

When looking at the 31 papers that were review in this work that used TL CNN for plant leaf disease classification, then one can get a good understanding of the recent trends and practices used in the field. As becomes very obvious in Figure 2.1, PlantVillage is by far the most used

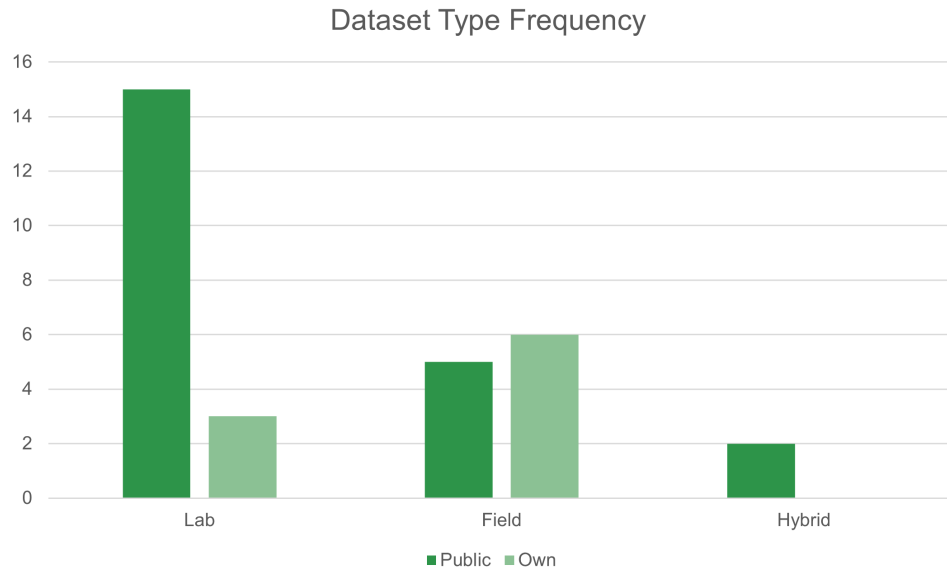


Figure 2.2: Frequency of used dataset types in papers review for this work.

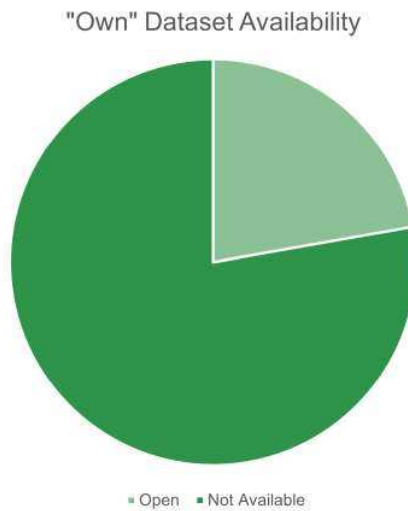


Figure 2.3: Availability of datasets newly introduced in review papers.

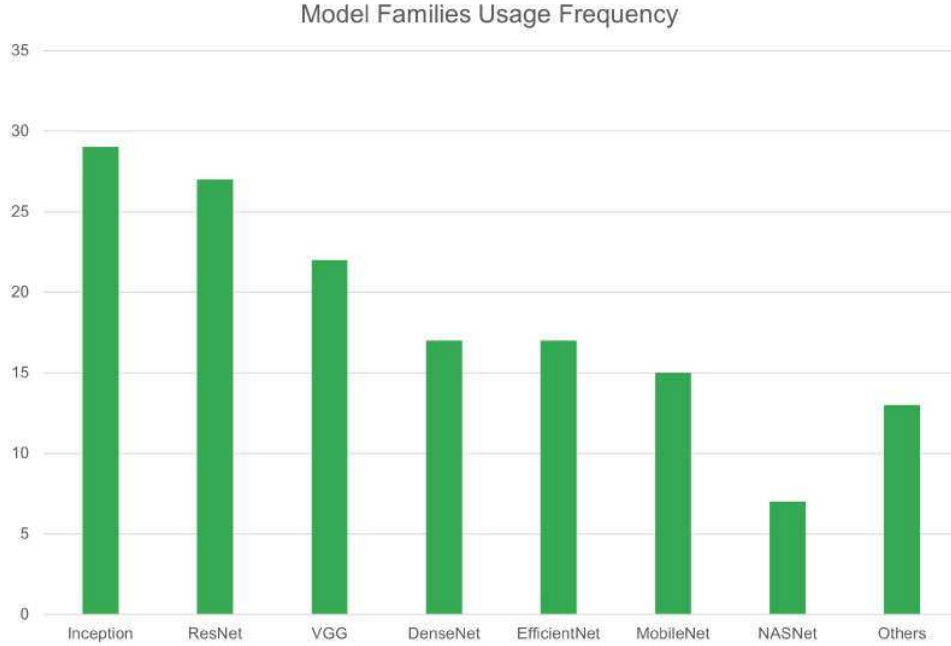


Figure 2.4: The most used model families that were used in the review papers.

dataset among the review papers. While PlantVillage is used in 12 of the review works (over 1/3), no other dataset is used more than once. It is technically not a bad thing to have dataset consistency across different studies, but PlantVillage is a lab condition dataset, which is much easier for models to handle and therefore makes comparability harder since all models tend to over-perform on such lab data. Also, lab data trained models do not generally perform well in real field conditions [15]. This trend towards lab data can also be observed across all datasets. Figure 2.2 shows that among publicly downloaded datasets a total of 15 were taken in lab conditions (12 are PlantVillage) and only 5 were in field conditions, with another 2 being hybrid. Out of the datasets that were specifically collected for the studies a total of 6 were field datasets and only 3 lab (a much better ratio in terms of field images), but sadly out of those 9 datasets that were collected as part of the studies only 2 were shared with the public and 7 were kept private (see Figure 2.3). This shows that datasets are indeed sparse, since most researchers use PlantVillage (which is a lab set and therefore not ideal) or other lab datasets, and most of the newly created sets are not even shared with the public. This further showcases the need for a large scale dataset in field or hybrid conditions that can challenge models and offer the grounds for true comparability.

When looking at the model usage, the picture is quite different. Where in terms of datasets

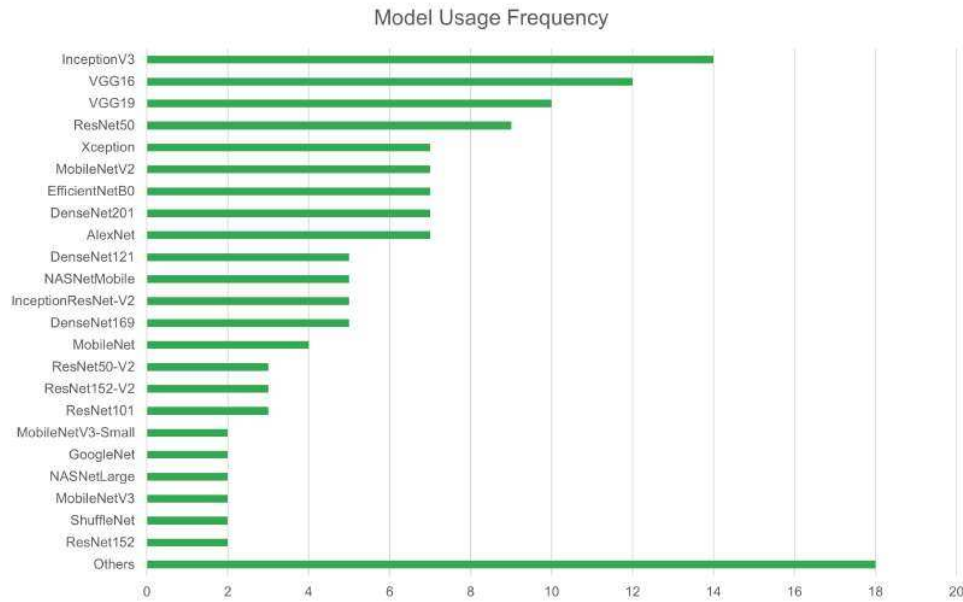


Figure 2.5: The most used models in review work.

most researchers worked with the same option (all though it comes with drawbacks), in model selection there seems to be no consensus as to which model or even model family to gravitate towards. A large number of different models from different architecture families see frequent use (see Figure 2.5). InceptionV3 sees the most usage with VGG16, VGG19, ResNet50, Xception, MobileNetV2, EfficientNetB0, DenseNet201, and AlexNet also seeing a lot of application. Numerous other models also saw repeated usage in the papers studied. Even when looking at the model family usage in Figure 2.4, it becomes apparent that there is no clear agreement about which models are better suited to be applied and tested in plant leaf disease classification tasks.

Overall, through this review it becomes apparent that data is an issue in plant leaf disease classification that needs solving. Ideally a new large scale dataset that does not only contain lab condition images would help solve this issue. Such a field or hybrid dataset could be used to test, compare, benchmark, and pre-train future models, which could lessen the reliance on the PlantVillage dataset. Additionally, a better understanding of which models are inherently better suited to be applied to plant leaf disease classification tasks would be desirable. If such a understanding could be reached, then future work could focus more on using models that are better suited and spend less time working with models that are generally subpar when applied

to this field. Additionally, all these models are general CNN model. A dedicated model maybe even one with pre-trained weights and knowledge in the field of plant leaf disease classification, could help future research by providing a dedicated model architecture to work with and by allowing future work to be based in said model, potentially even use it as a pre-trained BM for TL could save future work time, and computational resources, since it could help models to train faster, more stable, more robust and even with less new data.

3. Background

3.1 Image Classification using Deep Learning

Deep Learning and Neural Networks have seen a ton of usage, work, development, and application in recent years. With the rapid development and increase in computational power, of newer hardware, GPU in particular, neural networks have not only become feasible, but in this day and age they have become very powerful and they have become common place in many areas and also in many people's everyday life. One area that has benefited heavily from the increase in computational power and has subsequently seen a lot of recent work is the field of image processing using AI methods. One popular, efficient and effective method to build AI models that handle images are CNN. Before CNN and DL became computationally viable, traditional methods were employed, where feature extractors had to be built by hand. While the resulting models can be very strong and efficient, they require a lot of work, expert knowledge and need to be redone for any new domain-specific task that one might need a model for. This means that they were often laborious, time consuming and expensive in making. CNNs on the other hand, can be trained automatically, as long as sufficient (and often labeled) data is present. CNN can learn feature extractors through the learning process, without developers having to design any of them on their own. Only the model needs to be constructed, but there are numerous popular and proven CNN model architectures readily available for use in publications and online. Fundamentally speaking, they are all somewhat based on the initial idea of convolutional layers paired with pooling layers to automatically train feature maps, which can then later be used for classification by adding a classifier top to the end of the convolutional block.

These convolutional layers are made up of so called kernels, which parse over the image. Kernels are usually square, often of the size of 3x3 pixels, and parse over the image from the top left to the bottom right pixel by pixel (see Figure 3.1 and Figure 3.2), multiplying their

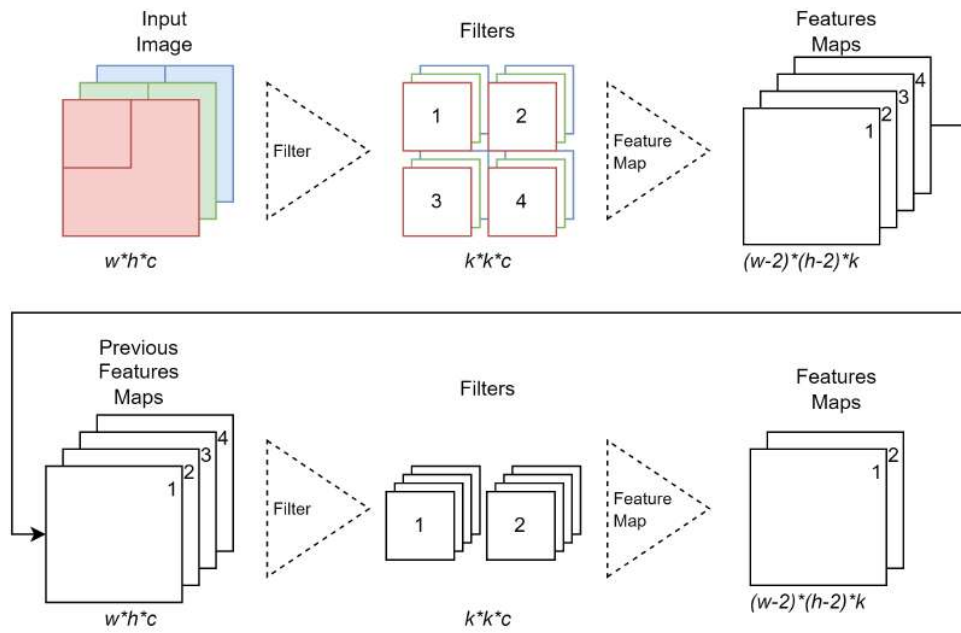


Figure 3.1: This figure explains how kernels parse over the image and extract feature maps from them.

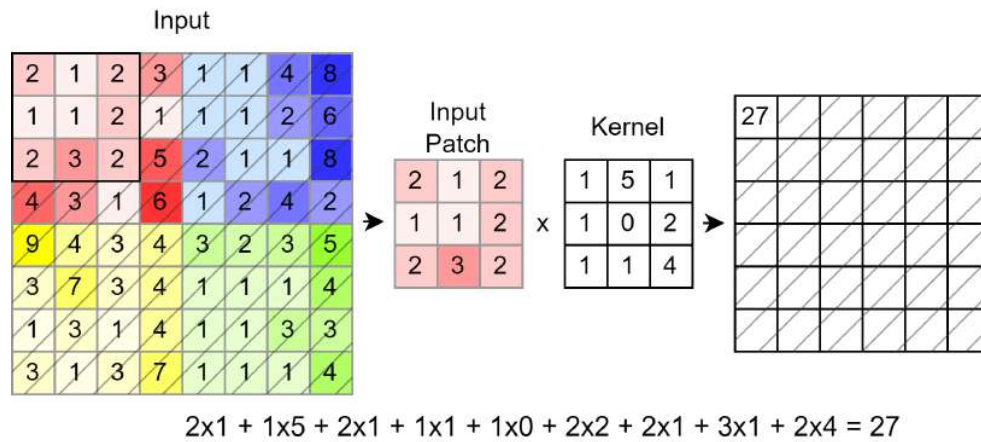


Figure 3.2: Kernel operation visualized.

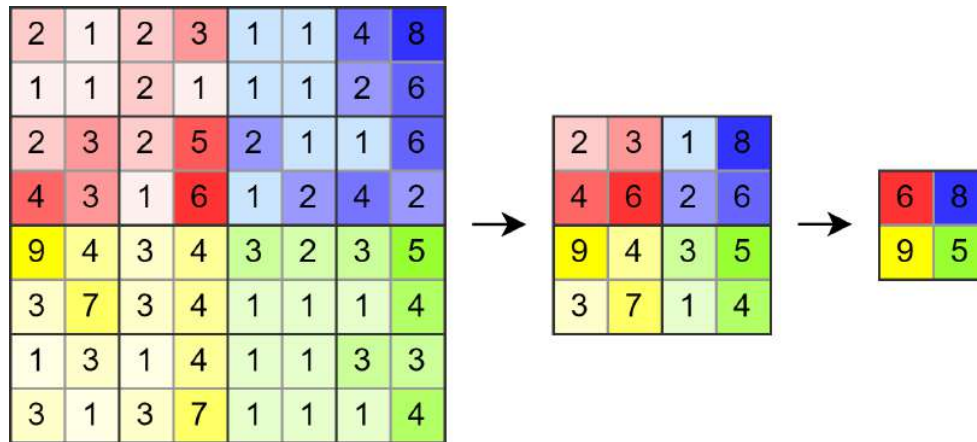


Figure 3.3: Max Pooling process explained and visualized. 2 max pooling operations are shown in this figure.

own values with the image pixel values to generate automated feature maps. Early convolutional layers generally learn basic features, with deeper layers learning features that are more nuanced. Deeper layers also learn features on a more global level, and across a larger area of the image, whereas early layers usually learn more local features over a smaller part of the image. This is due to the nature of the pooling layers that often appear in between stacks of convolutional layers. Pooling layers, max-pooling being the most commonly used one for this task, reduce the image in size and only keep the values one chooses to keep. In a 2x2 max-pooling layer, which is the standard, an image gets reduced to half its size, with each 2x2 block of original pixels in the image being reduced to a single pixel in the resulting pooled image, with the largest of the 4 values in the 2x2 square being kept (see Figure 3.3).

After the CNN feature extractor has learned and constructed all feature maps, a classifier is needed to take the provided features and turn them into class predictions. There are various different classifiers that one can choose from, ranging from ML classifiers such as random forest or SVM classifiers to neural network based classifiers. Generally speaking, all classifiers need the features to be condensed into a 1 dimensional vector, as they are not meant to be trained with data of higher dimensionality. Feature vectors are provided in 3D tuples, so they need to be converted into 1 dimensionality first. The two most common ways of doing this are flattening and global average pooling. Flattening simply takes all the pixels of all channels and orders them into a long 1 dimensional vector where all pixels are simply a long list. Global average pooling takes the average value per channel and returns that, creating a 1D list of one

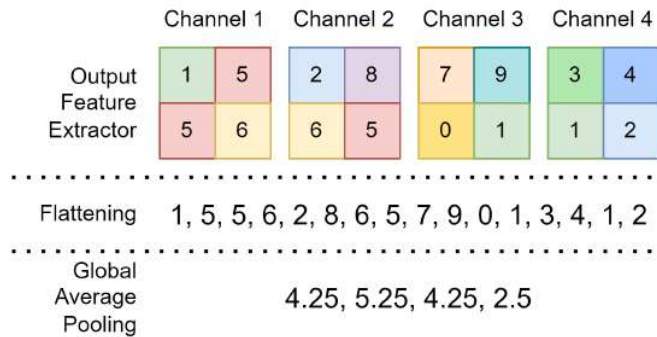


Figure 3.4: Flatten and Pooling visually explained.

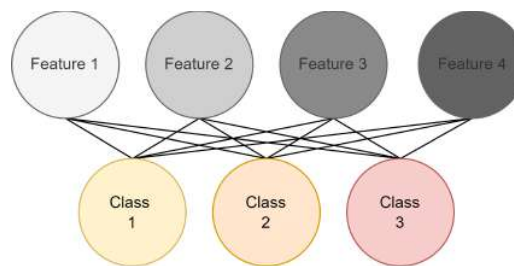


Figure 3.5: A fully connected neural network classifier top.

single value per channel (see Figure 3.4).

Then the converted 1D vector can be forwarded to the classifier. A neural network based classifier which is most often used would then for example be a fully connected network with the 1D vector as input and a final layer with softmax activation that has the number of classes as neurons.

3.1.1 Domain Adaptation

3.1.1.1 Transfer-Learning

One way, which could be classified as the standard way, to train image classification models is to just initialize the models weights and other parameters at random. This means that before training, the model has no knowledge of this task or any other domain and starts of by essentially guessing at random and starting completely from scratch. This can generate well performing models that are only trained on the domain specific data. If, however, data is limited, or there is not enough time available for training, or if the computational resources are limited, then one might want to pivot to Transfer-Learning (TL) instead of training the model from

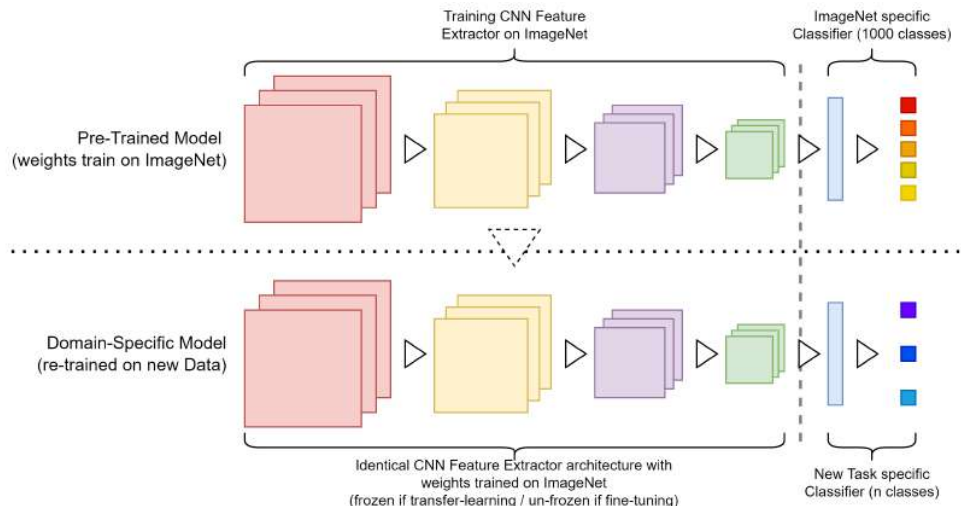


Figure 3.6: Transfer-Learning method visualized

scratch. This process uses a pre-trained model, a model that has previously been trained on a different dataset, and then trains that model, with the old weights still intact, to now work on the new domain specific data. Pre-trained models are usually trained on the ImageNet [58] dataset, a huge scale dataset with over 1.2 million images belonging to 1,000 classes. Through this training, the model will already learn many general features that are applicable to a wide range of topics which can be applied to the new domain-specific topic through Transfer-Learning. Pure TL takes the pre-trained feature extractor and freezes all parameters (they become not trainable, meaning they will not be updated during training on the new domain-specific data) and trains only the classifier top. Because of freezing all the CNN layers, the computational cost during training is heavily reduced, allowing models trained in this manner to be trained on machines much weaker than the ones that would be needed for train from scratch. Additionally, because all feature extractor layers are already intact, training will also be much quicker and because the features already exist, the change of overfitting is much reduced (see Figure 3.6).

3.1.1.2 Fine-Tuning

If the results are not strong enough, or if one wants to improve the model's results as much as possible, then FT on top of the TL model is possible. To do this, the model would, after all the updates made to it via TL, be un-frozen, meaning that all layers and parameters are now trainable. This does increase computational costs again and it will also add additional training time, but it will allow each parameter to be adjusted slightly to better match the target domain-

specific data from the original ImageNet features. This can extract extra accuracy percentages as the model will be even better adjusted to the target data and the resulting model will benefit from the pre-trained weights based on ImageNet, the TL adjustments, and lastly the improvements made through FT (see Figure 3.6).

3.1.1.3 One-Shot Learning

In One-Shot Learning (OSL), one does not train the model in the standard sense of deep learning. Rather than that, one will use the pre-trained model, use it as a feature extractor only, and use said features as class embeddings to compare future feature embeddings to. The features are collected after the global average pooling layer, with the rest of the model's classifier top being disregarded. To do this, the pre-trained model (with the classifier top removed) is taken, and then each image for each class, one image per class, is fed into the network in inference mode to obtain the feature embeddings, which are saved for each class. This feature embedding is now the representation for said class. Future test images will be fed into the image and then their distance will be calculated for all class embeddings. The shortest distance from the test image's embeddings to any class embedding will be the projected class. As such, the model is more light weight than before (since the classifier top is removed) and no training is needed at all, only one inference run per class is required during "training".

3.1.1.4 Few-Shot Learning

Few-Shot Learning (FSL) works essentially the same way One-Shot Learning does, with one difference. Instead of a single image per class, here n images, say 5, are present during training to generate the embeddings. Each image is fed into the network, embeddings are averaged per class (if 5 images per class are used then all 5 embeddings are generated and then averaged, with the averaged embeddings being used for predictions) and used for future distance calculations and predictions.

3.1.2 Base Models & Foundational Models

In this work the term Foundational Model (FM) refers to large scale CNN Base Model that are trained on a large dataset to later be used to be potentially adapted, transferred, and retrained for other (potentially) related tasks [16] (but FM can generally also refer to more general AI

models). Examples of such CNN architectures commonly used as Foundational Model include models such as ResNet, DenseNet, ConvNeXt, MobileNet, and more, just to name a few. These model architectures are then most often pre-trained on the ImageNet dataset, with these pre-trained weights being available to download by the public, which can then use these pre-trained models to apply them to their area of need (as mentioned above through TL and FT). ImageNet as the base dataset to pre-train the model on comes with certain advantages and disadvantages. Firstly, ImageNet is a huge dataset with over 1.2 million images across 1,000 classes. This offers the models a diverse, large scale and high quality dataset to train on, with low risks of overfitting and low risks of being too centered on a single domain. Resulting models trained on ImageNet therefore boast feature maps with a knowledge base that encompass a very large variety of different image types and classes, and therefore offers a great base on which one could build models for a wide variety of different target domain topics. However, ImageNet does, as a result of the wide variety offered, contain a large number of classes and images that will inevitably not be related to the target task, and only contain a small number of images and classes that are directly related to said task, if any at all. While the features learned on other images are still valuable and can still be used to retrain models to a new task area, they are most likely not fine-tuned for specific tasks that rely on very specific features, that one might not obtain when differentiating between bookcases and brooms on ImageNet for example. As a result, to achieve the best performance, one would have to fully fine-tune these models which is computationally expensive [17]. A model already trained on a large dataset that is related, or even identical, to the target domain, can overcome these shortcomings of potentially having to re-train the entire model in FT mode, and learns domain-specific knowledge during pre-training already. As such, the resulting model does not necessarily need to be entirely fine-tuned before being applied to the domain-specific task, because it was trained on related data, and does perform better on said data without full FT due to the presence of domain-specific knowledge in the FM weights [17]. This means that a domain-specific Foundational Model can potentially learn faster, more robust, more consistent, more powerful models on less data, while not necessarily requiring full FT.

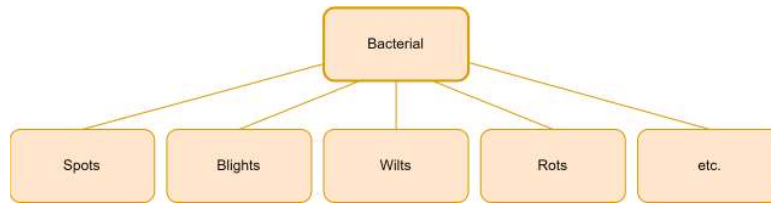


Figure 3.7: Bacterial Diseases

3.2 Plant Pathology using Deep Learning

These DL methods have been applied to many different fields in recent years and due to the capabilities of CNN to automatically learn features based on the labeled data, CNN are perfectly capable of being applied in many different fields successfully, granted the availability of sufficient data. For the field of plant leaf disease classification this equates to large image datasets depicting images of leaves both with and without disease symptoms that have been classified into healthy and diseased (one class per disease). This classification needs to be carried out by experts that can reliably differentiate between the different plant diseases without error to make sure that the dataset is accurate, because a faulty dataset will lead to faulty models.

3.2.1 Disease Types

Plant diseases can generally be grouped into 3 subcategories, based on which pathogen has infected the plant. These three categories are viral, bacterial, and fungal diseases.

3.2.1.1 Bacterial

When bacteria enters a plant through openings in the plant, they can cause the plant to suffer from bacterial plant diseases. The opening through which the bacteria enter the plant can be caused by external damage (hail, heavy rain, animals, humans, etc.) or they can be natural opening of the plant for water and gas exchange for example [59, 60, 12, 61]. They then infect seeds which can spread the disease, but it can also spread from plant to plant, for example through water. Some examples of bacterial diseases are spots, scabs and rots (see Figure 3.7). Bacterial diseases are often not curable, and the plants need to be removed from the field to prevent further spreading [12].

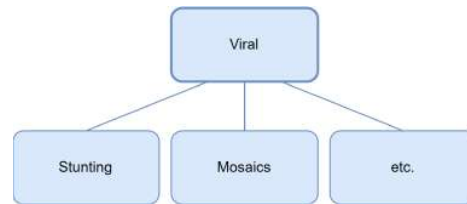


Figure 3.8: Examples of Viral Diseases

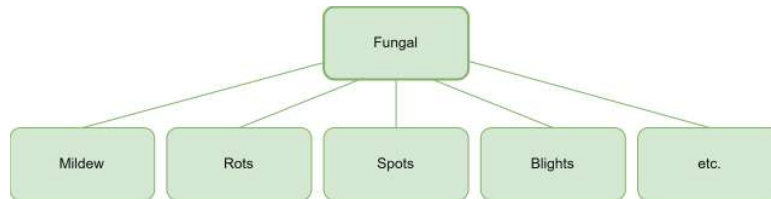


Figure 3.9: Fungal Disease Examples

3.2.1.2 Viral

Viral diseases can modify the DNA of plant host cells, which will make them produce new viruses, helping them reproduce. Viral diseases can be transmitted through water, but also via insects that move from one plant to the next [60]. Some viral diseases are mosaic, mop-top, etc. [60, 12] (see Figure 3.8). Viral diseases tend to be very hard to identify [61].

3.2.1.3 Fungal

Fungal diseases are often contracted through air, water or soil and can cause diseases such as blights, mildew, etc. [60] (see figure 3.9). They are often transmitted through spores that can travel quite far. Plants infected with fungal diseases can be treated by removing the infected parts of the plant and only leaving behind parts of the plants that are still healthy [12].

3.2.2 Datasets

Datasets, in this field, are collections of images depicting healthy images as well as images containing a set of different diseases. Datasets, disregarding the types of diseases, can be divided into two categories: field and lab datasets. As the name suggests, field datasets are taken in field (in real field conditions), while lab datasets are taken in lab (in ideal conditions). These two different capturing methods create widely different datasets with different characteristics.

3.2.2.1 Lab Datasets

Lab datasets, datasets that were taken in laboratory like conditions, are a type of datasets in which leaves and backgrounds are prepared before images are taken. This means that leaf images are usually taken one leaf at a time, with the leaf separated from the plant itself on a single color (often white) background. As such, these datasets are rather simple in terms of complexity. Where a real plant leaf is surrounded by other plants, leaves, soil, etc. the isolated leaves in the images in lab plant leaf datasets have no such distracting noise. Models trained on such data are, as a result, facing a much smaller challenge during training. They do not have to learn how to differentiate between background and foreground. This leads to models trained exclusively on lab data achieving high results on said lab data, in some cases making it hard to differentiate the trained models, since they all reach high score close to one another. Such models are, however, said to be less capable when used in real field conditions [15]. The most used dataset in the field, PlantVillage [19] is a lab dataset. Sample image of a lab dataset can be seen in Figure 4.1.

3.2.2.2 Field Datasets

Field datasets, in contrast to the afore mentioned lab datasets, are taken in real in field conditions. Field datasets are taken with the leaf still attached to the plant and therefore with a lot of noise in the vicinity of the leaf that one wishes to analyze. This noise makes it quite a lot harder for DL models to work with the data, since unlike perfect lab data, here the model needs to not only analyze the leaf for symptoms, but also the image itself for the location of the leaf within in. Sadly, there is no field dataset of the size, variety, and quality of PlantVillage, so often when researchers pick open datasets, they gravitate towards the lab dataset PlantVillage. Many datasets collected by researchers are field datasets, but they are often not released to the public, leading to somewhat of a shortage of field data. Field data being more challenging makes it easier to differentiate the performance of different architectures and also train more robust and generalizable models that can also be used in field conditions. Sample images of a field dataset can be seen in Figure 4.2.

3.2.2.3 Hybrid Datasets

Hybrid datasets combine image data taken in field and image data taken in lab. This can take the form of one class being exclusively field data and another class being only lab data, which can cause problems, as the model might focus more on learning the difference between data types and less on the actual disease symptoms. Other hybrid datasets are made up in a way in which each class has data of both types. This can lead to the model learning how to handle both types of data, and this can alleviate some of the drawbacks of lab data and create robust systems that can function in different scenarios [62, 63, 64].

4. Datasets

As is true with every kind of Deep Learning, a large amount of high quality data is also needed for the problem of plant disease classification as well. If the data is too small, not diverse enough, of too low quality, or has other problems, then the model can not learn properly. A lack of sufficient data of good quality, for example, can lead to the model overfitting to the training data and not generalizing to the actual problem being studied, which will render the model useless, although the training results might initially sound promising. This requirement needs to be met for all classes being trained, and ideally all classes should be well balanced to encourage the model to actually analyze all images in detail to make its predictions, instead of exploiting issues with the training data, as heavily imbalanced data could make the model lean and bias towards one class per default, simply because it has a much higher probability of being correct due to the possible imbalance. Data should also be uniform across all classes, so that the model needs to solve and discriminate based on the actual problem being studied, instead of learning to simply predict based on other differences across classes (e.g. if one class has all images taken in front of a red background and the second class only features blue backgrounds, then the model, in all likelihood will learn only that, instead of focusing on the actual foreground of the image). All this proves that the dataset is an incredibly important factor in the training of a successful model and therefore needs to be well chosen and constructed, maybe also pre-processed and augmented, to end up with a dataset that allows the model to train properly and well.

Creating datasets for this plant disease use-case is not easy, as one needs access to a large enough amount of plants, invest a lot of time and effort to take pictures of adequate quality, and then have an expert label said image data by disease type. This is why, as part of this thesis, no new data is collected. Instead this work falls back on image datasets that are available online and adjust and modify them to fit the goals and scope of this work. In this chapter the

different datasets chosen will be discussed. First all datasets will be introduced. All datasets will be explained through a table of key information, sample images for each class, as well as a plot showcasing the distribution of images across all classes. These datasets will be used to test a wide variety of models to find a suitable baseline model to build a new architecture on, and then a selection of these datasets will be combined to train said new model on. When discussing image datasets for plant disease identification, there are 2 major distinct groups among them. One group contains plant images taken in the lab, while the other group includes image datasets taken in field. Lab images are inherently easier for DL models to handle, as the leaf is completely isolated in the image and the background is uniform and without any complexities (see Figure 4.1).

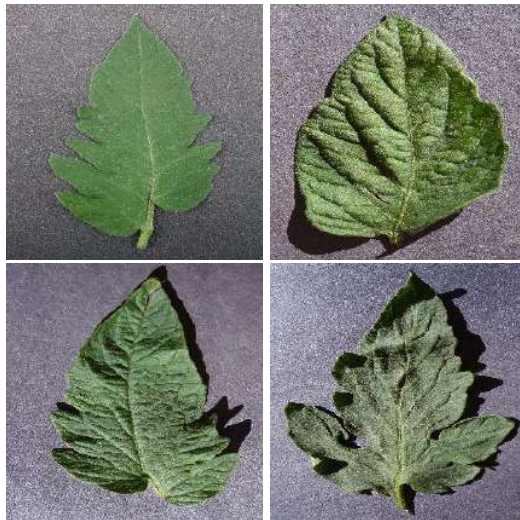


Figure 4.1: Sample of Tomato Leaf images taken under Lab conditions from the Plant Village dataset [19].

Images taken in field are much more complex and difficult to predict since the background, instead of being just one uniform color, they often feature soil, other plants, and other more complex features, that the model needs to handle. But while these images are more complex and harder to train, they also produce better performing classifiers that can be used in real world applications in the end [11]. While lab image trained networks work well as proof of concepts, they fail when one tries to use them with in field images, as would be the case if farms would move to DL models for practical use. As such, it is better to use field image datasets or hybrid sets that include or combine the two, because field images datasets essentially mirror the way

images would look like if someone were to take them in field when inspecting their field for diseases with a camera or phone (see Figure 4.2) and should therefore translate to real world application much more easily [62, 63, 64].

Datasets also vary by which plants are included as well as which diseases are present in it. Multi-plant datasets, as well as datasets that only contain a single plant can be found publicly available online. Datasets also vary in the number of diseases per plant type that are included within, ranging from simple binary classification to multi-class problems. Lastly, the amount of images per class also heavily fluctuates between datasets, with some datasets having images in the hundreds, while other datasets offer tens of thousands of images, both to varying degrees in terms of per-class-distribution.



Figure 4.2: Sample of Potato Leaf images taken taken in the field conditions from the novel Potato dataset [65].

With all that, as part of this thesis, openly available datasets will be presented, categorized and analyzed in this chapter. First lab image datasets will be introduced, then field datasets and after that hybrid sets will be listed. More detailed information for each dataset can be found in Appendix A.

4.1 Lab Datasets

4.1.1 Plant Village (plantVillage)

The Plant Village Dataset [66, 19, 67] might currently be the most popular and commonly used dataset in plant disease classification. It contains various different plants and their corresponding diseases all taken under lab conditions (see Figure A.2) at different research stations across the USA. The distribution of images per dataset is rather imbalanced (see Figure A.1). It is also one of the biggest openly available datasets in terms of image numbers. Classes per plant range from 1 to 10 with a healthy class always included (see Table A.1). It has been used in numerous papers [68, 69] and tends to produce very strong results, with the caveat that lab images are much easier to handle.

4.1.2 Tomato Village (tomatoVillage)

The Tomato Village dataset [70, 71] is a single plant dataset focusing on tomato plant leaf diseases. It includes 7 diseases as well as a healthy class (see Table A.2), all of which are taken under laboratory conditions (see Figure A.4). Classes are mostly imbalanced in this dataset (see Figure A.3). This dataset, when compared to the tomato images in the Plant Village dataset [19], does have some overlap in diseases, but does also introduce new diseases as well. This is due to the nature of this dataset being captured at three different locations in India, where other diseases are prominent. Tomato Village has seen prior use in research projects [72].

4.1.3 Potato Disease Leaf Dataset (pld)

The PLD Potato Leaf Disease dataset [73] is a dataset of potato leaves collected in Pakistan under lab conditions as can be seen in Figure A.6. The dataset contains healthy potato leaf images alongside 2 more classes of diseases, totaling 4,062 images across all 3 classes (see Table A.3) which are fairly well balanced (see Figure A.5). PLD has been used in research before as well [74].

4.1.4 Tea Sickness Dataset (tea)

The Tea sickness dataset [75] includes tea leaf images from 8 different classes (see Table A.4) captured in eastern Africa. All images were taken in laboratory like conditions (see Figure A.8), resulting in a dataset with 885 total images, which have proven to train strong models in prior work [76]. When looking at the distribution of those images across all classes, one can see that the dataset is rather well balanced (see Figure A.7).

4.2 Field Datasets

4.2.1 Cassava Leaf Disease Classification (cassava)

The Cassava Leaf Disease Classification dataset [77, 78] was originally used for a Kaggle coding competition, but has since also found use in various research papers [79, 80]. All images are taken in field (see Figure A.10) in Uganda. It contains 5 classes, 4 of which are diseased leaves with the fifth being the healthy leaf class, totaling 21,397 images (see Table A.5). While the dataset is heavily imbalanced (see Figure A.9), it is one of the bigger and high quality datasets of infield plant disease images.

4.2.2 CD&S Dataset (cbs)

The CD&S dataset [81, 82] is a corn plant leaf disease dataset. Images were acquired in West Lafayette, IN, USA at Purdue University and all images were taken in field (see Figure A.12). The dataset contains a total of 3 classes (see Table A.6), all of which are disease classes. One thing of note is the near perfect distribution of images per class, as can be seen in Figure A.11. Prior work has shown good results with this dataset [83].

4.2.3 Cucumber Disease Recognition Dataset (cucumber)

The Cucumber Disease Recognition Dataset [84, 85] contains images of both cucumber fruits as well as cucumber plant leaves. Since this thesis focuses on leaf images only, the fruit image classes have been discarded and not considered. They will also not be present in the tables and images below. The dataset contains 5 leaf classes (see Table A.7), one of which is healthy leaf images (see A.14). The distribution across classes is near perfect (see Figure A.13). The dataset

was successfully used in [86] for example.

4.2.4 DiaMOS Plant (diaMos)

The DiaMOS Plant Dataset [87, 88], just like the aforementioned Cucumber Dataset, also includes fruit images alongside leaf images, and just like with the Cucumber Dataset, here too the fruit images will be ignored and, therefore, not listed in this work. Severity data is also present in this dataset, but that data too will not be considered. Pear leaf images are divided into 4 heavily imbalanced (see Figure A.15 and Table A.8) distinct classes, one of which includes healthy images. All images were taken in field (see Figure A.16) in Italy and the dataset has already been applied in plant disease related research [89].

4.2.5 Paddy Doctor (paddy)

The Paddy Doctor Dataset [90, 91] is a dataset of in field images of rice leaves taken in paddies in India, for samples see Figure A.18. The dataset contains 10,407 images over 10 classes (see Table A.9), which are somewhat imbalanced as can be seen in Figure A.17. [92] is an example of the Paddy Doctor dataset being used in academic work.

4.2.6 Plant Pathology 2020 - FGVC7 (fgvc7)

The Plant Pathology 2020 - FGVC7 Dataset [93, 94] is a dataset comprised of apple leaf images including a total of over 1,500 apple leaf images, all of which were captured in field in the US (see Figure A.20). The dataset was originally used for the Plant Pathology Challenge at the Fine-Grained Visual Categorization (FGVC) workshop at the 2020 CVPR conference. The dataset includes two distinct diseases and a multi-disease class (see Table A.10). When looking at Figure A.19, one can see that the FGVC7 dataset's distribution is pretty even, except for the multi-disease class. And due to its high popularity and exposure at the conference, it has seen a vast amount of research interest ([95, 96]).

4.2.7 Plant Pathology 2021 - FGVC8 (fgvc8)

One year after the above mentioned Plant Pathology 2020 - FGVC7 challenge, the challenge was renewed with an extended dataset as the Plant Pathology 2021 - FGVC8 challenge and dataset [97, 98] (see Figure A.22 for sample images). This newer dataset now features over

18,000 images divided into 12 classes (see Table A.11) that overlap and also vary in complexity, which are unbalanced, as can be seen in Figure A.21. This popular dataset has seen use in research work, e.g. [99, 100].

4.2.8 PDD271: Plant Disease Recognition Dataset (pdd271)

The PDD271 dataset [101, 102] is a very large dataset originally containing a total of 271 different classes across 220,592 total images, all taken in field. This dataset, however, is proprietary and not open to the public. Only a sample containing 10 images per class can be accessed online, except for 10 classes that seem to be unaltered and still seem to contain all images. In this thesis only these 10 classes will be considered for training. This subset of PDD271 now contains a total of 7,555 field images (see Figure A.24), of 5 different plants (see Table A.12) with reasonably well balanced classes, as shown in Figure A.23.

4.2.9 Strawberry Disease Detection Dataset (sms)

The Strawberry Disease Dataset [103, 104] contains images of leaves, fruits as well as blossoms. Due to the nature of this thesis working with leaf images exclusively, the blossom images as well as the fruit images have been discarded. As such, these classes and their images will also not be listed here. One more thing to note, it seems as if the dataset has already been enlarged by a lot of augmentation. As is, the dataset contains a total of 3 classes, all diseases, after removing the blossoms and fruits, as can be seen in Table A.13. Images are all taken in field (see Figure A.26), resulting in a rather well balanced dataset (see Figure A.25). This data has been utilized in a number of studies (e.g. [105, 106]).

4.3 Hybrid Datasets

4.3.1 plantDoc

The plantDoc dataset [15, 107] is a multi-plant dataset that features a wide variety of plant across 28 total classes (see Table A.14). It includes images are taken in field, but when looking at figure A.28, it becomes clear that the dataset also includes images that realistically should have been excluded from the dataset (e.g. PowerPoint slides). Class distribution is not too bad,

except for some outlier classes (see Figure A.27). Regardless, planDoc has seen researcher attention [108].

4.3.2 Taiwan Tomato (taiwanTomato)

The Taiwan Tomato Dataset [109] is a dataset that includes images for 5 different classes of tomato diseases as well as a class for healthy images. The classes contain both, images taken in the field as well as images taken under lab conditions (see Figure A.30). The dataset also includes images taken from the Plant Village dataset [19], but these were not included in this work. Augmented images were also ignored, as this work applies its own set of augmentations. As can be seen in Table A.15, the dataset is rather small but the distribution is not as imbalanced as it is in other datasets. The Taiwan Tomato dataset has already seen use in research in the past [110].

4.3.3 Potato Leaf Disease Dataset in Uncontrolled Environment (novelPotato)

This novel Potato image dataset for leaf disease classification [65, 111] contains a total of 7 classes, one of which is healthy, taken in field and lab-like conditions (see Table A.16 and Figure A.32) in Indonesia. The per-class distribution is unbalanced, especially when looking at the "Nematode" class. This dataset had seen prior use in research (e.g. [112]).

4.3.4 Rice Leaf Diseases Dataset (rlidd)

The Rice Leaf Diseases Dataset [113] by Antony and Prasanth is a dataset that contains 3 classes, all of which are diseased (see Table A.17). The dataset is rather small in size and it seems as if some amount of augmentation has already been used to expand the bacterial blight class, which as a result of that is now much larger than the other 2 (see Figure A.33). Images seem to be taken under varying conditions, some taken in conditions somewhat similar to the ones found in lab datasets, while others are taken in field, as can be seen in Figure A.34.

4.3.5 Sugarcane Leaf Dataset (sugar)

This Dataset containing sugarcane images [114, 115] originally contained a total of 11 classes, one of which is dried leaves. This work will not consider the dried leaf class, so the modified dataset totals 10 classes (see Table A.18), containing a healthy class. Images were acquired in

India and the dataset includes both field images and also images taken under lab-like conditions (see Figure A.36). The number of images per class varies rather heavily (see Figure A.35). This dataset has proven to work well in recently published papers [116, 117].

5. Models

Datasets are essential to assure good performing models. But just like the datasets, choosing the right model architecture has large impact on the final result. As such, one must consider which model to use wisely. CNN models have come a long way in recent years, with new FM being published that introduced new methods. However, different models perform differently depending on the way they are applied but also depending on which domain they are being applied to. In order to build a new dedicated plant leaf disease classification model or to improve an existing model to perform better, one first needs to learn which models are inherently potent in the field. This chapter will introduce and briefly explain some of the FM that see usage these days which will be tested on their performance on all the datasets mentioned before in a Transfer-Learning fashion, in order to gain insights and learn which model architecture and methods can be built upon for the new model.

5.1 ResNet

The ResNet architecture [118] utilizes so-called residual connections (see Figure B.1). These residual connections pointwise add the input of a layer to its output to preserve features captured in earlier layers and to provide a more direct path to earlier layers which improves the gradient flow during learning. To enable such connections, the layers outputs need to be of the same dimensionality as the inputs so padding is set to same within the blocks and the dimensionality only changes through stride 2 convolutional layers in the beginning of each block.

5.2 VGG

The VGG [119] model architecture is a rather simple model when looking at the blocks is is build out of (see Figure B.2). The blocks are simply made up of regular convolutional layers

and max pooling layers at the end of each block.

5.3 Inception

The Inception [120] family of CNN models makes use of Multi-Scale Processing (MSP), batch normalization, Factorized Convolutions (FtC), and label smoothing. Multi-Scale Processing is the method of using different sized kernels across the network (often in parallel) to recognize differently sized features, batch normalization normalizes the outputs of a layer to stabilize training. Factorized Convolutions split kernels into 2 (e.g. a 5x5 kernel into a 1x3 and into a 3x1 kernel) which minimizes the amount of parameters needed. Lastly, label smoothing improves generalization.

5.4 EfficientNet

EfficientNet [121] is a model architecture family that is based on the ideas of dropout layers and stochastic depth, swish activation, and Mobile Inverted Bottleneck (MIB) convolution. The dropout layers ignore certain connections per layer to improve generalization, whereas stochastic depth ignore entire layers for the same effect. Swish is a activation function that improves the normally used ReLU and Mobile Inverted Bottleneck convolutions use Pointwise Convolution (PwC) and Depthwise Convolution (DwC) to reduce parameter counts. Depthwise Convolution only operate on a single channel (regular convolutions operate on all) and Pointwise Convolution are essentially 1D convolutions that only look at 1 pixel per channel but across all channels. In MIB convolutions, first a PwC layer increases the number of channels, before a DwC, followed by another PwC (in a Depthwise Separable Convolution (DSC) block) layer parse the image for features.

5.5 NASNet

NASNet [122] is a architecture that was made with optimization algorithms including Reinforcement Learning (RL). It is made up of different blocks and cells with max pooling, average pooling, regular convolutions, and Depthwise Separable Convolution.

5.6 MobileNet

MobileNet [22] is a family of models mainly concerned with building models that are efficient and light-weight. To achieve these goals methods such as the above mentioned Mobile Inverted Bottleneck, and Squeeze & Excitation (SE) were employed. Squeeze & Excitation is a attention mechanism that focuses on channel attention by using a global average pooling layer with an MLP to identify the importance of the given channels.

5.7 ConvNeXt

ConvNeXt [123] is a model architecture that is based on the principles of Vision Transformer (ViT), since they have managed to achieve high levels of performance in recent works. As such, the creators of ConvNeXt built a model with similar characteristics based on CNN to rival these Vision Transformer and to combine the advantages of both. It does that by including techniques such as large kernels (7x7), layer normalization, residual connections GELU activations and inverted bottleneck (see Figure B.3).

5.8 DenseNet

The DenseNet [124] family of networks is also based on residual type connections (see Figure B.4), but unlike ResNet, here dense connections are used. They work differently where, instead of adding layers, they append the channels to one another, also preserving earlier features and reducing the vanishing gradient problem in the mean time.

6. Benchmarking

To this day there seems to be no real consensus on which model is best suited to handle the task of plant leaf disease classification. This understanding is helpful and even somewhat essential when trying to choose a model for a new project in the field. But not just for picking already existing models does one require this knowledge, but also to build a new and better model, one best first find out which model is inherently well suited to be used as a baseline, and also to see which techniques might be better applied to the task than others. Additionally, as mentioned in earlier chapters, datasets are a part of this field that requires improvement. So, while benchmarking the models, a number of datasets will be tested at the same time. This will eliminate the bias any given model might have to a certain dataset and therefore generate much more generalizable and robust data, while also giving insight into the currently available datasets. In this chapter the methods of benchmarking, in an effort to find suitable data for training and a suitable baseline model, will be explained and the results gathered will be presented and contextualized. Based on these results, in later chapters, a new dataset and model will be built with a sole focus of improving performances in the field of plant leaf disease classification.

6.1 Benchmarking Methods

In this benchmark, to find a suitable baseline model to build upon and datasets to combine and train on, a total of 23 foundation models have been trained on 18 different plant leaf disease datasets. Each model was trained for up to 200 epochs (unless early-stopping triggered) for both TL and FT on each dataset (models are pre-trained on ImangeNet). Each combination was trained 5 times each to get more comparable and representative results. A full list of all datasets can be found in Table 6.1 and all models are listed in Table 6.2, with key information

being provided for both. The workflow can be seen in Algorithm 1 and in Figure 6.1. This chapter is based on [125]. The experiments in the paper are run for 5 iterations, while in this thesis they were only run for 2. For more generalized results, read [125].

6.1.1 Datasets

As pointed out in prior work [14, 11, 126], datasets for plant leaf disease classification are still at a point where they are far from being abundant. New datasets are still often kept private, many datasets are rather small in size, popular datasets are often taken only in lab conditions, and often datasets are somewhat limited in the selection of plants, or diseases, or classes that they contain. In an effort to learn which datasets are better equipped to be used to train a large scale model on them, a set of 18 datasets (see Figure 6.1) that are openly available to the public have been selected for this benchmarking. Based on these results a new dataset can be constructed that contains images from datasets that show good characteristics and based on their performance in this benchmark.

Table 6.1: List of all the datasets considered in this benchmark with all key-metrics.

Ref.	Dataset	Type	Plant	Num. Class	Total Img.
[77]	cassava	Field	Cassava	5	21,397
[81]	cds	Field	Corn	3	1,571
[85]	cucumber	Field	Cucumber	5	800
[87]	diaMOS	Field	Pear	4	3,006
[93]	fgvc7	Field	Apple	4	1,821
[97]	fgvc8	Field	Apple	12	18,632
[65]	novelPotato	Hybrid	Potato	7	3,076
[90]	paddy	Field	Rice	10	10,407
[101]	pdd271	Field	Multi	10	7,555
[15]	plantDoc	Hybrid	Multi	28	2,577
[19]	plantVillage	Lab	Multi	38	54,304
[73]	pld	Lab	Potato	3	4,062
[113]	rldd	Hybrid	Rice	3	524
[104]	sms	Field	Strawberry	3	1,583
[114]	sugar	Hybrid	Sugarcane	10	6,405
[109]	taiwanTomato	Hybrid	Tomato	6	622
[75]	tea	Lab	Tea	8	885
[70]	tomatoVillage	Lab	Tomato	8	4,526

6.1.2 Models

Since this benchmarking is based on the idea of Transfer-Learning, to both extract high level performance out of the models while also doing so in less time, models have been picked

based on their performance potential, reputation, renown, their usage in recent works, and their availability of pre-trained ImageNet weights. Following these criteria, the models picked to be trained in this benchmark are listed below. A total of 23 models (see Table 6.2) belonging to various different Foundational Model architectures have been selected to be trained in order to find which models are better suited to be used in plant leaf diseases classification and which ones are not so suitable. Based on these findings, the later process of building/improving a new BM will be more streamlined and better informed.

Table 6.2: A list of all the models that will be considered for the benchmark in this work. The metrics were obtained from the official TensorFlow implementations via the model summary [127].

Ref.	Model	Total Params	Train. Params	Total Mem.	Train. Mem.
[123]	ConvNeXtSmall	49.45M	49.45M	188.65	188.65
[123]	ConvNeXtTiny	27.82M	27.82M	106.13	106.13
[124]	DenseNet121	7.04M	6.95M	26.85	26.53
[124]	DenseNet169	12.64M	12.48M	48.23	47.62
[124]	DenseNet201	18.32M	18.09M	69.89	69.02
[121]	EfficientNetV2B0	5.92M	5.86M	22.58	22.35
[121]	EfficientNetV2B1	6.93M	6.86M	26.44	26.17
[121]	EfficientNetV2B2	8.77M	8.69M	33.45	33.14
[121]	EfficientNetV2B3	12.93M	12.82M	49.33	48.91
[121]	EfficientNetV2M	53.15M	52.86M	202.75	201.64
[121]	EfficientNetV2S	20.33M	20.18M	77.56	76.97
[120]	InceptionV3	21.80M	21.77M	83.17	83.04
[128]	InceptionResNetV2	54.34M	54.28M	207.28	207.05
[129]	MobileNetV3Large	2.99M	2.97M	11.43	11.34
[129]	MobileNetV3Small	0.94M	0.93M	3.58	3.54
[122]	NASNetLarge	84.92M	84.72M	323.93	323.18
[122]	NASNetMobile	4.27M	4.23M	16.29	16.15
[118]	ResNet50V2	23.56M	23.52M	89.89	89.72
[118]	ResNet101V2	42.63M	42.53M	162.61	162.23
[118]	ResNet152V2	58.33M	58.19M	222.52	221.97
[119]	VGG16	14.71M	14.71M	56.13	56.13
[119]	VGG19	20.02M	20.02M	76.39	76.39
[130]	Xception	20.86M	20.81M	79.58	79.37

6.1.3 Benchmark Workflow

To identify which models and datasets are indeed better performing, each model has been trained on each dataset once only using TL and once with FT added on top. Each model was trained for 200 epochs each (TL & FT) with early stopping enabled with a patience of 50 to eliminate overfitting. After training is completed, the model will be reset to its best performing epoch based on the checkpoint callback considering the validation loss. Then that best model

will be tested on the train set, the validation set, and the test set one more time and metrics such as accuracy, F1-score, etc. will be recorded, compared, contextualized, and analyzed. Each model is run for 2 iterations, and results are the average across both runs, in order to obtain and present more representative results.

Algorithm 1 Loop used to train all models on all datasets for benchmarking based on [125]. This loop is carried out twice for each model-dataset combination and then results are averaged.

```

1: for each pre-trained CNN model  $F$  do:
2:   for each Dataset  $D$  do:
3:     Init Dataset  $D$ 
4:     Init Hyperparameters
5:     Init Checkpoint  $C$  & Early-Stopping  $e$  with patience = 50
6:     Init Feature Extractor CNN  $F$  with ImageNet weights  $\theta$ 
7:     Init Classifier  $C$  with random weights  $\gamma$ 
8:     Init Model  $M$  by merging  $F$  with  $C$ 
9:     # Transfer-Learning
10:    Freeze  $F$ 
11:    Train  $M$  with  $D$  until num_epochs or until  $e$ 
12:    Load Best weights for  $M$  from  $c$ 
13:    Eval Model  $M$  for  $D(train)$ ,  $D(val)$ ,  $D(test)$ 
14:    # Fine-Tuning
15:    Un-Freeze  $F$ 
16:    Train  $M$  with  $D$  until num_epochs_tuning or until  $e$ 
17:    Load Best weights for  $M$  from  $c$ 
18:    Eval Model  $M$  for  $D(train)$ ,  $D(val)$ ,  $D(test)$ 
19:    Log Results
20:   end for
21: end for

```

6.2 Benchmarking Results

When looking at the results obtained during the benchmarking experiments some trends become apparent. Table 6.3 shows the weaknesses that some of the datasets currently available pose. Datasets such as plantDoc and taiwanTomato show rather weak overall performances when looking at the test results. PlantDoc as a dataset is made up of images that are well suited to the task, but also of images that are far from the domain (e.g. PowerPoint slides). With these suboptimal images being part of the dataset, it is hardly possible to train a robust model with strong feature maps. Datasets such as taiwanTomato, novelPotato, fgvc8, cassava, and fgvc7 show low F1-Scores, which implies imbalanced data which leads to overfitting and biasing to larger classes, while not properly learning the features that make up less represented classes. One the other end of the spectrum datasets such as pld, plantVillage, and pdd271 stick out due

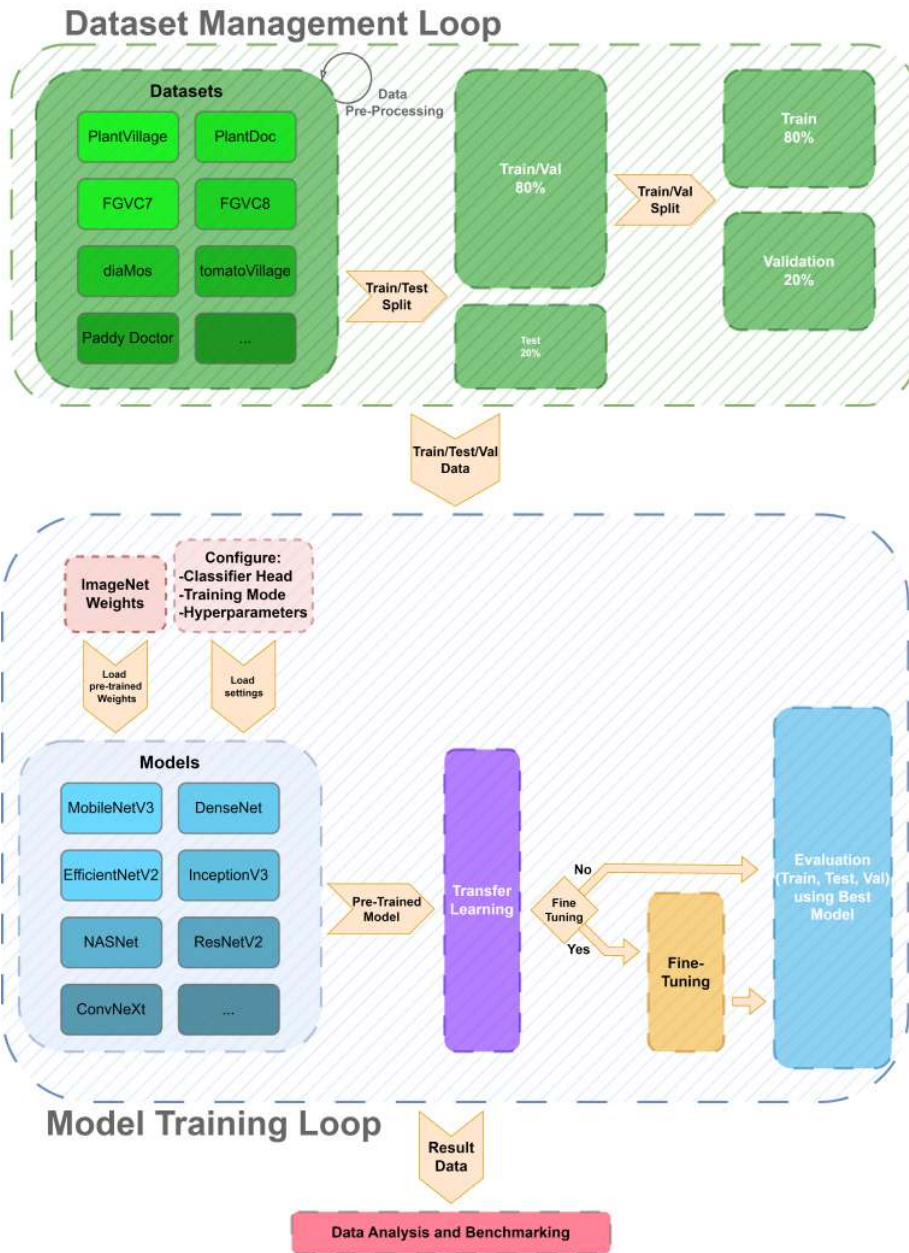


Figure 6.1: The workflow used during benchmarking

to their very high performance scores. PlantVillage and pld are lab datasets with adequately large classes (images per class). Lab datasets are easier to learn, making these datasets inherently less challenging, but the well balanced and well sized classes most likely further help to reach these levels of performance. However, lab datasets are not very robust to training in real world applications in field [15], so purely lab data trained models are not, while the results might suggest otherwise, the ideal choice. The pdd271 dataset on the other hand is taken in field, but does come with the caveat that only 10 classes are available with only 5 plant types (out of which 2 only have a single class). This showcases that a model trained on well balanced and high quality data, even if it is taken in field, can achieve results that are outstanding, signifying the importance for a solid high quality dataset. These findings will be considered when creating a new dataset for training and benchmarking.

Table 6.3: The average performance metrics for each models averaged per dataset. All values are the 5 run average and all of the metrics are based on the test dataset, except for epochs which are taken during testing. FT stands for fine-tuned.

Dataset	Acc.	F1	Epochs	Acc. FT	F1 FT	Epochs FT
pdd271	0.9748	0.9739	84.2609	0.9904	0.9903	88.6522
plantVillage	0.9747	0.9662	68.1739	0.9934	0.9906	60.3478
pld	0.9721	0.9707	48.0217	0.9872	0.9865	13.5652
rldd	0.9584	0.9432	130.0870	0.9685	0.9559	27.7609
cds	0.9340	0.9331	90.0652	0.9723	0.9719	64.5435
sugar	0.9166	0.8736	68.5652	0.9171	0.8726	4.4565
sms	0.9081	0.9075	116.9130	0.9310	0.9309	63.8261
paddy	0.8779	0.8665	113.1522	0.9209	0.9109	17.8043
tomatoVillage	0.8474	0.8213	85.1957	0.8722	0.8491	6.1087
tea	0.8418	0.8372	125.3913	0.8852	0.8809	30.3478
cucumber	0.8322	0.8317	72.0217	0.8586	0.8578	6.4565
diaMos	0.8252	0.7539	38.7391	0.8544	0.8227	2.9348
fgvc7	0.8234	0.6681	49.2826	0.8794	0.7627	6.3696
cassava	0.7521	0.5780	20.8261	0.7911	0.6447	3.9348
fgvc8	0.7480	0.4042	44.1304	0.8121	0.4715	5.6304
novelPotato	0.7196	0.6809	53.9565	0.7650	0.7350	5.6739
taiwanTomato	0.6450	0.6061	59.1739	0.6705	0.6315	4.1304
plantDoc	0.4959	0.4669	75.8043	0.5151	0.4915	3.3696

When inspecting the results grouped by model (Table 6.4 and Table 6.5), one can again see large deviations between the performances near the top and the performances near the bottom of the models compared. Even after Fine-Tuning, which helped many of the less performing models to "catch-up" so to speak, the difference in performance is still very noticeable. Models such as the models of the NASNet family, the Inception family, and the more traditional

ResNet family models can generally be found towards the bottom in terms of training accuracy. This leads to the assumptions that technologies such as the residual connections, as they are present in ResNet, or the FtC and the Multi-Scale Processing, of Inception models tend to not work as well in the field of plant leaf disease classification. Even models such as VGG19 and VGG16, which are built solely without any such advanced features have managed to consistently outperform the above mentioned models. On the other hand, models such as EfficientNet models, DenseNet models, MobileNet models and ConvNeXt models are found near the top, showcasing that the methods that are employed in their architectures (e.g. advanced activation functions, dense connections, Depthwise Separable Convolution, larger kernels, etc.) seem to be more powerful and well suited in this field. These results are helpful and will therefore be considered when constructing the Federated Learning. As mentioned above, all these results are based on [125].

Table 6.4: This list displays the average performance metrics of each model averaged across all datasets and iterations. Again, all of the metrics are based on the test dataset, except for epochs which are taken during testing. FT stands for fine-tuned.

Model	Acc.	F1	Epochs	Acc. FT	F1 FT	Epochs FT
EfficientNetV2B2	0.8699	0.8223	76.3889	0.8842	0.8420	26.2778
MobileNetV3Large	0.8698	0.8180	79.5000	0.8841	0.8363	35.4722
EfficientNetV2S	0.8680	0.8139	78.4722	0.8839	0.8395	25.0278
EfficientNetV2B0	0.8670	0.8166	77.5000	0.8844	0.8442	28.2778
EfficientNetV2B1	0.8655	0.8181	76.1389	0.8829	0.8420	28.5556
EfficientNetV2B3	0.8648	0.8134	72.8056	0.8822	0.8357	30.3333
ConvNeXtTiny	0.8611	0.8167	108.7500	0.8862	0.8419	37.1944
DenseNet201	0.8580	0.8108	64.2778	0.8775	0.8372	16.8333
ConvNeXtSmall	0.8568	0.8085	112.3889	0.8791	0.8312	28.0833
DenseNet169	0.8534	0.8024	75.4722	0.8761	0.8342	20.2222
DenseNet121	0.8530	0.8047	96.2778	0.8761	0.8339	21.2222
MobileNetV3Small	0.8491	0.7935	96.2778	0.8650	0.8131	35.3056
EfficientNetV2M	0.8424	0.7894	85.6111	0.8784	0.8352	20.0278
ResNet101V2	0.8215	0.7623	45.6389	0.8536	0.8076	13.3056
ResNet50V2	0.8188	0.7646	44.9722	0.8450	0.7986	16.3333
VGG16	0.8133	0.7636	94.3611	0.8667	0.8193	24.3333
ResNet152V2	0.8130	0.7496	46.5556	0.8511	0.8042	14.8611
VGG19	0.8130	0.7590	84.7778	0.8628	0.8144	25.0556
InceptionResNetV2	0.8050	0.7512	85.0278	0.8427	0.7979	11.8056
Xception	0.8011	0.7370	59.6111	0.8399	0.7902	17.3611
NASNetMobile	0.7891	0.7298	69.3611	0.8387	0.7877	25.7500
NASNetLarge	0.7871	0.7255	40.5556	0.8385	0.7879	14.1111
InceptionV3	0.7862	0.7242	46.3056	0.8347	0.7820	15.6944

Table 6.5: The model average accuracy rankings represent the models average accuracy across all datasets and rank them accordingly, while the average model rank takes the model rank per dataset (based on accuracy per dataset) and averages that value.

Model Rank By Avg. Acc after FT			Model Rank By Avg. Rank after FT		
Rank	Model	Average Acc.	Rank	Model	Average Rank
1	ConvNeXtTiny	0.8862	1	EfficientNetV2B2	6.4444
2	EfficientNetV2B0	0.8844	2	EfficientNetV2B0	6.5556
3	EfficientNetV2B2	0.8842	3	EfficientNetV2S	6.7222
4	MobileNetV3Large	0.8841	4	DenseNet201	6.9444
5	EfficientNetV2S	0.8839	5	EfficientNetV2B1	7.0556
6	EfficientNetV2B1	0.8829	6	ConvNeXtTiny	7.1667
7	EfficientNetV2B3	0.8822	7	EfficientNetV2M	7.3333
8	ConvNeXtSmall	0.8791	8	MobileNetV3Large	7.8333
9	EfficientNetV2M	0.8784	9	EfficientNetV2B3	8.0556
10	DenseNet201	0.8775	10	ConvNeXtSmall	8.3889
11	DenseNet169	0.8761	11	DenseNet121	8.5000
12	DenseNet121	0.8761	12	DenseNet169	9.5556
13	VGG16	0.8667	13	VGG19	11.3333
14	MobileNetV3Small	0.8650	14	VGG16	13.3889
15	VGG19	0.8628	15	MobileNetV3Small	14.0000
16	ResNet101V2	0.8536	16	ResNet152V2	15.8333
17	ResNet152V2	0.8511	17	ResNet101V2	16.1111
18	ResNet50V2	0.8450	18	InceptionResNetV2	17.6667
19	InceptionResNetV2	0.8427	19	ResNet50V2	18.5000
20	Xception	0.8399	20	NASNetLarge	18.8889
21	NASNetMobile	0.8387	21	NASNetMobile	19.4444
22	NASNetLarge	0.8385	22	Xception	20.1111
23	InceptionV3	0.8347	23	InceptionV3	20.1667

6.2.1 ViT comparison

Additionally, the CNN models were also compared to ImageNet pre-trained ViT (b16) [131, 132], to verify that CNN are the correct choice and indeed better performing than the ViT. The CNN were not trained again, so their results remain identical to above, but the ViT was trained under the same conditions and its results are compared with the CNN model’s results. ViT results are kept separate and are not included in any average scores beyond this subsection.

When looking at the scores that ViT achieved in comparison to the CNN models, then we can see that it did achieve competitive results, but was constantly beat out by CNN models, such as EfficientNet models, ConvNeXt models, and DenseNet models. This showcases that overall, CNN models do seem to still generate better results in the field. One could still consider comparing ViT to other models for their use cases, since the results are still competitive and superior to models such as NASNet, ResNet, and Inception based models in this benchmark. However, based on these results, and based on the fact that transformers are computationally

heavier and bigger than CNN and that they tend to require more data [131], here we will keep using CNN models. They performed better and with them being more lightweight and data efficient, they suit the field of plant leaf disease detection, with its limitations, better.

Table 6.6: Model ranking comparisons (same methods as in Table 6.5), including the comparison with ViT.

Model Rank By Avg. Acc after FT			Model Rank By Avg. Rank after FT		
Model	Avg. FT Test Acc	Rank	Model	Average Rank	Rank
ConvNeXtTiny	88.62%	1	EfficientNetV2B2	6.78	1
EfficientNetV2B0	88.44%	2	EfficientNetV2B0	6.89	2
EfficientNetV2B2	88.42%	3	EfficientNetV2S	7.11	3
MobileNetV3Large	88.41%	4	DenseNet201	7.33	4
EfficientNetV2S	88.39%	5	EfficientNetV2B1	7.33	5
EfficientNetV2B1	88.29%	6	ConvNeXtTiny	7.44	6
EfficientNetV2B3	88.22%	7	EfficientNetV2M	7.72	7
ViT	88.14%	8	MobileNetV3Large	8.33	8
ConvNeXtSmall	87.91%	9	EfficientNetV2B3	8.44	9
EfficientNetV2M	87.84%	10	ConvNeXtSmall	8.78	10
DenseNet201	87.75%	11	DenseNet121	8.89	11
DenseNet169	87.61%	12	DenseNet169	10.11	12
DenseNet121	87.61%	13	ViT	10.56	13
VGG16	86.67%	14	VGG19	11.89	14
MobileNetV3Small	86.50%	15	VGG16	14.06	15
VGG19	86.28%	16	MobileNetV3Small	14.78	16
ResNet101V2	85.36%	17	ResNet152V2	16.67	17
ResNet152V2	85.11%	18	ResNet101V2	16.89	18
ResNet50V2	84.50%	19	InceptionResNetV2	18.61	19
InceptionResNetV2	84.27%	20	ResNet50V2	19.22	20
Xception	83.99%	21	NASNetLarge	19.78	21
NASNetMobile	83.87%	22	NASNetMobile	20.33	22
NASNetLarge	83.85%	23	Xception	21.00	23
InceptionV3	83.47%	24	InceptionV3	21.06	24

7. Data Augmentation Assessment

Datasets in the field are still considered to be sparse [14, 11, 126] and image collection is tedious and laborious and requires many prerequisites such as access to a large field of crops, equipment, hardware, expert staff, collection staff, labeling, and large amounts of time. This is not always possible due to different factors. However, if not enough data is available, training sufficient models can be difficult if not even impossible. One way to enlarge datasets artificially is augmentation. Data augmentation is the process of altering the images in a way where they are different enough from the original so that they pose an additional challenge and learning point to the model, while not losing the important and classifying features. Like this, without the hassle of collecting new plant leaf data, one can extend the dataset and improve model performance. To ensure that this is true in this case as well, a set of experiments were carried out to validate these claims. The experiments, along with the results and analysis are based on the findings found in [133].

7.1 Augmentation Techniques

Augmentation comes in different types in which it can be applied. Here noise based augmentation, transformation based augmentation, and color based augmentation techniques will be applied, used, and compared to find the best possible augmentation methods for dataset enlargement and model training in the field of plant leaf disease classification. Color, noise and transformation based methods were used due to the fact that they are non-invasive to the features of the images while also being fast, easily reproducible and adjustable.

Table 7.1: List of methods and values for color augmentation.

Method	Value
Brightness	-0.75, 0.75
Hue Shift	-20, 20
Contrast	-0.25, 0.25
Channel Shift	75

Table 7.2: The noise augmentation method with the values used during augmentation.

Method	Value
Gaussian Noise	mean: 0, stddev: 1

7.1.1 Color

Color based augmentation methods change the images by changing the colors of the image. These augmentations can simulate the way different camera equipment might differ in how it captures images or how the same plant might look different in different conditions (e.g. weather). Common and effective ways of making these changes are achieved by adjusting the brightness, contrast or by shifting the image’s hue or channels. These methods all, if done within certain thresholds, do not disturb the image enough to a point where features would get lost, but change the image enough to where models would have to learn more robust features. The values with which we tested the effects of color augmentation on plant leaf disease classification are listed in Table 7.1 and the effects on the base image can be seen in Figure 7.1.

7.1.2 Noise

Noise augmentation adds noise to the image to add imperfections to the images. These imperfections simulate different imperfections that could appear during image capturing (e.g. camera, light conditions, compression, etc.). The added noise adds complexity to the image in a way that is not helpful to the classification task, and as such the model needs to learn how to form feature maps that are robust to such noisy imperfections. The values used can be seen Table 7.2 and the effect are shown in Figure 7.2.

7.1.3 Transformation

Transformation based augmentation methods change the image by transforming it. In this study rotation and flipping (mirroring) were applied to the image. This simulates the different ways

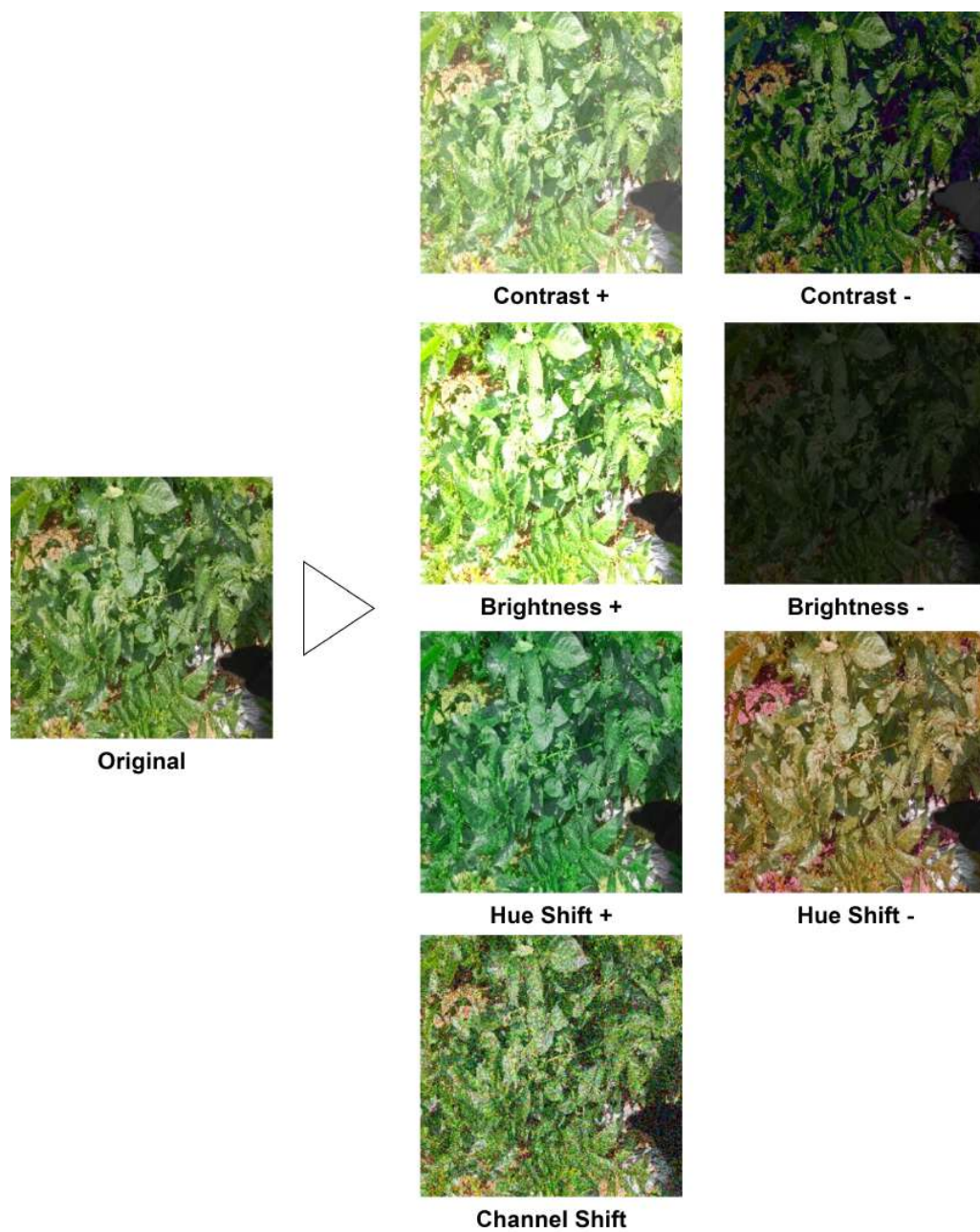


Figure 7.1: The different color based data augmentation techniques used in this paper visualized. Images are taken from the novelPotato [65] dataset.



Figure 7.2: The noise based data augmentation technique used in this paper visualized. Images are taken from the novelPotato [65] dataset.

Table 7.3: Transformation augmentation methods.

Method	Value
Rotation	90deg, 180deg, 270deg
Flip	horizontal, vertical

of taking images could affect how they are represented in the dataset. Simply taking the image from another angle or another direction can easily happen during image capturing and through the augmentation methods listed below these differences can be simulated and applied to an already captured dataset. This will expose the model to more different data and can lead to better performance in more different scenarios. The methods and values are listed in Table 7.3 and the effects can be seen in Figure 7.3.

7.2 Augmentation Methodology

To obtain representative results without having to run an equally, if not more, intensive, complex, and time consuming set of experiments, to obtain the results for augmentations only a subset of datasets and models has been selected. To keep other variable at a constant, 2 datasets have been chosen (novelPotato and pld, see Table 7.4), both of which are of potato leaves, but one is taken in lab with the other one having been taken in field. This allows an analysis of the effect on both different types of data. The models chosen here represent a wide variety of the families of models present in the benchmark, to obtain results for many different models, from which generalization will be possible. Each dataset will once be augmented with only color techniques, once with only noise techniques, once with only transformation techniques, and once with all three techniques combined (see Table 7.6 for dataset sizes post augmentation). Then each model will be trained on each of the 5 variations (no augmentation, color, noise,

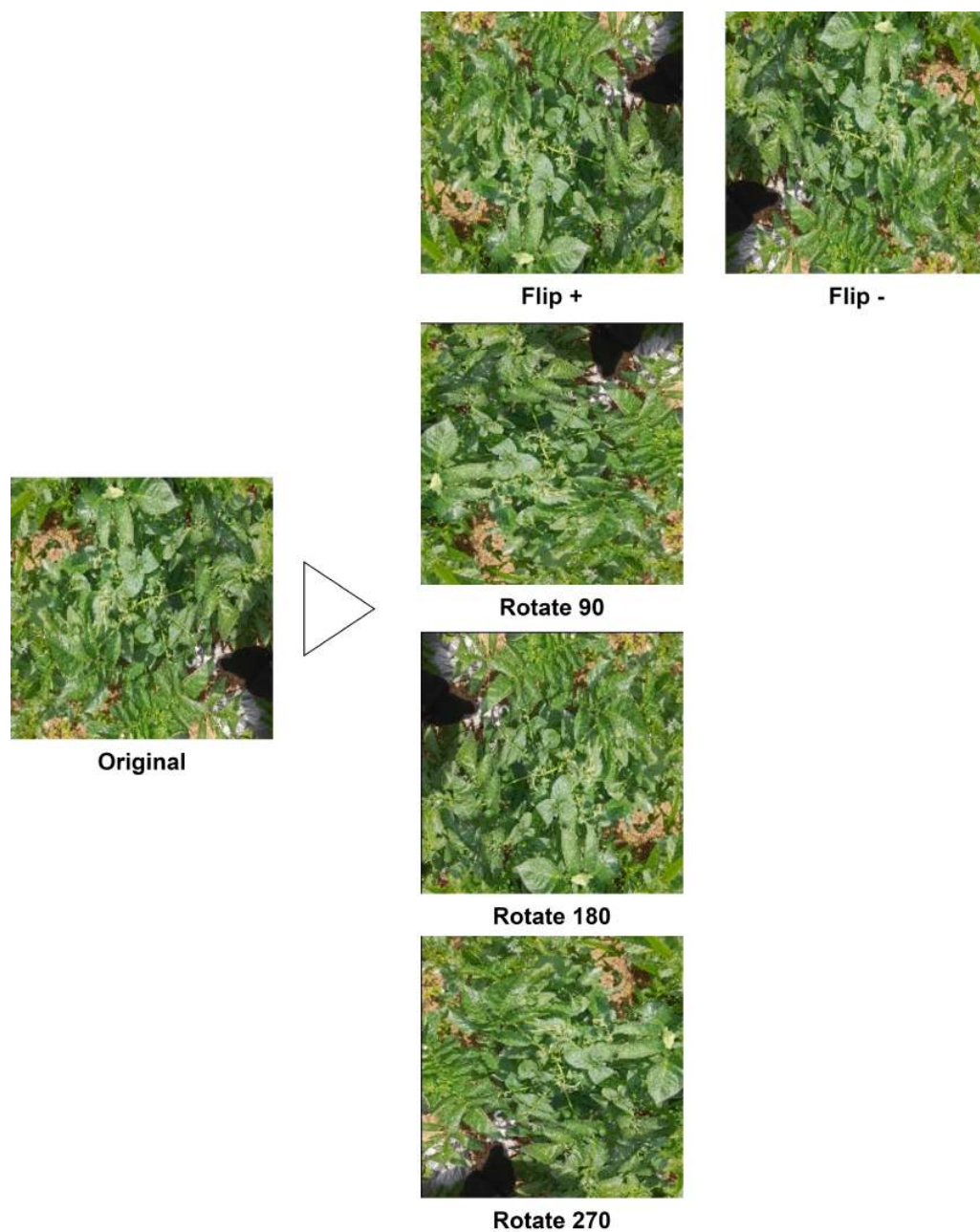


Figure 7.3: The different transformation based data augmentation techniques used in this paper visualized. Images are taken from the novelPotato [65] dataset.

Table 7.4: List of all the datasets considered in the augmentation experiments runs.

Ref.	Dataset	Type	Plant	Num. Class	Total Img.
[65]	novelPotato	Hybrid	Potato	7	3,076
[73]	pld	Lab	Potato	3	4,062

Table 7.5: Models used for the augmentation experiments.

Ref.	Model	Total Params	Train. Params	Total Mem.	Train. Mem.
[129]	MobileNetV3Large	2.99M	2.97M	11.43	11.34
[124]	DenseNet121	7.04M	6.95M	26.85	26.53
[124]	DenseNet201	18.32M	18.09M	69.89	69.02
[121]	EfficientNetV2B0	5.92M	5.86M	22.58	22.35
[121]	EfficientNetV2B2	8.77M	8.69M	33.45	33.14
[118]	ResNet50V2	23.56M	23.52M	89.89	89.72
[118]	ResNet152V2	58.33M	58.19M	222.52	221.97
[123]	ConvNeXtSmall	49.45M	49.45M	188.65	188.65
[119]	VGG19	20.02M	20.02M	76.39	76.39

transformation, all augmentations) for both datasets.

7.3 Augmentation Results

The results, as can be seen in Tables 7.7 and 7.8, showcase that employing augmentation methods to extend datasets in the field of plant leaf disease classification, lead to better performing and more robust models. While no actual new data (as in new pictures taken in field) has been added to the datasets, the challenges provided by these augmented images, through image altering methods such as flipping, mirroring, contrast and brightness adjustments and noise, do lead to better results when compared to the results obtained by models without augmentation, and

Table 7.6: Datasets sizes for the different augmented datasets.

Dataset	Healthy	E. Blight	L. Blight
pld	918	1,466	1,273
pld + Color	7,344	11,728	10,184
pld + Transform	5,508	8,796	7,638
pld + Noise	1,836	2,932	2,546
pld + Combined	13,770	21,990	19,095
Dataset	Healthy	Fungal	Bacterial
novelPotato	160	598	455
novelPotato + Color	1,280	4,784	3,640
novelPotato + Transform	960	3,588	2,730
novelPotato + Noise	320	1,196	910
novelPotato + Combined	2,400	8,970	6,825

Table 7.7: The average test scores of each augmentation techniques across all models and datasets.

Augmentation	Accuracy	F1-Score	Recall	Precision
Augmentation Combined	98.82%	98.64%	98.82%	98.82%
Augmentation Transform	98.60%	98.36%	98.60%	98.62%
Augmentation Color	97.89%	97.67%	97.89%	97.90%
Augmentation None	97.58%	97.08%	97.58%	97.63%
Augmentation Noise	97.22%	96.79%	97.20%	97.22%

Table 7.8: The test scores for each augmentation method across all models based on the dataset.

Augmentation	Dataset	Accuracy	F1-Score	Recall	Precision
Augmentation Transform	pld	99.86%	99.86%	99.86%	99.86%
Augmentation Combined	pld	99.78%	99.78%	99.78%	99.78%
Augmentation Color	pld	99.42%	99.42%	99.42%	99.45%
Augmentation None	pld	99.34%	99.28%	99.34%	99.34%
Augmentation Noise	pld	99.04%	99.04%	98.98%	99.04%
Augmentation Combined	novelPotato	97.85%	97.50%	97.85%	97.85%
Augmentation Transform	novelPotato	97.34%	96.85%	97.34%	97.38%
Augmentation Color	novelPotato	96.36%	95.92%	96.36%	96.36%
Augmentation None	novelPotato	95.81%	94.87%	95.81%	95.92%
Augmentation Noise	novelPotato	95.41%	94.53%	95.41%	95.41%

that is true for the lab and the field dataset. Combining all methods into one big augmentation pool and applying them to all images managed to yield the best results when combining the results for both datasets and it also did so for the novelPotato dataset taken in field. The pld lab dataset achieved slightly better results only using transformation, suggesting that transformation is the most powerful of the tested methods. However, since combining all 3 did perform best in the field+lab test and in the field only tests, moving forward, all methods will be combined to create a new dataset. Using transformation only would be slightly faster, but since that is not an issue, and since "augmentation combined" was best on hybrid and field only data, which the new dataset will be, these results carry the most weight in this case.

All this is possible without having to spend any additional time or money on obtaining new images in field, a task that is not feasible, or even impossible for many. These findings will be implemented into the dataset construction. Results are an extension of the work in [133].

8. Dataset Construction

In order to construct a dataset that is large enough and diverse enough, the methods identified in Chapters 6 and 7 will be applied. Since it is not possible, as part of this work, to collect new data, due to the unavailability of fields and crops, existing datasets will be combined, merged, adjusted, and augmented in order to achieve a dataset with the desired characteristics. The final dataset will be a dataset with hybrid image sources (field and lab) to expose the model to as many different image types, in terms of diseases, plants, and conditions, in order to train a model that is as robust and generalizable as possible [62, 63, 64]. All classes will be set up in a way in which they will be perfectly balanced to support actual learning and to avoid biases in the trained weights. The dataset introduced here was submitted for publication as part of the following paper [134]. As such, chapter is based on the findings presented in this paper.

8.1 Dataset Construction Methods

Selected based on the benchmark, as well as on the original composition of each dataset, a set of 9 datasets have been chosen to be combined into a single large scale benchmarking dataset for this work. The datasets of choice can be found in Table 8.1. Other datasets have not been selected based on their weak performance in the benchmark (plantDoc, taiwanTomato, novelPotato), due to their redundancy (fgvc7 has been updated to fgvc8, tomatoVillage is a tomato dataset in lab conditions which plantVillage already covers, and pld is a lab potato dataset that again plantVillage already includes), and their small size (rldd, tea, cucumber). Also, during construction, an eye was kept on the distribution of lab to field images, to make sure that a good balance is kept. As a result the resulting dataset, after simply combining all the directories would end up being 95 classes with around 125,000 images. However, this does not consider overlap in classes between different datasets, where both the plant and the disease

Table 8.1: List of all the datasets that are considered to be part of the new benchmarking dataset. Given are all key metrics and performance metrics from the benchmarking [125].

Dataset	Type	Plant	Num. Class	Total Img.	Acc.	F1	Acc. FT	F1 FT
cds	Field	Corn	3	1,571	93.338%	93.248%	97.323%	97.286%
fgvc8	Field	Apple	12	18,632	74.810%	40.618%	81.754%	48.848%
plantVillage	Lab	Multi	38	54,304	97.492%	96.654%	99.377%	99.117%
paddy	Field	Rice	10	10,407	87.844%	86.671%	92.389%	91.461%
sugar	Hybrid	Sugarcane	10	6,405	91.582%	87.267%	91.634%	87.139%
cassava	Field	Cassava	5	21,397	75.175%	57.688%	79.427%	64.935%
pdd271	Field	Multi	10	7,555	97.495%	97.410%	99.058%	99.052%
sms	Field	Strawberry	3	1,583	91.144%	91.090%	93.278%	93.276%
diaMOS	Field	Pear	4	3,006	82.412%	75.049%	86.201%	84.002%

Table 8.2: Classes that were deleted from the dataset and the reason they were.

Dataset	Class	Reason for exclusion
fgvc8	Apple Powdery Mildew Complex	too small
fgvc8	Apple Rust Complex	too small
fgvc8	Apple Rust Frog Eye Leaf Spot	too small
fgvc8	Apple Frog Eye Leaf Spot Complex	too small
fgvc8	Apple Scab Frog Eye Leaf Spot Complex	too small
fgvc8	Complex	complex
fgvc8	Scab Frog Eye Leaf Spot	multi disease
PlantVillage	Potato Healthy	too small
diaMOS	Pear Healthy	too small
diaMOS	Pear Curl	too small

are the same and it does also not consider some of the weaknesses observed in the benchmark.

8.1.1 Class Cleanup

To ensure that each class truly represents a plant-disease combination that is not present in any other class and to make sure that all classes follow the same principles while also assuring class balance, some classes need to be combined while others need to be deleted from the dataset. Classes chosen for deletion (see Table 8.2) were picked based on a few criteria. On one hand classes with 200 or less images were deleted to preserve a adequate number of unique images before augmentation. Additionally, two more fgvc8 classes were deleted as they were complex and multi-disease classes, that did not fit with the rest of the classes that were all single disease.

With the deletion of 10 classes, the dataset now has 85 classes, not all of which are unique though. To ensure uniqueness a total of 10 classes need to be combined, as there are classes that contain the same plant-disease combination. These 10 classes will be combined into 5 corresponding classes ensuring uniqueness for the resulting dataset. The classes to be combined

Table 8.3: Classes that were combined in order to create unique classes for the final dataset.

Dataset 1	Class 1	Dataset 2	Class 2
cds	Gray Leaf Spot	PlantVillage	Cercospora Leaf Spot Gray Leaf Spot
cds	Northern Leaf Blight	fgvc8	Northern Leaf Blight
fgvc8	Healthy	PlantVillage	Apple Healthy
fgvc8	Rust	PlantVillage	Cedar Apple Rust
fgvc8	Scab	PlantVillage	Apple Apple Scab

Table 8.4: Metrics of the new dataset.

Number of Different Plants	25
Number of Classes	80
Number of Images Total	304,507
Train-Test Split (before val split)	80-20
Number of Images Train (before val split)	280,000
Number of Images Test	24,507
Train-Val-Test Split (after val split)	64-16-20
Number of Images Train (after val split)	224,000
Number of Images Validation (after val split)	56,000
Image Size	224x224x3

can be seen in Table 8.3.

Post deletion and combination the dataset is 80 classes in size, but the classes are heavily imbalanced, with some classes also being undersized. To ensure perfect balancing and, as part of that, to lower the risk of biasing during training, all classes will be set to be of the same size. First, to guarantee that robustness can be observed during training, the dataset will be split 80-20 into a train set and a test set (the test set will not be augmented). Then, each train class will be expanded through the augmentation techniques introduced and discussed in Chapter 7, due to their proven positive impact on training. Next, each class will be cutdown to exactly 3,500 images per class, creating a perfectly balanced dataset. Out of the augmented set, each class will randomly sample 3,500 images for the final dataset, creating a final train dataset of 304,507 images across 80 classes. Before training, the train set will be further split 80-20 into actual train data and validation data, to keep track of unseen image performance during training, before the final model will be tested on the un-augmented test set at the end. The key metrics for the new dataset, which is called PLDC-80, are listed in Table 8.4.

8.1.2 Dataset Method Availability

Due to the fact that the dataset is a merger of preexisting datasets, all of which come with different kinds of licenses, uploading the final dataset is not possible, since some dataset's

licenses prohibit redistribution. Instead, a detailed method for how one can reconstruct the dataset is available at [135].

9. Model Construction

A dedicated Base Model for the field of plant leaf disease classification would potentially offer advantages such as faster, more robust, and more stable training, even in scenarios where data is sparse (as is often the case in this field). Such a model needs to first be constructed (based on an existing and already powerful architecture) before being trained on the PLDC-80 dataset to construct powerful and domain relevant feature extractors that contain feature maps that are relevant to the field specifically. This includes a multi-step process of first identifying a baseline model to base the architecture upon, then, if possible, improving said baseline to help it achieve even better results. Then that model, with the pre-trained weights, needs to be compared to the baseline model trained on general data, e.g. ImageNet, to see if it does indeed improve training and final results. This step requires yet another new dataset, that is unknown to the model, meaning data that is not part of the PLDC-80 dataset, and ideally also contains data that does not correspond to plant-disease class combinations found in PLDC-80 (as much as possible). The model and findings presented in this chapter will be submitted for publication in [136]. This chapter is based on the referenced paper, which is written as part of the work towards this thesis.

To build a new improved model architecture one needs to identifying potential baseline models and technologies that could improve the model and then implement them to assess their performance. To compare the models in a constant test environment with no outside inconsistencies, that allow for fair and accurate comparisons of the models performance only (to make sure that the model is truly the variable that is being tested and compared), the following settings were used and they remain constant across all tests for all models. The values kept constant can be seen in Table 9.1.

Table 9.1: Constant setup during model training and evaluation across all architectures.

Parameter/Setting	Value
Batch Size	128
Epochs	150
Optimizer	Adam
Callbacks	Checkpoint (Val. Acc.)
Train Dataset	224,000
Val. Dataset	56,000
Test Dataset	24,507
Number of Classes	80
Input Size	224x224x3
Loss	Categorical Crossentropy
Machine	CPU: Intel Xeon Gold 6330, GPU: NVIDIA A100 SXM4 40GB, RAM: 125GB
Evaluation	Based on the best performing epoch Checkpoint

Table 9.2: List of the models that were compared in the benchmark.

Ref.	Model	Total Params	Train. Params	Total Mem.	Train. Mem.
[124]	DenseNet201	18.32M	18.09M	69.89	69.02
[121]	EfficientNetV2B2	8.77M	8.69M	33.45	33.14
[121]	EfficientNetV2S	20.33M	20.18M	77.56	76.97
[123]	ConvNeXtSmall	49.45M	49.45M	188.65	188.65
[123]	ConvNeXtTiny	27.82M	27.82M	106.13	106.13

9.1 Baseline Model search

Based on these settings, different baseline models were trained (based on the top performing benchmarking models) to find the best performing model to then use it as the baseline model to built upon and compare to. The models used can be seen in Table 9.2. Models were trained on the new PLDC-80 dataset and then compared on their performance on the test set (which is both unseen to the trained model as well as un-augmented). After 150 epochs of training the model is reset to the best performing epoch (based on validation accuracy). This best performing model is then used for evaluation on all 3 sets (train, validation, test). As mentioned earlier, the models will be judged on their accuracy score on the test set, to evaluate which model is best performing. Results for these baseline model tests can be seen in Table 9.3.

Table 9.3: Baseline model performance comparison.

Model	Train Accuracy	Validation Accuracy	Test Accuracy
ConvNeXtTiny	99.38%	90.71%	83.86%
ConvNeXtSmall	99.44%	91.43%	84.07%
EfficientNetV2B2	99.47%	94.62%	89.35%
EfficientNetV2S	99.45%	94.64%	89.57%
DenseNet201	99.38%	95.07%	91.10%

Based on the results observed in Table 9.3, one can conclude that DenseNet201 is ideal to be used as the basis of the new model, as it is both top performing and also modular and block based. It managed to outperform even the best of the other models by over 1%, which is quite significant in a scenario where the dataset is this large and where all models already managed to achieve good results. As such, as mentioned earlier, the DenseNet201 model architecture has been chosen to be used as the baseline model to be built upon.

9.2 Model Improvement Methodology

With the new PLDC-80 dataset in place and through the findings of the benchmarks as well as the test, constructing the new model based on the DenseNet201 baseline is the next step. The improved model should be able to outperform other CNN baselines on the new PLDC-80 dataset and then, after training, manage to outperform the baseline in a Transfer-Learning task, where the trained model with the weights obtained during training will be compared with the baseline model trained on ImageNet when exposed to another plant leaf disease classification dataset. Ideally the new model can train TL model faster, more stable, and at the end of training perform better.

9.2.1 Model Architecture

Based on the findings of the benchmark, as well as after additional testing on the new dataset, the baseline model that this model will be based on will be the DenseNet201 architecture, which has proven to be very capable of training strong plant leaf disease classifying models during the benchmark and also during the experiments here. DenseNet201, as can be seen in Chapter 5 and Appendix B, is a model that features dense residual connection, which allow the model to carry attention maps into deeper layers, which improve gradient flow, lessen the vanishing gradient problem, and allow feature reuse. DenseNet201's architecture can be seen in Figure 9.1.

It feeds input images into the pre-amble which houses a padded convolutional layer with kernel size 7 and stride 2 to get a large kernel look at the image before downsizing the input for the actual dense blocks. Then a batch normalization layer is applied to the output of the convolutional layer and following that is the relu activation. Next is a padding layer before max

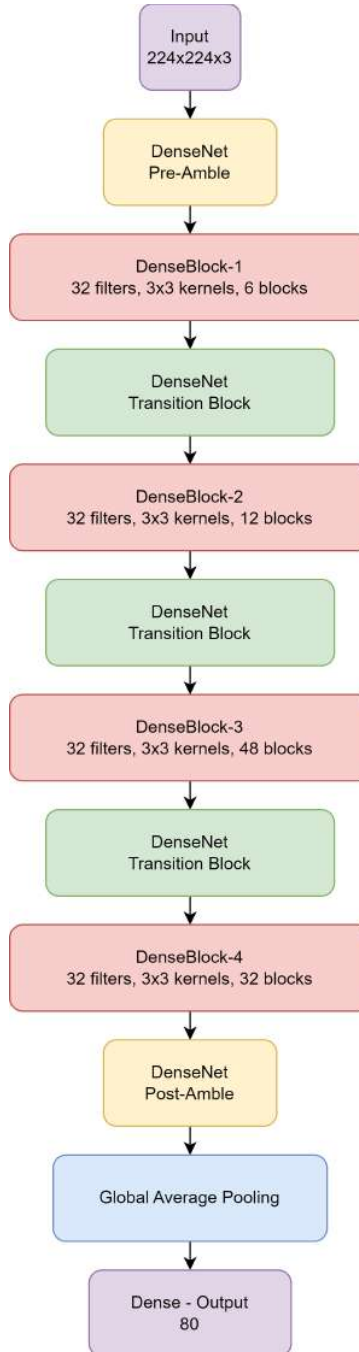


Figure 9.1: DenseNet201's architecture before modification

pooling with stride 2. Then come the dense blocks, which are stacks of the dense layer blocks as seen in Figure B.4 (e.g. the first dense block as seen in Figure 9.1 would have 6 Figure B.4 layer blocks stacked on top of each other). Each layer block receives the concatenated input of all previous layer's outputs in said block. These dense blocks are divided by transition blocks. These transition blocks break up the dense connections, meaning they only exist within any given block but not across blocks, as they need to be of the same dimensions (width and height), which is not given after transition. The transition blocks first apply batch normalization to the input, then a relu activation before applying a Pointwise Convolution (a 1x1 convolution) that reduces large depth dimension of the input to a given new channel size. This is then followed by an average pooling layer with stride 2, reducing the width and height dimensions. After several stacks of these dense and transition blocks, follows the post-ambly. The post-ambly simply includes a batch normalization layer after which comes a relu activation, which completes the classifier. With these methods an un-edited model can already achieve high level results, as it is already fine-tuned to work in large scale, multi-class image classification tasks.

9.2.2 Possible Improvements

To improve models such as DenseNet201, a lot of different techniques can be implemented, be it from other Foundational Model that are based on different philosophies, or additional on techniques such as attention blocks, etc. However, since models like DenseNet are already finely tuned to work extremely well on large datasets for image classification, one needs to act thoughtfully and carefully when implementing such new concepts into the architecture, since small changes to the model are not guaranteed to improve the performance, but on top also run the risk of instead lowering the performance the model can achieve. As such, methods need to be well considered and tested, to make sure that they do indeed help the model achieve better results, as opposed to simply creating a different more complex model, that does however not manage to achieve any better results. Methods considered for improving the baseline model included, but were not limited to:

- GELU Activations
- Larger Kernels
- Layer Normalization

- ConvNeXt Blocks
- More filters
- More Dense Layers per block
- Dropout
- Progressive receptive field expansion
- Squeeze & Excitation (SE)
- Convolutional Block Attention Module (CBAM)
- Spatial Attention (SA)
- Large Kernel Attention
- Super Latent Connections
- Swish Activations
- Channel Attention (CA)

Many of these approaches were tested in different configurations. Large kernels were for example tested in 5x5 and 7x7, and also in progressive receptive field expansion setups, both per block and inside the blocks. Many of these methods were tested in such different setups, to find the ideal selection and combination of methods that improve the performance of DenseNet201 specifically for the field of plant leaf disease classification.

These methods and technologies now need to be applied to said DenseNet201 architecture and compared, in order to identify the ideal combination of model and additional methods to create the architecture for the Base Model. In testing the following results were observed which can be seen in table 9.4.

9.2.3 Successful Improvements

As seen in Table 9.4, the best performing model resulting from the numerous testing runs was DenseNet201 with Swish Activations in all blocks and a Channel Attention Block at the end of the CNN classifier. This model managed to outperform the baseline model on the test dataset

Table 9.4: Model modification comparison results. Here DN201 stands for DenseNet201. The Train, Val and Test columns list the accuracy for each set.

Baseline	Added Methods	Train	Val	Test
DN201	Swish + Channel Attention Block	99.41%	94.80%	91.46%
DN201	Channel Attention Block	99.44%	95.08%	91.40%
DN201	Swish	99.41%	94.72%	91.40%
DN201	Spatial Attention Block	99.42%	94.91%	91.21%
DN201	Channel Attention + Bigger Kernel per Block (1st Block 3x3, 2nd Block 5x5, 3rd Block 7x7)	99.37%	94.77%	91.20%
DN201	Kernel Size 5x5 all Blocks	99.44%	95.22%	91.11%
DN201	None	99.38%	95.07%	91.10%
DN201	Large Kernel Attention Block	99.31%	94.71%	90.70%
DN201	Swish + CBAM Attention Block + Bigger Kernel per Block (1st Block 3x3, 2nd Block 5x5, 3rd Block 7x7)	99.41%	95.02%	90.66%
DN201	Swish + Channel Attention Block (Swish also in Channel Attention Block)	99.41%	94.94%	90.65%
DN201	CBAM Block	99.38%	94.98%	90.64%
DN201	Swish + Channel Attention (After every Dense Block)	99.32%	94.50%	90.51%
DN201	Squeeze & Excitation Attention Block	99.46%	94.99%	90.48%
DN201	Channel Attention + Super Latent Connections	99.49%	94.68%	90.46%
DN201	Deeper Last Block (48 Dense Layers in Last Block)	99.43%	94.89%	90.44%
DN201	Swish + Channel Attention Block + 5x5 kernel in all Blocks	99.37%	94.86%	90.34%
DN201	Bigger Kernel per Block (1st Block 3x3, 2nd Block 5x5, 3rd Block 7x7)	99.35%	94.94%	90.21%
DN201	Kernel Size 7x7 all Blocks	99.39%	94.76%	90.11%
DN201	Last Dense Block with growth rate 48, 48 layers and 7x7 kernel	99.38%	94.69%	90.09%
DN201	Growth rate 48 in 3rd Dense Block and 64 in last Dense block	99.45%	94.72%	90.03%
DN201	Replacing Dense Convolution Layers with ConvNeXt like blocks (and ConvNeXt depth and width) while maintaining Dense Connections	99.34%	94.12%	89.97%
DN201	Channel Attention (After every Dense Block)	99.31%	94.63%	89.67%
DN201	Light Super Latent Connection	99.44%	94.70%	89.57%
DN201	Light Plus Super Latent Connection	99.46%	94.27%	89.54%
DN201	Super Latent Connection	99.50%	94.60%	89.54%
DN201	Channel Attention Block + 7x7 kernel size in last Dense Block	99.40%	94.80%	89.51%
DN201	Bigger Kernel inside each Block (first 1/3rd of layers in Block 3x3, 2nd 1/3 5x5, 3rd 1/3 7x7)	99.37%	94.52%	89.22%
DN201	Replacing Dense Convolution Layers with ConvNeXt like blocks while maintaining Dense Connections	99.15%	92.70%	88.03%
DN201	Adding ConvNeXt block after last Dense Block	99.09%	93.29%	87.89%

with 91.46%, where the baseline model reached 91.10%. This might not seem like a large improvement at first, but with the dataset being this large, it does favor large scale models, meaning the baseline is already well suited as is (as is also proven by the benchmarks and the comparison on the dataset to other models). Also, with DenseNet201 already performing as well as it did with over 91% the room for further improvements is small and limited. As such, 0.36% does actually show fairly decent improvements and it is a 4.04% decrease of miss classifications over the whole test dataset. It does also equal around 88 more images that were classified correctly in the test set, which could make a difference in on field applications.

The two techniques that managed to elevate the performance of the baseline model were SiLU/Swish-1 activations and Channel Attention. Both methods as well as the resulting model architecture look and work as follows:

9.2.3.1 Swish Activation (SiLU)

Swish Activations, also known as Swish-1 or SiLU (Sigmoid Linear Unit) (Equations (9.1) and (9.2)) [137, 138, 139], as they are used in EfficientNet architectures (which have also performed well in the benchmarks) are an activation function that, unlike the ReLU used in DenseNet, does not set all negative inputs to 0, which helps it overcome the dying ReLU problem of vanishing gradients. SiLU is self-gated, meaning that it multiplies the result of the sigmoid function of the input by the input itself, scaling the output by the activation level. As can be seen in Figure 9.2, SiLU is a smooth activation function, especially when compared with the very sharp ReLU activation. This smoothness allows better gradient flow through the network which can improve learning. SiLU is non-monotonic, not increasing linear after 0, this allows it to achieve better generalization and can help learn more complex patterns.

$$f(x) = x * sigmoid(x) \tag{9.1}$$

$$sigmoid(x) = \frac{1}{1 + e^{-x}} \tag{9.2}$$

Implementing SiLU into the DenseBlocks improved the performance of the DenseNet201 architecture when looking at the test dataset performance, which is best suited to showcase the robustness and generalization ability of the final model.

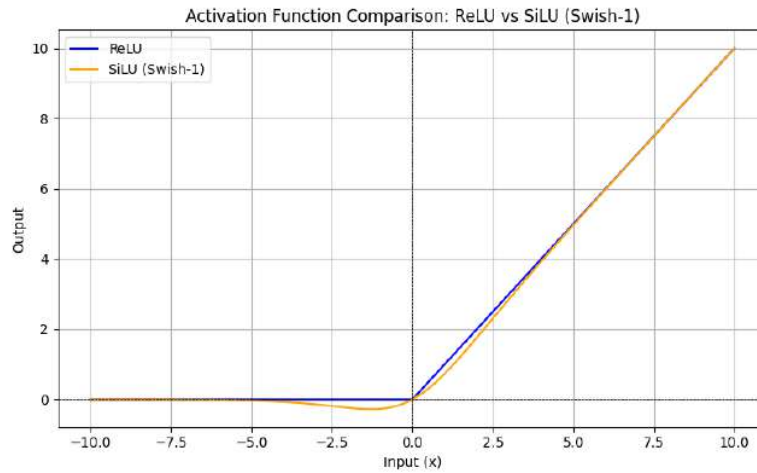


Figure 9.2: A visual comparison of the ReLU and the SiLU/Swish activation functions.

9.2.3.2 Channel Attention

The second mechanism that managed to improve the performance of DenseNet201 was adding a Channel Attention block [140, 141] to the end of the DenseNet201 model. Channel Attention is a mechanism that ranks input channels based on their importance to the classification task and weights them accordingly. Channel Attention does that by first reducing each channel to a single value, once through global average pooling and global max pooling. Both of these feature vectors of size $1 \times 1 \times \text{channel size}$ are then passed into an encoder-decoder fully connected block separately, before being added. Then, after sigmoid activation, each channel is multiplied by said sigmoid value to scale them based on their importance to the task. This allows the model to focus on important feature maps that actually help the model classify images into the correct class and focus less on feature maps that are not as useful to the task at hand. See Figure 9.3 for a visual representation of that method.

9.2.3.3 Combined Model

As a result of both of the above mentioned techniques managing to improve the performance of the baseline DenseNet201 architecture for the field of plant leaf disease classification, the next step is to combine them into one model to benefit from the advantages they both present. The resulting PLDC-Net architecture replaces all the ReLU connections in the Dense Preamble, the Dense Blocks and also in the Dense Postamble. The CA Block still uses ReLU, since

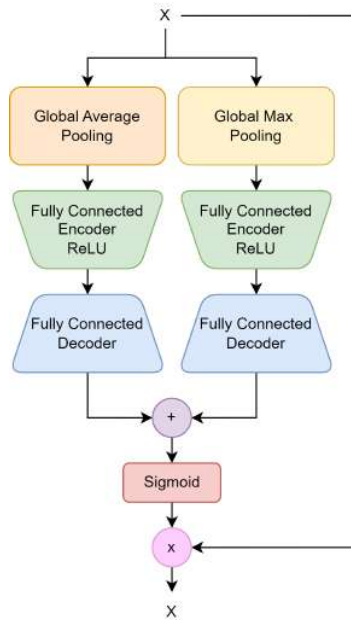


Figure 9.3: Flowchart of the Channel Attention Block.

experiments of also using Swish in the attention block yielded worse results. The CA block is positioned right after the dense post-amble block and before the global average pooling layer, where it produced the best results, when compared to other positioning and also when compared to using multiple CA blocks across the network. This resulting model will be called PLDC-Net, more details can be found in [136].

9.3 Transfer-Learning

To validate that the resulting pre-trained model did not only achieve better generalization results on the PLDC-80 test dataset, one now needs to create yet another dataset that the pre-trained model can now be transfer-learned on. Ideally, this dataset does not have much overlap with the PLDC-80 dataset in terms of classes (plant-disease overlap) and it should not contain any images that were in the PLDC-80 dataset during training.

9.3.1 PLDC-6

To facilitate these further TL experiments, a new dataset needs to be constructed that is, as mentioned earlier, relevant to the field of plant leaf disease classification, representative of a dataset one might collect in future research, and different enough from the original PLDC-80,

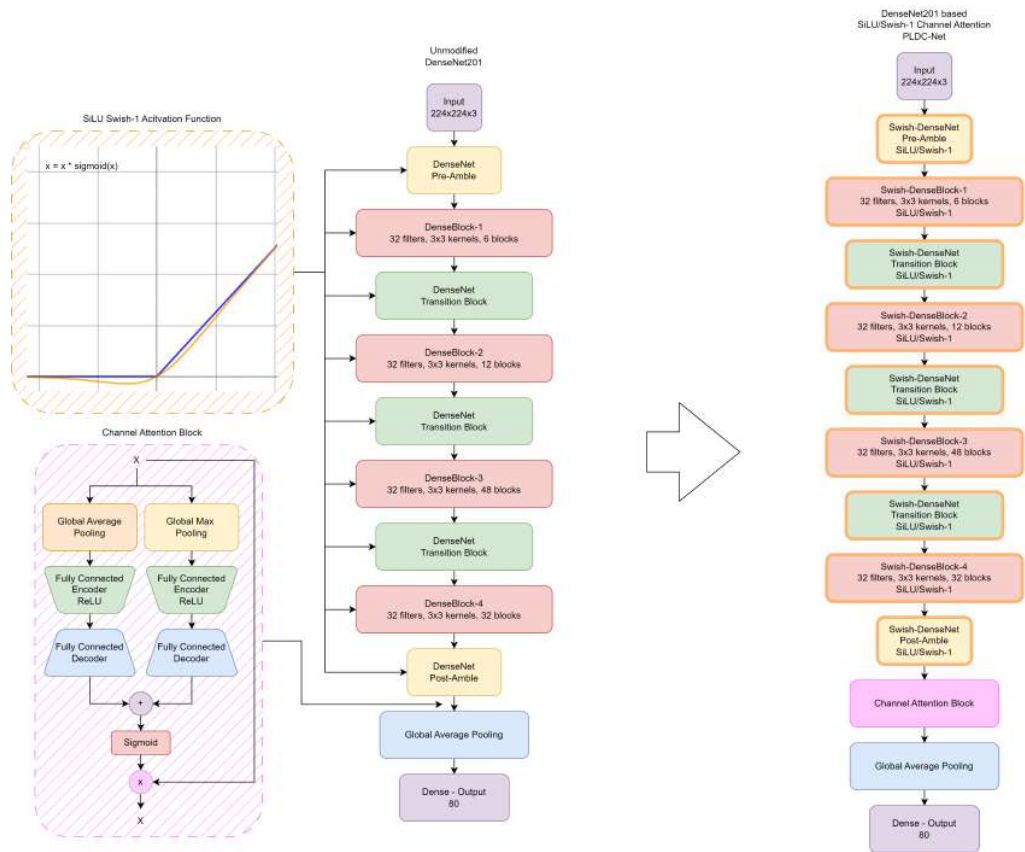


Figure 9.4: The proposed PLDC-Net architecture based on the DenseNet201 baseline model with a Channel Attention Block and Swish-1 SiLU activations.

Table 9.5: The 2 datasets used to combine into PLDC-6 for TL testing.

Ref.	Dataset	Type	Plant	Num. Class	Total Img.
[143, 144]	mignoniSoy	Field	Soybean	3	6,410
[142]	iBean	Field	Beans	3	1,296

Table 9.6: Metrics of the new PLDC-6 dataset.

Number of Different Plants	2
Number of Classes	6
Number of Images Total	7,706
Image Size	224x224x3
Images Per Class	<ul style="list-style-type: none"> • Soybean Healthy - 896 • Soybean Caterpillar - 3309 • Soybean Diabrotica speciosa - 2205 • Bean Healthy - 428 • Bean Angular Leaf Spot - 432 • Bean Bean Rust - 436

to actually test TL capabilities. To achieve these design goals, another 2 datasets have been obtained and combined to create the new dataset. In this case no augmentation and balancing was carried out, to more resemble a dataset that would be collected by someone that would go out into the field to simply collect and label data. The datasets chosen for this 6 class version PLDC transfer dataset for TL purposes is made up of the iBean dataset [142] and the Soybean images dataset [143, 144] (see Table 9.5).

To combine the datasets, they were simply combined to create a 6 class, 2 plant dataset with 7,706 images in total. As earlier mentioned, this data will not be augmented or adjusted for good balance. Also iBean data has been un-split (it originally comes in a pre train-validation-test split) (see Appendix F for more information about the original datasets). The resulting combined PLDC-6 dataset's information can be seen in Table 9.6.

As one can see in Table 9.6, the dataset is largely imbalanced. This can happen with data taken in field, and does as such not only pose an extra challenge, but also represents what real conditions might produce. Due to this imbalance, in the TL experiments the focus will be put on the F1-Score rather than the accuracy. Another possible limitation that real field datasets might suffer from is small image counts (a small dataset). To simulate this limitation, the dataset will be train-test split in different ratios (see Table 9.7). these ratios are:

- train 10% - test 90%
- train 30% - test 70%
- train 50% - test 50%
- train 70% - test 30%
- train 90% - test 10%

These different ratios will give an insight into the effects the pre-trained PLDC-Net Base Model has on small datasets, at different levels, ending with fairly large datasets in the end.

9.3.2 Transfer-Learning Methodology

With the dataset prepared, the pre-trained models can now be trained on it to compare how well they adjust to the new data. The two models that will be compared in these experiments are the PLDC-80 pre-trained PLDC-Net and the baseline DenseNet201 on the ImageNet Dataset. Each model will be trained on each of the different train-test splits mentioned above, once with the classifier frozen and once with it un-frozen. Frozen training is beneficial in terms of computational costs, since only the classifier top needs to be retrained, and the huge CNN model with all its parameters remains unchanged (see Table 9.8). As a result, in total 20 models will be trained, 5 train-test splits, frozen (batch size 128) and un-frozen (batch size 32) and all that for ImageNet DenseNet201 and PLDC-80 pre-trained PLDC-Net. Each model is trained for 50 epoch. The best performing epoch is used for evaluation using the checkpoint callback.

9.3.3 Results

Each of the train-test split experiments, both for frozen as well as for un-frozen, will then compare the performance of the PLDC-80 pre-trained PLDC-Net and the ImageNet trained DenseNet201 baseline. Performance will be compared on speed, robustness, adaptability and final performance results. As mentioned earlier, the goal of developing a new Base Model for the domain of plant leaf disease classification is that the resulting model can train a domain-specific model faster and with less resources by utilizing the domain related knowledge obtained during the pre-training phase.

Table 9.7: Train-Test split results for TL experiments

Train-Test Split (0.1-0.9)		
	Train	Test
Soybean Healthy	90	806
Soybean Caterpillar	331	2978
Soybean Diabrotica speciosa	220	1984
Bean Healthy	43	385
Bean Angular Leaf Spot	43	389
Bean Bean Rust	44	392
Total	771	6934
Train-Test Split (0.3-0.7)		
	Train	Test
Soybean Healthy	269	627
Soybean Caterpillar	993	2316
Soybean Diabrotica speciosa	662	1544
Bean Healthy	128	300
Bean Angular Leaf Spot	130	302
Bean Bean Rust	131	305
Total	2313	5394
Train-Test Split (0.5-0.5)		
	Train	Test
Soybean Healthy	448	448
Soybean Caterpillar	1654	1654
Soybean Diabrotica speciosa	1102	1102
Bean Healthy	214	214
Bean Angular Leaf Spot	216	216
Bean Bean Rust	218	218
Total	3852	3852
Train-Test Split (0.7-0.3)		
	Train	Test
Soybean Healthy	627	269
Soybean Caterpillar	2316	993
Soybean Diabrotica speciosa	1544	662
Bean Healthy	300	128
Bean Angular Leaf Spot	302	130
Bean Bean Rust	305	131
Total	5394	2313
Train-Test Split (0.9-0.1)		
	Train	Test
Soybean Healthy	806	90
Soybean Caterpillar	2978	331
Soybean Diabrotica speciosa	1984	220
Bean Healthy	385	43
Bean Angular Leaf Spot	389	43
Bean Bean Rust	392	44
Total	6934	771

Table 9.8: Model parameter comparison for frozen and un-frozen models.

		Model	
		Baseline	PLDC-Net
Frozen	Total Params.	18,333,510	19,255,110
	Trainable Params.	11,526	11,526
	Non-Trainable Params.	18,321,984	19,243,584
Unfrozen	Total Params.	18,333,510	19,255,110
	Trainable Params.	18,104,454	19,026,054
	Non-Trainable Params.	229,056	229,056

Table 9.9: The results of the frozen TL results on the frozen 10-90 split. The percentage values given are the test F-1 scores.

Frozen 10-90	
Baseline	69.19%
At Epoch	49
PLDC-Net	79.21%
At Epoch	39
Overtake PLDC-Net	69.32%
At Epoch	10

Less resources are used when the model is frozen and when only the classifier top is used, making this scenario the most desirable one. On top of that, as this field does lack data, good performance on small datasets is deemed the most important aspect.

9.3.3.1 Frozen

This section will showcase the frozen model TL performance.

10% Train Data - 90% Test Data The results obtained when the PLDC-6 dataset is split into only 10% data used for training, simulating a very small and imbalanced dataset (see Table 9.7), showcase the following results that can be seen in Table 9.9 and Figure 9.5.

As can easily be seen in both the table and the figure, the results in the hardest train-test split in the frozen, and therefore more computationally efficient setting that relies and benefits more from pre-trained data, the PLDC-Net manages to outperform the baseline model by over 10% in terms of F1-score on the before un-seen test dataset. The PLDC-Net model also manages to outperform the baseline model after only 10 epochs, to reach a value higher than the baseline’s max score for which it needed 49 epochs. This showcases the validity of such a domain relevant and domain related pre-trained Base Model for the field of plant leaf disease classification. The proposed PLDC-Net does not only heavily outperform the baseline on this

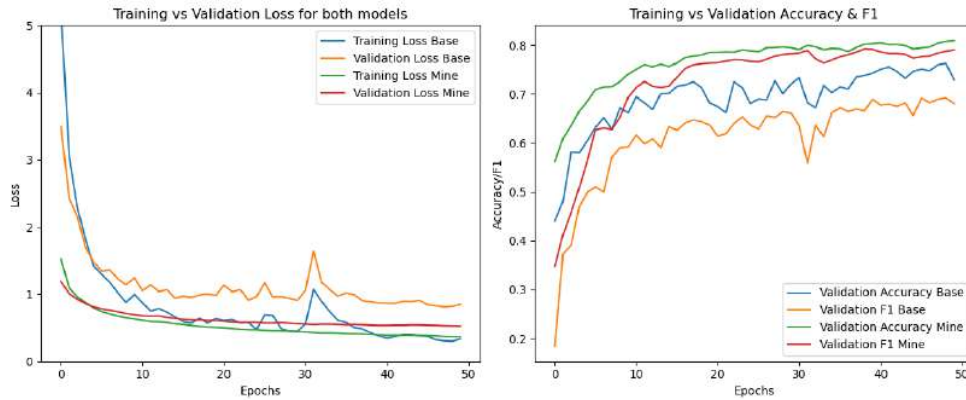


Figure 9.5: The result graph of the frozen TL results on the frozen 10-90 split.

Table 9.10: The results of the frozen TL results on the frozen 30-70 split. The percentage values given are the test F-1 scores.

Frozen 30-70	
Baseline	77.50%
At Epoch	50
PLDC-Net	86.31%
At Epoch	47
Overtake PLDC-Net	77.73%
At Epoch	5

small and imbalanced dataset, but also does so faster and more robust.

30% Train Data - 70% Test Data With the dataset split 30-70 and frozen CNN layers, the results that can be seen in Figure 9.6 and 9.10 have been achieved.

With this somewhat bigger but still rather small (and imbalanced) train set, the baseline model managed 77.50% F1-Score. The PLDC-Net managed to outperform that score after only 5 epochs with 77.63% and with a max score of 86.31% PLDC-Net managed to outperform the baseline model nearly 9%. Figure 9.6 also showcases the difference in biasing between PLDC-Net and the baseline model. Whereas the baseline model shows significant differences between accuracy and F1-Score, indicating a bias towards some classes, PLDC-Net actually showcases a (slightly) better F1-Score when compared with the accuracy, showing no bias, signifying that the model handles the imbalanced data well.

50% Train Data - 50% Test Data With a 50-50 split, the train set starts to become somewhat large. It is still just as imbalanced as it was in the previous experiments, but with over 3,800

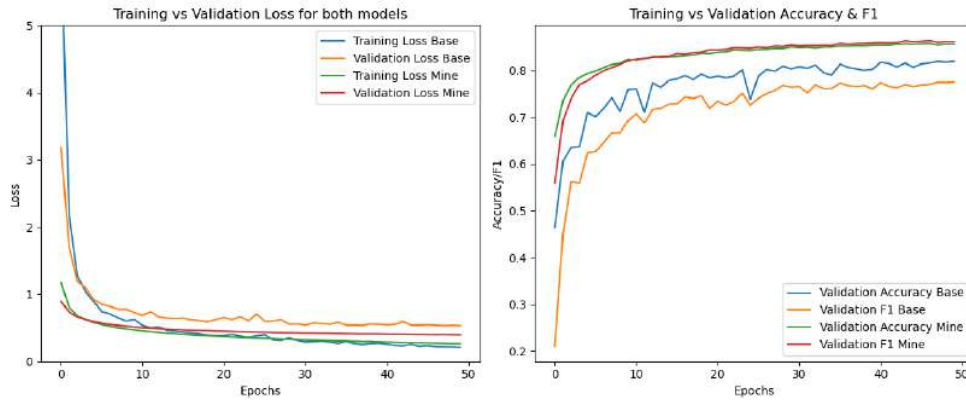


Figure 9.6: The result graph of the frozen TL results on the frozen 30-70 split.

Table 9.11: The results of the frozen TL results on the frozen 50-50 split. The percentage values given are the test F-1 scores.

Frozen 50-50	
Baseline	81.53%
At Epoch	45
PLDC-Net	88.02%
At Epoch	45
Overtake PLDC-Net	82.24%
At Epoch	7

images in the training set, the dataset now enters an image count that one might no longer consider to be "too small", however due to said imbalance, the bean classes are still only just over 200 images per class. Results are listed and showcased in Table 9.11 and Figure 9.7.

The experiments on the 50-50 split dataset have, even though data is becoming increasingly bigger, produced results that are similar to the ones from the earlier and smaller dataset runs. The PLDC-Net model manages to outperform the baseline by over 6%. The proposed model manages to outperform the baseline's max score after only 5 epochs and it does again learn much more stable, faster and more robust, with the F1-Score to accuracy ratio being much more desirable.

70% Train Data - 30% Test Data With the 70-30 split, and a subsequent training set of over 5,300 images, the dataset is starting to resemble a larger dataset. However, due to the heavy imbalance, the smaller classes still only contain roughly 300 images. The frozen model's performance can be seen in Table 9.12 and Figure 9.8.

When comparing the performance of the frozen PLDC-Net and the baseline model on the

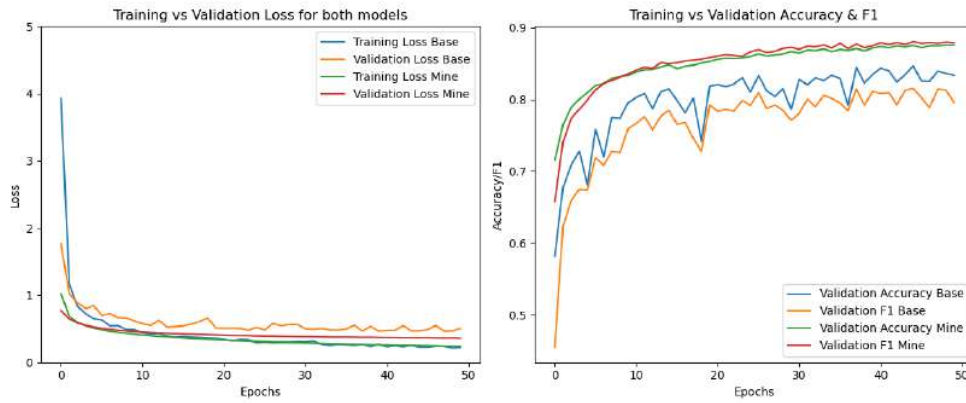


Figure 9.7: The result graph of the frozen TL results on the frozen 50-50 split.

Table 9.12: The results of the frozen TL results on the frozen 70-30 split. The percentage values given are the test F-1 scores.

Frozen 70-30	
Baseline	82.25%
At Epoch	43
PLDC-Net	88.63%
At Epoch	47
Overtake PLDC-Net	83.10%
At Epoch	5

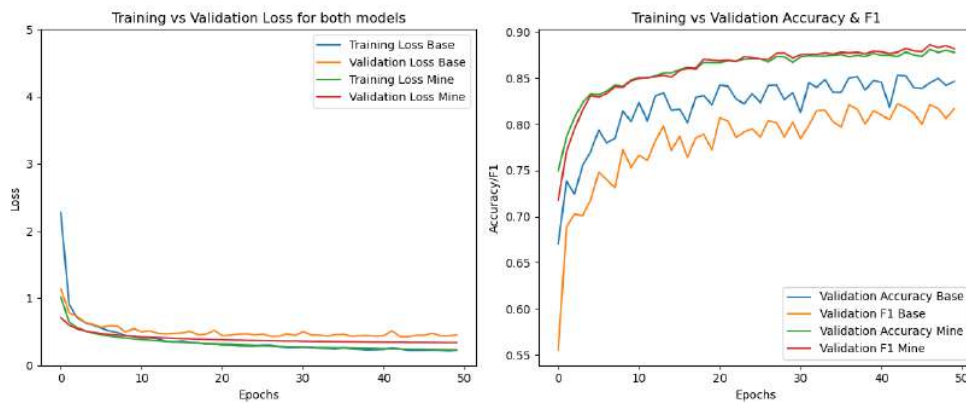


Figure 9.8: The result graph of the frozen TL results on the frozen 70-30 split.

Table 9.13: The results of the frozen TL results on the frozen 90-10 split. The percentage values given are the test F-1 scores.

Frozen 90-10	
Baseline	85.06%
At Epoch	30
PLDC-Net	90.13%
At Epoch	40
Overtake PLDC-Net	85.23%
At Epoch	7



Figure 9.9: The result graph of the frozen TL results on the frozen 90-10 split.

70-30 split of PLDC-6, one can see that the PLDC-Net model again managed to catch up and overtake the baselines max score of 82.25% in only 5 epochs. PLDC-Net managed a score with an over 6% better F1-Score of 88.63% in the end. The graph also showcases similar findings to before, where the PLDC-Net's training scores showcase more robust and faster learning, while the baseline's show a rift between the F1-Score and the accuracy, suggesting some biasing in the baselines weights.

90% Train Data - 10% Test Data The largest test data split - with 90% of the PLDC-6 data being used for training, allows both models to now utilize a fairly decently large dataset for training. While still imbalanced, this dataset of now nearly 7,000 images with all classes almost topping 400 images, is now of a size where many researchers or farmers would need to spend significant amounts of time into collecting and annotating the data, if they can even muster this many images per class from the plant available in their fields. Results can be seen in Figure 9.9 and Table 9.13.

Results obtained from these runs again showcase that PLDC-Net manages to outperform

the baseline model when comparing max performance, with PLDC-Net reaching 90.13% on the F1-Score, while the baseline model only managed 85.06%. PLDC-Net managed to outperform these 85.06% after only 7 epochs, where PLDC-Net was already up to 85.23%. The graph also again shows the same story, where the PLDC-Net's accuracy and F-1 scores are almost identical, with F1 actually being higher, while there is a gap in the performance of the baseline model.

Frozen Results Summary The results obtained by training the frozen PLDC-Net model and the baseline model on the PLDC-6 dataset show how significant the advantage a domain-related and domain-relevant Base Model can have over a general Foundational Model. PLDC-Net managed to outperform the baseline consistently on each of the different dataset splits, with the model managing a higher performance with 10% training data than the baseline did with 30%, meaning it did better with only 1/3 of the data, while the baseline with 3x the data still fell behind. PLDC-Net with only 30% of the data also managed to beat the baseline that was trained on 90% of the data, again showing that it can be 3x as data efficient and still more powerful. It does all that in a setting with limited data, with a frozen classifier, meaning it does that in a setting where it is computationally lighter than it would be to re-train the entire model. It is also, across the board, much faster, much more stable, much more robust, and performs better without exception when using the computationally more efficient and therefore more desirable method to locations without high end computers and countless training data (such as many farms). These results more than validate PLDC-Net and the idea of domain-specific BM.

9.3.3.2 Unfrozen

Here the results of the unfrozen experiments will be presented and analyzed. Unfrozen training runs are much more computationally expensive (see Table 9.8, since each parameter needs to be trained during these runs. This is also why the batch size had to be reduced from 128 to only 32, since the machine used for testing can not handle the full 128 batch size in un-frozen mode. As such, they are less applicable to use-cases where computational power is at an impasse, which can include farms. Unfrozen Transfer-Learning also is much more prone to overfit on small data, since the TL domain specific dataset influences every weight in the model. However, unfrozen training can lead to stronger overall results, barring all the downsides listed.

Table 9.14: The results of the unfrozen TL results on the unfrozen 10-90 split. The percentage values given are the test F-1 scores.

Unfrozen 10-90	
Baseline	79.50%
At Epoch	43
PLDC-Net	83.88%
At Epoch	33
Overtake PLDC-Net	80.57%
At Epoch	6

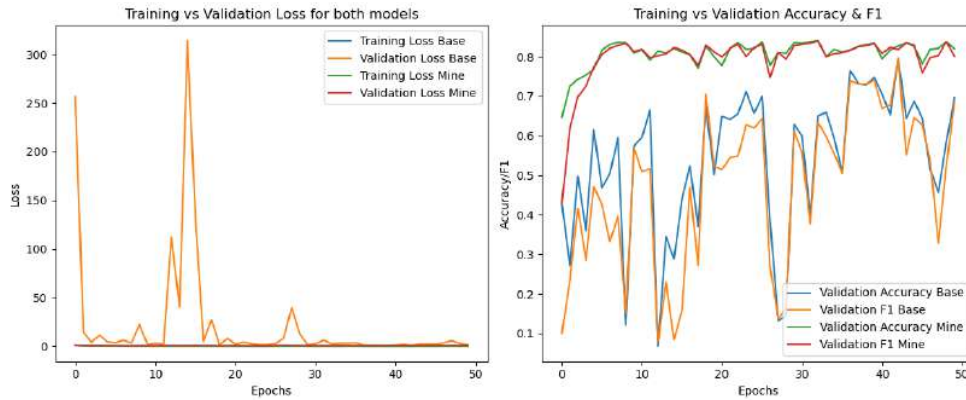


Figure 9.10: The result graph of the unfrozen TL results on the unfrozen 10-90 split.

10% Train Data - 90% Test Data The smallest train split (see Table 9.7) with less than 800 total images across 6 classes and with only around 40 images per bean class, used for training on the un-frozen models produced the results in Table 9.14 and in Figure 9.10, with Figure 9.11 providing a zoomed in view to the loss, as the validation loss of the baseline model is too high to see the more subtle trends of PLDC-Net.

Results showcase that PLDC-Net managed to outperform the baseline model by over 5% in overall performance, and it managed to overtake the max performance posted by the baseline after only 6 epochs. This shows that PLDC-Net manages to perform better on the most difficult train dataset split and it does also learn much faster. Even more obvious are the findings observed in the Figures (Figures 9.10 and 9.11). Here it becomes obvious how much the baseline model fluctuates, with performance being incredibly instable during the entire training period. PLDC-Net, on the other hand, performs much more stable and robust. PLDC-Net is, based on the results observed, much more suited to handle this task.

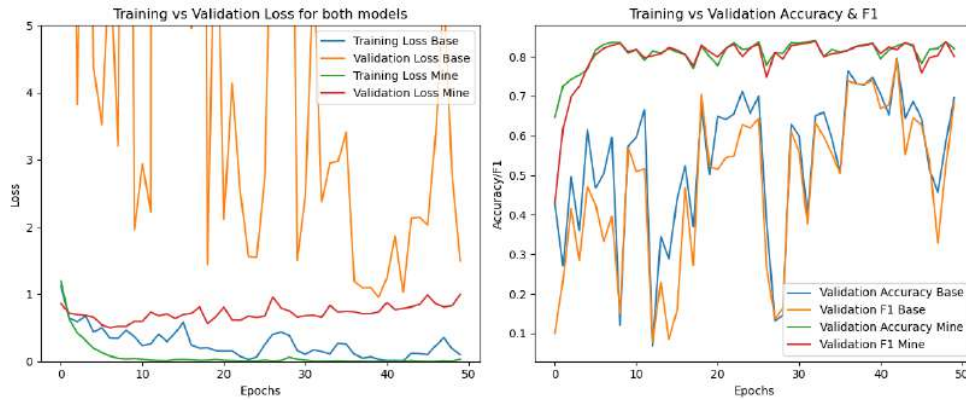


Figure 9.11: The zoomed in result graph of the unfrozen TL results on the unfrozen 10-90 split.

Table 9.15: The results of the unfrozen TL results on the unfrozen 30-70 split. The percentage values given are the test F-1 scores.

Unfrozen 30-70	
Baseline	90.75%
At Epoch	46
PLDC-Net	89.94%
At Epoch	7
Overtake PLDC-Net	None
At Epoch	None

30% Train Data - 70% Test Data Increasing the training dataset size by a factor of 3 to a 30-70 split shows a sharp increase in overall performance for both models, as they can now make use of significantly more data. Results are available in Table 9.15 and Figure 9.12.

This is the first test scenario where the baseline model managed to achieve a higher overall F1-Score than PLDC-Net. However, one can also see that PLDC-Net manages it's 89.95% F1 max score after only 7 epochs, while the baseline took 46 to reach 90.75%, only less than 1% more. The max score achieved by PLDC-Net after 7 epochs is only outperformed by the baseline after 46 epochs of training. The graphs also indicate that the baseline model is much more vulnerable to overfitting and trains much less stable and much more erratic with high variance in performance epoch to epoch.

50% Train Data - 50% Test Data The 50-50 split dataset with the un-frozen model again shows improved performance for both models. Results are shown in Table 9.16 and Figure 9.13.

Here too the baseline did manage to score higher in overall performance with an around

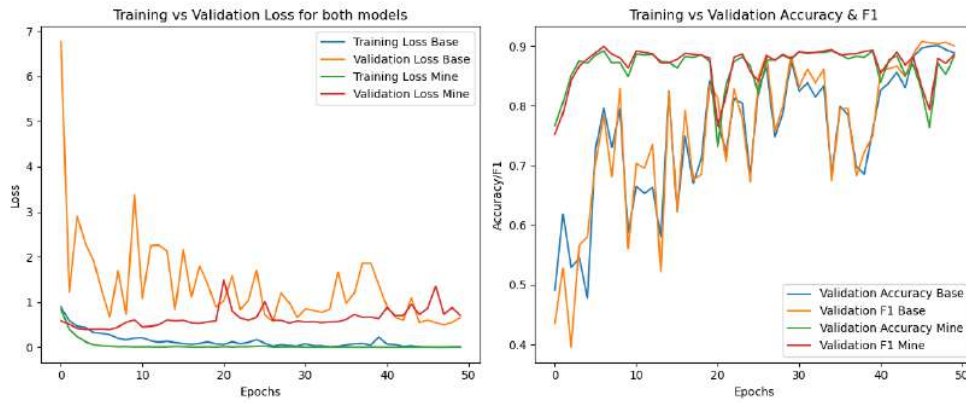


Figure 9.12: The result graph of the unfrozen TL results on the unfrozen 30-70 split.

Table 9.16: The results of the unfrozen TL results on the unfrozen 50-50 split. The percentage values given are the test F-1 scores.

Unfrozen 50-50	
Baseline	92.63%
At Epoch	44
PLDC-Net	91.99%
At Epoch	11
Overtake PLDC-Net	None
At Epoch	None

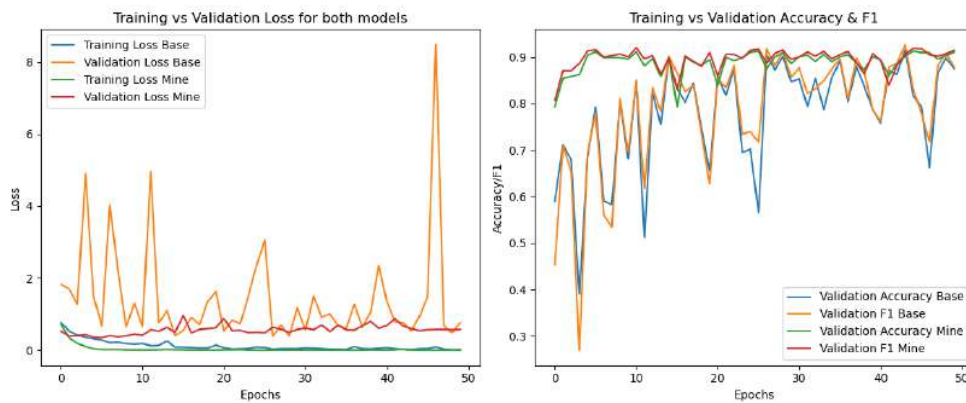


Figure 9.13: The result graph of the unfrozen TL results on the unfrozen 50-50 split.

Table 9.17: The results of the unfrozen TL results on the unfrozen 70-30 split. The percentage values given are the test F-1 scores.

Unfrozen 70-30	
Baseline	91.74%
At Epoch	39
PLDC-Net	93.08%
At Epoch	24
Overtake PLDC-Net	92.50%
At Epoch	8

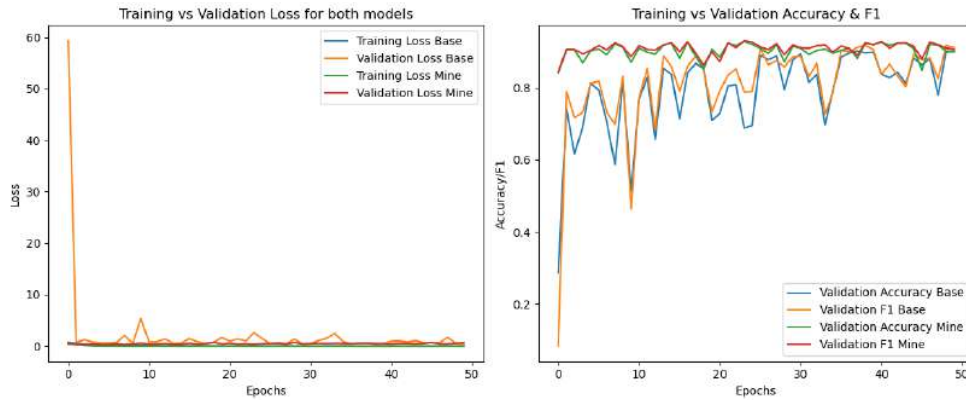


Figure 9.14: The result graph of the unfrozen TL results on the unfrozen 70-30 split.

0.6% better F1-Score, but as was the case with the 30-70 split, PLDC-Net managed its high score after only 11 epochs, while it took the baseline model 44 epochs to outscore that. The graphs also paint a similar picture to the graphs obtained by the previous un-frozen experiments, with the baseline model being very unstable and erratic, while the PLDC-Net model trains much more smoothly and stable, with no sudden variance and no sudden large drop-offs.

70% Train Data - 30% Test Data Again, with the 70% split used for training, the dataset starts to resemble a somewhat large scale dataset, one that might not easily be collected without significant time and financial investments, and only if enough plants per disease are available in field. Results of the un-frozen models on this larger dataset are presented in Table 9.17 and Figures 9.14 and the zoomed in Figure 9.15.

Results of this 70-30 split un-frozen run showcase that PLDC-Net managed to outperform the baseline again, reaching a max score of 93.08% compared to the 91.74% achieved by the baseline. This is also a step back in performance of the baseline when compared to the 50-50 split. One can also see that the PLDC-Net model managed to outscore the baseline's

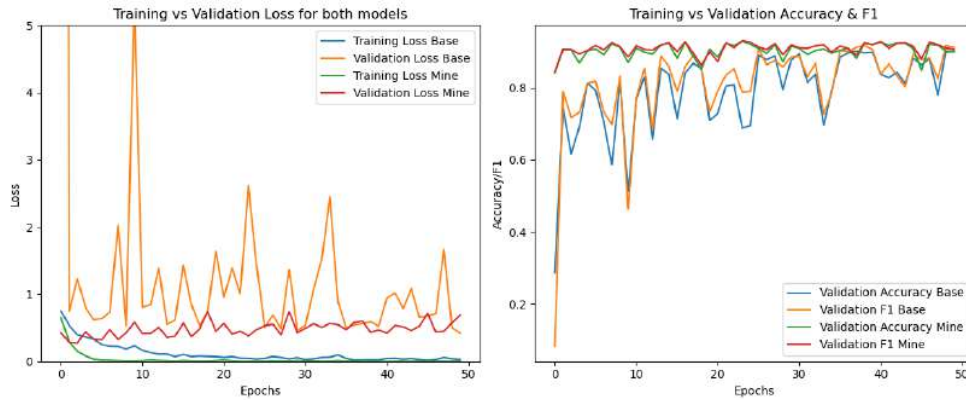


Figure 9.15: The zoomed in result graph of the unfrozen TL results on the unfrozen 70-30 split.

Table 9.18: The results of the unfrozen TL results on the unfrozen 90-10 split. The percentage values given are the test F-1 scores.

Unfrozen 90-10	
Baseline	94.53%
At Epoch	36
PLDC-Net	95.09%
At Epoch	20
Overtake PLDC-Net	94.82%
At Epoch	19

91.74% after only 8 epochs, at which PLDC-Net already managed to score 92.50%. Again, the plots showcase a much more erratic performance by the baseline, with the PLDC-Net model performing much more stable. Although one has to point out that the baseline is less variant on the larger dataset than it was on previous splits.

90% Train Data - 10% Test Data The largest train split, with 90% of the data in PLDC-6, does come with a size that is not easy to collect, but does come with the best setup for un-frozen training. Results are shown in Table 9.18 and Figures 9.16 and 9.17 with the latter being the zoomed in representation.

Results showcase both models achieving their overall highest scores across all experiments, which is to be expected with the un-frozen (but heavy and time consuming) training on a rather large (but hard to collect) dataset. However, even here the PLDC-Net model managed a higher score than the baseline model did. It also managed to achieve said higher score after only 19 epochs of training. The figures also, again, showcase that the baseline model is much less stable and much more erratic than the PLDC-Net.

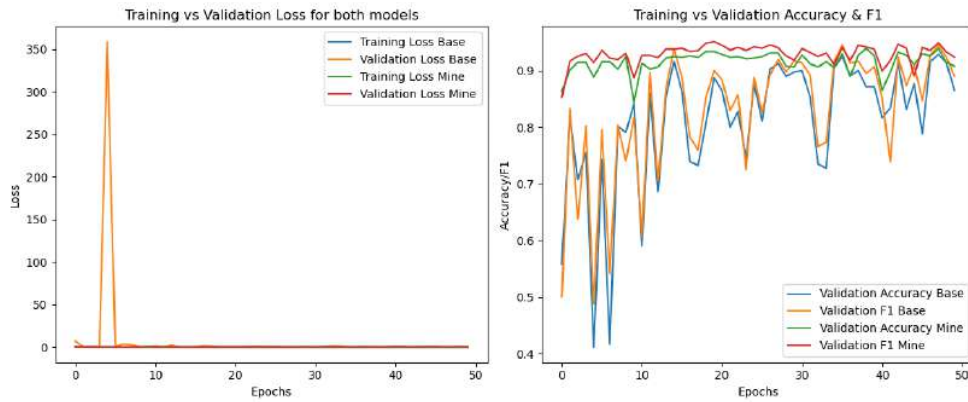


Figure 9.16: The result graph of the unfrozen TL results on the unfrozen 90-10 split.

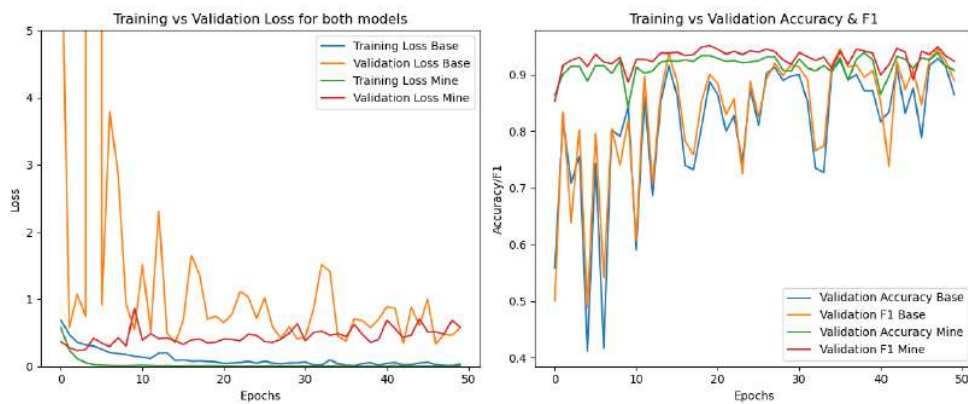


Figure 9.17: The zoomed in result graph of the unfrozen TL results on the unfrozen 90-10 split.

Frozen Results Summary In the un-frozen set of experiments, which are more computationally expensive and more time consuming, the PLDC-Net model managed to outperform the baseline model in 3 of 5 cases. In the 2 cases where the baseline model did manage higher max scores, the PLDC-Net model did manage results that are not too far of the baseline model's, while achieving said comparable scores much faster. Maybe more noticeable is the volatility that the baseline model operates with. All figures show that the baseline's results are very erratic, volatile, variant, and unstable. Loss, accuracy and F1-Scores of the PLDC-Net, however, are much more stable, with no large drop-offs in performance from one epoch to the other. PLDC-Net also manages to learn much faster than the baseline did, on top of being much more stable, as just mentioned.

9.3.3.3 Transfer-Learning Results Summary

Through these TL experiments and the results obtained from them, once can see that PLDC-Net managed to outperform the baseline model in each case when using the preferred frozen training method, with large improvements in each case, especially so in cases where the dataset was more limited. With data being sparse, these frozen and low data count cases are the most relevant and most interesting results obtained. With PLDC-Net being this much more powerful in these test-cases, its applicability in real world scenarios, where large data and advanced computational power and time might not be guaranteed, it sets itself apart as the better, faster, more powerful, more stable, and cheaper alternative to the baseline approach. When using the un-frozen approach, which is heavier in terms of time and computation, the baseline model did manage to score a higher overall score in 2 out of 5 cases. The difference to PLDC-Net was, however, not very large and PLDC-Net still managed to learn much faster. One thing that was even more noticeable in the un-frozen experiments was the inconsistency and erraticness that the baseline model trained with. While PLDC-Net still trained stable and fast, the baseline model was extremely volatile and unstable during training, especially so in the use-cases where data was limited.

Overall these results showcase the validity of PLDC-Net and the improvements it brings to the field of plant leaf disease classification. This domain-related and domain-relevant BM trained on the PLDC-80 dataset uses the related feature maps it obtained from the PLDC-80 dataset and transfers them to the new unseen PLDC-6 dataset much more effectively than the

baseline DenseNet201 model that was pre-trained on the general ImageNet dataset.

9.4 One-Shot and Few-Shot Learning

To further test the robustness and adaptability of PLDC-Net, especially in low data environments, one-shot and few-shot learning was employed. The above mentioned bean dataset was used, but without merging it with the soybean dataset to have more consistent data, which these techniques rely upon. Only a very small number of images (1 and 5) per class was used during "training" of the classifier. The models, PLDC-Net and ImageNet pre-trained DenseNet201 as the baseline, are not re-trained, or fine-tuned, nor is the dense layer at the end, at all during this. Instead they are simply used as feature extractors to provide embeddings of the one-shot images and then compare future images based on those embeddings.

9.4.1 Dataset

The dataset used here, as mentioned above, is the iBean dataset [142] with 3 classes taken in somewhat similar conditions. Depending on the experiments, one-shot or few-shot, a different amount of images will be used for "training", with the rest being used for testing. In one-shot learning, only 1 image per class will be used during "training", 3 in total, while in few-shot learning 5 per class (15 in total) are used.

Table 9.19: iBean dataset used for few-shot learning.

iBean Dataset	
Images	1,296
Classes	3
Images per Class	<ul style="list-style-type: none">• Healthy - 428• Angular Leaf Spot - 432• Bean Rust - 436

9.4.2 Methodology

In the few-shot learning experiments here, the models (PLDC-Net and ImageNet pre-trained DenseNet201) are not trained at all. The models are only used in inference mode. Each model

is cut off at the max pooling layer, deleting the classifier top. This feature extractor output of the max pooling layer is used for few shot learning as embeddings for the classes.

Each of the image support samples (training images), so 1 per class for one-shot and 5 per class for few-shot, are fed to the network and the predicted feature extractor embeddings are saved (and averaged in the case of few-shot). These embeddings (which represent the class of the support image(s) that generated it), which are a vector of 1920, are then used to predict classes for future images of the query (testing data). Each testing query image is also fed into the same model, and its embeddings are compared to the set of 3 prototype embeddings (1 per class) of the training support embeddings saved earlier using Euclidean distance (see (9.3)).

$$d(\mathbf{x}, \mathbf{y}) = \sqrt{\sum_{i=1}^n (x_i - y_i)^2} \quad (9.3)$$

Here d is the Euclidean distance between the predicted query image and the saved prototype support image embedding, x_i is the i -th dimensional position value of the prototype embedding, y_i is the i -th dimensional embedding of the new query test image, and n is the number of dimensions, which is 1920 in this case for both models.

Then the the prototype embedding (and with that the class it is representing) with the smallest distance to the new test image will be used as the predicted class and compared to the images true value, to obtain accuracy scores. Like this, the model does not need to be retrained, which would be near impossible with a single image per class, saves computational cost since it does not need to train, only inference, and even makes the model more light weight, since the dense layer at the end can be omitted. All this allows the model to be adjusted to classify new image classes of before unseen plants, diseases and classes (cross-domain), with incredibly limited data.

9.4.3 Results

When looking at the results of both models (PLDC-Net and ImageNet trained DenseNet201), we will differentiate 2 different approaches and their results. Each model was once used for one-shot learning, and once for 5-shot few-shot learning.

9.4.3.1 Cross-Domain One-Shot Classification

In one-shot learning, where each class was only embedded with a single image (train image set of 1 image per class and therefore 3 images in total), we can see the models performing decently well considering the limitations (see Table 9.20 for results). The baseline model manages almost 54% accuracy and PLDC-Net reaches almost 61%. Both of these outperform randomness (which would be around 33% for 3 classes) significantly, proving they are indeed properly predicting. The PLDC-Net, however, manages to outperform the baseline by nearly 7%, showing significant improvement over the baseline in highly limited data.

Table 9.20: The results of both models One-Shot Learning on the iBean dataset.

1-Shot Learning	
Baseline	53.95%
PLDC-Net	60.91%

9.4.3.2 Cross Domain Few-Shot Classification

In the test case where each class is represented by 5 images during training, with average embeddings, the PLDC-Net manages to outperform the baseline by an even bigger margin, achieving a nearly 14% better accuracy score (PLDC-Net 75.70%, Baseline 61.89% - see Table 9.21). As a result, here too the PLDC-Net manages to provide significantly better and therefore more valuable predictions, in conditions that are still highly limited in terms of image count for training.

Table 9.21: The results of both models Five-Shot Learning on the iBean dataset.

5-Shot Learning	
Baseline	61.80%
PLDC-Net	75.70%

9.4.3.3 One and Few-Shot Result Summary

Overall, just like it was the case with TL, one-shot and few-shot learning results show that the PLDC-Net model pre-trained on domain relevant and domain related data manages to produce features that are better and more helpful to predict new plant, diseases and classes in cross-domain settings. The five-shot baseline model only managed to slightly outperform the one-shot PLDC-Net model by less than 1% in a case where the baseline had 5x the images. The

PLDC-Net model was significantly strong in both scenarios, proving it can produce stronger plant leaf disease classifiers in data and resource constraint scenarios, which are real limitations that the field is faced with, making the PLDC-80 pre-trained PLDC-Net the stronger and better choice for domain adaptation when compared to the baseline.

10. Discussion

Through thorough, step-by-step research, PLDC-80, PLDC-Net and PLDC-6 were created in an effort to create a Base Model that is specifically tailored to the field of plant leaf disease classification. Whereas before, as pointed out by prior work [14, 11], datasets are an issue, with large scale diverse high quality field or hybrid datasets being sparse. After having conducted a detailed and extensive benchmark, suitable datasets and models have been identified that could be utilized for future steps such as creating a large scale benchmarking dataset that can be used for large scale models and a set of models that could be used as baseline comparisons as well as the basis for improvements. While collecting a totally new dataset is out of scope of this work, and as such would still be a worthwhile and desirable addition to the field, PLDC-80 combines, merges, augments (using proven methods), and filters 9 pre-existing benchmarked datasets (hybrid, lab, and field). Through this process PLDC-80 manages to reach over 300,000 images across 80 classes, representing 25 different plant species. This size, diversity (both in terms of plant types, diseases, and capturing conditions), and quality make for a uniquely capable dataset for the field of plant leaf disease classification. This dataset allows the opportunity to properly train a large scale CNN classifying model in a way in which it would not be possible with other openly available datasets. Using this dataset, a large number of models were trained to compare their robustness and generalization ability on PLDC-80's test set. DenseNet201 was the best performing baseline model, so it was chosen to be the basis of improvements. The improvements chosen were Channel Attention and Swish-1 SiLU activation. This new model, called PLDC-Net, managed to outperform the other models on the PLDC-80 dataset in terms of test performance. As such, it was used for another set of experiments, by using it as a foundational pre-trained model for TL, comparing it to the commonly used ImageNet pre-trained DenseNet201 baseline. In these experiments, on the PLDC-6 dataset, the model managed to outperform the baseline in most cases, learning faster, more robust, less volatile

weights and features. These experiments prove that the domain-specific Base Model, specific to the field of plant leaf disease classification, provides better training conditions for scenarios with small dataset and lower computational capacity. All in all, this proves the need for and the validity of PLDC-Net and the PLDC-80 dataset, as it improves the TL abilities for this field, allowing future research to train more robust models with less data in a shorter time frame.

11. Future Work

With PLDC-80, PLDC-6, and PLDC-Net now having been developed, future work can be built upon them. Future directions following these developments could go in a few different directions. For one, future work could try to improve PLDC-Net by trying even more different methods to change the architecture in hopes of managing better scores on the PLDC-80 benchmarking set. Alternatively, one could try to build a completely new model architecture for this field, although this task would be very difficult, since existing architectures like DenseNet201 already achieve great results

One could also make use of the benchmarking results to better select models for future experiments. The results showcase a clear difference between different model families and architectures, which should help future works to make a better informed pick for as to which model to pick.

The same benchmark, in combination with the results of the augmentation assessment, can also be used to enhance already existing datasets or even during the creation of new datasets, that are yet to be collected. Collecting new datasets is laborious, time consuming, and also potentially costly, so utilizing the benchmarking results to see what dataset size, diversity, and type are best suited for the field, as well as understanding which augmentations are most beneficial, can make creating more new datasets less of a problem.

Another option, one that could have large impact, but one that comes with a hefty cost, would be to create a completely new, large scale, diverse, high quality benchmarking dataset, completely collected in field (and maybe also in lab) conditions specifically for this field. One could then either use that dataset to train future BM, or use that new dataset in combination with PLDC-80 to create a even larger and potentially better dataset to train future models.

One could also try observe and asses different methods for training models for plant leaf disease classification. One option would be to use distributed methods such as the decentralized

federated learning method, to train models not on one dataset and one machine alone, but on a cluster or a network of multiple machines at the same time, which could reduce dataset requirements and computational costs per node.

12. Conclusion

This thesis first presents an extensive review of current literature in the field of plant leaf disease classification. This review provides a good look at the current state of the field and identifies current trends and best practices in the field. Following this literature review, this thesis explains a lot of the background information related to the field as well as relevant and essential information regarding CNN Deep Learning methods, upon which this thesis builds in later chapters. The background chapter also explains methods and ideas specific to plant leaf diseases and classification of such. Following that is a deep look into a large number of open datasets for plant leaf disease classification, giving an overview of possible options as well as giving a good overview of each datasets characteristics such as collection conditions, size, number of classes, class balance, etc. Next, relevant and popular large scale CNN classifier models are introduced and explained. These models make up a large number of the models used in current literature and also introduce a large number of currently popular methods. As such, this chapter gives good insight into the current state of CNN classifiers and these findings are later utilized in model construction. The next chapter contains the benchmarking experiments and results conducted as part of this research. This benchmark offers very insightful and important information into the field of plant leaf disease classification, identifying which datasets are better suited to be used for classification tasks as well as pointing out which models are more powerful when applied to plant leaf classification datasets. The benchmark shows significant differences between different datasets and models in terms of performance and applicability to this field and shows useful trends that can be utilized to chose the right combination for future work. The augmentation experiments offer further insights that can be implemented when enriching or even when creating datasets for plant leaf disease classification experiments. To solve the problem of insufficient data, PLDC-80 was introduced. A 80 class, 25 plant species and 300,000 images large hybrid dataset that can be use to benchmark models, as well as to train a domain-

related and domain-relevant Base Model, due to its size, diversity, conditions and quality. Such a Base Model was then conceptualized, constructed, and tested on the PLDC-80 dataset where it was also compared with baseline models to verify its legitimacy and relevance, as well as to point out its performance gains. This PLDC-Net model was, after pre-training on the large scale PLDC-80 dataset, used for TL on another, smaller, related dataset that has no overlap with PLDC-80, called PLDC-6, since it contains 6 classes (unseen to the pre-trained PLDC-Net). Transfer-Learning experiments showcase the power of PLDC-Net, when compared to the baseline DenseNet201 model pre-trained on ImageNet. PLDC-Net was faster, more robust, more stable, and better performing, especially in low data scenarios when using the computationally lighter frozen TL approach. PLDC-Net trained on PLDC-80 managed to outperform the baseline model by over 10% F1-Score on 10-90 train-test split PLDC-6 using frozen CNN layers, signifying the substantial improvement made in terms of low data and computational availability, which is heavily beneficial in the field of plant leaf disease classification. The model also showcased better learning characteristics on top of the afore mentioned numbers, with it learning much faster, it being less erratic, volatile, and variant during training, while the baseline model suffers from all these problems. This positions PLDC-Net as a powerful domain-informed Base Model for plant leaf disease classification with many beneficial and desirable characteristics.

Bibliography

- [1] FAO, IFAD, UNICEF, WFP and WHO, *The State of Food Security and Nutrition in the World 2024 – Financing to end hunger, food insecurity and malnutrition in all its forms*, ser. The State of Food Security and Nutrition in the World (SOFI). Rome, Italy: FAO, IFAD, UNICEF, WFP, WHO, 2024, no. 2024. doi: 10.4060/cd1254en .
- [2] FAO, *World Food and Agriculture – Statistical Yearbook 2023*, ser. FAO Statistical Yearbook – World Food and Agriculture. Rome, Italy: FAO, 2023, no. 2023. doi: 10.4060/cc8166en .
- [3] ———, *The Future of Food and Agriculture: Trends and Challenges*, 1st ed. Rome, Italy: FAO, 2017. [Online]. Available: <https://openknowledge.fao.org/handle/20.500.14283/i6583e>
- [4] J. B. Ristaino, P. K. Anderson, D. P. Bebber, K. A. Brauman, N. J. Cunniffe, N. V. Fedoroff, C. Finegold, K. A. Garrett, C. A. Gilligan, C. M. Jones *et al.*, “The persistent threat of emerging plant disease pandemics to global food security,” *Proceedings of the National Academy of Sciences*, vol. 118, no. 23, p. e2022239118, 2021. doi: 10.1073/pnas.2022239118 .
- [5] FAO, *The State of Food and Agriculture 2023 – Revealing the true cost of food to transform agrifood systems*, ser. The State of Food and Agriculture (SOFA). Rome, Italy: FAO, 2023, no. 2023. doi: 10.4060/cc7724en .
- [6] D. C. Clay, C. G. Carlson, and K. Dalsted, *iGrow Wheat: Best Management Practices for Wheat Production*. Brookings, S.D.: South Dakota State University, College of Agriculture and Biological Sciences. SDSU Extension, 2012, agronomy,

Horticulture, and Plant Science Books. 1., ISBN: 978-0-9856309-0-4. [Online]. Available: https://openprairie.sdstate.edu/plant_book/1

- [7] R. O. for Europe, *Monitoring and Surveillance of Cereals Pests, Diseases and Weeds*, 1st ed. Sub-regional Office of FAO for Central Asia: FAO, 2012, fAO Job Number: AQ295E. [Online]. Available: <https://openknowledge.fao.org/handle/20.500.14283/aq295e>
- [8] M. Koyshibayev and H. Muminjanov, *GUIDELINES FOR MONITORING DISEASES, PESTS AND WEEDS IN CEREAL CROPS*, 1st ed. Rome, Italy: FAO, 2016. [Online]. Available: <https://openknowledge.fao.org/handle/20.500.14283/i5550e>
- [9] M. Nagaraju and P. Chawla, “Systematic review of deep learning techniques in plant disease detection,” *International journal of system assurance engineering and management*, vol. 11, no. 3, pp. 547–560, 2020. doi: 10.1007/s13198-020-00972-1 .
- [10] L. Li, S. Zhang, and B. Wang, “Plant disease detection and classification by deep learning—a review,” *IEEE Access*, vol. 9, pp. 56 683–56 698, 2021. doi: 10.1109/ACCESS.2021.3069646 .
- [11] J. Lu, L. Tan, and H. Jiang, “Review on convolutional neural network (cnn) applied to plant leaf disease classification,” *Agriculture*, vol. 11, no. 8, p. 707, 2021. doi: 10.3390/agriculture11080707 .
- [12] C. Sarkar, D. Gupta, U. Gupta, and B. B. Hazarika, “Leaf disease detection using machine learning and deep learning: Review and challenges,” *Applied Soft Computing*, vol. 145, p. 110534, 2023. doi: 10.1016/j.asoc.2023.110534 .
- [13] W. B. Demilie, “Plant disease detection and classification techniques: a comparative study of the performances,” *Journal of Big Data*, vol. 11, no. 1, p. 5, 2024. doi: 10.1186/s40537-023-00863-9 .
- [14] M. Xu, H. Kim, J. Yang, A. Fuentes, Y. Meng, S. Yoon, T. Kim, and D. S. Park, “Embracing limited and imperfect training datasets: opportunities and challenges in plant disease recognition using deep learning,” *Frontiers in Plant Science*, vol. 14, p. 1225409, 2023. doi: 10.3389/fpls.2023.1225409 .

- [15] D. Singh, N. Jain, P. Jain, P. Kayal, S. Kumawat, and N. Batra, “Plantdoc: A dataset for visual plant disease detection,” in *Proceedings of the 7th ACM IKDD CoDS and 25th COMAD*. New York, NY, USA: Association for Computing Machinery, 2020, pp. 249–253. doi: 10.1145/3371158.3371196.
- [16] M. Awais, M. Naseer, S. Khan, R. M. Anwer, H. Cholakkal, M. Shah, M.-H. Yang, and F. S. Khan, “Foundation models defining a new era in vision: a survey and outlook,” *IEEE Transactions on Pattern Analysis and Machine Intelligence*, 2025. doi: 10.1109/TPAMI.2024.3506283.
- [17] F. Chen, M. V. Giuffrida, and S. A. Tsaftaris, “Adapting vision foundation models for plant phenotyping,” in *Proceedings of the IEEE/CVF International Conference on Computer Vision*, 2023, pp. 604–613. doi: 10.1109/ICCVW60793.2023.00067.
- [18] D. J. Richter, M. I. Bappi, S. S. Kolekar, and K. Kim, “A systematic review of the current state of transfer learning accelerated cnn-based plant leaf disease classification,” 2025. doi: 10.1109/ACCESS.2025.3584404., in press.
- [19] S. P. Mohanty, D. P. Hughes, and M. Salathé, “Using deep learning for image-based plant disease detection,” *Frontiers in plant science*, vol. 7, p. 1419, 2016. doi: 10.3389/fpls.2016.01419.
- [20] D. Mamba Kabala, A. Hafiane, L. Bobelin, and R. Canals, “Image-based crop disease detection with federated learning,” *Scientific Reports*, vol. 13, no. 1, p. 19220, 2023.
- [21] K. He, X. Zhang, S. Ren, and J. Sun, “Deep residual learning for image recognition,” in *Proceedings of the IEEE conference on computer vision and pattern recognition*, 2016, pp. 770–778.
- [22] A. G. Howard, M. Zhu, B. Chen, D. Kalenichenko, W. Wang, T. Weyand, M. Andreetto, and H. Adam, “Mobilenets: Efficient convolutional neural networks for mobile vision applications,” *arXiv preprint arXiv:1704.04861*, 2017. doi: 10.48550/arXiv.1704.04861.

- [23] S. Mehta, V. Kukreja, and A. Gupta, "Transforming agriculture: Federated learning cnns for wheat disease severity assessment," in *2023 8th International Conference on Communication and Electronics Systems (ICCES)*. IEEE, 2023, pp. 792–797.
- [24] P. Dhiman, V. Kukreja, P. Manoharan, A. Kaur, M. Kamruzzaman, I. B. Dhaou, and C. Iwendi, "A novel deep learning model for detection of severity level of the disease in citrus fruits," *Electronics*, vol. 11, no. 3, p. 495, 2022.
- [25] F. S. Khan, S. Khan, M. N. H. Mohd, A. Waseem, M. N. A. Khan, S. Ali, and R. Ahmed, "Federated learning-based uavs for the diagnosis of plant diseases," in *2022 International Conference on Engineering and Emerging Technologies (ICEET)*. IEEE, 2022, pp. 1–6.
- [26] G. Idoje, T. Dagiuklas, and M. Iqbal, "Federated learning: Crop classification in a smart farm decentralised network," *Smart Agricultural Technology*, vol. 5, p. 100277, 2023.
- [27] D. R. Hammou and M. Boubaker, "Tomato plant disease detection and classification using convolutional neural network architectures technologies," in *Networking, Intelligent Systems and Security: Proceedings of NISS 2021*. Springer, 2022, pp. 33–44. doi: 10.1007/978-981-16-3637-0_3.
- [28] B. Tej, F. Nasri, and A. Mtibaa, "Detection of pepper and tomato leaf diseases using deep learning techniques," in *2022 5th international conference on advanced systems and emergent technologies (IC_ASET)*. IEEE, 2022, pp. 149–154. doi: 10.1109/IC_ASET53395.2022.9765923.
- [29] R. Nagi and S. S. Tripathy, "Grapevine leaf disease identification using transfer learning," in *2021 IEEE International Women in Engineering (WIE) Conference on Electrical and Computer Engineering (WIECON-ECE)*. IEEE, 2021, pp. 43–46. doi: 10.1109/WIECON-ECE54711.2021.9829703.
- [30] L. Li, S. Zhang, and B. Wang, "Apple leaf disease identification with a small and imbalanced dataset based on lightweight convolutional networks," *Sensors*, vol. 22, no. 1, p. 173, 2021. doi: 10.3390/s22010173.

- [31] B. N. Naik, R. Malmathanraj, and P. Palanisamy, "Detection and classification of chilli leaf disease using a squeeze-and-excitation-based cnn model," *Ecological Informatics*, vol. 69, p. 101663, 2022. doi: 10.1016/j.ecoinf.2022.101663 .
- [32] P. Pradhan, B. Kumar, and S. Mohan, "Comparison of various deep convolutional neural network models to discriminate apple leaf diseases using transfer learning," *Journal of Plant Diseases and Protection*, vol. 129, no. 6, pp. 1461–1473, 2022. doi: 10.1007/s41348-022-00660-1 .
- [33] M. Reda, R. Suwwan, S. Alkafri, Y. Rashed, and T. Shanableh, "Agroid: A mobile app system for visual classification of plant species and diseases using deep learning and tensorflow lite," in *Informatics*, vol. 9. MDPI, 2022, p. 55. doi: 10.3390/informat-ics9030055 .
- [34] H. D. Mafukidze, G. Owomugisha, D. Otim, A. Nechibvute, C. Nyamhere, and F. Mazunga, "Adaptive thresholding of cnn features for maize leaf disease classification and severity estimation," *Applied Sciences*, vol. 12, no. 17, p. 8412, 2022.
- [35] G. Latif, S. E. Abdelhamid, R. E. Mallouhy, J. Alghazo, and Z. A. Kazimi, "Deep learning utilization in agriculture: Detection of rice plant diseases using an improved cnn model," *Plants*, vol. 11, no. 17, p. 2230, 2022. doi: 10.3390/plants11172230 .
- [36] A. Bruno, D. Moroni, R. Dainelli, L. Rocchi, S. Morelli, E. Ferrari, P. Toscano, and M. Martinelli, "Improving plant disease classification by adaptive minimal ensembling," *Frontiers in Artificial Intelligence*, vol. 5, p. 868926, 2022. doi: 10.3389/frai.2022.868926 .
- [37] J. Eunice, D. E. Popescu, M. K. Chowdary, and J. Hemanth, "Deep learning-based leaf disease detection in crops using images for agricultural applications," *Agronomy*, vol. 12, no. 10, p. 2395, 2022. doi: 10.3390/agronomy12102395 .
- [38] S. Albahli and M. Masood, "Efficient attention-based cnn network (eanet) for multi-class maize crop disease classification," *Frontiers in Plant Science*, vol. 13, p. 1003152, 2022. doi: 10.3389/fpls.2022.1003152 .

- [39] D. Novtahaning, H. A. Shah, and J.-M. Kang, “Deep learning ensemble-based automated and high-performing recognition of coffee leaf disease,” *Agriculture*, vol. 12, no. 11, p. 1909, 2022. doi: 10.3390/agriculture12111909 .
- [40] P. Alirezazadeh, M. Schirrmann, and F. Stolzenburg, “Improving deep learning-based plant disease classification with attention mechanism,” *Gesunde Pflanzen*, vol. 75, no. 1, pp. 49–59, 2023. doi: 10.1007/s10343-022-00796-y .
- [41] B. A. Fulle, C. Ma, X. Shi, W. Zhu, Z. Yemataw, and E. Assefa, “Efficient early warning system in identifying enset bacterial wilt disease using transfer learning,” in *2023 International Joint Conference on Neural Networks (IJCNN)*. IEEE, 2023, pp. 1–8. doi: 10.1109/IJCNN54540.2023.10191617 .
- [42] M. Mavaddat, M. Naderan, and S. E. Alavi, “Classification of rice leaf diseases using cnn-based pre-trained models and transfer learning,” in *2023 6th International Conference on Pattern Recognition and Image Analysis (IPRIA)*. IEEE, 2023, pp. 1–6. doi: 10.1109/IPRIA59240.2023.10147178 .
- [43] E. Paiva-Peredo, “Deep learning for the classification of cassava leaf diseases in unbalanced field data set,” in *International Conference on Advanced Network Technologies and Intelligent Computing*. Springer, 2022, pp. 101–114. doi: 10.1007/978-3-031-28183-9_8 .
- [44] D. Mohapatra and N. Das, “A precise model for accurate rice disease diagnosis: a transfer learning approach,” *Proceedings of the Indian National Science Academy*, vol. 89, no. 1, pp. 162–171, 2023. doi: 10.1007/s43538-022-00149-3 .
- [45] A. Diker, A. Elen, C. Közkurt, S. Kılıçarslan, E. Dönmez, K. Arslan, and E. C. Kuran, “An effective feature extraction method for olive peacock eye leaf disease classification,” *European Food Research and Technology*, vol. 250, no. 1, pp. 287–299, 2024. doi: 10.1007/s00217-023-04386-8 .
- [46] M. G. Lanjewar, P. Morajkar, and P. P., “Modified transfer learning frameworks to identify potato leaf diseases,” *Multimedia Tools and Applications*, vol. 83, no. 17, pp. 50401–50423, 2024. doi: 10.1007/s11042-023-17610-0 .

- [47] R. Ramya and P. Kumar, “High-performance deep transfer learning model with batch normalization based on multiscale feature fusion for tomato plant disease identification and categorization,” *Environmental Research Communications*, vol. 5, no. 12, p. 125015, 2023. doi: 10.1088/2515-7620/ace594 .
- [48] K. Shaheed, I. Qureshi, F. Abbas, S. Jabbar, Q. Abbas, H. Ahmad, and M. Z. Sajid, “Efficientrmt-net—an efficient resnet-50 and vision transformers approach for classifying potato plant leaf diseases,” *Sensors*, vol. 23, no. 23, p. 9516, 2023. doi: 10.3390/s23239516 .
- [49] J. An, N. Zhang, and W. H. Mahmoud, “Transfer learning-based deep learning model for corn leaf disease classification,” in *International Symposium on Neural Networks*. Springer, 2024, pp. 163–173. doi: 10.1007/978-981-97-4399-5_16 .
- [50] A. Salam, M. Naznine, N. Jahan, E. Nahid, M. Nahiduzzaman, and M. E. Chowdhury, “Mulberry leaf disease detection using cnn-based smart android application,” *IEEE Access*, 2024. doi: 10.1109/ACCESS.2024.3407153 .
- [51] R. K. Bania, N. A. Talukdar, and D. J. Bora, “Cutting-edge hybrid deep transfer learning approach for potato leaf disease classification,” *International Journal of Agricultural and Natural Sciences*, vol. 17, no. 1, pp. 111–123, 2024. doi: 10.5281/zenodo.10727496 .
- [52] Y. Hang, X. Meng, and Q. Wu, “Application of improved lightweight network and choquet fuzzy ensemble technology for soybean disease identification,” *IEEE Access*, 2024. doi: 10.1109/ACCESS.2024.3365829 .
- [53] A. L. A. Haikal, N. Yudistira, and A. Ridok, “Comprehensive mixed-based data augmentation for detection of rice leaf disease in the wild,” *Crop Protection*, p. 106816, 2024. doi: 10.1016/j.cropro.2024.106816 .
- [54] S. K. Shah, V. Kumbhar, and T. Singh, “Grape (*vitis vinifera*) leaf disease detection and classification using deep learning techniques: A study on real-time grape leaf image dataset in india,” *International Journal of Engineering*, vol. 37, no. 8, pp. 1522–1533, 2024. doi: 10.5829/ije.2024.37.08b.06 .

- [55] M. K. A. Mazumder, M. M. Kabir, A. Rahman, M. Abdullah-Al-Jubair, and M. Mridha, “Densenet201plus: Cost-effective transfer-learning architecture for rapid leaf disease identification with attention mechanisms,” *Heliyon*, vol. 10, no. 15, 2024. doi: 10.1016/j.heliyon.2024.e35625 .
- [56] S. Winiarti, A. Pujiyanta *et al.*, “Identification of chili plant diseases based on leaves using hyperparameter optimization architecture convolutional neural network.” *International Journal of Advanced Computer Science & Applications*, vol. 15, no. 11, 2024. doi: 10.14569/IJACSA.2024.0151185 .
- [57] A. Batool, J. Kim, S.-J. Lee, J.-H. Yang, and Y.-C. Byun, “An enhanced lightweight t-net architecture based on convolutional neural network (cnn) for tomato plant leaf disease classification,” *PeerJ Computer Science*, vol. 10, p. e2495, 2024. doi: 10.7717/peerj-cs.2495 .
- [58] J. Deng, W. Dong, R. Socher, L.-J. Li, K. Li, and L. Fei-Fei, “Imagenet: A large-scale hierarchical image database,” in *2009 IEEE conference on computer vision and pattern recognition*. Ieee, 2009, pp. 248–255. doi: 10.1109/CVPR.2009.5206848 .
- [59] J. E. Bidlack and S. Jansky, *Stern’s introductory plant biology*, 12th ed. New York, USA: McGraw-Hill New York, 2010, ISBN-10: 0073040525, ISBN-13: 978-0073040523.
- [60] Penn State Extension, “Plant disease basics and diagnosis,” 2012, accessed: 2024-11-11. [Online]. Available: <https://extension.psu.edu/plant-disease-basics-and-diagnosis>
- [61] A. Patel and B. Joshi, “A survey on the plant leaf disease detection techniques,” *International Journal of Advanced Research in Computer and Communication Engineering*, vol. 6, no. 1, pp. 229–231, 2017. doi: 10.17148/IJARCCE.2017.6143 .
- [62] F. A. Guth, S. Ward, and K. McDonnell, “From lab to field: An empirical study on the generalization of convolutional neural networks towards crop disease detection,” *European Journal of Engineering and Technology Research*, vol. 8, no. 2, pp. 33–40, 2023. doi: 10.24018/ejeng.2023.8.2.2773 .

- [63] A. Ahmad, A. El Gamal, and D. Saraswat, "Toward generalization of deep learning-based plant disease identification under controlled and field conditions," *IEEE Access*, vol. 11, pp. 9042–9057, 2023. doi: 10.1109/ACCESS.2023.3240100.
- [64] K. P. Ferentinos, "Deep learning models for plant disease detection and diagnosis," *Computers and electronics in agriculture*, vol. 145, pp. 311–318, 2018. doi: 10.1016/j.compag.2018.01.009.
- [65] N. H. Shabrina, S. Indarti, R. Maharani, D. A. Kristiyanti, N. Prastomo *et al.*, "A novel dataset of potato leaf disease in uncontrolled environment," *Data in Brief*, vol. 52, p. 109955, 2024. doi: 10.1016/j.dib.2023.109955.
- [66] D. P. Hughes and M. Salathe, "An open access repository of images on plant health to enable the development of mobile disease diagnostics," *arXiv e-prints*, pp. arXiv–1511, 2015. doi: 10.48550/arXiv.1511.08060.
- [67] S. P. Mohanty, "Plantvillage dataset," <https://github.com/spMohanty/PlantVillage-Dataset>, 2016, accessed: 2024-10-21.
- [68] F. Mohameth, C. Bingcai, and K. A. Sada, "Plant disease detection with deep learning and feature extraction using plant village," *Journal of Computer and Communications*, vol. 8, no. 6, pp. 10–22, 2020.
- [69] W. Albattah, M. Nawaz, A. Javed, M. Masood, and S. Albahli, "A novel deep learning method for detection and classification of plant diseases," *Complex & Intelligent Systems*, pp. 1–18, 2022.
- [70] M. Gehlot, R. K. Saxena, and G. C. Gandhi, "'tomato-village': a dataset for end-to-end tomato disease detection in a real-world environment," *Multimedia Systems*, vol. 29, no. 6, pp. 3305–3328, 2023. doi: 10.1007/s00530-023-01158-y.
- [71] M. Gehlot, "Tomato-village dataset," <https://www.kaggle.com/datasets/mamtag/tomato-village>, 2023, accessed: 2024-10-21.
- [72] Y. Sun, L. Ning, B. Zhao, and J. Yan, "Tomato leaf disease classification by combining efficientnetv2 and a swin transformer," *Applied Sciences*, vol. 14, no. 17, p. 7472, 2024.

- [73] M. R. Saeed and D. J. Rashid, "Potato disease leaf dataset(pld)," 2021. doi: 10.34740/KAGGLE/DS/1562973. [Online]. Available: <https://www.kaggle.com/ds/1562973>
- [74] J. Rashid, I. Khan, G. Ali, S. H. Almotiri, M. A. AlGhamdi, and K. Masood, "Multi-level deep learning model for potato leaf disease recognition," *Electronics*, vol. 10, no. 17, p. 2064, 2021.
- [75] A. Kimutai, Gibson; Förster, "tea sickness dataset," 2022. doi: 10.17632/j32xdt2ff5.2. [Online]. Available: <https://data.mendeley.com/datasets/j32xdt2ff5/2>
- [76] Q. Heng, S. Yu, and Y. Zhang, "A new ai-based approach for automatic identification of tea leaf disease using deep neural network based on hybrid pooling," *Heliyon*, vol. 10, no. 5, 2024.
- [77] E. Mwebaze, T. Gebru, A. Frome, S. Nsumba, and J. Tsubira, "icassava 2019 fine-grained visual categorization challenge," *arXiv preprint arXiv:1908.02900*, 2019. doi: 10.48550/arXiv.1908.02900.
- [78] E. Mwebaze, J. Mostipak, Joyce, J. Elliott, and S. Dane, "Cassava leaf disease classification," 2020, accessed: 2024-10-21. [Online]. Available: <https://kaggle.com/competitions/cassava-leaf-disease-classification>
- [79] O. O. Abayomi-Alli, R. Damaševičius, S. Misra, and R. Maskeliūnas, "Cassava disease recognition from low-quality images using enhanced data augmentation model and deep learning," *Expert Systems*, vol. 38, no. 7, p. e12746, 2021.
- [80] D. O. Oyewola, E. G. Dada, S. Misra, and R. Damaševičius, "Detecting cassava mosaic disease using a deep residual convolutional neural network with distinct block processing," *PeerJ Computer Science*, vol. 7, p. e352, 2021.
- [81] A. Ahmad, D. Saraswat, A. E. Gamal, and G. Johal, "Cd&s dataset: Handheld imagery dataset acquired under field conditions for corn disease identification and severity estimation," *arXiv preprint arXiv:2110.12084*, 2021. doi: 10.48550/arXiv.2110.12084.
- [82] A. Ahmad, "CD&S Dataset," 2021. doi: 10.17605/OSF.IO/S6RU5., accessed: 2024-10-21. [Online]. Available: <https://osf.io/s6ru5/>

- [83] L. Divyanth, A. Ahmad, and D. Saraswat, "A two-stage deep-learning based segmentation model for crop disease quantification based on corn field imagery," *Smart Agricultural Technology*, vol. 3, p. 100108, 2023.
- [84] N. Sultana, S. B. Shorif, M. Akter, and M. S. Uddin, "A dataset for successful recognition of cucumber diseases," *Data in Brief*, vol. 49, p. 109320, 2023.
- [85] —, "Cucumber Disease Recognition Dataset," 2022. doi: 10.17632/y6d3z6f8z9.1 ., accessed: 2024-10-21. [Online]. Available: <https://data.mendeley.com/datasets/y6d3z6f8z9/1>
- [86] X. Wang and J. Liu, "Detection of small targets in cucumber disease images through global information perception and feature fusion," *Frontiers in Sustainable Food Systems*, vol. 8, p. 1366387, 2024.
- [87] G. Fenu and F. M. Mallocci, "Diamos plant: A dataset for diagnosis and monitoring plant disease," *Agronomy*, vol. 11, no. 11, p. 2107, 2021. doi: 10.3390/agronomy11112107 .
- [88] —, "Diamos plant dataset: A dataset for diagnosis and monitoring plant disease," 2021. doi: 10.5281/zenodo.5557313 ., accessed: 2024-10-21. [Online]. Available: <https://zenodo.org/records/5557313>
- [89] K. Alshammari, R. Alshammari, A. Alshammari, and T. Alkhudaydi, "An improved pear disease classification approach using cycle generative adversarial network," *Scientific Reports*, vol. 14, no. 1, p. 6680, 2024.
- [90] Petchiammal, B. Kiruba, Murugan, and P. Arjunan, "Paddy doctor: A visual image dataset for automated paddy disease classification and benchmarking," in *Proceedings of the 6th Joint International Conference on Data Science & Management of Data (10th ACM IKDD CODS and 28th COMAD)*, 2023, pp. 203–207. doi: 10.1145/3570991.3570994 .
- [91] Petchiammal and P. Arjunan, "Paddy disease classification," <https://kaggle.com/competitions/paddy-disease-classification>, 2022, kaggle.

- [92] V. Garg, S. Agarwal, and S. Sharma, “Deep learning-based paddy doctor for sustainable agriculture,” in *2023 Seventh International Conference on Image Information Processing (ICIIP)*. IEEE, 2023, pp. 485–490.
- [93] R. Thapa, K. Zhang, N. Snavely, S. Belongie, and A. Khan, “The plant pathology challenge 2020 data set to classify foliar disease of apples,” *Applications in plant sciences*, vol. 8, no. 9, p. e11390, 2020. doi: 10.1002/aps3.11390.
- [94] C. Kaeser-Chen and M. S. Dane, “Plant pathology 2020 - fgvc7,” <https://kaggle.com/competitions/plant-pathology-2020-fgvc7>, 2020, kaggle.
- [95] V. Acharya and V. Ravi, “Apple foliar leaf disease detection through improved capsule neural network architecture,” *Multimedia Tools and Applications*, vol. 83, no. 16, pp. 48 585–48 605, 2024.
- [96] S. Nain, N. Mittal, and A. Jain, “Recognition of apple leaves infection using densenet121 with additional layers,” in *International Conference on Micro-Electronics and Telecommunication Engineering*. Springer, 2023, pp. 297–307.
- [97] R. Thapa, Q. Wang, N. Snavely, S. Belongie, and A. Khan, “The plant pathology 2021 challenge dataset to classify foliar disease of apples,” in *CVPR FGVC8 Workshop*. Cornell University, 2021, accessed: 2024-10-21. [Online]. Available: <https://vision.cornell.edu/se3/wp-content/uploads/2021/09/029.pdf>
- [98] R. Thapa, K. Zhang, N. Snavely, S. Belongie, and A. Khan, “Plant pathology 2021 - fgvc8,” Kaggle, 2021, accessed: 2024-10-21. [Online]. Available: <https://kaggle.com/competitions/plant-pathology-2021-fgvc8>
- [99] M. Chilinski, P. Góralewski, T. Lehmann, and J. Stypulkowska, “Fgvc8 based foliar diseases identification with use of multi-label classifiers,” *International Journal of Computer Information Systems and Industrial Management Applications*, vol. 14, pp. 8–8, 2022.
- [100] A. Ait Nasser and M. A. Akhloufi, “A hybrid deep learning architecture for apple foliar disease detection,” *Computers*, vol. 13, no. 5, p. 116, 2024.

- [101] X. Liu, W. Min, S. Mei, L. Wang, and S. Jiang, "Plant disease recognition: A large-scale benchmark dataset and a visual region and loss reweighting approach," *IEEE Transactions on Image Processing*, vol. 30, pp. 2003–2015, 2021. doi: 10.1109/TIP.2021.3049334.
- [102] —, "Pdd271: Plant disease recognition dataset," <https://github.com/liuxindazz/PDD271>, 2020, gitHub Repository.
- [103] U. Afzaal, "Strawberry disease detection dataset," 2021, accessed: October 23, 2024. [Online]. Available: <https://www.kaggle.com/datasets/usmanafzaal/strawberry-disease-detection-dataset>
- [104] U. Afzaal, B. Bhattarai, Y. R. Pandeya, and J. Lee, "An instance segmentation model for strawberry diseases based on mask r-cnn," *Sensors*, no. 19, p. 6565, 2021. doi: 10.3390/s21196565.
- [105] S. Zhao, J. Liu, and S. Wu, "Multiple disease detection method for greenhouse-cultivated strawberry based on multiscale feature fusion faster r_cnn," *Computers and electronics in agriculture*, vol. 199, p. 107176, 2022.
- [106] S. Chen, Y. Liao, F. Lin, and B. Huang, "An improved lightweight yolov5 algorithm for detecting strawberry diseases," *IEEE Access*, vol. 11, pp. 54 080–54 092, 2023.
- [107] P. Kayal, "Plantdoc dataset," <https://github.com/pratikkayal/PlantDoc-Dataset>, 2020, accessed: 2024-10-21.
- [108] V. Menon, V. Ashwin, and R. K. Deepa, "Plant disease detection using cnn and transfer learning," in *2021 International Conference on Communication, Control and Information Sciences (ICCISc)*, vol. 1. IEEE, 2021, pp. 1–6.
- [109] M.-L. Huang and Y.-H. Chang, "Dataset of tomato leaves," 2020. doi: 10.17632/ngdgg79rzb.1. [Online]. Available: <https://data.mendeley.com/datasets/ngdgg79rzb/1>
- [110] M. Astani, M. Hasheminejad, and M. Vaghefi, "A diverse ensemble classifier for tomato disease recognition," *Computers and Electronics in Agriculture*, vol. 198, p. 107054, 2022.

- [111] N. H. Shabrina, S. Indarti, R. Maharani, D. A. Kristiyanti, I. Irmawati, N. Prastomo, and T. A. M, “Potato leaf disease dataset in uncontrolled environment,” <https://data.mendeley.com/datasets/ptz377bwb8/1>, 2023. doi: 10.17632/ptz377bwb8.1 ., mendeley Data.
- [112] C.-Y. Chang and C.-C. Lai, “Potato leaf disease detection based on a lightweight deep learning model,” *Machine Learning and Knowledge Extraction*, vol. 6, no. 4, pp. 2321–2335, 2024.
- [113] L. P. Lourdu Antony, “Rice leaf diseases dataset,” 2023. doi: 10.17632/dwtn3c6w6p.1 . [Online]. Available: <https://data.mendeley.com/datasets/dwtn3c6w6p/1>
- [114] S. Thite, Y. Suryawanshi, K. Patil, and P. Chumchu, “Sugarcane leaf dataset: A dataset for disease detection and classification for machine learning applications,” *Data in Brief*, vol. 53, p. 110268, 2024. doi: 10.1016/j.dib.2024.110268 .
- [115] S. Thite, Y. Suryawanshi, K. PATIL, and prawit chumchu, “Sugarcane leaf image dataset,” 2023. doi: 10.17632/9twjtv92vk.1 ., accessed: 2024-10-21. [Online]. Available: <https://doi.org/10.17632/9twjtv92vk.1>
- [116] İ. Kunderacıoğlu and İ. Paçal, “Deep learning-based disease detection in sugarcane leaves: Evaluating efficientnet models,” *Journal of Operations Intelligence*, vol. 2, no. 1, pp. 321–235, 2024.
- [117] İ. Paçal and İ. Kunderacıoğlu, “Data-efficient vision transformer models for robust classification of sugarcane,” *Journal of Soft Computing and Decision Analytics*, vol. 2, no. 1, pp. 258–271, 2024.
- [118] K. He, X. Zhang, S. Ren, and J. Sun, “Identity mappings in deep residual networks,” in *Computer Vision—ECCV 2016: 14th European Conference, Amsterdam, The Netherlands, October 11–14, 2016, Proceedings, Part IV 14*. Springer, 2016, pp. 630–645. doi: 10.1007/978-3-319-46493-0_38 .
- [119] K. Simonyan and A. Zisserman, “Very deep convolutional networks for large-scale image recognition,” *arXiv preprint arXiv:1409.1556*, 2014. doi: 10.48550/arXiv.1409.1556 .

- [120] C. Szegedy, V. Vanhoucke, S. Ioffe, J. Shlens, and Z. Wojna, “Rethinking the inception architecture for computer vision,” in *Proceedings of the IEEE conference on computer vision and pattern recognition*, 2016, pp. 2818–2826. doi: 10.1109/CVPR.2016.308 .
- [121] M. Tan and Q. Le, “Efficientnetv2: Smaller models and faster training,” in *International conference on machine learning*. PMLR, 2021, pp. 10 096–10 106. [Online]. Available: <https://proceedings.mlr.press/v139/tan21a.html>
- [122] B. Zoph, V. Vasudevan, J. Shlens, and Q. V. Le, “Learning transferable architectures for scalable image recognition,” in *Proceedings of the IEEE conference on computer vision and pattern recognition*, 2018, pp. 8697–8710. doi: 10.1109/CVPR.2018.00907 .
- [123] Z. Liu, H. Mao, C.-Y. Wu, C. Feichtenhofer, T. Darrell, and S. Xie, “A convnet for the 2020s,” in *Proceedings of the IEEE/CVF conference on computer vision and pattern recognition*, 2022, pp. 11 976–11 986. doi: 10.1109/CVPR52688.2022.01167 .
- [124] G. Huang, Z. Liu, L. Van Der Maaten, and K. Q. Weinberger, “Densely connected convolutional networks,” in *Proceedings of the IEEE conference on computer vision and pattern recognition*, 2017, pp. 4700–4708. doi: 10.1109/CVPR.2017.243 .
- [125] D. J. Richter and K. Kim, “Assessing the performance of domain-specific models for plant leaf disease classification: a comprehensive benchmark of transfer-learning on open datasets,” *Scientific Reports*, vol. 15, no. 1, pp. 1–31, 2025. doi: 10.1038/s41598-025-03235-w .
- [126] M. Xu, J.-E. Park, J. Lee, J. Yang, and S. Yoon, “Plant disease recognition datasets in the age of deep learning: challenges and opportunities,” *Frontiers in Plant Science*, vol. 15, p. 1452551, 2024.
- [127] TensorFlow, “tf.keras.applications - tensorflow core v2.13.0,” 2024, accessed: 2024-11-14. [Online]. Available: https://www.tensorflow.org/api_docs/python/tf/keras/applications
- [128] C. Szegedy, S. Ioffe, V. Vanhoucke, and A. Alemi, “Inception-v4, inception-resnet and the impact of residual connections on learning,” 2017. doi: 10.1609/aaai.v31i1.11231 .

- [129] A. Howard, M. Sandler, G. Chu, L.-C. Chen, B. Chen, M. Tan, W. Wang, Y. Zhu, R. Pang, V. Vasudevan *et al.*, “Searching for mobilenetv3,” in *Proceedings of the IEEE/CVF international conference on computer vision*, 2019, pp. 1314–1324. doi: 10.1109/ICCV.2019.00140.
- [130] F. Chollet, “Xception: Deep learning with depthwise separable convolutions,” in *Proceedings of the IEEE conference on computer vision and pattern recognition*, 2017, pp. 1251–1258. doi: 10.1109/CVPR.2017.195.
- [131] A. Dosovitskiy, L. Beyer, A. Kolesnikov, D. Weissenborn, X. Zhai, T. Unterthiner, M. Dehghani, M. Minderer, G. Heigold, S. Gelly *et al.*, “An image is worth 16x16 words: Transformers for image recognition at scale,” *arXiv preprint arXiv:2010.11929*, 2020. doi: 10.48550/arXiv.2010.11929.
- [132] F. Morales, “vit-keras: Keras implementation of vision transformer (vit),” <https://github.com/faustomorales/vit-keras>, 2020, accessed: 2025-06-04.
- [133] M. I. Bappi, D. J. Richter, and K. Kim, “Assessing the effectiveness of augmentation techniques in enhancing plant leaf disease classification,” *Smart Media Journal*, vol. 14, no. 1, pp. 17–25, 2025. doi: 10.30693/SMJ.2025.14.1.17.
- [134] D. J. Richter and K. Kim, “Pldc-80: A combined augmented hybrid plant leaf disease classification benchmarking dataset,” 2025, in press.
- [135] D. J. Richter, “Pldc-80,” <https://github.com/JDatPNW/PLDC-80>, 2025, accessed: 2025-03-27.
- [136] D. J. Richter and K. Kim, “Pldc-net: A domain specific base model for plant leaf disease classification,” manuscript in preparation.
- [137] D. Hendrycks and K. Gimpel, “Gaussian error linear units (gelus),” *arXiv preprint arXiv:1606.08415*, 2016. doi: 10.48550/arXiv.1606.08415.
- [138] S. Elfving, E. Uchibe, and K. Doya, “Sigmoid-weighted linear units for neural network function approximation in reinforcement learning,” *Neural networks*, vol. 107, pp. 3–11, 2018. doi: 10.1016/j.neunet.2017.12.012.

- [139] P. Ramachandran, B. Zoph, and Q. V. Le, “Swish: a self-gated activation function,” *arXiv preprint arXiv:1710.05941*, vol. 7, no. 1, p. 5, 2017. doi: 10.48550/arXiv.1710.05941 .
- [140] L. Chen, H. Zhang, J. Xiao, L. Nie, J. Shao, W. Liu, and T.-S. Chua, “Sca-cnn: Spatial and channel-wise attention in convolutional networks for image captioning,” in *Proceedings of the IEEE conference on computer vision and pattern recognition*, 2017, pp. 5659–5667. doi: 10.1109/CVPR.2017.667 .
- [141] J. Hu, L. Shen, and G. Sun, “Squeeze-and-excitation networks,” in *Proceedings of the IEEE conference on computer vision and pattern recognition*, 2018, pp. 7132–7141. doi: 10.1109/CVPR.2018.00745 .
- [142] M. A. Lab. (2020, January) Bean disease dataset. [Online]. Available: <https://github.com/AI-Lab-Makerere/ibean/>
- [143] M. E. Mignoni, “Images of soybean leaves,” 2021. doi: 10.17632/bycbh73438.1 . [Online]. Available: <https://doi.org/10.17632/bycbh73438.1>
- [144] M. E. Mignoni, A. Honorato, R. Kunst, R. Righi, and A. Massuquetti, “Soybean images dataset for caterpillar and diabrotica speciosa pest detection and classification,” *Data in Brief*, vol. 40, p. 107756, 2022. doi: 10.1016/j.dib.2021.107756 .

식물 잎 질병 분류를 위한 강력한 사전 학습 기본 모델 개발

David Jona Richter

전남대학교대학원 인공지능융합학과

(지도교수: 김정백)

(국문초록)

식물, 작물, 그리고 그 수확물은 우리 생존에 필수적입니다. 우리 사회는 식량을 농업과 농부에게 크게 의존하지만, 질병과 해충은 매년 큰 손실을 초래합니다. 따라서 질병을 조기에 발견하고 적절히 치료하여 가능한 한 확산을 막는 것이 매우 중요합니다. 수작업 및 전통적인 방법은 전문 지식을 갖춘 인력이 밭을 직접 돌아다니며 증상을 "손으로" 확인하거나 현미경과 같은 실험실 장비를 사용하여 식물의 질병을 분석해야 합니다. 이는 당연히 매우 힘들고 시간이 많이 소요되며 숙련된 인력도 필요합니다. 따라서 이 과정을 자동화해야 할 필요성이 대두되었습니다. 그 결과 머신러닝(ML) 기법이 적용되어 유망한 결과를 얻었지만, 머신러닝에는 단점이 있습니다. 특히 이미지 데이터(일반 이미지, 다중 스펙트럼 이미지, 초분광 이미지 모두)에서 연구자가 특징을 추출해야 합니다. 딥러닝(DL) 기법은 이러한 문제를 해결할 뿐만 아니라 기존 머신러닝보다 성능이 더 우수한 경향이 있습니다. CNN 모델은 수동 특징 생성 없이 이미지에서 특징을 자동으로 추출한 후 분류기(ML 또는 DL)에 입력할 수 있으므로 특히 효율적입니다. 그 이후로 다양한 DL 모델이 제안되어 식물 질병을 식별하는 데 사용되었으며, 그 성공률은 다양했습니다. 그중 대부분은 이미지 데이터를 입력으로 사용하는 CNN 아키텍처였습니다. CNN을 비롯한 모든 DL 방법은 제대로 학습하려면 방대한 양의 데이터가 필요하기 때문에, 데이터 세트는 모델의 최종 성능에 큰 영향을 미칩니다. 데이터 세트가 분야에 미치는 중요성에도 불구하고, 공개적으로 사용 가능한 데이터 세트와 완전한 기능을 갖춘 모델을 충분히 학습하는 데 필요한 데이터 세트 간에는 여전히 약간의 차이가 있는 것으로 보입니다. 이러한 단점을 극복하기 위해 본 논문

에서는 식물 잎 질병 분류 분야의 공개 데이터 세트를 파악하고, 이를 기반으로 학습 가능한 모델을 선정했으며, 적합성을 확인하기 위한 광범위한 벤치마크를 수행했습니다. 그런 다음 이러한 결과와 증강 적용성 연구 결과를 바탕으로 새로운 데이터 세트를 구성했습니다. 이 데이터 세트는 DenseNet201 아키텍처를 기반으로 하는 새로운 모델을 훈련하는 데 사용될 예정이며, 해당 새로운 데이터 세트에서 기존 모델보다 우수한 성능을 보였을 뿐만 아니라 다른 새로운 데이터 세트에서 식물 잎 질병 분류 도메인 특정 전이 학습 실험에서도 기존 모델보다 우수한 성능을 보였습니다.

A. Appendix Datasets

A.1 Lab Datasets

A.1.1 Plant Village

Table A.1: Information about the Plant Village Dataset.

Plants	<ol style="list-style-type: none"> 1. Corn (Maize) 2. Potato 3. Pepper (Bell) 4. Tomato 5. Blueberry 	<ol style="list-style-type: none"> 6. Cherry 7. Squash 8. Orange 9. Raspberry 10. Apple 	<ol style="list-style-type: none"> 11. Grape 12. Peach 13. Strawberry 14. Soybean
Diseases	<ol style="list-style-type: none"> 1. Apple <ul style="list-style-type: none"> • Healthy • Cedar Apple Rust • Apple Scab • Apple Black Rot 2. Blueberry <ul style="list-style-type: none"> • Healthy 3. Cherry <ul style="list-style-type: none"> • Healthy • Powdery Mildew 4. Corn <ul style="list-style-type: none"> • Healthy • Common Rust • Northern Leaf Blight • Gray Leaf Spot 	<ol style="list-style-type: none"> 5. Grape <ul style="list-style-type: none"> • Healthy • Leaf Blight • Black Measles • Black Rot 6. Orange <ul style="list-style-type: none"> • Citrus Greening 7. Peach <ul style="list-style-type: none"> • Healthy • Bacterial Spot 8. Bell Pepper <ul style="list-style-type: none"> • Healthy • Bacterial Spot 9. Potato <ul style="list-style-type: none"> • Healthy • Early Blight • Late Blight 10. Raspberry <ul style="list-style-type: none"> • Healthy 	<ol style="list-style-type: none"> 11. Soybean <ul style="list-style-type: none"> • Healthy 12. Squash <ul style="list-style-type: none"> • Powdery Mildew 13. Strawberry <ul style="list-style-type: none"> • Healthy • Leaf Scorch 14. Tomato <ul style="list-style-type: none"> • Healthy • Leaf Mold • Leaf Spot • Early Blight • Late Blight • Spider Mites • Bacterial Spot • Mosaic Virus • Yellow Leaf Curl Virus • Target Spot
Number of Classes	38		
Number of Images	54,304		

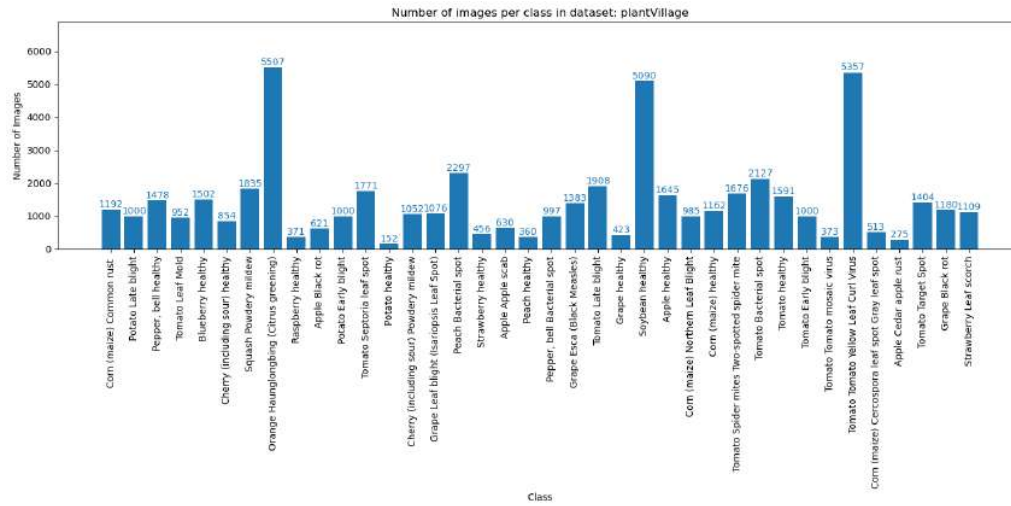


Figure A.1: Class Distribution of the Plant Village Dataset.

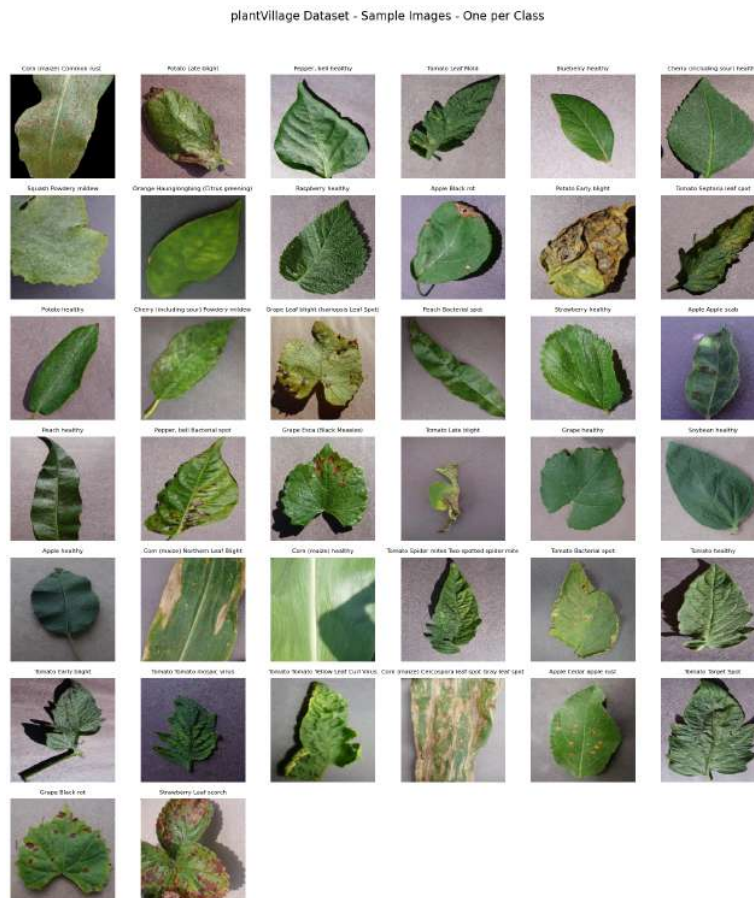


Figure A.2: A sample image of each class present in the Plant Village Dataset.

A.1.2 Tomato Village

Table A.2: Information about the Tomato Village Dataset.

Plants	Tomato
Diseases	<ol style="list-style-type: none">1. Healthy2. Leaf Miner3. Pottasium Deficiency4. Spotted with Virus5. Magnesium Deficiency6. Early Blight7. Late Blight8. Nitrogen Deficiency
Number of Classes	8
Number of Images	4,526

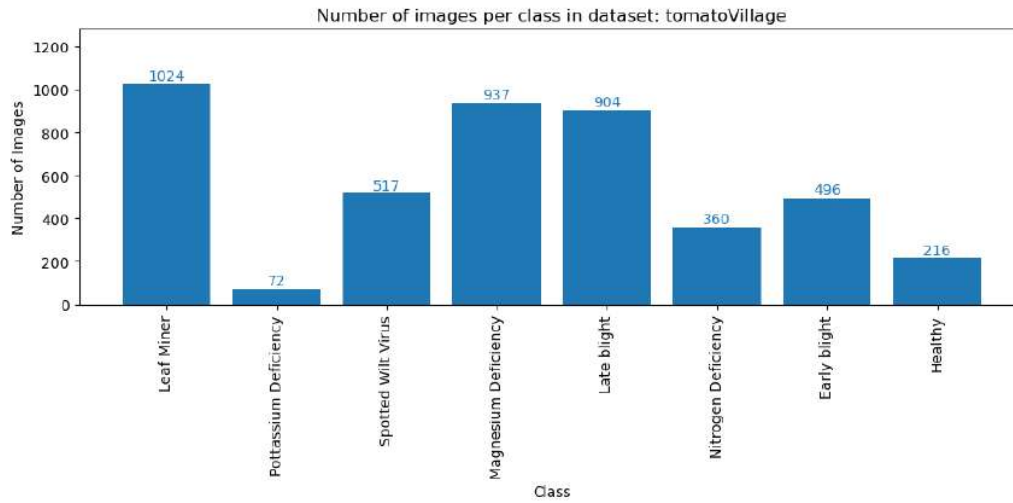


Figure A.3: Class Distribution of the Tomato Village Dataset.

tomatoVillage Dataset - Sample Images - One per Class

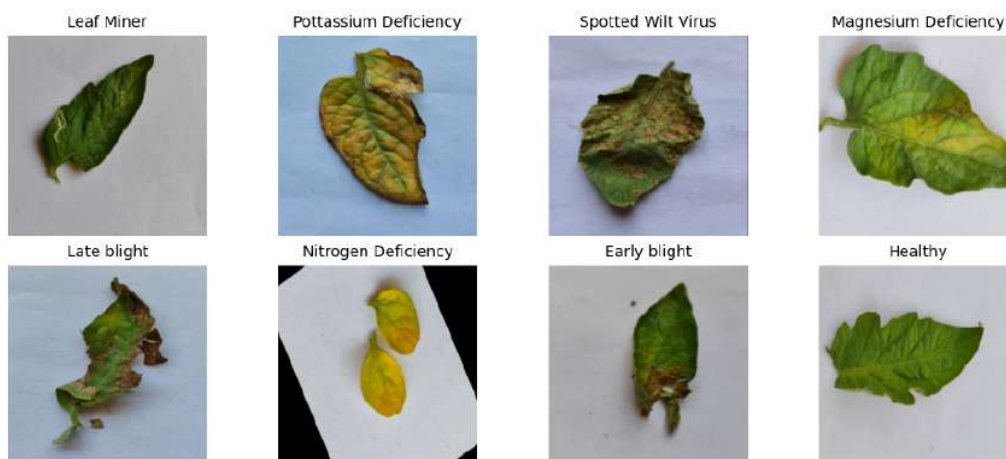


Figure A.4: A sample image of each class present in the Tomato Village Dataset.

A.1.3 Potato Disease Leaf Dataset (PLD)

Table A.3: Information about the PLD Dataset.

Plants	Potato
Diseases	<ol style="list-style-type: none"> 1. Healthy 2. Early Blight 3. Late Blight
Number of Classes	3
Number of Images	4,062

pld Dataset - Sample Images - One per Class

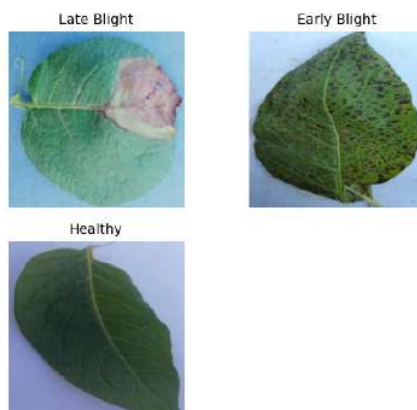


Figure A.6: A sample image of each class present in the PLD Dataset.

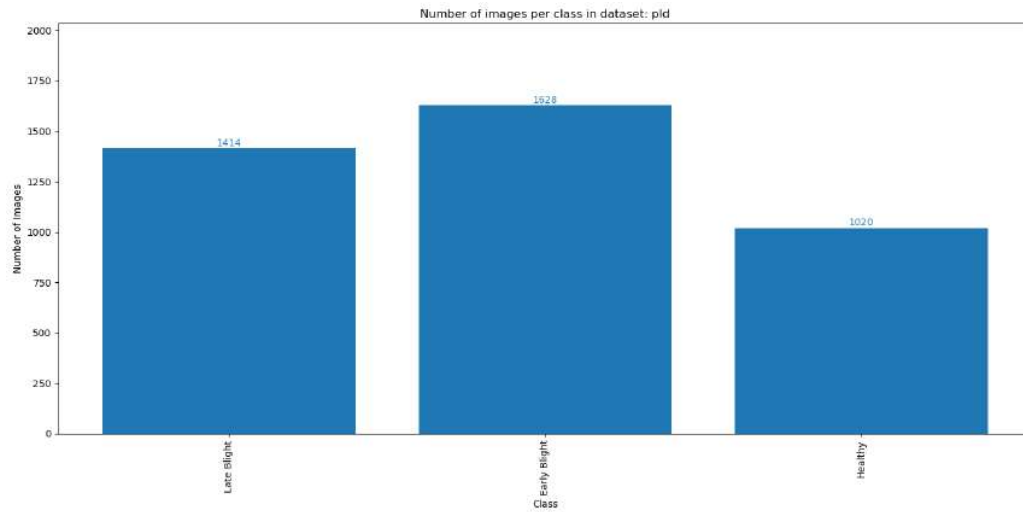


Figure A.5: Class Distribution of the PLD Dataset.

A.1.4 Tea Sickness Dataset

Table A.4: Information about the Tea Leaf Dataset.

Plants	Tea
Diseases	<ol style="list-style-type: none"> 1. Healthy 2. Red Leaf Spot 3. Bird Eye Spot 4. Anthracnose 5. Gray Light 6. Brown Blight 7. Algal Leaf 8. White Spot
Number of Classes	8
Number of Images	885

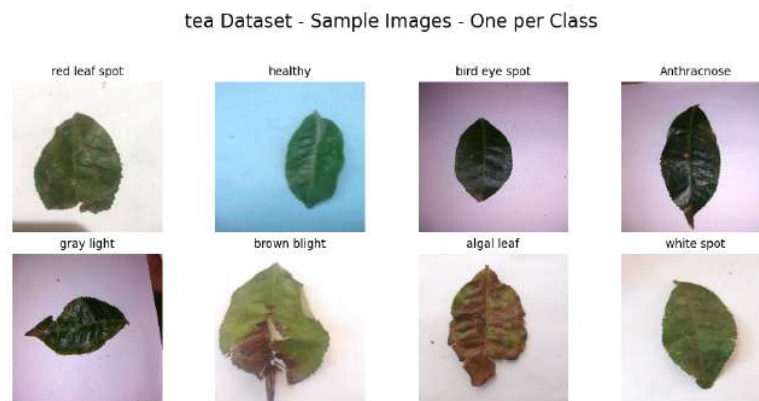


Figure A.8: A sample image of each class present in the Tea Dataset.

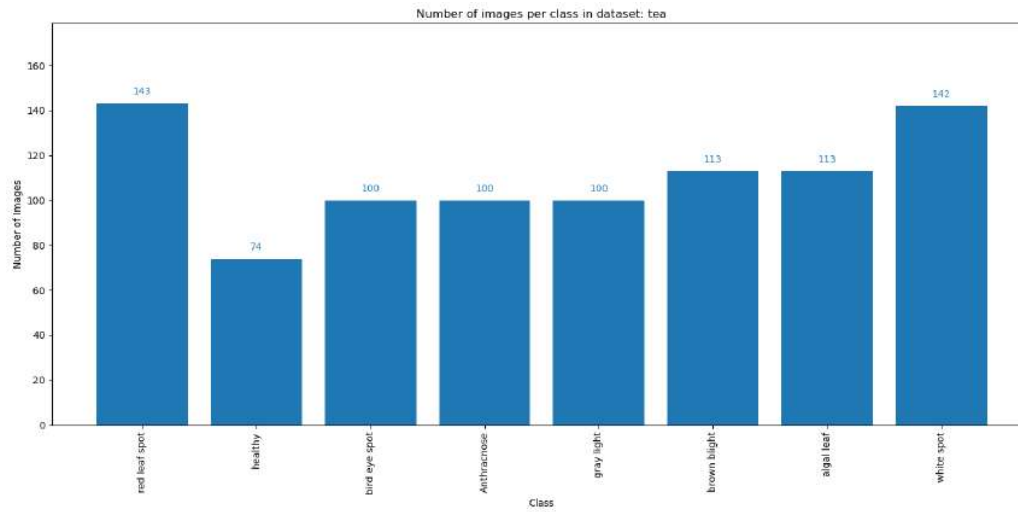


Figure A.7: Class Distribution of the Tea Dataset.

A.2 Field Datasets

A.2.1 Cassava Leaf Disease Classification

Table A.5: Information about the Cassava Dataset.

Plants	Cassava
Diseases	1. Healthy 2. Cassava Bacterial Blight 3. Cassava Mosaic Disease 4. Cassava Green Mottle 5. Cassava Brown Streak Disease
Number of Classes	5
Number of Images	21,397

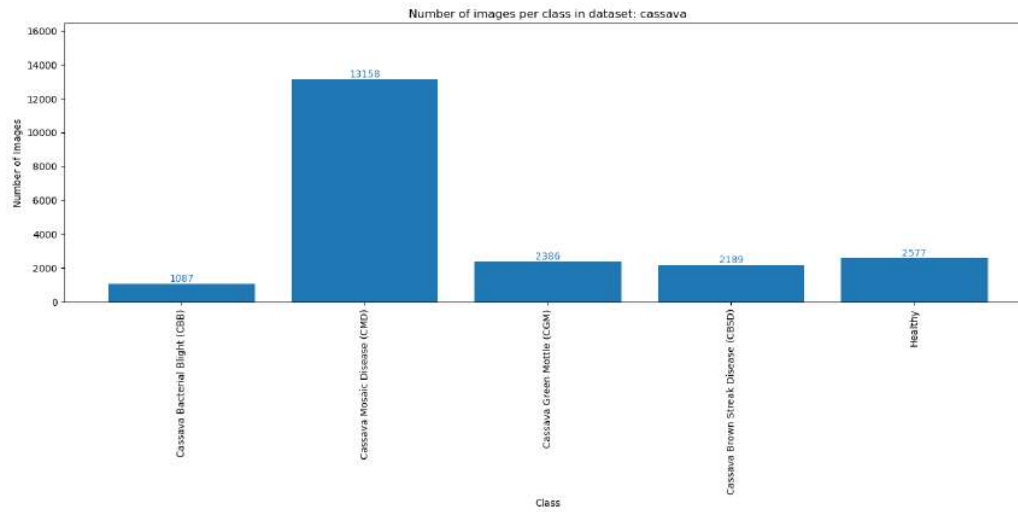


Figure A.9: Class Distribution of the Cassava Dataset.

cassava Dataset - Sample Images - One per Class



Figure A.10: A sample image of each class present in the Cassava Dataset.

A.2.2 CD&S Dataset

Table A.6: Information about the CD&S Dataset.

Plants	Corn
Diseases	1. Northern Leaf Blight 2. Gray Leaf Spot 3. Northern Leaf Spot
Number of Classes	3
Number of Images	1,571

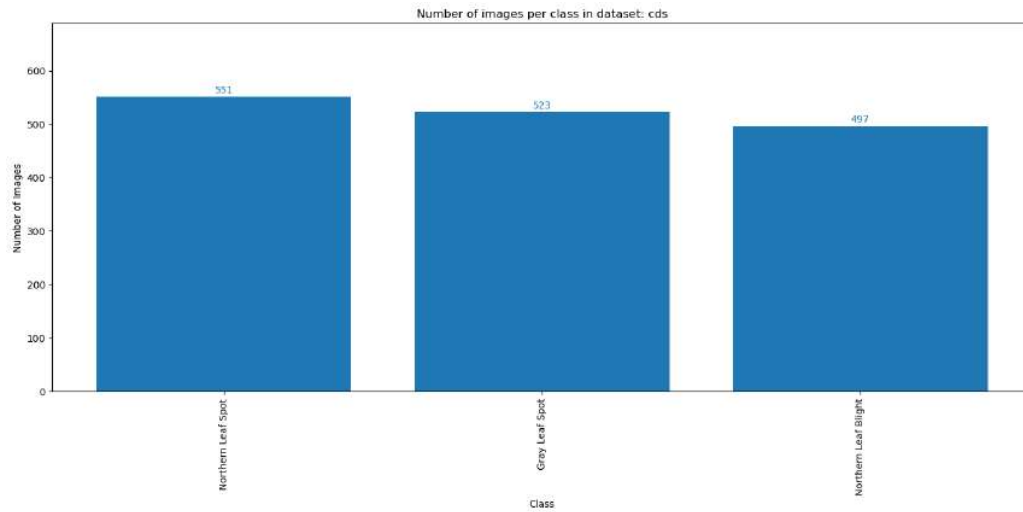


Figure A.11: Class Distribution of the CD&S Dataset.

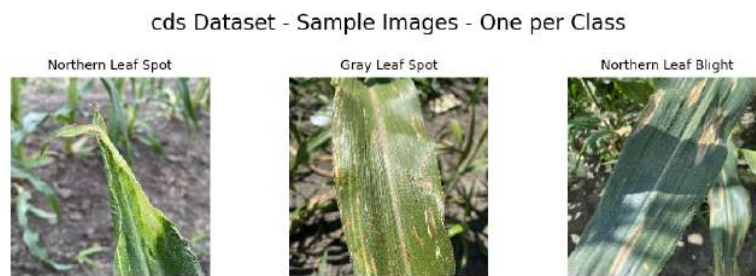


Figure A.12: A sample image of each class present in the CD&S Dataset.

A.2.3 Cucumber Disease Recognition Dataset

Table A.7: Information about the Cucumber Dataset.

Plants	Cucumber
Diseases	1. Healthy 2. Downy Mildew 3. Gummy Stem Blight 4. Anthracnose 5. Bacterial Wilt
Number of Classes	5
Number of Images	800

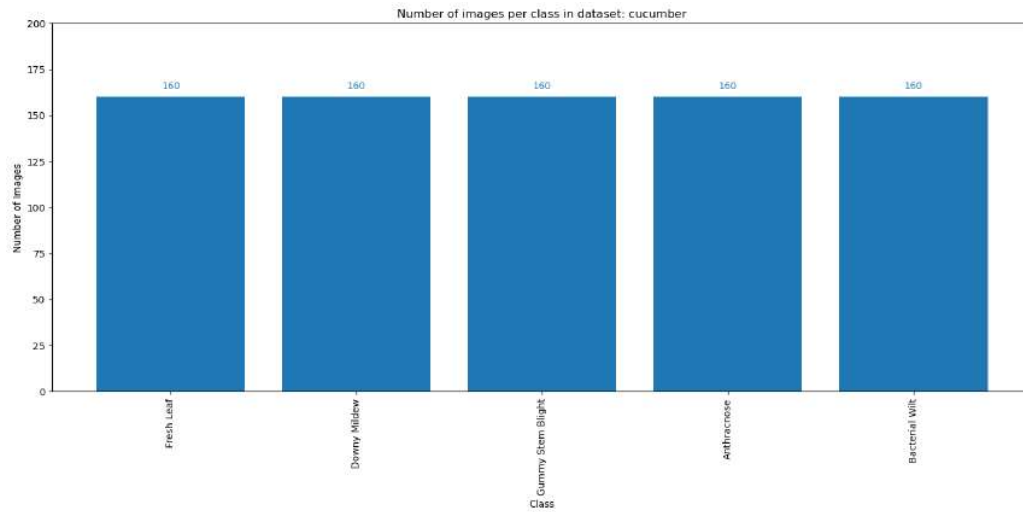


Figure A.13: Class Distribution of the Cucumber Dataset.

cucumber Dataset - Sample Images - One per Class

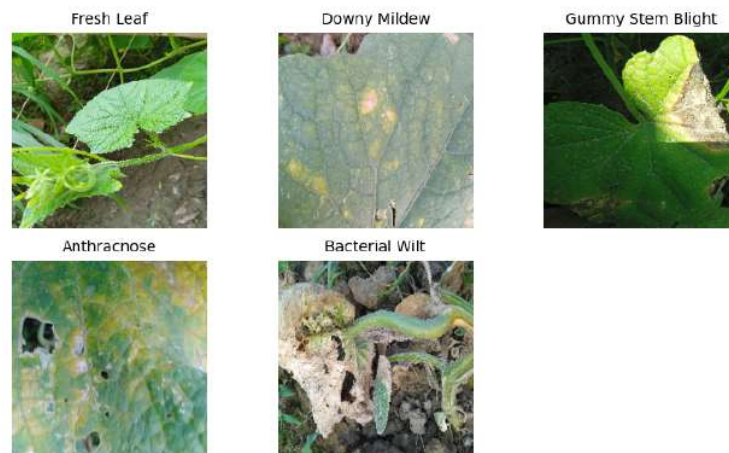


Figure A.14: A sample image of each class present in the Cucumber Dataset.

A.2.4 DiaMOS Plant

Table A.8: Information about the diaMOS Dataset.

Plants	Pear
Diseases	1. Healthy 2. Slug 3. Spot 4. Curl
Number of Classes	4
Number of Images	3,006

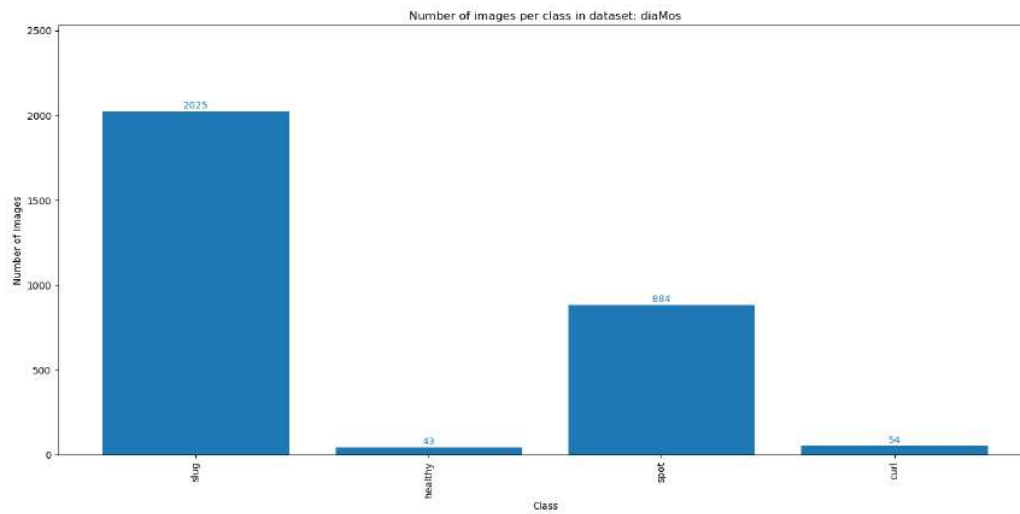


Figure A.15: Class Distribution of the diaMOS Dataset.

diaMos Dataset - Sample Images - One per Class



Figure A.16: A sample image of each class present in the diaMOS Dataset.

A.2.5 Paddy Doctor

Table A.9: Information about the Paddy Doctor Dataset.

Plants	Rice
Diseases	<ol style="list-style-type: none"> 1. Healthy 2. Bacterial Leaf Streak 3. Tungro 4. Brown Spot 5. Dead Heart 6. Hispa 7. Downy Mildew 8. Bacterial Panicle Blight 9. Blast 10. Bacterial Leaf Blight
Number of Classes	10
Number of Images	10,407

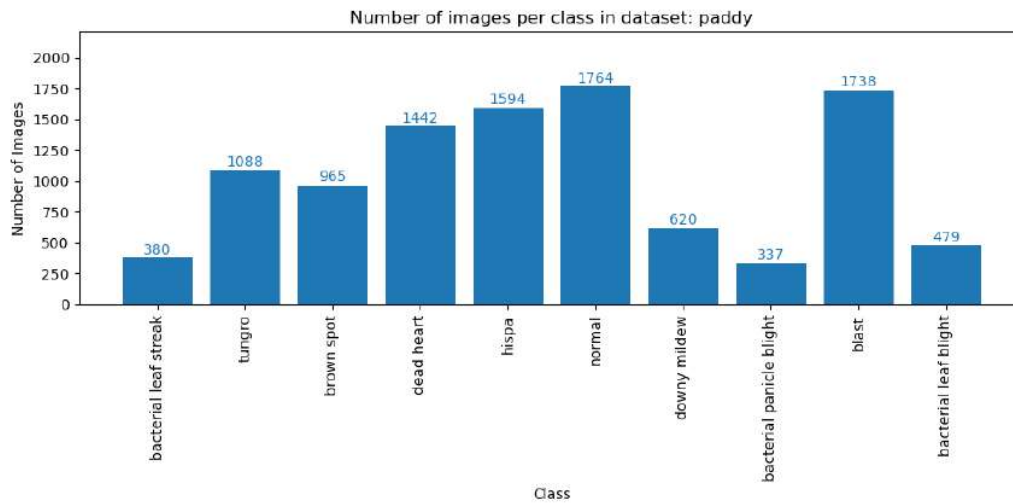


Figure A.17: Class Distribution of the Paddy Doctor Dataset.



Figure A.18: A sample image of each class present in the Paddy Doctor Dataset.

A.2.6 Plant Pathology 2020 - FGVC7

Table A.10: Information about the FGVC7 Dataset.

Plants	Apple
Diseases	1. Healthy 2. Rust 3. Scab 4. Multi-Disease
Number of Classes	4
Number of Images	1,821

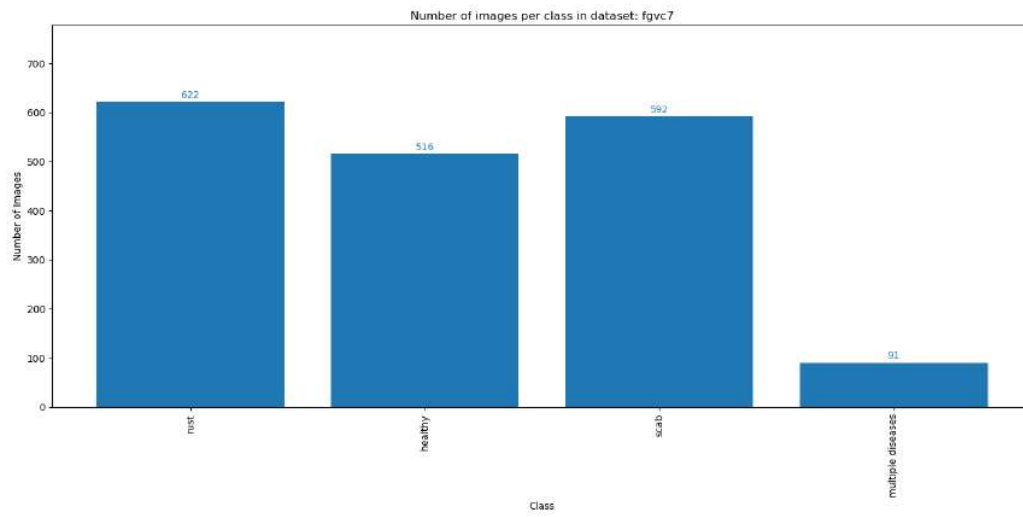


Figure A.19: Class Distribution of the FGVC7 Dataset.

fgvc7 Dataset - Sample Images - One per Class



Figure A.20: A sample image of each class present in the FGVC7 Dataset.

Table A.11: Information about the FGVC8 Dataset.

Plants	Apple
Diseases	<ol style="list-style-type: none"> 1. Healthy 2. Rust 3. Rust (complex) 4. Rust Frog Eye Leaf Spot 5. Scab 6. Scab (complex) 7. Scab Frog Eye Leaf Spot 8. Frog Eye Leaf Spot 9. Frog Eye Leaf Spot (complex) 10. Complex 11. Powdery Mildew 12. Powdery Mildew (complex)
Number of Classes	12
Number of Images	18,632

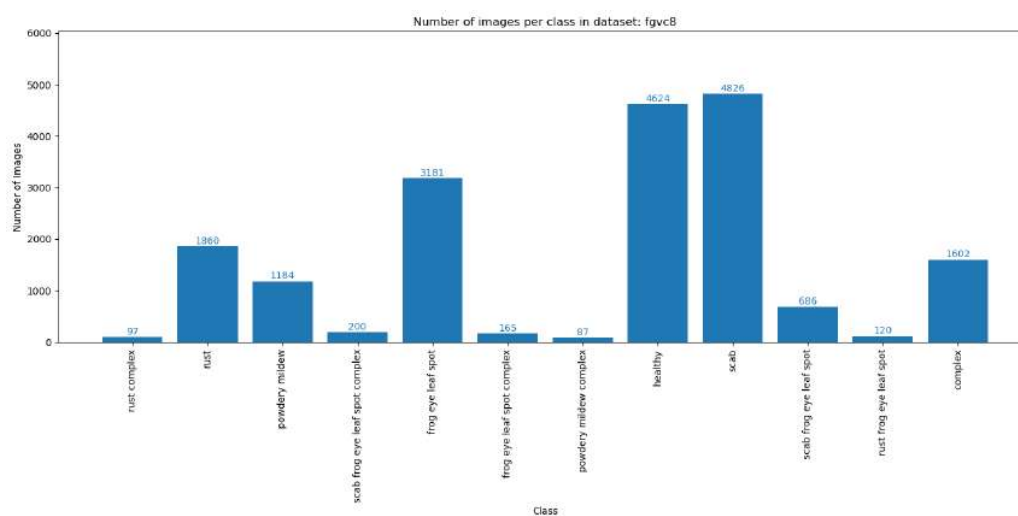


Figure A.21: Class Distribution of the FGVC8 Dataset.

A.2.7 Plant Pathology 2021 - FGVC8



Figure A.22: A sample image of each class present in the FGVC8 Dataset.

A.2.8 PDD271: Plant Disease Recognition Dataset

Table A.12: Information about the PDD271 Dataset.

Plants	<ol style="list-style-type: none"> 1. Leek 2. Sweet Potato 3. Mung Bean 	<ol style="list-style-type: none"> 4. Radish 5. Ginger
Diseases	<ol style="list-style-type: none"> 1. Leek <ul style="list-style-type: none"> • Gray Mold • Hail Damage 2. Sweet Potato <ul style="list-style-type: none"> • Healthy • Sooty Mold • Magnesium Deficiency 	<ol style="list-style-type: none"> 3. Mung Bean <ul style="list-style-type: none"> • Brown Spot 4. Radish <ul style="list-style-type: none"> • Black Spot • Mosaic Virus • Wrinkle Virus 5. Ginger <ul style="list-style-type: none"> • Anthracnose
Number of Classes	10	
Number of Images	7,555	

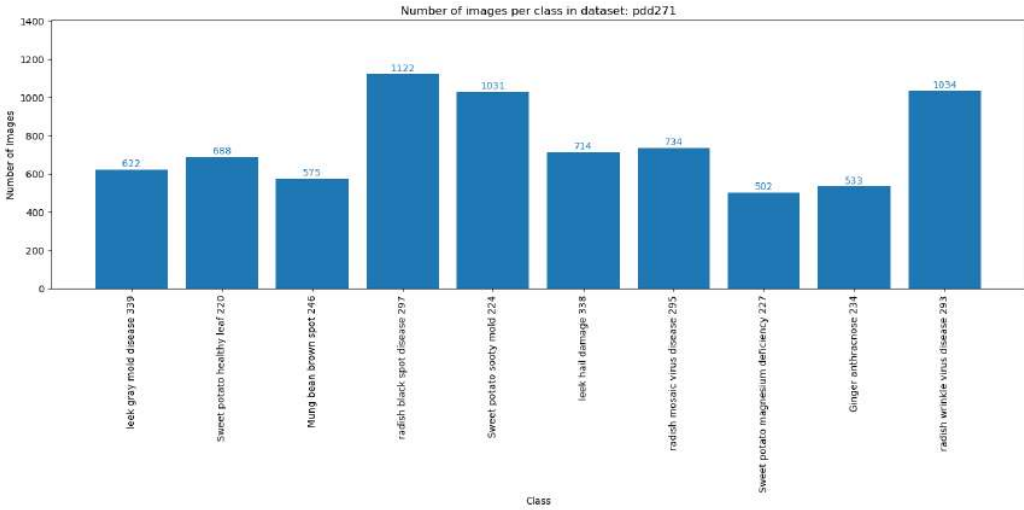


Figure A.23: Class Distribution of the PDD271 Dataset.



Figure A.24: A sample image of each class present in the PDD271 Dataset.

A.2.9 Strawberry Disease Detection Dataset

Table A.13: Information about the Strawberry Dataset.

Plants	Strawberry
Diseases	<ol style="list-style-type: none"> 1. Leaf Smut 2. Brown Spot 3. Powdery Mildew Bacterial Blight
Number of Classes	3
Number of Images	1583

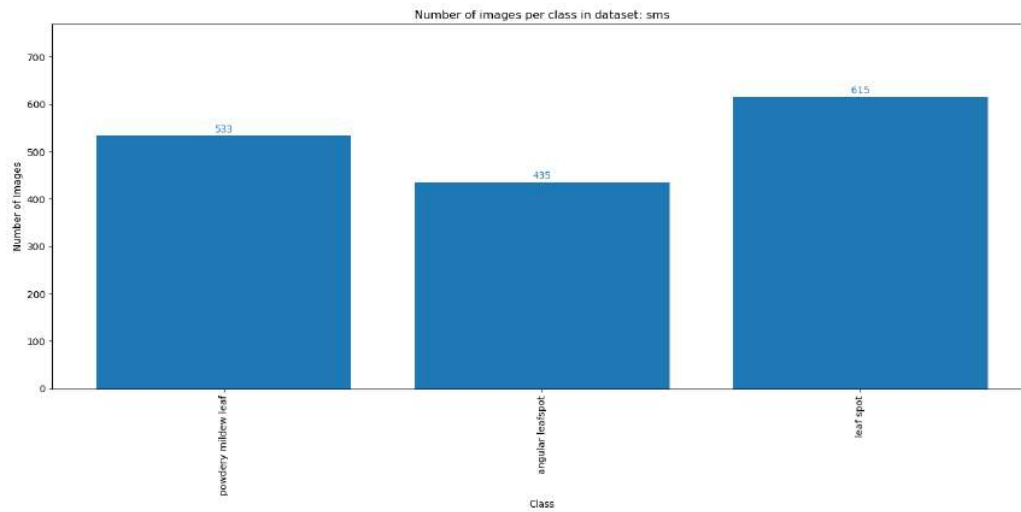


Figure A.25: Class Distribution of the Strawberry Dataset.



Figure A.26: A sample image of each class present in the Strawberry Dataset.

A.3 Hybrid Datasets

A.3.1 plantDoc

Table A.14: Information about the plantDoc Dataset.

Plants	<ol style="list-style-type: none"> 1. Squash 2. Bell Pepper 3. Tomato 4. Strawberry 5. Grape 	<ol style="list-style-type: none"> 6. Blueberry 7. Corn 8. Cherry 9. Apple 10. Potato 	<ol style="list-style-type: none"> 11. Soybean 12. Raspberry 13. Peach
Diseases	<ol style="list-style-type: none"> 1. Squash <ul style="list-style-type: none"> • Powdery Mildew 2. Bell Pepper <ul style="list-style-type: none"> • Healthy • Leaf Spot 3. Tomato <ul style="list-style-type: none"> • Healthy • Septoria Leaf Spot • Yellow Virus • Bacterial Spot • Mosaic Virus • Two Spotted Spider Mites • Mold • Early Blight • Late Blight 4. Strawberry <ul style="list-style-type: none"> • Healthy 5. Grape <ul style="list-style-type: none"> • Healthy • Black Rot 6. Potato 	<ol style="list-style-type: none"> 7. Blueberry <ul style="list-style-type: none"> • Healthy 8. Corn <ul style="list-style-type: none"> • Rust Leaf • Gray Leaf Spot • Leaf Blight 9. Cherry <ul style="list-style-type: none"> • Cherry leaf Healthy 10. Apple <ul style="list-style-type: none"> • Healthy • Scab • Rust Leaf 	<ol style="list-style-type: none"> 11. Soybean <ul style="list-style-type: none"> • Late Blight • Early Blight 12. Raspberry <ul style="list-style-type: none"> • Healthy 13. Peach <ul style="list-style-type: none"> • Healthy
Number of Classes	28		
Number of Images	2,577		

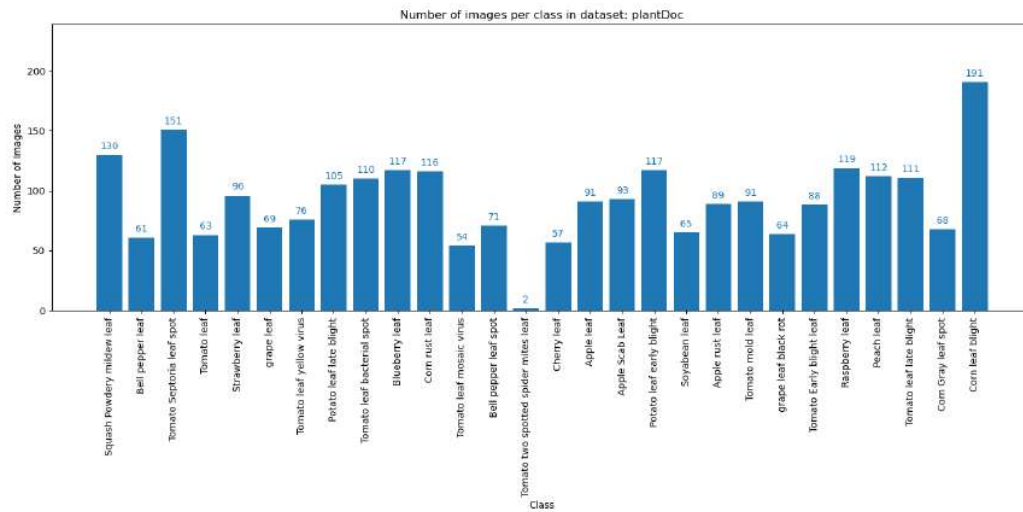


Figure A.27: Class Distribution of the plantDoc Dataset.

plantDoc Dataset - Sample Images - One per Class

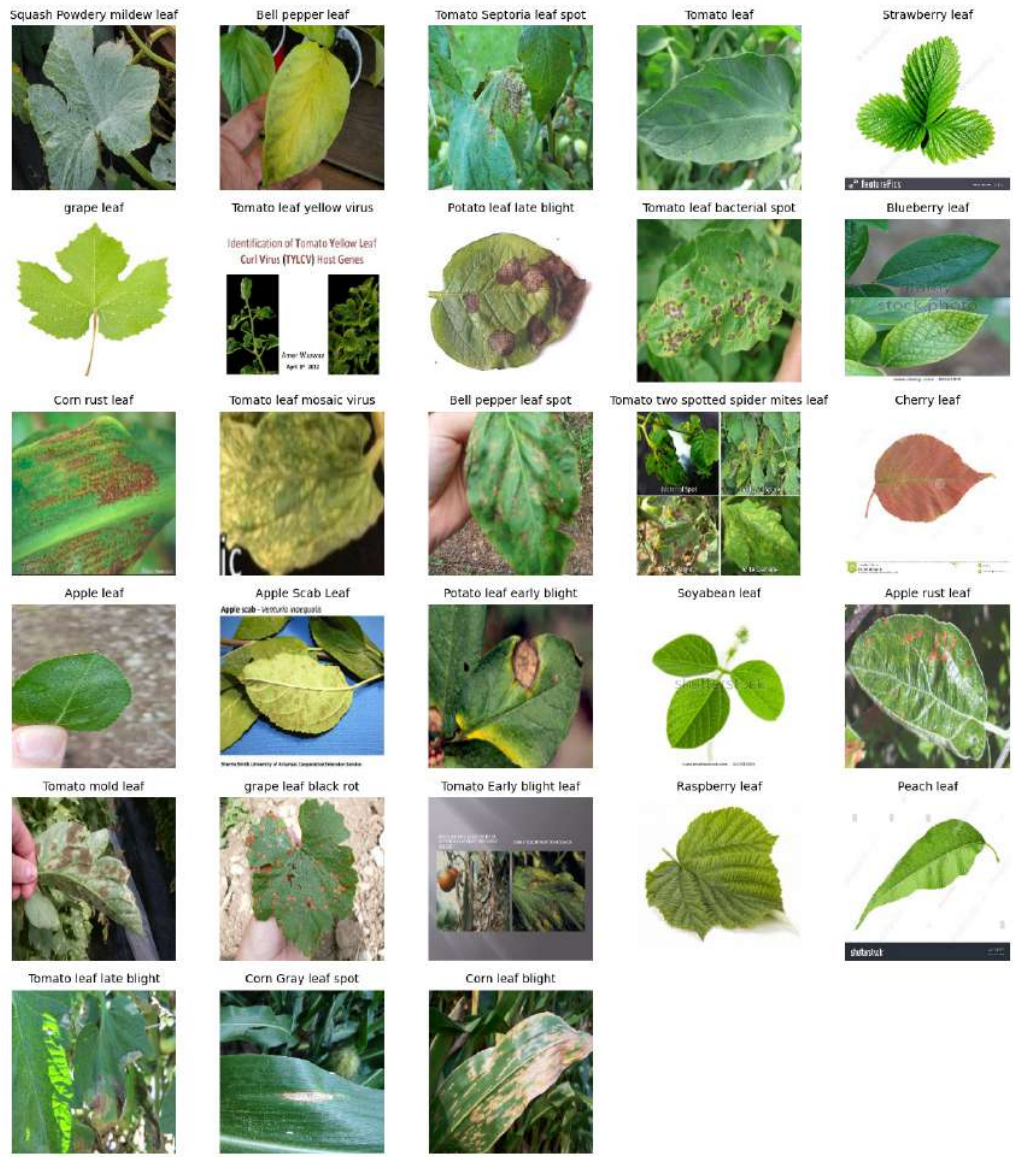


Figure A.28: A sample image of each class present in the plantDoc Dataset.

A.3.2 Taiwan Tomato

Table A.15: Information about the Taiwan Tomato Dataset.

Plants	Tomato
Diseases	1. Healthy 2. Bacterial Spot 3. Gray Spot 4. Late Blight 5. Powdery Mildew 6. Black Mold
Number of Classes	6
Number of Images	622

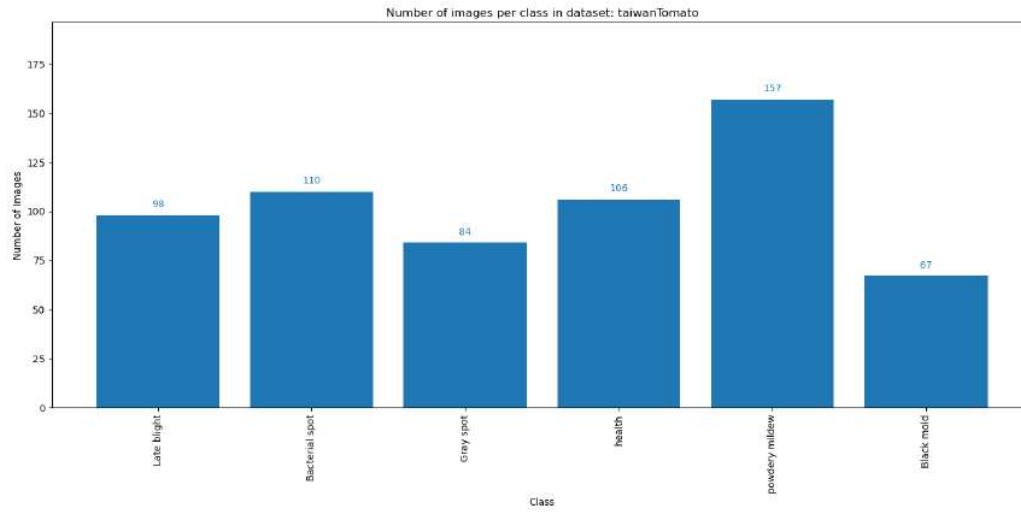


Figure A.29: Class Distribution of the Taiwan Tomato Dataset.

taiwanTomato Dataset - Sample Images - One per Class

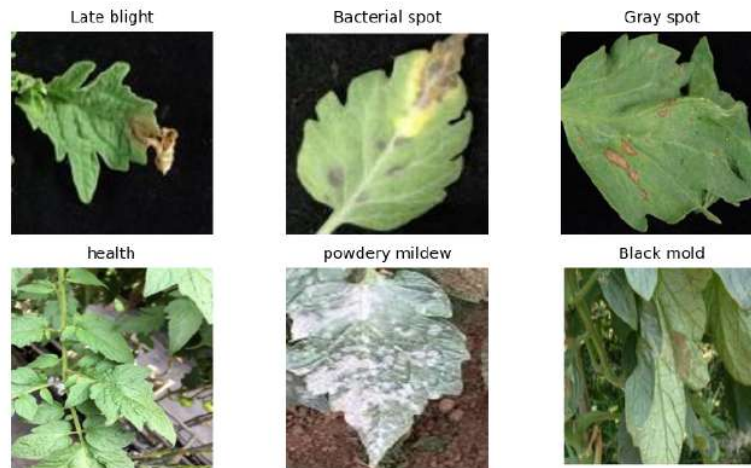


Figure A.30: A sample image of each class present in the Taiwan Tomato Dataset.

A.3.3 Potato Leaf Disease Dataset in Uncontrolled Environment

Table A.16: Information about the Novel Potato Dataset.

Plants	Potato
Diseases	<ol style="list-style-type: none"> 1. Healthy 2. Bacteria 3. Phytophthora 4. Nematode 5. Pest 6. Virus 7. Fungi
Number of Classes	7
Number of Images	3,076

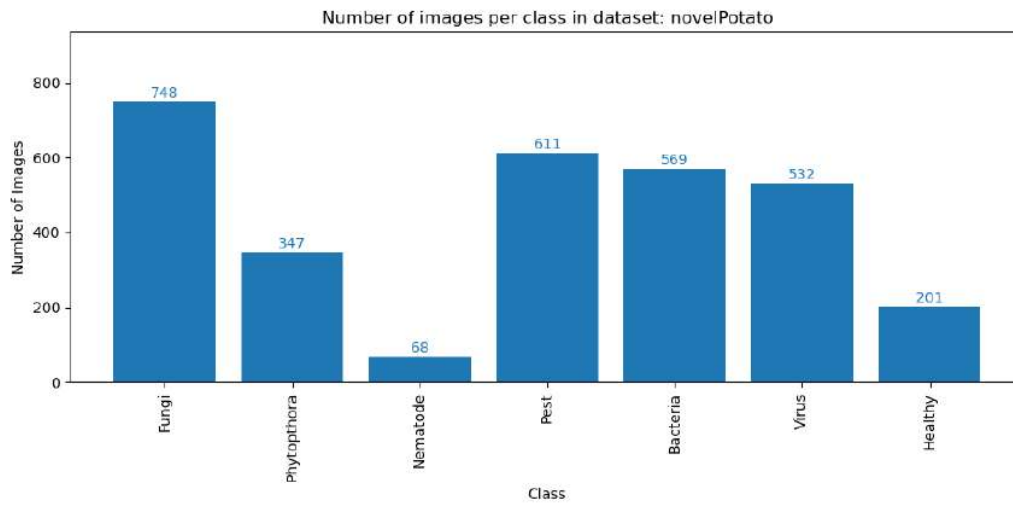


Figure A.31: Class Distribution of the Novel Potato Dataset.

novelPotato Dataset - Sample Images - One per Class

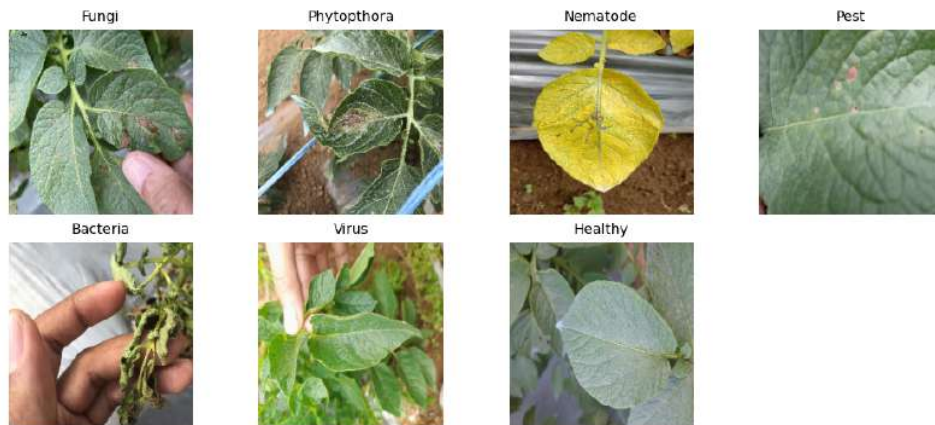


Figure A.32: A sample image of each class present in the Novel Potato Dataset.

A.3.4 Rice Leaf Diseases Dataset

Table A.17: Information about the RLDD Dataset.

Plants	Rice
Diseases	1. Bacterial Blight 2. Brown Spot 3. Leaf Smut
Number of Classes	3
Number of Images	524

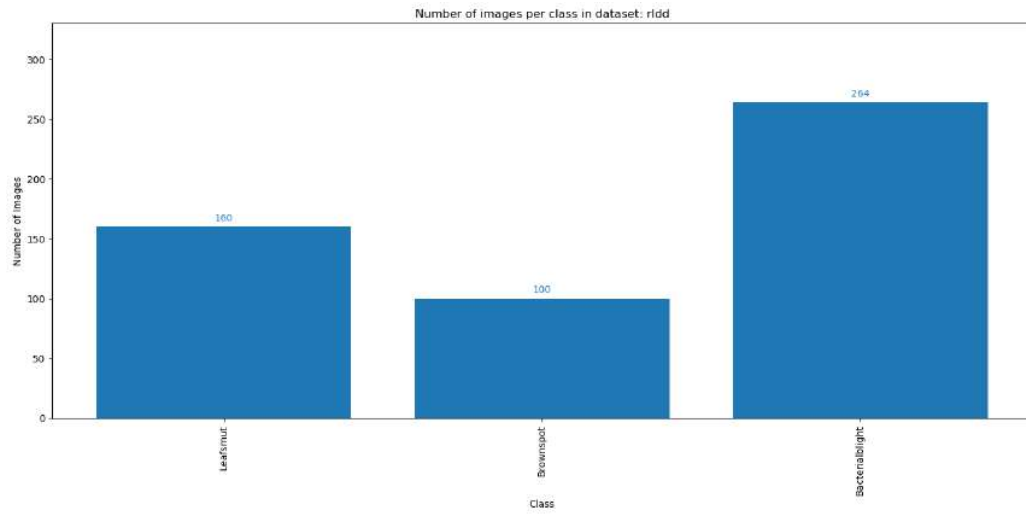


Figure A.33: Class Distribution of the RLDD Dataset.

rldd Dataset - Sample Images - One per Class



Figure A.34: A sample image of each class present in the RLDD Dataset.

Table A.18: Information about the Sugarcane Dataset.

Plants	Sugarcane
Diseases	<ol style="list-style-type: none"> 1. Healthy 2. Viral Disease 3. Banded Chlorosis 4. Grassy shoot 5. Yellow Leaf 6. Pokkah Boeng 7. Brown Spot 8. Brown Rust 9. Smut 10. Sett Rot
Number of Classes	10
Number of Images	6,405

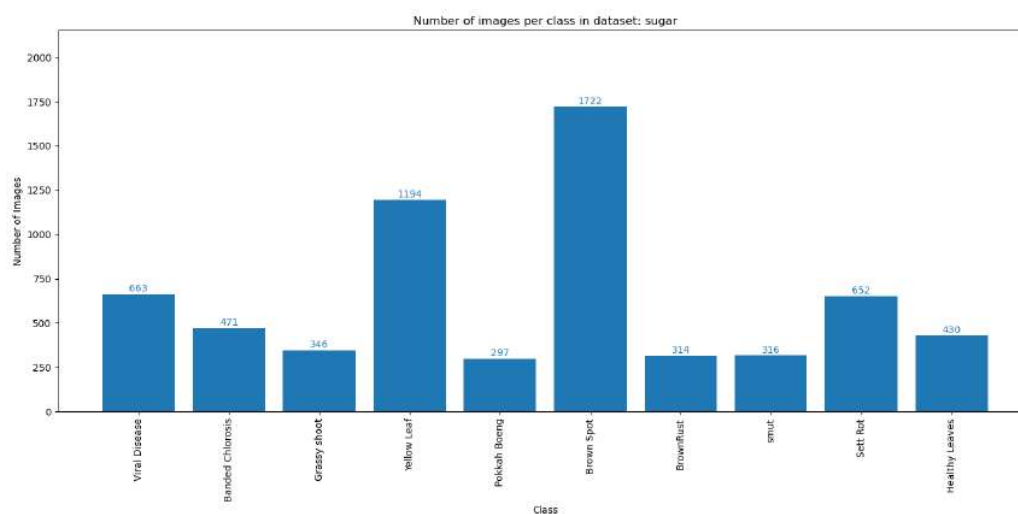


Figure A.35: Class Distribution of the Sugarcane Dataset.

A.3.5 Sugarcane Leaf Dataset



Figure A.36: A sample image of each class present in the Sugarcane Dataset.

B. Appendix Datasets

B.1 ResNet

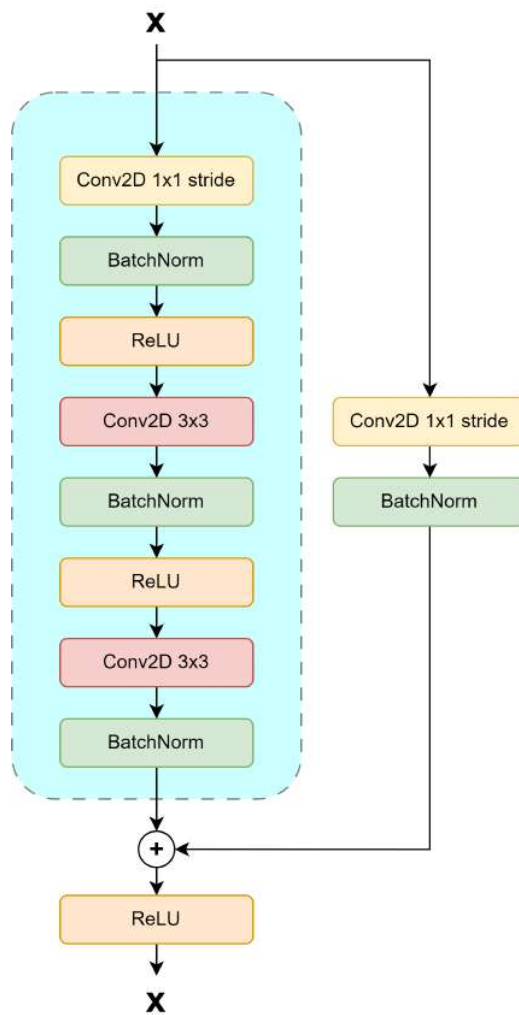


Figure B.1: A ResNet block with the residual connection. The stride in is defaulted to 1 but set to 2 if this is the first block in the layer-block. Based on TensorFlow implementation [127].

B.2 VGG

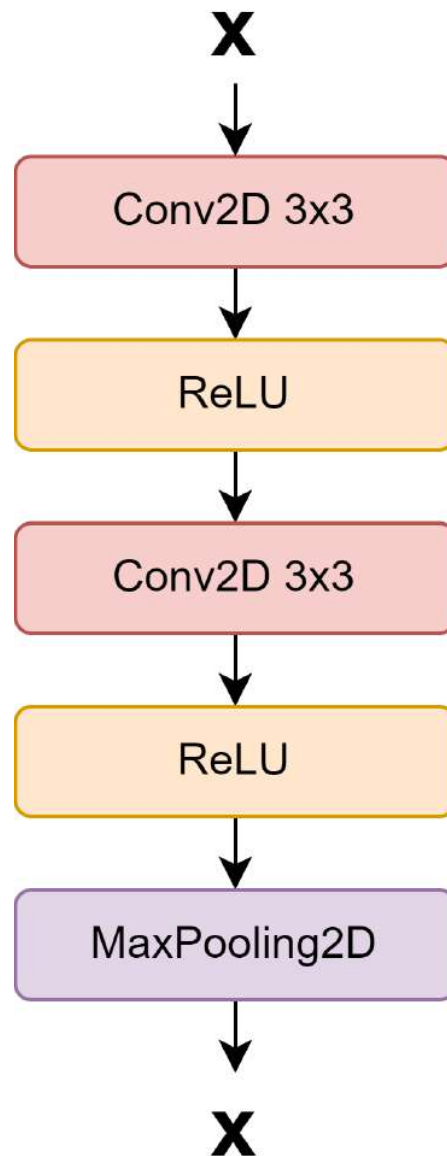


Figure B.2: VGG block of convolutional layers with pooling. Based on TensorFlow implementation [127].

B.3 ConvNeXt

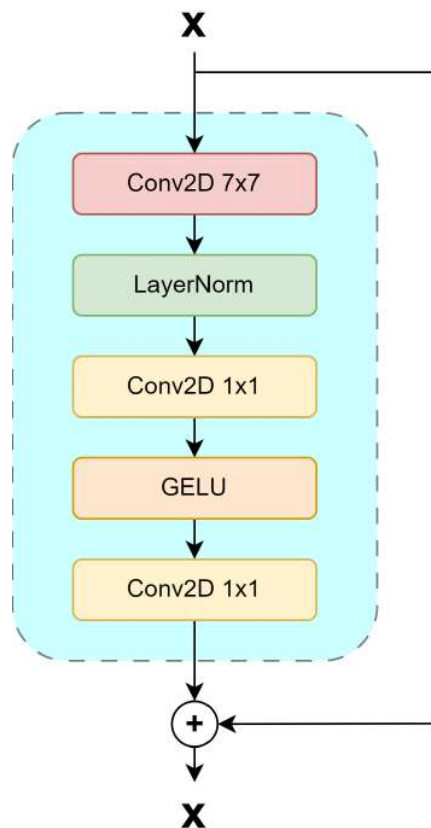


Figure B.3: ConvNeXt block with large kernel, pointwise convolutions, GELU and residual connections. Based on TensorFlow implementation [127].

B.4 DenseNet

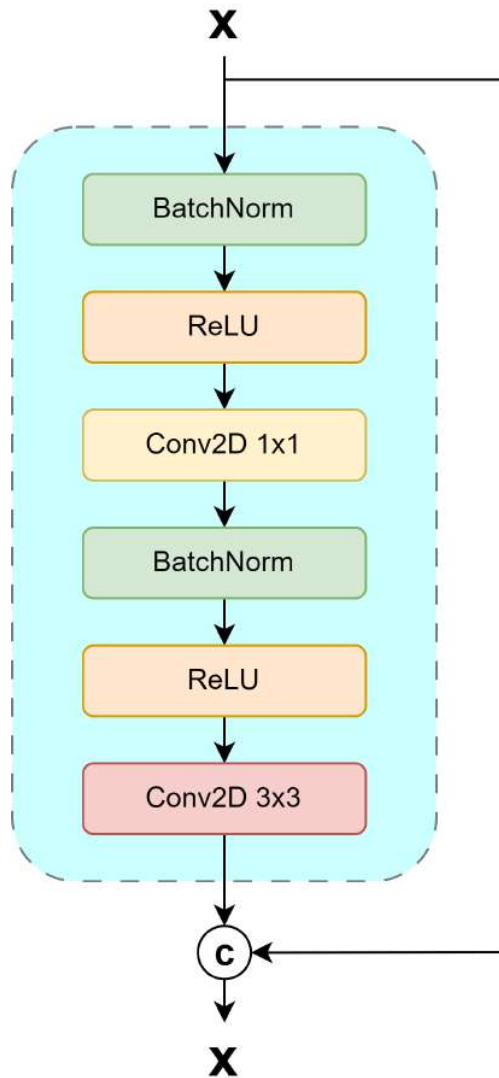


Figure B.4: DenseNet block with bottleneck and dense connection connections. Based on TensorFlow implementation [127].

C. Appendix Benchmark

In this appendix more detailed results will be given for each combination of all 23 models across all 18 datasets, resulting in 414 different combinations, all trained first using only transfer-learning and then again with fine-tuning in addition. This is done 5 times for each combination, resulting in a total of 4,140 models having been trained. Here, in Table C.2 all 414 combinations will be listed with the corresponding results for transfer-learning only and including fine-tuning. All results are averaged results over the 5 repetitions.

Table C.1: The models rank per dataset for each combination. Column name legend: 1 = cassava, 2 = cds, 3 = cucumber, 4 = diaMos, 5 = fgvc7, 6 = fgvc8, 7 = novelPotato, 8 = paddy, 9 = pdd271, 10 = plantDoc, 11 = plantVillage, 12 = pld, 13 = rlDD, 14 = sms, 15 = sugar, 16 = taiwanTomato, 17 = tea, 18 = tomatoVillage, 19 = Avg. Rank, 20 = Worst Rank, 21 = Best Rank, 22 = Avg. Rank STD.

	1	2	3	4	5	6	7	8	9	10	11	12	13	14	15	16	17	18	19	20	21	22
ConvNeXtSmall	1	13	18	1	4	4	7	2	5	8	8	20	8	14	16	10	11	1	8.39	20	1	5.96
ConvNeXtTiny	2	4	5	2	13	1	10	3	9	3	6	16	16	2	20	5	2	10	7.17	20	1	5.81
DenseNet121	13	7	11	5	9	13	11	16	4	5	5	5	10	8	7	9	10	5	8.50	16	4	3.43
DenseNet169	14	8	15	13	11	12	14	9	1	10	4	13	11	3	10	6	5	13	9.56	15	1	4.19
DenseNet201	6	9	9	3	3	16	9	6	2	9	3	1	2	9	4	13	12	9	6.94	16	1	4.28
EfficientNetV2B0	8	2	2	9	10	11	3	12	6	1	9	2	3	6	11	8	8	7	6.56	12	1	3.58
EfficientNetV2B1	5	10	7	6	7	3	1	1	11	11	11	6	6	11	8	7	14	2	7.06	14	1	3.78
EfficientNetV2B2	7	1	6	4	6	5	4	10	3	2	12	9	4	20	2	2	13	6	6.44	20	1	4.84
EfficientNetV2B3	10	6	8	14	15	9	6	7	15	6	10	7	5	4	5	1	9	8	8.06	15	1	3.76
EfficientNetV2M	4	12	3	10	2	7	5	5	8	12	1	3	14	12	3	19	1	11	7.33	19	1	5.17
EfficientNetV2S	3	3	13	11	8	2	2	4	12	4	2	10	12	7	6	4	15	3	6.72	15	2	4.38
InceptionResNetV2	16	22	22	16	16	15	20	18	16	15	19	14	23	15	12	23	20	16	17.67	23	12	3.33
InceptionV3	22	18	23	23	19	17	23	21	17	18	20	23	19	13	21	21	22	23	20.17	23	13	2.79
MobileNetV3Large	9	15	4	7	5	6	8	13	10	7	13	12	1	5	15	3	4	4	7.83	15	1	4.30
MobileNetV3Small	15	11	1	19	14	14	15	20	18	13	16	19	9	19	19	11	7	12	14.00	20	1	4.99
NASNetLarge	18	23	21	17	17	18	19	17	21	21	17	17	20	22	17	15	19	21	18.89	23	15	2.22
NASNetMobile	23	17	14	20	18	23	21	22	20	20	22	18	7	23	23	16	21	22	19.44	23	7	4.08
ResNet101V2	17	16	16	22	21	19	16	14	19	14	18	15	13	1	14	20	16	19	16.11	22	1	4.57
ResNet152V2	19	19	17	15	20	20	17	8	13	16	15	11	15	18	13	17	18	14	15.83	20	8	3.20
ResNet50V2	20	21	20	18	23	21	22	19	22	19	21	8	18	10	18	18	17	18	18.50	23	8	3.87
VGG16	12	14	12	12	1	8	12	15	14	22	14	21	21	17	9	14	6	17	13.39	22	1	5.34
VGG19	11	5	19	8	12	10	13	11	7	23	7	4	17	16	1	22	3	15	11.33	23	1	6.42
Xception	21	20	10	21	22	22	18	23	23	17	23	22	22	21	22	12	23	20	20.11	23	10	3.72

Table C.2: All of the results obtained during benchmarking. Each of the 23 model 18 dataset combinations are given. Each row represents the 5 run average results. Results originate from [125].

Model	Dataset	Acc	F1	Acc SD	F-1 SD	Acc FT	F1 FT	Acc FT	SD FT	F-1 FT	SD FT	Best Epoch	Best Epoch FT
ConvNeXtSmall	cassava	0.78001	0.62425	0.00117	0.14137	0.82496	0.69262	0.00689	0.12900	34	5.5		
ConvNeXtTiny	cassava	0.78328	0.63023	0.00047	0.14031	0.82415	0.69385	0.00631	0.12505	35.5	6		
DenseNet121	cassava	0.75747	0.60116	0.00105	0.14537	0.79496	0.66093	0.00841	0.13004	30	3.5		
DenseNet169	cassava	0.76845	0.60971	0.00058	0.14469	0.79426	0.65234	0.01401	0.13566	21.5	1.5		
DenseNet201	cassava	0.77265	0.62075	0.00245	0.13852	0.81282	0.68416	0.00829	0.12165	19.5	2.5		
EfficientNetV2B0	cassava	0.78643	0.63889	0.00222	0.13538	0.80862	0.67394	0.00736	0.13252	17.5	6		
EfficientNetV2B1	cassava	0.78211	0.63017	0.00093	0.13845	0.81364	0.67905	0.00187	0.12862	17	5		
EfficientNetV2B2	cassava	0.78515	0.63138	0.00047	0.14088	0.81119	0.67578	0.00082	0.13248	19	3		
EfficientNetV2B3	cassava	0.77802	0.62022	0.00199	0.14717	0.80184	0.65205	0.00362	0.14849	18.5	3		
EfficientNetV2M	cassava	0.75829	0.59184	0.00047	0.15247	0.81773	0.69511	0.00666	0.11830	21.5	2		
EfficientNetV2S	cassava	0.78164	0.62902	0.00280	0.14037	0.81831	0.68998	0.00140	0.12639	20.5	3		
InceptionResNetV2	cassava	0.73552	0.55229	0.00245	0.16508	0.77861	0.62860	0.00187	0.13799	27.5	2.5		
InceptionV3	cassava	0.72069	0.51887	0.00327	0.17793	0.75479	0.59427	0.00444	0.15118	14	1.5		
MobileNetV3Large	cassava	0.77721	0.62504	0.00070	0.13600	0.80220	0.66483	0.00677	0.12958	19	7.5		
MobileNetV3Small	cassava	0.75315	0.58684	0.00234	0.14969	0.78234	0.63672	0.00257	0.13387	27	14		

Continued on next page

Table C.2 - continued from previous page

Model	Dataset	Acc	F1	Acc SD	F-1 SD	Acc FT	F1 FT	Acc SD FT	F-1 SD FT	Best Epoch	Best Epoch FT
NASNetLarge	cassava	0.70213	0.48395	0.00175	0.19411	0.76273	0.59598	0.01051	0.15526	10	2
NASNetMobile	cassava	0.71976	0.52050	0.00304	0.17424	0.75058	0.58012	0.00560	0.15615	20	5
ResNet101V2	cassava	0.73027	0.53108	0.00117	0.17458	0.76436	0.59547	0.01028	0.15580	13	1.5
ResNet152V2	cassava	0.72279	0.52208	0.00257	0.17665	0.76133	0.58455	0.01775	0.16701	12.5	1.5
ResNet50V2	cassava	0.72980	0.53629	0.00140	0.17492	0.76039	0.59074	0.01355	0.15854	12.5	1
VGG16	cassava	0.72875	0.53920	0.00245	0.16608	0.80044	0.66208	0.02067	0.13597	27	5.5
VGG19	cassava	0.71952	0.51435	0.00187	0.17995	0.80056	0.65480	0.00794	0.13737	25	5.5
Xception	cassava	0.72560	0.53492	0.00304	0.17237	0.75525	0.59027	0.01308	0.15398	17	2
ConvNeXtSmall	cds	0.96994	0.96945	0.00791	0.01403	0.98259	0.98238	0.00158	0.00511	143	39.5
ConvNeXtTiny	cds	0.96835	0.96774	0.00000	0.01838	0.99051	0.99024	0.00316	0.00797	101.5	48
DenseNet121	cds	0.96519	0.96497	0.00633	0.00882	0.98734	0.98734	0.00316	0.00461	172.5	56
DenseNet169	cds	0.96677	0.96622	0.00158	0.01683	0.98576	0.98558	0.00158	0.00577	76	82.5
DenseNet201	cds	0.97152	0.97117	0.00316	0.00990	0.98418	0.98394	0.00316	0.00851	89.5	24.5
EfficientNetV2B0	cds	0.98101	0.98077	0.00316	0.00827	0.99367	0.99364	0.00000	0.00231	78.5	89
EfficientNetV2B1	cds	0.97627	0.97582	0.00158	0.01251	0.98418	0.98386	0.00316	0.00941	89.5	44.5
EfficientNetV2B2	cds	0.96835	0.96781	0.00000	0.01339	0.99525	0.99512	0.00158	0.00399	64.5	119

Continued on next page

Table C.2 - continued from previous page

Model	Dataset	Acc	F1	Acc SD	F-1 SD	Acc FT	F1 FT	Acc FT	SD FT	F-1 FT	SD FT	Best Epoch	Best Epoch FT
EfficientNetV2B3	cds	0.97152	0.97111	0.00316	0.01170	0.98892	0.98873	0.00158	0.00560	103.5	97		
EfficientNetV2M	cds	0.95411	0.95377	0.00475	0.01189	0.98259	0.98257	0.00158	0.00362	156.5	68.5		
EfficientNetV2S	cds	0.97943	0.97903	0.00158	0.01067	0.99209	0.99194	0.00158	0.00460	74.5	49.5		
InceptionResNetV2	cds	0.84019	0.83703	0.00158	0.04516	0.92880	0.92798	0.00158	0.02322	65.5	10.5		
InceptionV3	cds	0.83070	0.82909	0.00158	0.04169	0.94620	0.94517	0.00000	0.02506	50.5	29		
MobileNetV3Large	cds	0.96361	0.96338	0.00158	0.00700	0.97785	0.97781	0.00000	0.00370	111.5	75.5		
MobileNetV3Small	cds	0.97468	0.97418	0.00000	0.01513	0.98259	0.98243	0.00475	0.00864	116	125		
NASNetLarge	cds	0.84968	0.84730	0.00475	0.05216	0.91930	0.91798	0.02057	0.04176	35.5	21		
NASNetMobile	cds	0.87658	0.87488	0.00000	0.02972	0.96677	0.96644	0.00158	0.01037	94.5	73.5		
ResNet101V2	cds	0.91772	0.91733	0.00000	0.02671	0.97152	0.97128	0.01582	0.01955	47	18		
ResNet152V2	cds	0.90032	0.89906	0.00475	0.02857	0.94620	0.94583	0.00633	0.01566	61.5	71		
ResNet50V2	cds	0.89557	0.89414	0.00000	0.04335	0.94146	0.94079	0.02057	0.03197	54.5	8.5		
VGG16	cds	0.94304	0.94268	0.00633	0.01272	0.98101	0.98089	0.00633	0.01022	131	144.5		
VGG19	cds	0.94146	0.94072	0.00791	0.01817	0.99051	0.99044	0.00316	0.00406	105.5	119		
Xception	cds	875.00000	0.87348	0.00475	0.03620	0.94304	0.94213	0.00000	0.01913	49	71		
ConvNeXtSmall	cucumber	0.81875	0.81721	0.01875	0.11032	0.84375	0.84344	0.00000	0.09871	115.5	12		

Continued on next page

Table C.2 - continued from previous page

Model	Dataset	Acc	F1	Acc SD	F-1 SD	Acc FT	F1 FT	Acc FT	SD FT	F-1 FT	SD FT	Best Epoch	Best Epoch FT
ConvNeXtTiny	cucumber	0.86563	0.86652	0.01563	0.07333	0.89375	0.89313	0.00625	0.05209	115.5	29		
DenseNet121	cucumber	0.84062	0.84082	0.00313	0.10035	0.86875	0.86702	0.01250	0.07383	75	2		
DenseNet169	cucumber	0.82813	0.82875	0.01563	0.08853	0.85313	0.85208	0.00312	0.07025	56	4		
DenseNet201	cucumber	0.86250	0.86106	0.00000	0.06093	0.87813	0.87518	0.00313	0.07824	53.5	3		
EfficientNetV2B0	cucumber	0.88125	0.88196	0.00625	0.07104	0.89687	0.89769	0.00312	0.05553	58.5	11.5		
EfficientNetV2B1	cucumber	0.86562	0.86351	0.00938	0.08855	0.88125	0.87999	0.00625	0.08022	56.5	15		
EfficientNetV2B2	cucumber	0.86250	0.86349	0.01250	0.08288	0.88438	0.88592	0.00938	0.07105	50	10		
EfficientNetV2B3	cucumber	0.85000	0.85159	0.01250	0.07936	0.88125	0.88188	0.00625	0.06592	71	14		
EfficientNetV2M	cucumber	0.85313	0.85315	0.02813	0.08377	0.89687	0.89825	0.00938	0.06460	85	7.5		
EfficientNetV2S	cucumber	0.86250	0.86378	0.00625	0.07255	0.86875	0.86866	0.00000	0.07907	73.5	4.5		
InceptionResNetV2	cucumber	0.73750	0.73738	0.01875	0.12725	0.79063	0.78799	0.04063	0.13374	118	1		
InceptionV3	cucumber	0.74375	0.74095	0.00625	0.13858	0.77500	0.77154	0.03125	0.14104	50	1.5		
MobileNetV3Large	cucumber	0.89687	0.89606	0.00938	0.05367	0.89375	0.89341	0.00625	0.06767	67.5	1.5		
MobileNetV3Small	cucumber	0.91250	0.91108	0.00625	0.05778	0.89687	0.89592	0.00312	0.05804	110	7.5		
NASNetLarge	cucumber	0.75000	0.75064	0.01875	0.11984	0.79375	0.79340	0.03750	0.11990	45	2		
NASNetMobile	cucumber	0.80313	0.79795	0.01563	0.09004	0.86250	0.85916	0.03125	0.07576	71.5	5.5		

Continued on next page

Table C.2 - continued from previous page

Model	Dataset	Acc	F1	Acc SD	F-1 SD	Acc FT	F1 FT	Acc SD FT	F-1 SD FT	Best Epoch	Best Epoch FT
ResNet101V2	cucumber	0.79688	0.79432	0.00313	0.09929	0.84375	0.84105	0.01875	0.07297	36.5	2.5
ResNet152V2	cucumber	0.82500	0.82416	0.01250	0.08587	0.84375	0.84312	0.03125	0.08643	45	1
ResNet50V2	cucumber	0.81562	0.81491	0.00938	0.09511	0.82188	0.82169	0.00312	0.07182	39.5	1.5
VGG16	cucumber	0.82188	0.82181	0.03437	0.09345	0.86875	0.86823	0.02500	0.06336	100	5.5
VGG19	cucumber	0.80937	0.80940	0.01563	0.07588	0.83750	0.83840	0.04375	0.09318	85	4
Xception	cucumber	0.83750	0.83852	0.00000	0.08981	0.87188	0.87223	0.00938	0.07949	78.5	2.5
ConvNeXtSmall	diaMos	0.86213	0.84897	0.00498	0.08569	0.88040	0.85283	0.00498	0.06588	58.5	5
ConvNeXtTiny	diaMos	0.85880	0.83793	0.00664	0.11707	0.87708	0.84893	0.00332	0.11475	57.5	3.5
DenseNet121	diaMos	0.84718	0.83566	0.00332	0.12595	0.87043	0.88052	0.00166	0.07445	34.5	3
DenseNet169	diaMos	0.84718	0.73766	0.00000	0.18964	0.85797	0.83350	0.01080	0.11000	33	2
DenseNet201	diaMos	0.86545	0.86713	0.00332	0.05530	0.87458	0.88296	0.00581	0.05537	29.5	4
EfficientNetV2B0	diaMos	0.85382	0.84989	0.00332	0.06426	0.86296	0.87882	0.01412	0.07092	36.5	3
EfficientNetV2B1	diaMos	0.85963	0.84283	0.01080	0.10764	0.86960	0.87193	0.00083	0.06647	45	3
EfficientNetV2B2	diaMos	0.85299	0.80524	0.00748	0.10470	0.87375	0.86767	0.00166	0.06332	32.5	4
EfficientNetV2B3	diaMos	0.83638	0.80016	0.00083	0.11112	0.85216	0.84935	0.01329	0.08003	39	1
EfficientNetV2M	diaMos	0.82226	0.77528	0.00166	0.06816	0.86130	0.83250	0.01412	0.10182	48.5	3.5

Continued on next page

Table C.2 - continued from previous page

Model	Dataset	Acc	F1	Acc SD	F-1 SD	Acc FT	F1 FT	Acc FT	SD FT	F-1 FT	SD FT	Best Epoch	Best Epoch FT
EfficientNetV2S	diaMos	0.84551	0.76510	0.00332	0.18956	0.86130	0.81664	0.00914	0.12668	31.5	3.5		
InceptionResNetV2	diaMos	0.79485	0.77086	0.00083	0.08811	0.83970	0.83068	0.01744	0.07689	44.5	2		
InceptionV3	diaMos	0.78821	0.66302	0.01246	0.28057	0.82641	0.79891	0.02575	0.11158	30.5	2		
MobileNetV3Large	diaMos	0.84967	0.75074	0.00249	0.16749	0.86877	0.79644	0.00332	0.13719	30	2.5		
MobileNetV3Small	diaMos	0.82392	0.73654	0.00000	0.09735	0.83555	0.76536	0.00498	0.08361	59	3		
NASNetLarge	diaMos	0.75083	0.58548	0.00831	0.15768	0.83804	0.79104	0.02907	0.12968	17	2.5		
NASNetMobile	diaMos	0.79319	0.73738	0.00415	0.14046	0.83472	0.77049	0.02409	0.15828	43	4.5		
ResNet101V2	diaMos	0.80066	0.66903	0.00498	0.19162	0.82973	0.79110	0.01080	0.12124	24	1.5		
ResNet152V2	diaMos	0.80731	0.63650	0.00498	0.26020	0.84053	0.81604	0.02159	0.12358	26	1		
ResNet50V2	diaMos	0.80150	0.73303	0.00914	0.16123	0.83721	0.82918	0.01163	0.08373	27.5	1.5		
VGG16	diaMos	0.81561	0.76360	0.01329	0.12034	0.86130	0.78359	0.02575	0.17792	53.5	4.5		
VGG19	diaMos	0.81146	0.73417	0.01080	0.12653	0.86794	0.79256	0.00914	0.12899	62	4.5		
Xception	diaMos	0.79153	0.59321	0.00415	0.29989	0.83056	0.74193	0.02159	0.21693	28	2.5		
ConvNeXtSmall	fgvc7	0.85967	0.71583	0.00681	0.28318	0.90599	0.77388	0.00681	0.27519	61	13		
ConvNeXtTiny	fgvc7	0.85014	0.75550	0.00272	0.20168	0.89101	0.77237	0.01907	0.24835	95.5	10.5		
DenseNet121	fgvc7	0.83243	0.68355	0.00681	0.29268	0.89782	0.79357	0.00681	0.21757	69.5	7		

Continued on next page

Table C.2 - continued from previous page

Model	Dataset	Acc	F1	Acc SD	F-1 SD	Acc FT	F1 FT	Acc FT	SD FT	F-1 FT	SD FT	Best Epoch	Best Epoch FT
DenseNet169	fgvc7	0.83924	0.69955	0.00000	0.27186	0.89510	0.78923	0.02316	0.22254	44	2.5		
DenseNet201	fgvc7	0.84332	0.64892	0.00409	0.37519	0.90599	0.80389	0.00954	0.21137	41.5	5.5		
EfficientNetV2B0	fgvc7	0.86921	0.69105	0.00000	0.35367	0.89510	0.80029	0.00681	0.20116	57.5	8.5		
EfficientNetV2B1	fgvc7	0.84332	0.70901	0.00681	0.26612	0.90054	0.79336	0.01499	0.22689	44.5	10.5		
EfficientNetV2B2	fgvc7	0.86785	0.75891	0.00954	0.22070	0.90191	0.80841	0.01362	0.20808	41.5	5		
EfficientNetV2B3	fgvc7	0.83787	0.66849	0.00409	0.33284	0.87738	0.72236	0.01635	0.32486	52.5	6.5		
EfficientNetV2M	fgvc7	0.84469	0.70063	0.00272	0.28474	0.90872	0.78980	0.00954	0.24659	55.5	4.5		
EfficientNetV2S	fgvc7	0.88556	0.72589	0.00545	0.31462	0.90054	0.79349	0.00409	0.21983	56	3.5		
InceptionResNetV2	fgvc7	0.84196	0.68733	0.01090	0.31421	0.87057	0.75214	0.00954	0.26032	54	2		
InceptionV3	fgvc7	0.76158	0.59557	0.00681	0.32074	0.84605	0.69933	0.03134	0.31039	25	1		
MobileNetV3Large	fgvc7	0.87466	0.76169	0.01362	0.23266	0.90463	0.80751	0.00817	0.20164	40	11		
MobileNetV3Small	fgvc7	0.82834	0.63922	0.00272	0.36927	0.87738	0.71675	0.00000	0.32358	59	21.5		
NASNetLarge	fgvc7	0.76567	0.59957	0.00000	0.31924	0.85967	0.72154	0.02589	0.29223	24.5	2.5		
NASNetMobile	fgvc7	0.76703	0.59028	0.00409	0.34115	0.85559	0.73945	0.01362	0.24708	41.5	6.5		
ResNet101V2	fgvc7	0.79019	0.62003	0.00272	0.33214	0.83379	0.71219	0.01907	0.24976	42.5	2.5		
ResNet152V2	fgvc7	0.78883	0.61801	0.00681	0.32975	0.83787	0.74892	0.02316	0.19150	32.5	2		

Continued on next page

Table C.2 - continued from previous page

Model	Dataset	Acc	F1	Acc SD	F-1 SD	Acc FT	F1 FT	Acc SD FT	F-1 SD FT	Best Epoch	Best Epoch FT
ResNet50V2	fgvc7	0.79019	0.65148	0.00272	0.27253	0.82561	0.70557	0.01362	0.24273	38.5	2
VGG16	fgvc7	0.79292	0.63261	0.00817	0.31216	0.91417	0.80363	0.00681	0.22799	68.5	9.5
VGG19	fgvc7	0.79428	0.62217	0.00409	0.33410	0.89237	0.78148	0.01771	0.23919	57	7
Xception	fgvc7	0.76839	0.59111	0.00545	0.34203	0.82834	0.71290	0.02725	0.24180	31.5	2
ConvNeXtSmall	fgvc8	0.80287	0.44037	0.00067	0.38906	0.83892	0.46703	0.00616	0.39645	86	5.5
ConvNeXtTiny	fgvc8	0.80193	0.46220	0.00027	0.36778	0.84723	0.51126	0.00322	0.36425	78.5	7
DenseNet121	fgvc8	0.77057	0.42374	0.00161	0.36817	0.81694	0.45988	0.00027	0.37844	56	4.5
DenseNet169	fgvc8	0.76441	0.41911	0.00027	0.37086	0.82109	0.48338	0.00389	0.37173	38	7.5
DenseNet201	fgvc8	0.75905	0.41633	0.00456	0.36461	0.80434	0.49161	0.01555	0.35034	44.5	3
EfficientNetV2B0	fgvc8	0.80032	0.43265	0.00107	0.38954	0.82337	0.47979	0.00322	0.37342	47	7.5
EfficientNetV2B1	fgvc8	0.80582	0.44370	0.00067	0.38564	0.84093	0.48930	0.00121	0.37715	45.5	6.5
EfficientNetV2B2	fgvc8	0.79831	0.43618	0.00174	0.38533	0.83516	0.47725	0.00241	0.38311	41	6
EfficientNetV2B3	fgvc8	0.79241	0.43647	0.00067	0.37907	0.82726	0.48462	0.00737	0.37149	43	2.5
EfficientNetV2M	fgvc8	0.76159	0.39810	0.00121	0.38204	0.83128	0.49593	0.00201	0.36433	51	3
EfficientNetV2S	fgvc8	0.80099	0.44135	0.00147	0.38013	0.84361	0.51394	0.00791	0.35942	51	2.5
InceptionResNetV2	fgvc8	0.74765	0.39817	0.00281	0.36445	0.80541	0.47069	0.00750	0.35894	60	2

Continued on next page

Table C.2 - continued from previous page

Model	Dataset	Acc	F1	Acc SD	F-1 SD	Acc FT	F1 FT	Acc FT	SD FT	F-1 FT	SD FT	Best Epoch	Best Epoch FT
InceptionV3	fgvc8	0.68681	0.35759	0.00094	0.34461	0.79804	0.44809	0.01220	0.36924	25	4		
MobileNetV3Large	fgvc8	0.78196	0.41994	0.00255	0.38186	0.83463	0.48118	0.00724	0.37869	32	9		
MobileNetV3Small	fgvc8	0.76374	0.40846	0.00281	0.37619	0.81238	0.45943	0.00295	0.37302	51.5	25.5		
NASNetLarge	fgvc8	0.67649	0.35903	0.00456	0.33558	0.78397	0.44383	0.03189	0.36298	25	2		
NASNetMobile	fgvc8	0.66671	0.34277	0.00228	0.34291	0.75771	0.43410	0.00884	0.35203	45.5	6.5		
ResNet101V2	fgvc8	0.70866	0.38230	0.00456	0.34800	0.78169	0.45845	0.01756	0.35464	24.5	3.5		
ResNet152V2	fgvc8	0.70209	0.37233	0.00094	0.35390	0.78009	0.43756	0.02024	0.36509	25	2.5		
ResNet50V2	fgvc8	0.72755	0.39012	0.00013	0.35888	0.77191	0.45005	0.01689	0.35451	24.5	2.5		
VGG16	fgvc8	0.71000	0.39447	0.00241	0.33716	0.82806	0.49054	0.00925	0.36455	46.5	7.5		
VGG19	fgvc8	0.68655	0.36973	0.00255	0.33881	0.82337	0.47576	0.01474	0.37343	40	6		
Xception	fgvc8	0.68681	0.35185	0.00228	0.35145	0.77137	0.44130	0.02010	0.35655	34	3		
ConvNeXtSmall	novelPotato	0.75606	0.73006	0.00485	0.10755	0.79725	0.77121	0.00242	0.11059	71	19.5		
ConvNeXtTiny	novelPotato	0.72132	0.69857	0.00727	0.10969	0.78675	0.75902	0.00323	0.10402	93.5	22.5		
DenseNet121	novelPotato	0.74637	0.72272	0.00323	0.10347	0.78271	0.76615	0.00081	0.09476	64	5		
DenseNet169	novelPotato	0.74071	0.72908	0.00889	0.08927	0.76979	0.74928	0.00889	0.10239	50	4		
DenseNet201	novelPotato	0.74960	0.73595	0.01454	0.08407	0.78918	0.76043	0.03312	0.11420	54.5	2		

Continued on next page

Table C.2 - continued from previous page

Model	Dataset	Acc	F1	Acc SD	F-1 SD	Acc FT	F1 FT	Acc SD FT	F-1 SD FT	Best Epoch	Best Epoch FT
EfficientNetV2B0	novelPotato	0.77868	0.74319	0.00485	0.13013	0.80775	0.78651	0.01131	0.09571	38	6
EfficientNetV2B1	novelPotato	0.77302	0.74951	0.00404	0.11690	0.81987	0.80592	0.00242	0.09205	51.5	9.5
EfficientNetV2B2	novelPotato	0.78595	0.75768	0.00242	0.10515	0.80210	0.76551	0.00404	0.12744	54	5
EfficientNetV2B3	novelPotato	0.75848	0.71698	0.00565	0.14877	0.79725	0.75150	0.01212	0.14230	43.5	3
EfficientNetV2M	novelPotato	0.72294	0.68139	0.00404	0.13412	0.79806	0.78217	0.02262	0.08672	57	4.5
EfficientNetV2S	novelPotato	0.77868	0.72141	0.00162	0.14792	0.80937	0.78871	0.01292	0.09410	57.5	2.5
InceptionResNetV2	novelPotato	0.67124	0.62520	0.00404	0.13814	0.70840	0.68100	0.01696	0.11317	73.5	2
InceptionV3	novelPotato	0.61551	0.54641	0.01292	0.18519	0.68821	0.62337	0.02746	0.20032	31.5	3
MobileNetV3Large	novelPotato	0.77464	0.73683	0.00081	0.12030	0.78998	0.74740	0.00323	0.13979	49	4.5
MobileNetV3Small	novelPotato	0.74798	0.73297	0.01131	0.10175	0.76737	0.74989	0.01777	0.10368	67	7
NASNetLarge	novelPotato	0.65105	0.60857	0.00969	0.13528	0.71325	0.67753	0.02989	0.15628	25	1.5
NASNetMobile	novelPotato	0.65428	0.57941	0.00000	0.20936	0.70679	0.64430	0.01696	0.17954	58	3.5
ResNet101V2	novelPotato	0.72294	0.66344	0.00565	0.17463	0.73829	0.71156	0.01292	0.11916	37.5	1.5
ResNet152V2	novelPotato	0.67205	0.60692	0.00808	0.18439	0.73506	0.71535	0.03231	0.11212	29.5	2
ResNet50V2	novelPotato	0.67528	0.61586	0.00323	0.20776	0.70113	0.66073	0.01292	0.16085	34.5	1
VGG16	novelPotato	0.68821	0.67304	0.00323	0.09807	0.78110	0.75588	0.02342	0.09780	79.5	9.5

Continued on next page

Table C.2 - continued from previous page

Model	Dataset	Acc	F1	Acc SD	F-1 SD	Acc FT	F1 FT	Acc SD FT	F-1 SD FT	Best Epoch	Best Epoch FT
VGG19	novelPotato	0.68255	0.65140	0.01696	0.11670	0.77948	0.76140	0.02666	0.08908	76	10
Xception	novelPotato	0.68336	0.63319	0.00000	0.16357	0.72698	0.68976	0.01292	0.14069	45.5	1.5
ConvNeXtSmall	paddy	0.92107	0.91175	0.00408	0.03100	0.93930	0.93103	0.00264	0.02986	180.5	19
ConvNeXtTiny	paddy	0.92035	0.91148	0.00096	0.03798	0.93930	0.93078	0.00648	0.03381	188	26.5
DenseNet121	paddy	0.87908	0.86925	0.00384	0.04213	0.91579	0.90444	0.01080	0.03598	143	7
DenseNet169	paddy	0.89923	0.88820	0.00336	0.04266	0.92922	0.91750	0.00984	0.04038	111.5	12
DenseNet201	paddy	0.90787	0.90417	0.00192	0.03148	0.93666	0.92970	0.00528	0.03129	99	12.5
EfficientNetV2B0	paddy	0.91963	0.91048	0.00264	0.03148	0.92370	0.91587	0.00672	0.03184	137.5	1.5
EfficientNetV2B1	paddy	0.92850	0.91755	0.00336	0.03718	0.94218	0.93288	0.00120	0.02855	120	23
EfficientNetV2B2	paddy	0.91939	0.91090	0.00000	0.03491	0.92922	0.92256	0.00504	0.03593	104	17
EfficientNetV2B3	paddy	0.92202	0.91524	0.00312	0.02812	0.93330	0.92464	0.00816	0.02978	107	3.5
EfficientNetV2M	paddy	0.89803	0.88608	0.00024	0.03544	0.93690	0.92823	0.00600	0.02945	142.5	15
EfficientNetV2S	paddy	0.91483	0.90696	0.00744	0.03267	0.93738	0.92886	0.00984	0.02772	115.5	14.5
InceptionResNetV2	paddy	0.84405	0.82390	0.00480	0.05722	0.91099	0.89987	0.00840	0.03844	104	13
InceptionV3	paddy	0.80686	0.78986	0.00792	0.06084	0.90115	0.89162	0.00960	0.04031	60.5	25.5
MobileNetV3Large	paddy	0.90499	0.89595	0.00096	0.04295	0.92298	0.91352	0.00312	0.03440	112.5	15

Continued on next page

Table C.2 - continued from previous page

Model	Dataset	Acc	F1	Acc SD	F-1 SD	Acc FT	F1 FT	Acc SD FT	F-1 SD FT	Best Epoch	Best Epoch FT
MobileNetV3Small	paddy	0.88580	0.87581	0.00144	0.03723	0.90571	0.89631	0.00504	0.03444	140.5	31.5
NASNetLarge	paddy	0.81958	0.80516	0.00576	0.05489	0.91267	0.89951	0.00480	0.03445	67	35.5
NASNetMobile	paddy	0.80902	0.78593	0.00240	0.06561	0.88220	0.86636	0.01272	0.05516	87	12.5
ResNet101V2	paddy	0.86204	0.85447	0.00312	0.03967	0.91963	0.90913	0.00696	0.04142	71	10.5
ResNet152V2	paddy	0.85581	0.83416	0.00408	0.05529	0.93018	0.92295	0.00120	0.03177	73	51
ResNet50V2	paddy	0.84789	0.83700	0.00048	0.05411	0.90931	0.89647	0.00528	0.04132	66	9.5
VGG16	paddy	0.84717	0.83798	0.00360	0.04570	0.91915	0.90873	0.00888	0.03416	132.5	24.5
VGG19	paddy	0.84549	0.83944	0.00240	0.03999	0.92562	0.91938	0.01200	0.02698	152	25.5
Xception	paddy	0.83373	0.81732	0.00024	0.04852	0.87812	0.86039	0.01583	0.05227	88	4
ConvNeXtSmall	pdd271	0.99076	0.99164	0.00066	0.00817	0.99406	0.99448	0.00000	0.00474	151.5	172.5
ConvNeXtTiny	pdd271	0.99109	0.99133	0.00033	0.00769	0.99274	0.99288	0.00066	0.00611	180.5	120
DenseNet121	pdd271	0.98713	0.98775	0.00099	0.01201	0.99406	0.99403	0.00132	0.00531	85	25
DenseNet169	pdd271	0.98977	0.98904	0.00099	0.00889	0.99670	0.99657	0.00066	0.00428	56.5	95
DenseNet201	pdd271	0.98581	0.98546	0.00033	0.01059	0.99472	0.99461	0.00198	0.00517	82.5	52
EfficientNetV2B0	pdd271	0.98779	0.98817	0.00165	0.00775	0.99373	0.99395	0.00099	0.00359	80.5	177
EfficientNetV2B1	pdd271	0.98548	0.98496	0.00066	0.00878	0.99208	0.99200	0.00132	0.00564	68	67.5

Continued on next page

Table C.2 - continued from previous page

Model	Dataset	Acc	F1	Acc SD	F-1 SD	Acc FT	F1 FT	Acc FT	SD FT	F-1 FT	SD FT	Best Epoch	Best Epoch FT
EfficientNetV2B2	pdd271	0.99109	0.99130	0.00099	0.00705	0.99439	0.99466	0.00033	0.00465	113.5	49		
EfficientNetV2B3	pdd271	0.98779	0.98766	0.00099	0.00829	0.98911	0.98912	0.00297	0.00817	139	110.5		
EfficientNetV2M	pdd271	0.98548	0.98577	0.00066	0.00971	0.99274	0.99294	0.00000	0.00616	111	91.5		
EfficientNetV2S	pdd271	0.98548	0.98444	0.00066	0.00990	0.99109	0.99121	0.00033	0.00636	92	38.5		
InceptionResNetV2	pdd271	0.96139	0.95998	0.00033	0.02858	0.98845	0.98818	0.00099	0.00985	80	126.5		
InceptionV3	pdd271	0.95083	0.94697	0.00033	0.03588	0.98779	0.98679	0.00165	0.01055	47.5	47.5		
MobileNetV3Large	pdd271	0.98350	0.98357	0.00000	0.00995	0.99208	0.99270	0.00132	0.00663	76.5	120		
MobileNetV3Small	pdd271	0.97525	0.97387	0.00033	0.01588	0.98647	0.98627	0.00099	0.00731	68.5	122		
NASNetLarge	pdd271	0.94752	0.94423	0.00165	0.03676	0.98548	0.98495	0.00066	0.01113	52	53.5		
NASNetMobile	pdd271	0.94389	0.93925	0.00198	0.03974	0.98614	0.98622	0.00066	0.01216	71	129.5		
ResNet101V2	pdd271	0.96535	0.96302	0.00231	0.02391	0.98614	0.98573	0.00000	0.01039	41	49.5		
ResNet152V2	pdd271	0.96073	0.95941	0.00231	0.02845	0.99109	0.99079	0.00033	0.00719	47	56.5		
ResNet50V2	pdd271	0.96205	0.96058	0.00231	0.02625	0.98515	0.98509	0.00033	0.00921	49.5	139.5		
VGG16	pdd271	0.97426	0.97441	0.00066	0.01602	0.98977	0.98964	0.00033	0.00476	95	29.5		
VGG19	pdd271	0.97129	0.97073	0.00033	0.01954	0.99340	0.99330	0.00000	0.00497	85	60.5		
Xception	pdd271	0.95743	0.95626	0.00231	0.02898	0.98185	0.98138	0.00099	0.01389	65	106		

Continued on next page

Table C.2 - continued from previous page

Model	Dataset	Acc	F1	Acc SD	F-1 SD	Acc FT	F1 FT	Acc FT	SD FT	F-1 FT	SD FT	Best Epoch	Best Epoch FT
ConvNeXtSmall	plantDoc	0.50633	0.47354	0.01266	0.24134	0.54219	0.51282	0.01477	0.24550	120	10.5		
ConvNeXtTiny	plantDoc	0.51055	0.48895	0.00422	0.24082	0.56118	0.53864	0.00000	0.23024	106	26		
DenseNet121	plantDoc	0.52743	0.49128	0.00844	0.24912	0.55485	0.52134	0.00633	0.26440	100.5	3		
DenseNet169	plantDoc	0.54430	0.51867	0.00844	0.23776	0.53797	0.53326	0.01055	0.25685	74	4.5		
DenseNet201	plantDoc	0.54219	0.50797	0.01055	0.22551	0.54008	0.50536	0.01266	0.24440	74	2		
EfficientNetV2B0	plantDoc	0.55063	0.52007	0.00633	0.23558	0.58017	0.54747	0.02743	0.23682	82.5	1		
EfficientNetV2B1	plantDoc	0.52110	0.49484	0.00211	0.22620	0.53586	0.52806	0.00422	0.23081	82.5	1.5		
EfficientNetV2B2	plantDoc	0.54219	0.51480	0.01055	0.24146	0.56962	0.55690	0.00844	0.23671	69.5	2.5		
EfficientNetV2B3	plantDoc	0.54008	0.51097	0.00000	0.24688	0.55063	0.53645	0.01055	0.22282	66	1		
EfficientNetV2M	plantDoc	0.49578	0.46099	0.01055	0.21192	0.52532	0.49595	0.02743	0.22438	74.5	1		
EfficientNetV2S	plantDoc	0.55696	0.52960	0.00422	0.21822	0.55907	0.53078	0.00633	0.20914	85	2.5		
InceptionResNetV2	plantDoc	0.47257	0.44077	0.01266	0.25479	0.49367	0.48928	0.01688	0.25996	89	1.5		
InceptionV3	plantDoc	0.47468	0.43594	0.00211	0.21667	0.48101	0.44127	0.00844	0.25704	55.5	1		
MobileNetV3Large	plantDoc	0.52954	0.49688	0.00633	0.23420	0.54641	0.51422	0.00211	0.23648	63.5	3.5		
MobileNetV3Small	plantDoc	0.47890	0.44954	0.01055	0.21881	0.50211	0.47298	0.01266	0.22570	109	3.5		
NASNetLarge	plantDoc	0.45781	0.43575	0.00211	0.20073	0.46414	0.43497	0.00000	0.20437	40.5	1		

Continued on next page

Table C.2 - continued from previous page

Model	Dataset	Acc	F1	Acc SD	F-1 SD	Acc FT	F1 FT	Acc FT	SD FT	F-1 FT	SD FT	Best Epoch	Best Epoch FT
NASNetMobile	plantDoc	0.46835	0.43717	0.00000	0.21926	0.46835	0.43422	0.01266	0.22485	70	1.5		
ResNet101V2	plantDoc	0.48101	0.45639	0.00422	0.25660	0.50211	0.48097	0.01688	0.24731	44	1		
ResNet152V2	plantDoc	0.46624	0.43658	0.00211	0.22992	0.48734	0.46305	0.00211	0.26638	42	1.5		
ResNet50V2	plantDoc	0.48734	0.46941	0.01477	0.23171	0.47890	0.48336	0.01477	0.24384	47	2		
VGG16	plantDoc	0.40506	0.38695	0.00422	0.21006	0.46414	0.43812	0.02954	0.23697	96.5	3		
VGG19	plantDoc	0.41772	0.38441	0.00000	0.24315	0.41772	0.37304	0.03376	0.24476	87	1.5		
Xception	plantDoc	0.42827	0.39659	0.00633	0.20465	0.48523	0.47204	0.02532	0.22724	65	1		
ConvNeXtSmall	plantVillage	0.98667	0.98182	0.00009	0.02560	0.99568	0.99320	0.00000	0.01423	113.5	62.5		
ConvNeXtTiny	plantVillage	0.98667	0.97984	0.00028	0.03331	0.99600	0.99376	0.00041	0.01214	113.5	149.5		
DenseNet121	plantVillage	0.98299	0.97683	0.00037	0.03026	0.99632	0.99461	0.00009	0.00981	93	131		
DenseNet169	plantVillage	0.98271	0.97616	0.00018	0.03253	0.99637	0.99473	0.00023	0.01079	43	36		
DenseNet201	plantVillage	0.98750	0.98230	0.00046	0.02593	0.99646	0.99454	0.00005	0.01315	57.5	51		
EfficientNetV2B0	plantVillage	0.98722	0.98116	0.00028	0.02533	0.99554	0.99290	0.00051	0.01532	60	63		
EfficientNetV2B1	plantVillage	0.98796	0.98255	0.00037	0.02299	0.99513	0.99283	0.00064	0.01147	84	62.5		
EfficientNetV2B2	plantVillage	0.98750	0.98284	0.00000	0.02381	0.99481	0.99177	0.00051	0.01537	89	33.5		
EfficientNetV2B3	plantVillage	0.98506	0.97990	0.00032	0.02805	0.99545	0.99359	0.00032	0.01214	50.5	61.5		

Continued on next page

Table C.2 - continued from previous page

Model	Dataset	Acc	F1	Acc SD	F-1 SD	Acc FT	F1 FT	Acc SD FT	F-1 SD FT	Best Epoch	Best Epoch FT
EfficientNetV2M	plantVillage	0.98129	0.97569	0.00023	0.03028	0.99692	0.99524	0.00032	0.00903	89.5	85
EfficientNetV2S	plantVillage	0.98800	0.98405	0.00014	0.02116	0.99660	0.99496	0.00000	0.01157	81	39
InceptionResNetV2	plantVillage	0.96506	0.95263	0.00028	0.05297	0.99099	0.98708	0.00211	0.01711	88.5	13
InceptionV3	plantVillage	0.94221	0.92675	0.00106	0.06987	0.99039	0.98604	0.00106	0.02046	51.5	59
MobileNetV3Large	plantVillage	0.98676	0.98236	0.00083	0.02475	0.99361	0.99131	0.00023	0.01302	64.5	63
MobileNetV3Small	plantVillage	0.98396	0.97804	0.00023	0.02832	0.99159	0.98856	0.00051	0.01688	72	84
NASNetLarge	plantVillage	0.94373	0.92686	0.00129	0.06987	0.99159	0.98858	0.00069	0.01821	41	68
NASNetMobile	plantVillage	0.94874	0.93240	0.00005	0.06378	0.98740	0.98310	0.00092	0.02206	80.5	76
ResNet101V2	plantVillage	0.96998	0.95885	0.00005	0.04571	0.99104	0.98707	0.00106	0.01924	33.5	37
ResNet152V2	plantVillage	0.96865	0.95880	0.00009	0.04922	0.99223	0.98956	0.00097	0.01454	41	37
ResNet50V2	plantVillage	0.96980	0.96002	0.00051	0.04454	0.99030	0.98686	0.00143	0.01879	45	56
VGG16	plantVillage	0.97232	0.96422	0.00055	0.03996	0.99338	0.99052	0.00175	0.01545	54.5	35
VGG19	plantVillage	0.96897	0.96036	0.00041	0.04203	0.99572	0.99373	0.00032	0.00960	69.5	52.5
Xception	plantVillage	0.95380	0.93931	0.00115	0.06101	0.98506	0.97992	0.00216	0.02332	52	33
ConvNeXtSmall	pld	0.97160	0.97059	0.00123	0.00622	0.98272	0.98245	0.00000	0.00155	62	23
ConvNeXtTiny	pld	0.97531	0.97436	0.00000	0.00582	0.98642	0.98531	0.00123	0.00687	84.5	32.5

Continued on next page

Table C.2 - continued from previous page

Model	Dataset	Acc	F1	Acc SD	F-1 SD	Acc FT	F1 FT	Acc FT	SD FT	F-1 FT	SD FT	Best Epoch	Best Epoch FT
DenseNet121	p1d	0.98395	0.98298	0.00123	0.00633	0.99012	0.98969	0.00000	0.00310	67.5	10		
DenseNet169	p1d	0.97778	0.97673	0.00000	0.00622	0.98765	0.98648	0.00494	0.00854	35.5	8.5		
DenseNet201	p1d	0.97901	0.97840	0.00123	0.00563	0.99753	0.99719	0.00000	0.00206	44.5	20		
EfficientNetV2B0	p1d	0.99259	0.99173	0.00000	0.00478	0.99383	0.99344	0.00123	0.00262	73.5	18.5		
EfficientNetV2B1	p1d	0.98642	0.98521	0.00123	0.00702	0.99012	0.98894	0.00000	0.00667	43	34.5		
EfficientNetV2B2	p1d	0.98765	0.98692	0.00000	0.00438	0.98889	0.98838	0.00123	0.00433	35	8.5		
EfficientNetV2B3	p1d	0.98519	0.98390	0.00247	0.00787	0.99012	0.98894	0.00000	0.00667	31.5	4		
EfficientNetV2M	p1d	0.97778	0.97686	0.00247	0.00651	0.99136	0.99087	0.00123	0.00483	46.5	5.5		
EfficientNetV2S	p1d	0.98148	0.98018	0.00370	0.00986	0.98889	0.98802	0.00123	0.00850	41.5	23		
InceptionResNetV2	p1d	0.96049	0.95791	0.00247	0.01643	0.98642	0.98556	0.00123	0.00545	72.5	4.5		
InceptionV3	p1d	0.94198	0.94090	0.00370	0.00775	0.97778	0.97752	0.00247	0.00348	24	7.5		
MobileNetV3Large	p1d	0.98025	0.97915	0.00000	0.00812	0.98765	0.98716	0.00247	0.00396	45	5.5		
MobileNetV3Small	p1d	0.98148	0.98032	0.00123	0.00686	0.98272	0.98153	0.00000	0.00759	70.5	11		
NASNetLarge	p1d	0.95185	0.95047	0.00123	0.00937	0.98272	0.98268	0.00247	0.00464	25.5	5.5		
NASNetMobile	p1d	0.94321	0.94054	0.00247	0.01564	0.98272	0.98243	0.00247	0.00385	47.5	33		
ResNet101V2	p1d	0.96790	0.96560	0.00247	0.01363	0.98642	0.98615	0.00123	0.00538	40	2		

Continued on next page

Table C.2 - continued from previous page

Model	Dataset	Acc	F1	Acc SD	F-1 SD	Acc FT	F1 FT	Acc FT	SD FT	F-1 FT	SD FT	Best Epoch	Best Epoch FT
ResNet152V2	p1d	0.97407	0.97235	0.00123	0.01041	0.98889	0.98823	0.00123	0.00413	35.5	5		
ResNet50V2	p1d	0.97284	0.97173	0.00000	0.00672	0.99012	0.98930	0.00247	0.00523	36	16		
VGG16	p1d	0.96420	0.96291	0.00370	0.00946	0.98148	0.97987	0.00370	0.01188	56	9		
VGG19	p1d	0.96790	0.96604	0.00000	0.01119	0.99136	0.99060	0.00123	0.00579	51	18		
Xception	p1d	0.95309	0.95136	0.00247	0.01092	0.98025	0.97908	0.00000	0.00771	36	7		
ConvNeXtSmall	r1dd	0.98095	0.97236	0.00000	0.02157	0.97619	0.96606	0.00476	0.02694	190	48		
ConvNeXtTiny	r1dd	0.96667	0.95149	0.00476	0.03850	0.96667	0.95149	0.00476	0.03850	128	3		
DenseNet121	r1dd	0.97143	0.95805	0.00000	0.03316	0.97143	0.95853	0.00952	0.03680	170	36.5		
DenseNet169	r1dd	0.97143	0.95805	0.00000	0.03316	0.97143	0.95805	0.00000	0.03316	184.5	14		
DenseNet201	r1dd	0.98571	0.97934	0.00476	0.01836	0.98095	0.97236	0.00000	0.02157	107.5	38.5		
EfficientNetV2B0	r1dd	0.97143	0.95805	0.00000	0.03316	0.98095	0.97236	0.00000	0.02157	105.5	34.5		
EfficientNetV2B1	r1dd	0.96667	0.95070	0.00476	0.04042	0.97619	0.96520	0.00476	0.02887	84.5	55.5		
EfficientNetV2B2	r1dd	0.97143	0.95805	0.00000	0.03316	0.98095	0.97236	0.00000	0.02157	155.5	7.5		
EfficientNetV2B3	r1dd	0.97619	0.96566	0.00476	0.02788	0.98095	0.97236	0.00000	0.02157	92	12.5		
EfficientNetV2M	r1dd	0.93333	0.90623	0.00952	0.06875	0.96667	0.95070	0.00476	0.04042	185.5	34.5		
EfficientNetV2S	r1dd	0.97143	0.95938	0.00952	0.03437	0.97143	0.95853	0.00952	0.03680	159	42		

Continued on next page

Table C.2 - continued from previous page

Model	Dataset	Acc	F1	Acc SD	F-1 SD	Acc FT	F1 FT	Acc FT	SD FT	F-1 FT	SD FT	Best Epoch	Best Epoch FT
InceptionResNetV2	ridd	0.92857	0.91307	0.00476	0.03981	0.93810	0.92203	0.00476	0.04041	101.5	8.5		
InceptionV3	ridd	0.94286	0.92796	0.00952	0.03921	0.95714	0.94483	0.00476	0.03163	66.5	24		
MobileNetV3Large	ridd	0.97619	0.96606	0.00476	0.02694	0.98095	0.97236	0.00000	0.02157	166.5	63		
MobileNetV3Small	ridd	0.97143	0.96100	0.00000	0.02721	0.97143	0.95805	0.00000	0.03316	193.5	63.5		
NASNetLarge	ridd	0.94286	0.92054	0.00000	0.05590	0.95714	0.93806	0.01429	0.05378	105.5	4.5		
NASNetMobile	ridd	0.91905	0.89776	0.00476	0.05344	0.97619	0.96606	0.00476	0.02694	74	27.5		
ResNet101V2	ridd	0.96190	0.95032	0.00000	0.02946	0.97143	0.96120	0.00000	0.02712	79.5	30		
ResNet152V2	ridd	0.95238	0.93484	0.00000	0.04567	0.96667	0.95184	0.00476	0.03848	95.5	10.5		
ResNet50V2	ridd	0.94762	0.93046	0.00476	0.04311	0.96190	0.94612	0.00000	0.04039	72	15.5		
VGG16	ridd	0.94762	0.92825	0.00476	0.04784	0.95714	0.94312	0.00476	0.03485	196.5	33		
VGG19	ridd	0.95238	0.92966	0.00000	0.05511	0.96667	0.95138	0.00476	0.03905	187	24.5		
Xception	ridd	0.93333	0.91580	0.00952	0.04531	0.94762	0.93163	0.00476	0.04307	92	7.5		
ConvNeXtSmall	sms	0.92500	0.92522	0.00543	0.04110	0.92935	0.92962	0.00761	0.04162	173	1		
ConvNeXtTiny	sms	0.94674	0.94681	0.00109	0.02962	0.95652	0.95666	0.00217	0.02500	119	51		
DenseNet121	sms	0.92609	0.92600	0.00000	0.04133	0.94565	0.94573	0.00000	0.03083	139.5	23		
DenseNet169	sms	0.93370	0.93388	0.00761	0.03966	0.95543	0.95551	0.00978	0.02695	194.5	46.5		

Continued on next page

Table C.2 - continued from previous page

Model	Dataset	Acc	F1	Acc SD	F-1 SD	Acc FT	F1 FT	Acc SD FT	F-1 SD FT	Best Epoch	Best Epoch FT
DenseNet201	sms	0.92609	0.92588	0.00870	0.03811	0.94565	0.94588	0.00217	0.03379	60	49
EfficientNetV2B0	sms	0.92826	0.92744	0.02391	0.04596	0.94891	0.94897	0.00109	0.02582	152	17.5
EfficientNetV2B1	sms	0.93696	0.93665	0.00435	0.03042	0.93913	0.93891	0.00217	0.03034	189.5	148.5
EfficientNetV2B2	sms	0.91304	0.91289	0.00435	0.05656	0.91196	0.91175	0.00109	0.05721	195	167
EfficientNetV2B3	sms	0.94457	0.94458	0.00761	0.03108	0.95000	0.95009	0.00435	0.02763	139	198
EfficientNetV2M	sms	0.92935	0.93018	0.00109	0.02587	0.93696	0.93731	0.00217	0.02768	77.5	13.5
EfficientNetV2S	sms	0.94239	0.94238	0.00109	0.02196	0.94783	0.94785	0.00217	0.02565	137	176
InceptionResNetV2	sms	0.90978	0.91009	0.00109	0.02137	0.92826	0.92820	0.00000	0.02951	190.5	13
InceptionV3	sms	0.89783	0.89691	0.01522	0.05946	0.93696	0.93703	0.00870	0.03751	72	47
MobileNetV3Large	sms	0.93913	0.93867	0.00435	0.02545	0.94891	0.94875	0.00326	0.02227	167.5	192
MobileNetV3Small	sms	0.87609	0.87155	0.01304	0.06509	0.91522	0.91418	0.00217	0.03671	90.5	77.5
NASNetLarge	sms	0.84674	0.84852	0.00326	0.03488	0.87935	0.88119	0.00326	0.03910	32.5	18
NASNetMobile	sms	0.84348	0.84106	0.00652	0.07708	0.87174	0.87032	0.01739	0.07253	98	29
ResNet101V2	sms	0.91848	0.91902	0.00543	0.03889	0.95978	0.96003	0.00761	0.02301	69	57
ResNet152V2	sms	0.89783	0.89784	0.00870	0.03624	0.91630	0.91612	0.00326	0.02724	56.5	1.5
ResNet50V2	sms	0.90435	0.90511	0.00870	0.02985	0.94348	0.94351	0.01957	0.02923	46	25

Continued on next page

Table C.2 - continued from previous page

Model	Dataset	Acc	F1	Acc SD	F-1 SD	Acc FT	F1 FT	Acc FT	SD FT	F-1 FT	SD FT	Best Epoch	Best Epoch FT
VGG16	sms	0.85761	0.85419	0.00326	0.07896	0.91739	0.91727	0.01739	0.05392	104	28.5		
VGG19	sms	0.84022	0.83618	0.01630	0.07131	0.92283	0.92257	0.00761	0.03738	48.5	32.5		
Xception	sms	0.90326	0.90254	0.00109	0.05188	0.90435	0.90363	0.00435	0.05325	138	56		
ConvNeXtSmall	sugar	0.91680	0.87303	0.00078	0.12138	0.91563	0.86859	0.00039	0.13001	87	2.5		
ConvNeXtTiny	sugar	0.91369	0.86696	0.00156	0.13206	0.91446	0.86707	0.00078	0.13114	89	3		
DenseNet121	sugar	0.91602	0.87182	0.00233	0.12841	0.91913	0.87545	0.00233	0.12572	91.5	7		
DenseNet169	sugar	0.91991	0.87701	0.00311	0.12339	0.91757	0.87257	0.00078	0.12650	50	2.5		
DenseNet201	sugar	0.91796	0.87587	0.00039	0.12035	0.91991	0.87660	0.00078	0.12224	56	2.5		
EfficientNetV2B0	sugar	0.92224	0.88013	0.00078	0.12115	0.91757	0.87426	0.00000	0.12395	81.5	5		
EfficientNetV2B1	sugar	0.92302	0.88153	0.00078	0.11917	0.91835	0.87535	0.00078	0.12160	75.5	5		
EfficientNetV2B2	sugar	0.92341	0.88319	0.00117	0.11863	0.92107	0.87772	0.00739	0.12384	62	2.5		
EfficientNetV2B3	sugar	0.92185	0.88095	0.00039	0.11831	0.91991	0.87694	0.00233	0.12256	60.5	4		
EfficientNetV2M	sugar	0.91213	0.86541	0.00078	0.13132	0.92030	0.87747	0.00350	0.12232	62.5	4		
EfficientNetV2S	sugar	0.92224	0.88356	0.00078	0.11273	0.91991	0.87557	0.00078	0.12178	54.5	3		
InceptionResNetV2	sugar	0.91252	0.86760	0.00039	0.12353	0.91757	0.87403	0.00233	0.12162	112	3		
InceptionV3	sugar	0.91174	0.86753	0.00117	0.12410	0.91330	0.86642	0.00194	0.13068	58.5	8		

Continued on next page

Table C.2 - continued from previous page

Model	Dataset	Acc	F1	Acc SD	F-1 SD	Acc FT	F1 FT	Acc FT	SD FT	F-1 FT	SD FT	Best Epoch	Best Epoch FT
MobileNetV3Large	sugar	0.92379	0.88625	0.00078	0.11093	0.91680	0.87218	0.00000	0.12640	56.5	6		
MobileNetV3Small	sugar	0.91796	0.87403	0.00039	0.12404	0.91446	0.86999	0.00000	0.12661	90.5	13		
NASNetLarge	sugar	0.91213	0.87200	0.00078	0.11371	0.91524	0.87131	0.00156	0.12304	39	2.5		
NASNetMobile	sugar	0.90669	0.86298	0.00389	0.12393	0.90941	0.86393	0.00350	0.12775	86	4.5		
ResNet101V2	sugar	0.91524	0.87193	0.00078	0.12469	0.91719	0.87220	0.00272	0.12550	39	2		
ResNet152V2	sugar	0.91252	0.86704	0.00194	0.13254	0.91757	0.87436	0.00156	0.12379	49	2.5		
ResNet50V2	sugar	0.91407	0.86857	0.00039	0.12799	0.91485	0.86772	0.00194	0.13198	43	4.5		
VGG16	sugar	0.91835	0.87386	0.00233	0.12472	0.91796	0.87459	0.00194	0.12410	91	3		
VGG19	sugar	0.92030	0.87953	0.00039	0.11689	0.92302	0.88213	0.00700	0.11524	84.5	9.5		
Xception	sugar	0.90747	0.86222	0.00233	0.12825	0.91213	0.86438	0.00156	0.13253	58	3		
ConvNeXtSmall	taiwanTomato	0.64961	0.61041	0.00394	0.19342	0.67717	0.62739	0.00787	0.21015	74	8.5		
ConvNeXtTiny	taiwanTomato	0.69291	0.65217	0.01575	0.17401	0.71654	0.68086	0.02362	0.16097	70	18		
DenseNet121	taiwanTomato	0.67323	0.63490	0.00394	0.18072	0.67717	0.64852	0.01575	0.16432	89.5	3		
DenseNet169	taiwanTomato	0.63780	0.60718	0.00787	0.19693	0.71260	0.68637	0.01181	0.14401	58.5	4		
DenseNet201	taiwanTomato	0.64173	0.61013	0.01181	0.18384	0.65748	0.61567	0.01181	0.18329	52.5	1.5		
EfficientNetV2B0	taiwanTomato	0.65354	0.60240	0.00787	0.19437	0.69685	0.66654	0.00394	0.15015	54.5	4.5		

Continued on next page

Table C.2 - continued from previous page

Model	Dataset	Acc	F1	Acc SD	F-1 SD	Acc FT	F1 FT	Acc FT	SD FT	F-1 FT	SD FT	Best Epoch	Best Epoch FT
EfficientNetV2B1	taiwanTomato	0.68110	0.63758	0.00394	0.18297	0.70079	0.65509	0.01575	0.19098	53.5	5.5		
EfficientNetV2B2	taiwanTomato	0.74409	0.71225	0.00394	0.16147	0.74016	0.71106	0.01575	0.17241	60	5.5		
EfficientNetV2B3	taiwanTomato	0.71654	0.67415	0.00787	0.19439	0.74803	0.71218	0.00787	0.17379	58.5	7		
EfficientNetV2M	taiwanTomato	0.59055	0.55584	0.00787	0.20906	0.63780	0.60465	0.01575	0.18905	57.5	2		
EfficientNetV2S	taiwanTomato	0.70866	0.66703	0.00787	0.16376	0.72047	0.67831	0.01969	0.17900	63	3		
InceptionResNetV2	taiwanTomato	0.61024	0.56941	0.01181	0.19420	0.59449	0.54194	0.06693	0.24530	81.5	1		
InceptionV3	taiwanTomato	0.60630	0.56519	0.01575	0.19871	0.61417	0.57232	0.04724	0.21336	40.5	1.5		
MobileNetV3Large	taiwanTomato	0.72047	0.68392	0.00394	0.17217	0.73228	0.70010	0.00000	0.15974	71	1.5		
MobileNetV3Small	taiwanTomato	0.65354	0.60044	0.01575	0.19865	0.66142	0.60057	0.00787	0.23549	90.5	1		
NASNetLarge	taiwanTomato	0.62598	0.59094	0.01181	0.17441	0.64567	0.61207	0.04724	0.18459	26.5	2		
NASNetMobile	taiwanTomato	0.57874	0.52630	0.01181	0.21748	0.64567	0.61967	0.00787	0.17367	31	14		
ResNet101V2	taiwanTomato	0.63386	0.59668	0.00394	0.18217	0.63386	0.60876	0.01181	0.17034	39.5	2		
ResNet152V2	taiwanTomato	0.57874	0.53880	0.01969	0.17672	0.64567	0.59309	0.00787	0.21611	31.5	1		
ResNet50V2	taiwanTomato	0.62598	0.59060	0.00394	0.18307	0.64173	0.57734	0.03543	0.25968	37.5	1		
VGG16	taiwanTomato	0.59055	0.56380	0.03937	0.18926	0.65354	0.61630	0.03150	0.19438	92.5	5		
VGG19	taiwanTomato	0.61811	0.58424	0.02756	0.18938	0.60630	0.56301	0.04724	0.23638	84.5	1		

Continued on next page

Table C.2 - continued from previous page

Model	Dataset	Acc	F1	Acc SD	F-1 SD	Acc FT	F1 FT	Acc FT	SD FT	F-1 FT	SD FT	Best Epoch	Best Epoch FT
Xception	taiwanTomato	0.60236	0.56532	0.02756	0.15885	0.66142	0.63185	0.02362	0.19049	43	1.5		
ConvNeXtSmall	tea	0.84637	0.84034	0.00838	0.10723	0.89106	0.88605	0.00279	0.08587	166.5	42.5		
ConvNeXtTiny	tea	0.89106	0.88498	0.00279	0.09197	0.92458	0.91931	0.00279	0.06800	173	96.5		
DenseNet121	tea	0.87151	0.86606	0.00559	0.09215	0.89106	0.88905	0.00838	0.08281	143	44		
DenseNet169	tea	0.89106	0.89064	0.00838	0.06795	0.91341	0.91321	0.00279	0.05713	159.5	27.5		
DenseNet201	tea	0.88268	0.87815	0.01117	0.09176	0.88827	0.88163	0.01117	0.10691	119	23		
EfficientNetV2B0	tea	0.85475	0.85099	0.00559	0.09818	0.90782	0.90452	0.00838	0.07205	135.5	54		
EfficientNetV2B1	tea	0.86592	0.86597	0.00559	0.08003	0.88827	0.88973	0.00559	0.07433	121.5	12		
EfficientNetV2B2	tea	0.87151	0.86783	0.00000	0.09206	0.88827	0.88177	0.00000	0.09909	105.5	24		
EfficientNetV2B3	tea	0.88268	0.87568	0.01117	0.09357	0.90503	0.89872	0.00559	0.08280	110	15		
EfficientNetV2M	tea	0.87989	0.87730	0.00279	0.07816	0.92737	0.92408	0.01117	0.06271	120.5	10.5		
EfficientNetV2S	tea	0.84637	0.83814	0.01397	0.13286	0.88547	0.87965	0.01397	0.10119	138	35		
InceptionResNetV2	tea	0.74581	0.73822	0.01397	0.11962	0.82961	0.82566	0.01955	0.11707	81.5	2.5		
InceptionV3	tea	0.75419	0.74581	0.00559	0.09605	0.82123	0.81231	0.01117	0.10362	75.5	17		
MobileNetV3Large	tea	0.91620	0.90992	0.00559	0.08557	0.92179	0.91417	0.00000	0.09072	182	50		
MobileNetV3Small	tea	0.89665	0.89124	0.00279	0.08426	0.90782	0.90316	0.00279	0.07935	196	21		

Continued on next page

Table C.2 - continued from previous page

Model	Dataset	Acc	F1	Acc SD	F-1 SD	Acc FT	F1 FT	Acc FT	SD FT	F-1 FT	SD FT	Best Epoch	Best Epoch FT
NASNetLarge	tea	0.77095	0.76284	0.01676	0.10449	0.86034	0.85484	0.00559	0.08292	65.5	27.5		
NASNetMobile	tea	0.76257	0.76145	0.00279	0.11468	0.82682	0.82378	0.01117	0.10563	146.5	27.5		
ResNet101V2	tea	0.81844	0.81320	0.00279	0.10909	0.88268	0.87957	0.00559	0.09470	89.5	13		
ResNet152V2	tea	0.80726	0.80332	0.00279	0.12217	0.86592	0.85995	0.01676	0.10792	77.5	16.5		
ResNet50V2	tea	0.83520	0.82847	0.00279	0.11025	0.87709	0.87065	0.02235	0.09898	83.5	4		
VGG16	tea	0.82961	0.82739	0.01397	0.09496	0.91061	0.90758	0.00000	0.06895	173	77		
VGG19	tea	0.86034	0.86039	0.00559	0.07989	0.92458	0.92041	0.01397	0.06838	132	51.5		
Xception	tea	0.77933	0.77736	0.00279	0.13377	0.82123	0.82183	0.02235	0.10848	89.5	6.5		
ConvNeXtSmall	tomatoVillage	0.87844	0.85596	0.00385	0.09042	0.90594	0.88736	0.00275	0.07742	136	15.5		
ConvNeXtTiny	tomatoVillage	0.85534	0.83308	0.00495	0.11388	0.88724	0.86835	0.00495	0.08991	128.5	17		
DenseNet121	tomatoVillage	0.87459	0.84713	0.00000	0.09414	0.89439	0.87393	0.00330	0.08298	109	11.5		
DenseNet169	tomatoVillage	0.85919	0.83749	0.00110	0.10458	0.87514	0.85643	0.01155	0.09321	72.5	9.5		
DenseNet201	tomatoVillage	0.86359	0.84535	0.00330	0.10398	0.88834	0.87404	0.00935	0.07942	72	6.5		
EfficientNetV2B0	tomatoVillage	0.88669	0.86938	0.00330	0.09981	0.89164	0.87499	0.00715	0.09293	98.5	1		
EfficientNetV2B1	tomatoVillage	0.88944	0.87374	0.00935	0.06896	0.90374	0.89314	0.00165	0.06730	99	4.5		
EfficientNetV2B2	tomatoVillage	0.88614	0.86014	0.00605	0.11533	0.89329	0.87218	0.01320	0.09320	83.5	4		

Continued on next page

Table C.2 - continued from previous page

Model	Dataset	Acc	F1	Acc SD	F-1 SD	Acc FT	F1 FT	Acc FT	SD FT	F-1 FT	SD FT	Best Epoch	Best Epoch FT
EfficientNetV2B3	tomatoVillage	0.88064	0.85709	0.00275	0.10317	0.89054	0.86953	0.00715	0.09445	85.5	2		
EfficientNetV2M	tomatoVillage	0.86194	0.83387	0.00275	0.11037	0.88174	0.85978	0.02365	0.09754	98.5	4.5		
EfficientNetV2S	tomatoVillage	0.87239	0.84801	0.00110	0.08970	0.89824	0.87401	0.00385	0.08204	81.5	5		
InceptionResNetV2	tomatoVillage	0.81023	0.77917	0.00715	0.10855	0.86799	0.84181	0.01760	0.09139	86.5	4		
InceptionV3	tomatoVillage	0.77503	0.74031	0.00165	0.16666	0.80913	0.77851	0.05226	0.14778	55	2.5		
MobileNetV3Large	tomatoVillage	0.87734	0.84756	0.00275	0.11085	0.89769	0.87829	0.00550	0.09231	76.5	7.5		
MobileNetV3Small	tomatoVillage	0.85809	0.83878	0.00220	0.08539	0.87624	0.85784	0.00385	0.08278	122	4		
NASNetLarge	tomatoVillage	0.80363	0.76654	0.00495	0.11218	0.82783	0.79325	0.01815	0.11410	53	2.5		
NASNetMobile	tomatoVillage	0.79978	0.76825	0.00660	0.09929	0.82453	0.78836	0.01485	0.12352	83	3.5		
ResNet101V2	tomatoVillage	0.82563	0.79410	0.00055	0.12222	0.85149	0.82471	0.00440	0.09901	50.5	4.5		
ResNet152V2	tomatoVillage	0.84158	0.80995	0.00440	0.10349	0.87239	0.83483	0.01760	0.09844	57.5	3.5		
ResNet50V2	tomatoVillage	0.83498	0.80572	0.00550	0.10196	0.85699	0.82987	0.01210	0.09980	52.5	3		
VGG16	tomatoVillage	0.83168	0.80292	0.00990	0.12369	0.86139	0.83633	0.01870	0.09466	101	4		
VGG19	tomatoVillage	0.82618	0.80987	0.00110	0.11067	0.87184	0.85418	0.00055	0.08572	94.5	18		
Xception	tomatoVillage	0.79868	0.76573	0.00220	0.12968	0.83388	0.80679	0.01210	0.10640	63	2.5		

D. Appendix Augmentation

In this appendix all the results used to achieve the augmentation benchmark results for plant leaf disease classification are listed in Table D.1. In the table Augmentation Combined corresponds to augmented all, Augmentation Transform corresponds to augmented trans, Augmentation Color is represented as augmented color, Augmentation None simply as none, and Augmentation Noise is listed as augmented noise.

Table D.1: Full results obtained during augmentation experiments. Results originate from [133].

Model	Dataset	Augmentation	Test Acc	Test F1	Test Recall	Val Precision
MobileNetV3Large	novelPotato	augmented all	98.69%	98.97%	98.69%	98.69%
DenseNet121	novelPotato	augmented all	97.70%	96.92%	97.70%	97.70%
DenseNet201	novelPotato	augmented all	98.03%	97.95%	98.03%	98.03%
EfficientNetV2B0	novelPotato	augmented all	99.34%	99.49%	99.34%	99.34%
EfficientNetV2B2	novelPotato	augmented all	98.36%	97.89%	98.36%	98.36%
ResNet50V2	novelPotato	augmented all	96.39%	96.13%	96.39%	96.39%
ResNet152V2	novelPotato	augmented all	96.72%	95.91%	96.72%	96.72%

Continued on next page

Table D.1 - continued from previous page

Model	Dataset	Augmentation	Test Acc	Test F1	Test Recall	Val Precision
ConvNeXtSmall	novelPotato	augmented all	99.02%	98.96%	99.02%	99.02%
VGG19	novelPotato	augmented all	96.39%	95.31%	96.39%	96.39%
MobileNetV3Large	pld	augmented all	99.75%	99.78%	99.75%	99.75%
DenseNet121	pld	augmented all	100.00%	100.00%	100.00%	100.00%
DenseNet201	pld	augmented all	99.75%	99.72%	99.75%	99.75%
EfficientNetV2B0	pld	augmented all	99.75%	99.78%	99.75%	99.75%
EfficientNetV2B2	pld	augmented all	100.00%	100.00%	100.00%	100.00%
ResNet50V2	pld	augmented all	99.26%	99.28%	99.26%	99.26%
ResNet152V2	pld	augmented all	100.00%	100.00%	100.00%	100.00%
ConvNeXtSmall	pld	augmented all	99.75%	99.72%	99.75%	99.75%
VGG19	pld	augmented all	99.75%	99.78%	99.75%	99.75%
MobileNetV3Large	novelPotato	augmented color	99.02%	99.23%	99.02%	99.02%
DenseNet121	novelPotato	augmented color	96.72%	96.22%	96.72%	96.72%
DenseNet201	novelPotato	augmented color	96.39%	96.13%	96.39%	96.39%
EfficientNetV2B0	novelPotato	augmented color	98.36%	98.71%	98.36%	98.36%
EfficientNetV2B2	novelPotato	augmented color	98.36%	97.89%	98.36%	98.36%
ResNet50V2	novelPotato	augmented color	94.10%	92.90%	94.10%	94.10%
ResNet152V2	novelPotato	augmented color	92.79%	92.55%	92.79%	92.79%

Continued on next page

Table D.1 - continued from previous page

Model	Dataset	Augmentation	Test Acc	Test F1	Test Recall	Val Precision
ConvNeXtSmall	novelPotato	augmented color	99.02%	99.23%	99.02%	99.02%
VGG19	novelPotato	augmented color	92.46%	90.38%	92.46%	92.46%
MobileNetV3Large	pld	augmented color	99.51%	99.51%	99.51%	99.75%
DenseNet121	pld	augmented color	99.26%	99.34%	99.26%	99.26%
DenseNet201	pld	augmented color	99.75%	99.78%	99.75%	99.75%
EfficientNetV2B0	pld	augmented color	99.51%	99.56%	99.51%	99.51%
EfficientNetV2B2	pld	augmented color	100.00%	100.00%	100.00%	100.00%
ResNet50V2	pld	augmented color	98.77%	98.65%	98.77%	98.77%
ResNet152V2	pld	augmented color	98.77%	98.74%	98.77%	98.77%
ConvNeXtSmall	pld	augmented color	100.00%	100.00%	100.00%	100.00%
VGG19	pld	augmented color	99.26%	99.21%	99.26%	99.26%
MobileNetV3Large	novelPotato	augmented noise	96.39%	95.77%	96.39%	96.39%
DenseNet121	novelPotato	augmented noise	96.07%	95.18%	96.07%	96.07%
DenseNet201	novelPotato	augmented noise	95.08%	93.99%	95.08%	95.08%
EfficientNetV2B0	novelPotato	augmented noise	97.70%	97.68%	97.70%	97.70%
EfficientNetV2B2	novelPotato	augmented noise	98.03%	97.38%	98.03%	98.03%
ResNet50V2	novelPotato	augmented noise	92.79%	91.12%	92.79%	92.79%
ResNet152V2	novelPotato	augmented noise	94.43%	93.96%	94.43%	94.43%

Continued on next page

Table D.1 - continued from previous page

Model	Dataset	Augmentation	Test Acc	Test F1	Test Recall	Val Precision
ConvNeXtSmall	novelPotato	augmented noise	98.69%	98.42%	98.69%	98.69%
VGG19	novelPotato	augmented noise	89.51%	87.30%	89.51%	89.51%
MobileNetV3Large	pld	augmented noise	99.01%	98.93%	99.01%	99.01%
DenseNet121	pld	augmented noise	98.77%	98.84%	98.77%	98.77%
DenseNet201	pld	augmented noise	99.01%	99.06%	99.01%	99.01%
EfficientNetV2B0	pld	augmented noise	98.77%	98.63%	98.77%	98.77%
EfficientNetV2B2	pld	augmented noise	99.51%	99.45%	99.51%	99.51%
ResNet50V2	pld	augmented noise	99.26%	99.28%	99.26%	99.26%
ResNet152V2	pld	augmented noise	98.02%	98.11%	97.78%	98.02%
ConvNeXtSmall	pld	augmented noise	99.75%	99.72%	99.75%	99.75%
VGG19	pld	augmented noise	99.26%	99.34%	99.01%	99.26%
MobileNetV3Large	novelPotato	augmented trans	97.70%	97.68%	97.70%	97.70%
DenseNet121	novelPotato	augmented trans	98.03%	97.94%	98.03%	98.03%
DenseNet201	novelPotato	augmented trans	98.36%	98.18%	98.36%	98.36%
EfficientNetV2B0	novelPotato	augmented trans	97.70%	97.35%	97.70%	97.70%
EfficientNetV2B2	novelPotato	augmented trans	98.36%	97.89%	98.36%	98.68%
ResNet50V2	novelPotato	augmented trans	95.41%	93.80%	95.41%	95.41%
ResNet152V2	novelPotato	augmented trans	96.72%	95.44%	96.72%	96.72%

Continued on next page

Table D.1 - continued from previous page

Model	Dataset	Augmentation	Test Acc	Test F1	Test Recall	Val Precision
ConvNeXtSmall	novelPotato	augmented trans	98.03%	97.92%	98.03%	98.03%
VGG19	novelPotato	augmented trans	95.74%	95.50%	95.74%	95.74%
MobileNetV3Large	pld	augmented trans	100.00%	100.00%	100.00%	100.00%
DenseNet121	pld	augmented trans	100.00%	100.00%	100.00%	100.00%
DenseNet201	pld	augmented trans	100.00%	100.00%	100.00%	100.00%
EfficientNetV2B0	pld	augmented trans	99.51%	99.44%	99.51%	99.51%
EfficientNetV2B2	pld	augmented trans	100.00%	100.00%	100.00%	100.00%
ResNet50V2	pld	augmented trans	100.00%	100.00%	100.00%	100.00%
ResNet152V2	pld	augmented trans	99.75%	99.78%	99.75%	99.75%
ConvNeXtSmall	pld	augmented trans	99.75%	99.78%	99.75%	99.75%
VGG19	pld	augmented trans	99.75%	99.73%	99.75%	99.75%
MobileNetV3Large	novelPotato		96.07%	95.18%	96.07%	96.07%
DenseNet121	novelPotato		96.39%	95.11%	96.39%	96.71%
DenseNet201	novelPotato		97.05%	97.13%	97.05%	97.37%
EfficientNetV2B0	novelPotato		94.75%	92.10%	94.75%	94.75%
EfficientNetV2B2	novelPotato		97.70%	97.41%	97.70%	97.70%
ResNet50V2	novelPotato		95.08%	93.95%	95.08%	95.39%
ResNet152V2	novelPotato		93.44%	91.97%	93.44%	93.44%

Continued on next page

Table D.1 - continued from previous page

Model	Dataset	Augmentation	Test Acc	Test F1	Test Recall	Val Precision
ConvNeXtSmall	novelPotato		98.03%	97.90%	98.03%	98.03%
VGG19	novelPotato		93.77%	93.11%	93.77%	93.77%
MobileNetV3Large	pId		99.26%	99.15%	99.26%	99.26%
DenseNet121	pId		99.26%	99.17%	99.26%	99.26%
DenseNet201	pId		99.75%	99.72%	99.75%	99.75%
EfficientNetV2B0	pId		99.26%	99.19%	99.26%	99.26%
EfficientNetV2B2	pId		99.51%	99.44%	99.51%	99.51%
ResNet50V2	pId		99.01%	98.90%	99.01%	99.01%
ResNet152V2	pId		99.26%	99.23%	99.26%	99.26%
ConvNeXtSmall	pId		99.75%	99.72%	99.75%	99.75%
VGG19	pId		99.01%	99.00%	99.01%	99.01%

E. Dataset Construction

The full list of plants and classes included in the PLDC-80 dataset. Each class has 3,500 training images.

PLDC-80

- └ cassava_cassava_Cassava Bacterial Blight (CBB)
- └ cassava_cassava_Cassava Brown Streak Disease (CBSD)
- └ cassava_cassava_Cassava Green Mottle (CGM)
- └ cassava_cassava_Cassava Mosaic Disease (CMD)
- └ cassava_cassava_Healthy
- └ cds_corn_Gray Leaf Spot_AND_plantvillage_Corn_Cercospora_leaf_spot Gray_leaf_spot
- └ cds_corn_Northern Leaf Blight_AND_plantvillage_Corn_Northern_Leaf_Blight
- └ cds_corn_Northern Leaf Spot
- └ diamos_pear_slug
- └ diamos_pear_spot
- └ fgvc8_apple_frog_eye_leaf_spot
- └ fgvc8_apple_healthy_AND_plantvillage_Apple__healthy
- └ fgvc8_apple_powdery_mildew
- └ fgvc8_apple_rust_AND_plantvillage_Apple___Cedar_apple_rust
- └ fgvc8_apple_scab_AND_plantvillage_Apple___Apple_scab
- └ paddy_rice_bacterial_leaf_blight
- └ paddy_rice_bacterial_leaf_streak
- └ paddy_rice_bacterial_panicle_blight
- └ paddy_rice_blast
- └ paddy_rice_brown_spot
- └ paddy_rice_dead_heart
- └ paddy_rice_downy_mildew
- └ paddy_rice_hispa
- └ paddy_rice_normal
- └ paddy_rice_tungro
- └ pdd271_Soybean_downy_mildew_135

- └ pdd271_Mung_bean_brown_spot_246
- └ pdd271_Sweet_potato_healthy_leaf_220
- └ pdd271_Sweet_potato_magnesium_deficiency_227
- └ pdd271_Sweet_potato_sooty_mold_224
- └ pdd271_leek_gray_mold_disease_339
- └ pdd271_leek_hail_damage_338
- └ pdd271_radish_black_spot_disease_297
- └ pdd271_radish_mosaic_virus_disease_295
- └ pdd271_radish_wrinkle_virus_disease_293
- └ plantvillage_Apple___Black_rot
- └ plantvillage_Blueberry___healthy
- └ plantvillage_Cherry_(including_sour)___Powdery_mildew
- └ plantvillage_Cherry_(including_sour)___healthy
- └ plantvillage_Corn_(maize)___Common_rust_
- └ plantvillage_Corn_(maize)___healthy
- └ plantvillage_Grape___Black_rot
- └ plantvillage_Grape___Esca_(Black_Measles)
- └ plantvillage_Grape___Leaf_blight_(Isariopsis_Leaf_Spot)
- └ plantvillage_Grape___healthy
- └ plantvillage_Orange___Haunglongbing_(Citrus_greening)
- └ plantvillage_Peach___Bacterial_spot
- └ plantvillage_Peach___healthy
- └ plantvillage_Pepper,_bell___Bacterial_spot
- └ plantvillage_Pepper,_bell___healthy
- └ plantvillage_Potato___Early_blight
- └ plantvillage_Potato___Late_blight
- └ plantvillage_Raspberry___healthy
- └ plantvillage_Soybean___healthy
- └ plantvillage_Squash___Powdery_mildew
- └ plantvillage_Strawberry___Leaf_scorch
- └ plantvillage_Strawberry___healthy
- └ plantvillage_Tomato___Bacterial_spot
- └ plantvillage_Tomato___Early_blight
- └ plantvillage_Tomato___Late_blight
- └ plantvillage_Tomato___Leaf_Mold
- └ plantvillage_Tomato___Septoria_leaf_spot
- └ plantvillage_Tomato___Spider_mites Two └spotted_spider_mite
- └ plantvillage_Tomato___Target_Spot

- └ plantvillage_Tomato___Tomato_Yellow_Leaf_Curl_Virus
- └ plantvillage_Tomato___Tomato_mosaic_virus
- └ plantvillage_Tomato___healthy
- └ sms_strawberry_angular_leafspot
- └ sms_strawberry_leaf_spot
- └ sms_strawberry_powdery_mildew_leaf
- └ sugar_cane_Banded Chlorosis
- └ sugar_cane_Brown Spot
- └ sugar_cane_BrownRust
- └ sugar_cane_Grassy shoot
- └ sugar_cane_Healthy Leaves
- └ sugar_cane_Pokkah Boeng
- └ sugar_cane_Set Rot
- └ sugar_cane_Viral Disease
- └ sugar_cane_Yellow Leaf
- └ sugar_cane_smut

F. Appendix PLDC-6 Datasets

F.1 iBean

Table F.1: Information about the iBean Dataset.

Plants	Beans
Diseases	1. Healthy 2. Angular Leaf Spot 3. Bean Rust
Number of Classes	3
Number of Images	1,296

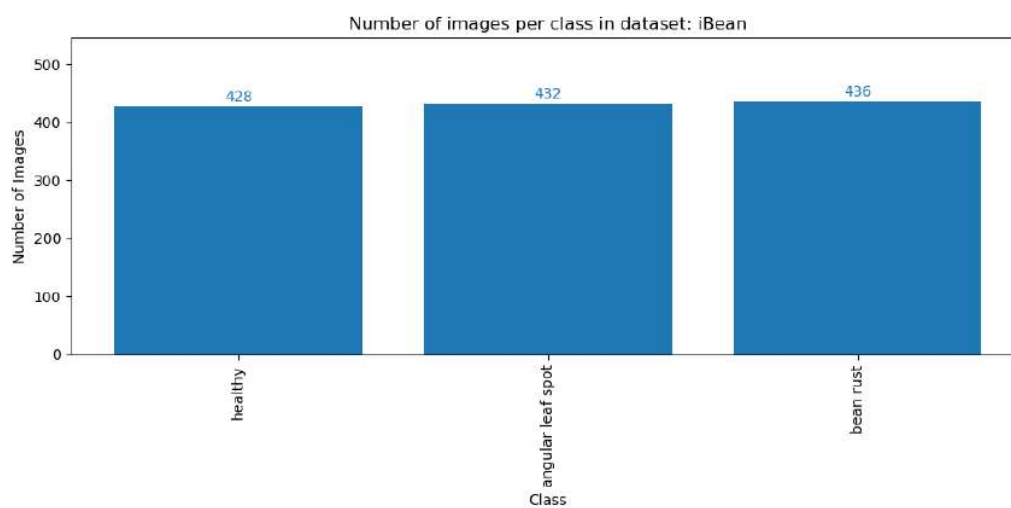


Figure F.1: Class Distribution of the iBean Dataset.

iBean Dataset - Sample Images - One per Class



Figure F.2: A sample image of each class present in the iBean Dataset.

F.2 Soybean

Table F.2: Information about the Soybean Dataset.

Plants	Soybean images dataset
Diseases	1. Healthy 2. Caterpillar 3. Diabrotica speciosa
Number of Classes	3
Number of Images	6,410

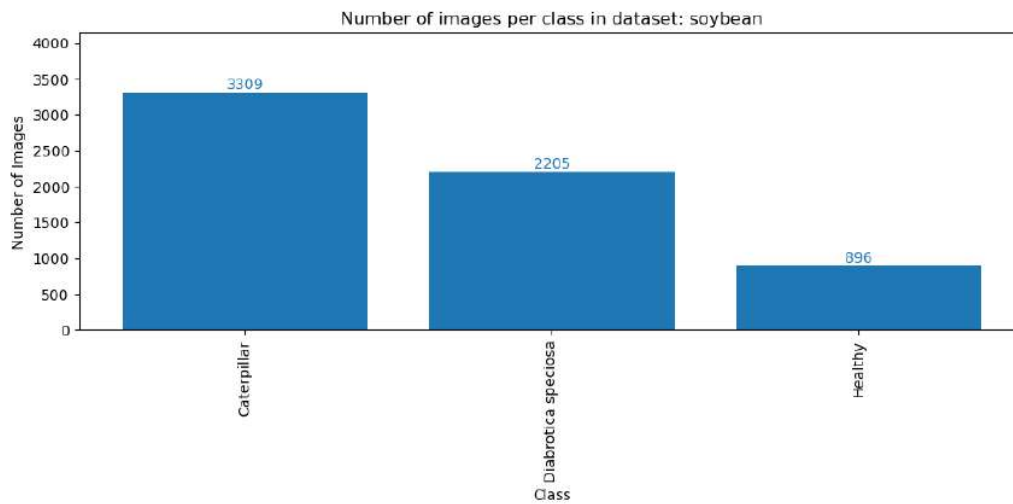


Figure F.3: Class Distribution of the Soybean Dataset.

soybean Dataset - Sample Images - One per Class

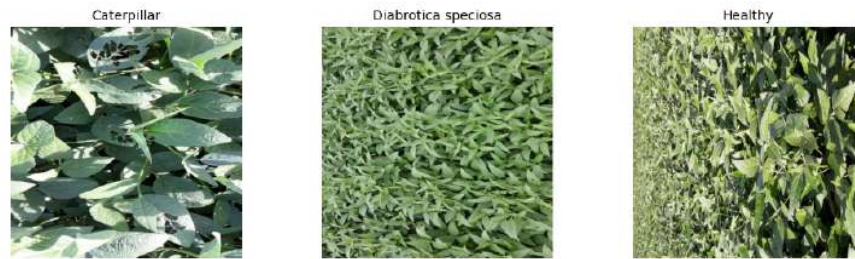


Figure F.4: A sample image of each class present in the Soybean Dataset.

F.3 Classes PLDC-6

PLDC-6

- └ soybean_Healthy
- └ soybean_Caterpillar
- └ soybean_Diabrotica speciosa
- └ iBean_Healthy
- └ iBean_Angular Leaf Spot
- └ iBean_Bean Rust

To my friends and family.

Acknowledgments

I want to thank my lab mates for helping me when I had any questions regarding this thesis or any of the other projects I worked on, my friends (both here in Korea and as well as back home and all over the world) and family for being there for me during the duration of this work. I also want to thank my professors here at CNU and outside that gave me valuable advice and always had an open ear. I also appreciate the high-performance GPU computing support of HPC-AI Open Infrastructure via GIST SCENT, without which many of the experiments in this thesis would not have been possible.